THE UNIVERSITY OF SOUTH ALABAMA
COLLEGE OF ARTS AND SCIENCES

LARVAL OYSTER (*CRASSOSTREA VIRGINICA*) SETTLEMENT AND
DISTRIBUTION IN A FRESHWATER-DOMINATED AND HUMAN-
INFLUENCED ESTUARY

BY

Haley Nicholson Gancel

A Dissertation

Submitted to the Graduate Faculty of the
University of South Alabama
in partial fulfillment of the
requirements for the degree of

Doctor of Philosophy

in

Marine Sciences

May 2020

Approved: Date:

                                                                            01/14/2020
Chair of Dissertation Committee: Dr. Ruth H. Carmichael

                                                                            1/14/2020
Committee Member: Dr. Kyeong Park

                                                                            01/14/2020
Committee Member: Dr. William Burkhardt III

                                                                            1/14/2020
Committee Member: Dr. Jeffrey W. Krause

                                                                            1/14/2020
Committee Member: Dr. Kelly Dorgan

                                                                            1/21/2020
Chair of Department: Dr. Sean P. Powers

                                                                            2/17/2020
Director of Graduate Studies: Dr. Eric J. Loomis

                                                                            3/12/2020
Dean of the Graduate School: Dr. J. Harold Pardue

LARVAL OYSTER (*CRASSOSTREA VIRGINICA*) SETTLEMENT AND
DISTRIBUTION IN A FRESHWATER-DOMINATED AND HUMAN-
INFLUENCED ESTUARY

A Dissertation

Submitted to the Graduate Faculty of the
University of South Alabama
in partial fulfillment of the
requirements for the degree of

Doctor of Philosophy
in

Marine Science

by
Haley Nicholson Gancel
B. S., University of Miami, 2013
May 2020

I dedicate this dissertation to my parents, Stephanie and Brendon Nicholson, and to my husband Jake.

TABLE OF CONTENTS

Page

LIST OF TABLES

Appendix
Table

xi

LIST OF FIGURES

Appendix
Figure

LIST OF SYMBOLS AND ABBREVIATIONS

1	2015
2	2016
$\Delta\,AIC_c$	Change in Akaike weight
α	Significance level
$\sum$	Sum
A	Adult
Ag	Agriculture
AICc	Akaike information criterion for small sample size
Al	Aluminum
ALC	Alizarin complexone
ANOVA	Analysis of variance
As	Arsenic
B	Boron
Ba	Barium
BBR	Bayou La Batre River
BLB	Bayou La Batre
BLB1	Bayou La Batre1
BLB2	Bayou La Batre2

BLB3	Bayou La Batre3
C	Cold
Ca	Calcium
Cd	Cadmium
Ce	Cerium
CFU	Colony Forming Units
Chl*a*	Chlorophyll *a*
CI	Confidence interval
Co	Cobalt
Cr	Chromium
Cu	Copper
df	Degrees of Freedom
DI	Deionized
DIN	Dissolved inorganic nitrogen
DMSO	Dimethyl sulfoxide
DO	Dissolved oxygen
Dog	Dog River
DON	Dissolved organic nitrogen
DR	Dog River
E	East
EC	*Escherichia coli*
EFR	East Fowl River
EMS	eastern Mississippi Sound

F	Statistical test of significance
Famp	Host *E. coli* resistant to streptomycin and ampicillin
FC	Fecal coliforms
Fe	Iron
FOV	Field of View
fps	Frames per second
FR	Fowl River
GF/F	Glass fiber filter
GLM	General linear model
GPS	Global Positioning System
H	High flow
HSD	Honestly Significant Difference
ICP-MS	Inductively coupled plasma mass spectrometry
L	Low flow
La	Lanthanum
LD	Linear discriminant
LDA	Linear discriminant function analysis
Li	Lithium
m-TEC	Agar for membrane filtration *E. coli* enumeration
MANOVA	Multivariate analysis of variance
MB	Mobile Bay
MB1	Mobile Bay 1

MB2	Mobile Bay2
MB-EMS	Mobile Bay-eastern Mississippi Sound
Me	Metal
Mg	Magnesium
Mn	Manganese
MR	Mobile River
MS	Mean square
MSC	Male-specific coliphage
n	Sample size
N	Nitrogen
N	North
$NaHCO_3$	Sodium bicarbonate
NE	Northeast
nGoM	North-central Gulf of Mexico
NH_4^+	Ammonium
Ni	Nickel
NIST	National Institute of Standards and Technology
NOAA	National Oceanic and Atmospheric Administration
NO_2^-	Nitrite
NO_3^-	Nitrate
NW	Northwest
p	Significance level
P	Phosphorus

Pb	Lead
PFU	Plaque Forming Unit
PO_4^{3-}	Phosphate
PPUI	Fluorescent particle per image
PVC	Polyvinyl chloride
R	River
R^2	Coefficient of determination
S	Settlement
S	South
SE	Standard error
SE	Southeast
Sn	Tin
Sr	Strontium
SW	Southwest
t	Statistical test of significance using student's t-test
t-test	Student's t-test
TC	Tetracycline
TDN	Total dissolved nitrogen
TE	Trace element
Ti	Titanium
TN	Total nitrogen
TNC	The Nature Conservancy

U	Uranium
U.K.	United Kingdom
U.S.	United States
USGS	United States Geological Survey
UV	Ultraviolet
V	Vanadium
VIF	Variance inflation factor
W	Warm
W	West
w	Akaike weights
WFR	West Fowl River
WTP	Wastewater treatment plant
Y	Yttrium
YSI Pro 2030	Yellow Springs Instrument water quality sonde
z	Statistical test of significance using *z* statistic
Zn	Zinc

ABSTRACT

Gancel Nicholson, Haley, Ph.D., University of South Alabama, May, 2020. Larval oyster (*Crassostrea virginica*) settlement and distribution in a freshwater-dominated and human-influenced estuary. Chair of Committee: Ruth H. Carmichael, Ph.D.

In many coastal systems, freshwater inputs influence the physical and chemical environment of estuarine organisms through changes in flow patterns, salinity, and conveyance of wastewater pollution. In areas with harvestable commercial fishery stocks, freshwater inputs may also pose an increasing public health risk. While freshwater-dominated systems exist world-wide, it is poorly understood how these freshwater-driven changes to the environment may act in tandem to affect the ecology of estuarine organisms with larval stages. The objective of this study was to assess the effects of freshwater discharge on the ecology of estuarine species with larval stages, using eastern oysters (*Crassostrea virginica*) and the freshwater-influenced Mobile Bay-eastern Mississippi Sound (MB-EMS) system as models. First, I used an artificial marker, calcein, to directly track oyster larval movements *in situ* to determine larval transport pathways under different freshwater flow regimes. Larvae were transported through dominant flow paths set up by freshwater inputs and winds, with stained larvae recaptured ($n = 2$) during a high salinity release and no larvae recaptured during a low salinity release, when larval number was likely lowered due to poor survival or flushing of larvae out of the system. Data validated a larval transport model and identified model

inputs for refinement to better track larval movements. Second, I used larval oyster settlement patterns and natural tags (trace element ratios in shell) to infer larval movements to corroborate how flows influenced settlement and to determine larval connectivity. Discharge affected connectivity by mediating changes in salinity and temperature, in turn affecting the magnitude, timing, and location of settlement and possible spawning events. During high discharge, settlement throughout the system was 4x lower than during low discharge, and oysters only settled in the higher salinity region, EMS, resulting in lower connectivity between EMS and MB populations. Trace element ratios indicated self-recruitment and connectivity within EMS, confirming observed settlement patterns and suggesting that EMS oysters are important larval sources to this system. Third, I used nutrients and bacterial and viral indicators of sanitary water quality to determine how changes in flows mediated point (wastewater treatment plants [WTPs]) and non-point (measured as riverine discharge) wastewater inputs and their influence on potential downstream oyster settlement sites. Overall, rivers were larger sources of nutrients and indicator microbes compared to WTPs, but seasonal differences in flow changed the relative influence of the two sources. Although discharge simultaneously affected larval life history and wastewater conveyance, oyster settlement was higher where wastewater inputs were lower (higher salinity) due to poorer oyster habitat suitability where wastewater input was higher (lower salinity). These data demonstrate the potential for freshwater discharge to affect species distributions and potential human health risk by mediating larval survival, settlement patterns, and population connectivity and determining when and where a commercially important fishery species may be contaminated by wastewater.

INTRODUCTION

Freshwater discharge can affect the persistence, growth, distribution, and connectivity of estuarine species by changing the physical environment and water quality. Increased discharge can reduce salinity and increase conveyance of nutrients and anthropogenic pollutants (Zuliani et al. 2005; Lane et al. 2007; Paerl et al. 2010). Increasing freshwater inputs in parts of Texas and Florida in the U.S. have resulted in increased benthic macrofauna abundance, including oyster populations, due to more favorable salinities for these species (Montagna and Kalke 1992; Wilber 1992), whereas damming of the Nile River in Africa lowered freshwater inputs and consequently decreased nutrient delivery and fisheries landings (Aleem 1972; Nixon 2003). Excess freshwater input, however, can also lead to mortality of fisheries such as oysters as occurred during Mississippi River flooding in the U.S. in 2011 (Soniat et al. 2012; DeHaan et al. 2012). Due to global changes in precipitation patterns, melting of ice due to warming temperatures, and anthropogenic water diversions, freshwater inputs to coastal systems are expected to change substantially in coming years (Milliman et al. 2008; Dai et al. 2009). Climate change, especially changes in the hydrological cycle (Huntington 2006), may exacerbate changing patterns of freshwater discharge (Vörösmarty et al. 2000), potentially prompting large-scale, but poorly understood, changes to species distributions in estuaries worldwide.

Estuarine organisms with larval life stages may be particularly responsive to changes in freshwater flow regimes that alter the physical, chemical, and biological environment (Skreslet 1986). Freshwater discharge, winds, and tides influence water circulation patterns (Kim and Park 2012), which can influence the distribution, transport, and retention of estuarine larvae (North and Houde 2003; Vargas et al. 2006; Landaeta et al. 2012). For example, Meerhoff et al. (2013) found that the distribution and abundance of larval squat lobster (*Munida gregaria*) was tightly linked to freshwater input and tides driving changes to physical circulation. Other studies have shown that increased freshwater inputs can lower the retention of larvae (*Gilchristella aestuaria*: Strydom et al. 2002), and a combined effect of increased freshwater discharge and wind-mixing can increase larval distributions (*Cancer irroratus*: Roman and Boicourt 1999). Discharge-associated changes to salinity, temperature, turbidity, and food supply can influence larval growth and survival (Kaartvedt and Aksnes 1992; Secor and Houde 1995; Grimes 2001; Landaeta and Castro 2006). Of these factors, salinity is the parameter most directly associated with freshwater discharge, and larval stages of many estuarine species have salinity-dependent growth and survival, making shifting discharge regimes potentially problematic for these species (Richmond and Woodin 1996; Anger 2002). Large-scale increases in freshwater discharge may push suitable salinity habitat farther down-estuary, reducing or altering recruitment and connectivity patterns (Powell et al. 2003; Shoji et al. 2006). Thus, it is important to understand how estuarine organisms with pelagic larval stages respond to fluctuations in freshwater discharge flows that may ultimately influence distribution and growth of adult populations and harvestable stocks.

Larval stages that settle and grow-out in areas affected by nutrient and anthropogenic pollutants delivered via freshwater inputs also may introduce a potential human health risk if adult stages are harvested in areas of poor water quality. Wastewater effluent and wastewater related contaminants are conveyed by freshwater discharge via point (sewage outfalls) and non-point (urban, industrial, and agricultural runoff) sources, potentially complicating the effects of flows on estuarine larval ecology. Wastewater treatment plant (WTP) outfalls deliver nutrients, such as nitrogen and phosphorus, to the estuarine system, affecting estuarine larval organisms by increasing primary production and consequently, food supply (Alexander 1998; Cloern 2001; Nixon and Buckley 2002; Carmichael et al. 2004). Effluent from WTPs can also be a source of bacterial and viral pollution, which can carry microbes that indicate human health risks, periodically prompting closures of harvest areas for shellfish (Calci et al. 1998; Burkhardt and Calci 2000; National Shellfish Sanitation Program 2015). Many management plans for shellfish harvest use riverine discharge as a proxy of microbial load to inform decisions about area closures (Alabama Department of Public Health 2012). Discharge rates, however, may not be the best indicator of human health risks as evidenced by the many shellfish-borne viral illnesses, 58.4% involving oyster consumption (Bellou et al. 2013), still occurring globally each year (Butt et al. 2004; Scallan et al. 2011). More study is warranted to understand differences in microbial load under high and low freshwater discharge, effects on nearby fisheries, and implications for human health risks.

Oysters, such as the eastern oyster (*Crassostrea virginica*), are good model organisms to study the influence of changing flow regimes on estuarine larval species. During planktonic larval stages, oysters are influenced by water flow, which is mediated

by freshwater discharge, winds, and tides. Following the 2–3 week larval stage, oysters settle onto substrate and are termed "spat" (Galtsoff 1964), and remain at settlement sites throughout their adult life. As oysters grow during planktonic and settled stages, they incorporate elements from the surrounding environment into tissues and shell, with growth and survival mediated by environmental conditions (Surge et al. 2003). Settled oysters form biologically and commercially important reefs in the estuarine environment, providing many ecosystem services, such as improving water quality by reducing particle loads and providing habitat for other organisms (Nelson et al. 2004; Newell, Fisher et al. 2005; Lenihan et al. 2001; Gutiérrez et al. 2003). Oyster landings (a proxy for oyster abundance) are generally inversely related to freshwater discharge (Turner 2006), but sustained periods of high or low freshwater discharge can depress oyster populations (Wilber 1992; Powell et al. 2003; Soniat et al. 2013). Furthermore, water quality declines and wastewater inputs from freshwater flows affect oyster harvesting activities in many regions globally (reviewed in Wetz and Yoskowitz 2013), making oysters useful sentinels of ecosystem level effects of freshwater discharge and associated changes in water quality.

North-central Gulf of Mexico (nGoM) estuaries are among the most freshwater-influenced estuaries in the world and are good model systems to study how changing freshwater inputs affect the ecology of estuarine organisms. North-central Gulf of Mexico estuaries have among the most productive fisheries and the highest native eastern oyster harvest in the world (O'Bannon 2001; Beck et al. 2011). Furthermore, many of these freshwater-influenced estuaries range from incipiently to highly altered by urbanization and industrial activities that may further affect freshwater flow regimes,

wastewater inputs, water quality, fisheries, and local ecology (Kirby 2004; Darrow 2015). Mobile Bay, AL, for example, has the highest freshwater inflow per estuary area out of all U.S. estuaries (Ward 1980) and is home to one of the few remaining harvestable oyster populations in the U.S. (Zu Ermgassen et al. 2012). In the nGoM, oyster populations are declining due to overfishing, habitat destruction, and nutrient loading, and in 2019 the Alabama oyster harvesting season was closed for the first time since the inception of commercial oyster harvesting in Mobile Bay in 1880 (Gulf States Marine Fisheries Commission 2012; Specker 2019). Furthermore, freshwater discharge to nGoM estuaries is potentially increasing as evidenced by the longest continuous opening of the Bonnet Carré spillway, a freshwater diversion located in LA, during 2019 (Snell 2019). Therefore, it is imperative to understand the interacting effects of freshwater discharge on oyster ecology of the nGoM to understand current and prevent future declines of oysters and other species with larval life stages.

To better understand how freshwater affects oyster ecology in terms of larval movement, retention, and connectivity within a system, traditional ecological observations can be combined with new data from artificial and natural biomarkers and transport modeling. Artificial markers, such as chemical dyes, can be used to directly track larval species and trace the influence of freshwater on larvae by defining larval transport pathways (Pineda et al. 2007). Calcein is a fluorescent marker that can be used to tag individual larva and show how larval stages move in response to changes in the estuarine environment (Day et al. 1995; Kaehler and McQuaid 1999; Linard et al. 2011; van der Geest et al. 2011; Fitzpatrick et al. 2013). Use of calcein as a method of direct tracking by mark-recapture has the advantage of following a cohort of known origin to a

recapture location and can explicitly define net larval dispersal. Such direct tracking methods provide information on how larval transport pathways may change under different flow conditions, and these data can be compared to available numerical transport models to test confluence of larvae and major flow pathways, with additional benefit of validating model outputs. Natural geochemical tags (trace element [TE] ratios) can be similarly used to infer larval connectivity by predicting the exchange of larvae from geographically separated subpopulations (Cowen et al. 2007; Cowen and Sponaugle 2009). Trace element ratios are derived from the physical and chemical environment and can be used to determine larval origins, define dispersal, and infer population connectivity by comparing the larval TE signatures to natal site-specific TE reference signatures (Thorrold et al. 2002; Becker et al. 2005). The ability to define location-specific variation in TE ratios is of particular interest in freshwater-dominated systems where large-scale mixing may occur, complicating larval dispersal processes and the understanding of population connectivity. This combination of tracers has not been tested *in situ* in freshwater-dominated systems to determine their utility to assess the effects of freshwater discharge on the ecology of oysters or other estuarine species with larval stages.

Thus, the three main objectives of my study were to: 1) use the artificial marker, calcein, to track larval movements *in situ* and validate larval transport pathways under different freshwater flow regimes in the Mobile Bay-eastern Mississippi Sound (MB-EMS) system, 2) use natural tags (TE ratios) and larval oyster settlement patterns to determine how freshwater inputs influence connectivity of oyster populations, and 3) determine the relative contribution and downstream influences of point (WTP outfalls)

6

and non-point (river discharges that represent a combination of different non-point sources; United States Environmental Protection Agency: epa.gov/nps/basic-information-about-nonpoint-source-nps-pollution; last accessed 2 March 2020) wastewater sources in different subsystems of the MB-EMS system, where a paired high flow WTP and river (high flow subsystem) could be compared to a paired low flow WTP and river (low flow subsystem). Determining how changes in freshwater flows influence the physical and chemical environment and in turn mediate factors crucial to larval survival, growth, transport, and settlement is imperative to understand spatial and temporal scales of larval connectivity. These data provide insight into how larvae respond to pulsed or chronic flow events and how these events influence changes in population dynamics or exposure to water-borne contaminants through time. These data can help sustain harvestable marine populations for species with larval stages and understand potential human health risks in freshwater-influenced estuaries worldwide.

CHAPTER 1

FIELD MARK-RECAPTURE OF CALCEIN-STAINED LARVAL OYSTERS (*CRASSOSTREA VIRGINICA*) IN A FRESHWATER-DOMINATED ESTUARY

Abstract

Knowledge of larval transport is important for restoration and management efforts, yet there are no established methods to determine larval transport *in situ*. Calcein staining of oyster larvae may help fill this void, and a two-part study was conducted to determine its effectiveness at tracking larval oyster transport in the field. First, it was tested whether oysters could be successfully stained, survive, and grow at estuarine salinities (15, 20, 26), and at sufficiently large numbers (millions of oysters) to support field mark-recapture studies. Second, the field-based application was tested by releasing 22 million stained larvae twice (high and low salinity) into a major estuary, and two methods (fluorescent microscopy and FlowCam) were used to detect recaptured larvae. Results were compared with expected larval movement patterns simulated by an existing larval transport model. Calcein concentrations (100 mg L^{-1}) did not affect larval growth or survival, but handling conditions (water salinity manipulations and tank size) did affect growth and survival during the post-staining period. Microscopy had double the detection capacity, but FlowCam was more practical and time efficient for the large-

volume, high particulate load field samples. Larvae ($n = 2$) were recaptured during the second, higher salinity release, and model comparison showed a 1–2 day time-lag between field recapture and model predictions, suggesting need for model refinement. Calcein has potential to be a useful marker to track larval movement at large-scales needed for field-based studies, providing critical information to aid in selection of restoration sites and management of commercially important shellfish species.

Introduction

To better manage populations with pelagic larval stages, knowledge of larval transport is important to help identify larval sources and understand connectivity and population dynamics (Levin 2006). Yet, larval transport is difficult to trace and quantify due to the small size of larvae, and the coupled bio-physical larval transport models typically used to determine larval transport are rarely field validated (Pineda et al. 2007). Field validation can include indirect and direct larval tracking efforts. Indirect tracking has been attempted using genetics (Gilg and Hillbish 2003; Taylor and Hellberg 2003; Galindo et al. 2010) and chemical tracers such as trace elements (DiBacco and Levin 2000; Zacherl et al. 2003; Becker et al. 2007; Kroll et al. 2016). These approaches have significant uncertainty among locations (Thorrold et al. 2002), making interpretation of larval dispersal difficult. Direct tracking by mark-recapture (i.e., marking a subset of the population and recapturing individuals) has the advantage of following a cohort of known origin to a recapture or settlement location and explicitly defining net larval dispersal. Mark-recapture, therefore, is a viable option to validate bio-physical models, assess larval dispersal, retention, and restoration efforts. This approach has not been widely used for

larvae, however, due to the difficulty of recapturing microscopic organisms in the field, where systems are affected by advection and high larval mortality (Levin 2006) and thereby potentially reducing the recapture yield and increasing the uncertainty. Hence, there is demand for development of field-viable mark-recapture methods for larvae (Levin 1990; Rumrill 1990).

While challenging, development of mark-recapture suitable field methods should be achievable. To be effective, mark-recapture methods require a mark that meets four criteria: 1) retained for an appropriate amount of time, 2) does not increase predation nor affect growth and/or survival, 3) cost-effective, and 4) readily detectable at recapture (Ricker 1956; Thorrold et al. 2002). Calcein is a fluorescent chemical marker that may be particularly useful for mark-recapture studies. Calcein can mark large cohorts in a short period of time (mussel and scallop: Moran and Marko 2005; Fitzpatrick et al. 2013), has a mark incorporation of 100% into calcified tissues (mussel and oyster: Kaehler and McQuaid 1999; Linard et al. 2011), is long lasting in the field (fish and limpet: Wilson et al. 1987; Clarke et al. 2004), does not affect standard activity/health metrics (predation by corals on planktonic invertebrates: Johnson and Shanks 2003), and does not increase predation in the field (fluoresces from a narrow range of blue light, 492–496 nm: Moran and Marko 2005). Currently, the major applications of calcein as a marker in bivalves have been for development of methods to mass-mark larvae without testing recapture success (Fitzpatrick et al. 2013; Stańczak et al. 2015; Chalupnicki et al. 2016) or for growth studies (Kaehler and McQuaid 1999; van der Geest et al. 2011; Andresen et al. 2013), but more study is needed to determine if calcein meets the core criteria to be an

effective mark-recapture method. Detection of calcein-marked larvae in large sample collections, with low recapture potential in each sample is also unknown.

Bivalves, such as the eastern oyster (*Crassostrea virginica*), are well-suited for mark-recapture studies. Oysters are commercially, ecologically, and biogeochemically important and hatchery-reared, making larvae readily available for laboratory marking and subsequent field release. There is high interest for understanding larval transport of commercially important species for restoration and management efforts (Fogarty and Botsford 2007), for which larval transport models have been developed and employed (e.g., Kim et al. 2010; Spires 2015). While methods for staining bivalve larvae with calcein have been largely developed and refined in the laboratory, these protocols have not considered salinity or holding conditions (Fitzpatrick et al. 2013; Moran and Marko 2005), which may be important for large-scale estuarine field applications. For example, bivalves inhabit dynamic habitats often dominated by large salinity fluctuations due to freshwater inputs (Pollack et al. 2011), and as a result, mark-recapture studies should examine a range of salinities to inform field applications by increasing larval survival and recapture success. Holding conditions (e.g., stocking density and salinity) and tank type (e.g., size and shape) may also be important considerations for marking the larger number of larvae needed for practicable field release, but it is unknown how holding conditions affect the staining process to affect overall survival, growth, and staining success. For broader use and application, more study is needed to determine the effectiveness of staining under representative field conditions where larvae occur.

I conducted a large-scale field-based study to refine calcein marking and detection methods, in which I measured growth and survival of calcein-stained oyster larvae at

different salinities common to oyster growing areas and in different holding tank characteristics for pre-release salinity acclimation. In addition, calcein detection methods were tested using a fluorescent microscope and FlowCam®VS series to determine the most efficient and accurate method for detection of calcein-stained larvae from field samples. Lastly, as a proof-of-concept to determine if calcein mark-recapture has potential for field-validation of a three-dimensional bio-physical oyster larval transport model (Kim et al. 2010; Kim and Park 2012) and to determine if larvae are transported through water trajectories set up in part by freshwater discharge, I released the calcein-stained oyster larvae into model-predicted dominant flow paths in the Mobile Bay-eastern Mississippi Sound system on the north-central Gulf of Mexico coast during low and high discharge conditions, which corresponded to a high and low salinity period. Sites along the flow path were sampled for marked larvae at 1, 2, 3, and 5 days after release and stained larvae were detected by both tested methods.

Methods

Calcein marking methods

Staining oyster larvae.

To test calcein marking methods, 3-day old veliger-stage oysters (*Crassostrea virginica*), reared at the Auburn University Shellfish Laboratory on Dauphin Island, AL, were held under low light conditions (Linard et al. 2011) in a 100 mg L^{-1} calcein solution (Fitzpatrick et al. 2013) for 48 hours. To encourage feeding and assimilation of calcein into shell, larvae were batch fed Shellfish Diet 1800™ (Reed Mariculture) twice daily

12

according to Rikard and Walton (2010), and the holding tank water was not changed during the staining process. Calcein powder (Fisher Scientific #NC0659213) was dissolved in 1 µm (pleated filter cartridge) filtered Gulf of Mexico seawater (salinity 23) according to Thébault et al. (2006), using one of two dissolution methods, depending on the volume of calcein required for each experiment.

For salinity treatments in which 1.7 million larvae were stained (detailed below), 13 g of calcein were dissolved in three 1-L batches. Each 1-L batch dissolved 4.3 g calcein L^{-1} over 24-hours while mixing on stir plates at 400 rpm. Because calcein is acidic, $NaHCO_3$ was progressively added (0.4 $NaHCO_3$ g per 1 g calcein) during the 24-hour mixing period to increase the pH to 7 and increase the solubility of calcein (Wilson et al. 1987; Fitzpatrick et al. 2013). Five hundred mL of stock solution was added to 9.5 L of 1 µm filtered seawater, to a final volume of 10 L and a final calcein concentration of 100 mg L^{-1} (used in all treatments). For holding tank treatments and field testing in which 35 million larvae were stained, a higher volume of calcein solution was needed (250 g in 2500 L of seawater), which required the calcein solution to be super-concentrated before adding solution to the holding tank. To make this solution, 62.5 g calcein L^{-1} were dissolved in four 1-L batches with the addition of 25 g $NaHCO_3$ on stir plates for 24 hours.

Salinity treatments.

To determine the effect of salinity on growth and survival of larvae during the calcein staining and post-staining, 3-day old veliger-stage larvae were stained and unstained at 3 salinity levels (15, 20, 26) with each treatment in duplicate. An unstained hatchery control was included to determine the effect of treatment water alone on larval

growth and survival, which resulted in a total of 13 treatments. Salinity treatments were

made by mixing 1 µm filtered Gulf of Mexico seawater with Instant Ocean® (to increase

salinity) or Deionized (DI) water (to decrease salinity), except hatchery control water,

which used unaltered filtered Gulf of Mexico seawater (salinity of 24–29). The staining

period was defined as the 48-hour calcein immersion time (3-day to 5-day old larvae),

and the post-staining period was defined as post-immersion until death or experiment

termination (5–20+ day old larvae). Treatments for the salinity experiment were done in

18.9 L (36.8 [height] $\times$ 29.8 [diameter] cm) round plastic buckets filled to 10 L at a

stocking density of 13 larvae mL^{-1}. Total water changes occurred every two days.

To further determine effects, if any, of water manipulation (addition of Instant

Ocean® or DI water) on larval growth during the salinity treatments, larval size was

compared to the salinity offset (difference in salinity units between hatchery control

water and target salinity: 15, 20, 26) for each treatment. Due to salinity fluctuations in

the hatchery control water, additions of Instant Ocean® or DI water were not the same

during each water change, and therefore the offset salinity varied for each water change.

A positive or negative offset reflects the addition of Instant Ocean® or DI water,

respectively. For example, an offset of -4 would occur when the hatchery control water

was 24 and DI water was added to achieve the salinity treatment of 20. The average

offset salinity was -6.8 for Instant Ocean® and 2.0 for DI water.

Holding tank effects.

To determine the potential effects of tank size on larval oyster growth and

survival post-staining and prior to field-release, larvae were grown out in two different

tank types following staining. First, 35 million 3-day old larvae were stained in 4000 L

round hatchery fiberglass tanks (246.4 [height] × 91.4 [diameter] cm) filled to 2500 L at a stocking density of 14 larvae mL^{-1}. Second, larvae were given a 24-hour recovery period post-staining in hatchery tanks filled to 3500 L with fresh 1 µm filtered ambient seawater at a stocking density of 5 larvae mL^{-1} before being left to grow out (post-staining period) in either: a) 1000 L round hatchery tanks (139.7 [height] × 91.4 [diameter] cm) or b) 37.6 L rectangular aquaria (32.1 [height] × 51.4 [length] × 26.7 [width] cm). Tank effects were tested at two salinity levels (15, 26). During the post-staining period, larvae were allowed to grow to settlement size to test longer-term survival. To accommodate settlement, 17 × 17 cm HardieBacker® Cement Boards were suspended in tanks with fishing line attached to a PVC pipe above the tanks. All tanks were held at an ambient temperature of 27–29°C and air stones were used for water circulation purposes.

Measuring growth and survival.

Size (maximum linear dimension) and counts of larvae were recorded every two days during water changes. Water from each bucket was decanted through a 70 µm sieve down to 1000 mL of water immediately after the staining period (at 48 hours) and 500 mL of water during the post-staining period (≥2 days) to concentrate larvae for counting. A smaller volume of water was needed following the post-staining period to accommodate the lower sample density due to mortality. Ten (at 48 hours) or five (≥2 days) 200 µL samples were collected and analyzed using a Sedgewick Rafter Counter slide on an Olympus BH-2 compound microscope (size: 10X magnification; counts: 5X magnification) equipped with an ocular scale bar under regular light. All live and dead larvae were counted and sizes of 10 haphazardly selected larvae were measured per 200 µL. Survival was only calculated immediately after the staining period (at 48 hours)

because dead larvae could not be excluded through sieving (70 µm), thus survivorship would be biased. For holding tank experiments, spat height was additionally measured with a SteREO Discovery V12 Zeiss microscope with AxioVision 4.6 software.

Calcein detection

Microscope vs. FlowCam.

To compare detection methods for stained larvae, immediately after the staining process (at 48 hours) a subsample of larvae from each treatment was preserved in 10% buffered formalin (which does not degrade the calcein mark: Bernhard et al. 2004) at an estimated concentration of 20–100 larvae mL^{-1}. To determine the estimated concentration in each preserved subsample, ten 200 µL samples were counted as described above, and an average count per mL was determined. Twenty-five mL was collected from the concentrated bucket sample (1000 mL) while continuously homogenizing using gentle stirring. To quantify detection, stained larvae were counted with an Olympus BH2-RFCA fluorescent microscope with FITC filter sets (λ_{ex} 470 nm; λ_{em} 509 nm) and using a FlowCam®VS series (Fluid Imaging Technologies Inc.) equipped with a blue laser (λ_{ex} 488 nm) and red/green filter (λ_{em} 525 ± 15 nm bandpass, and long-pass 650 nm). Results were compared to determine if the microscope or FlowCam was better for detecting stained oyster larvae. Before analyzing samples, a sample of non-stained larvae taken from the hatchery was tested with the FlowCam laser to ensure larvae did not autofluoresce. A handheld fluorescent light (SE-Mark™ Detector) was also tested as a possible method for manual quantification of stained larvae but was determined to not be a viable detection method because it could not be used in conjunction with a microscope.

Microscope and FlowCam settings.

       An Olympus BH2-RFCA fluorescent microscope, with a 10X objective was used

to analyze stained and unstained larvae. Stained larvae were analyzed under the FITC

filter sets and unstained larvae under regular transmitted light. The Field of View (FOV)

flow cell was used with a 2X objective to use the FlowCam for counts and image a large

sample volume. Trigger mode was used with stained larvae at a flow rate of 10 mL min^{-1}

with 13 frames per second (fps), which resulted in no double-imaging (common if flow

rate and fps are out of balance). Threshold for Trigger mode was set to 400 (default

settings) for all larval samples. After extended use, the threshold had to be lowered to

100 to detect stained larvae. When thresholds were met in either channel 1 (>650 nm

long-pass) or channel 2 (525 ± 15 nm bandpass) the field of view was imaged. In scatter

mode, the laser was continuously operating and any particle which scattered the laser was

imaged; in this mode, the fluorescence associated with each particle can also be recorded.

Channel 2 and scatter were used in trigger mode set to a threshold of 100. AutoImage

flow rate, used with non-stained larvae, was 8 mL min^{-1} with 19 fps. Stained larval

samples for salinity experiments were diluted with 25 mL of ultrapure water before

detection was tested on the FlowCam to decrease algal background and ensure one

fluorescent particle per image (PPUI) (Álvarez et al. 2011). Due to the different

orientation that the FlowCam can image larvae (Buskey and Hyatt 2006; Jakobsen and

Carstensen 2011), larvae were counted manually by visual inspection of FlowCam image

collages. The FOV flow cell was flushed three times (15.5 mL syringe) in between each

sample to ensure carry-over was insignificant.

Field mark-recapture and model simulations

To determine if calcein mark-recapture has potential for use in field studies I released and recaptured calcein-stained oyster larvae into the Mobile Bay-eastern Mississippi Sound system on the north-central Gulf of Mexico coast and compared the results to outputs from an existing oyster larval transport model (Kim et al. 2010). Calcein-stained 6-day old oyster larvae were released at two sites (1 and 2 in Fig. 1) in Mobile Bay along previously established model-predicted dominant larval flow paths (Kim et al. 2010) during ebb tide to maximize spatial distribution of released larvae. Larvae were stained and released twice in 2014 under lower and higher discharge conditions, that corresponded to higher and lower salinity release conditions. The first release on May 19 had a staining salinity of 15 and a release salinity of 5, and the second release on July 28 had a staining salinity of 26 and a release salinity of 21. For each release, 22 million larvae were released at the two sites (11 million per site), resulting in the overall release of 44 million larvae.

To recapture larvae, samples were taken using a 10 L Niskin sampler on days 1, 2, 3, and 5 after release at sites 1–4, which represent a range of expected larval concentrations based on model predictions (Kim et al. 2010). Niskin samples were chosen as the most efficient sampling method to capture location-specific samples during discrete time periods and validate the existing larval transport model. Two Niskin samples were taken vertically from 1 m above the bottom to the surface at each site to get a snapshot water column profile of bivalve abundance, sieved through a 150 and 420 µm sieve set (resulting in 150–419 µm and ≥420 µm samples), preserved in 10% buffered formalin (final volume: 250 mL), and stored in the dark. To detect stained and unstained

18

larvae in my high particulate background, high volume field samples, where recapture was expected to be low, I opted to use the FlowCam®VS series (parameters indicated above) because whole samples could be relatively quickly imaged. Salinity measurements were taken in the field with a YSI Pro 2030 handheld data probe.

I used an existing larval transport model (Kim et al. 2010) to simulate transport and distribution of the released stained larvae. Model simulations were conducted with physical transport processes only and with physical and biological movement (swimming and settling) of larvae. Both model runs were forced with the observed conditions for upriver freshwater discharge, surface wind, and water level along the open boundary for May and July releases. The simulated model results were compared with the observed salinity and recaptured stained larvae.

Statistical analyses

For the salinity treatments performed in round buckets, a *t*-test was used to determine that replicate treatments were not different. A general linear model was used with salinity (15, 20, 26), staining (stained, unstained) and time (i.e., duration of the experiment) (continuous variable) to determine if staining and/or salinity had an effect on larval size (maximum linear dimension). A two-way ANOVA with salinity (15, 20, 26) and staining (stained, unstained) determined if staining and/or salinity had an effect on larval survival immediately after the staining period. A one-way ANOVA with offset as the factor (3 levels: -6.8, 0, 2.0) determined the effect of water manipulation (addition of Instant Ocean® or DI water) on larval size. Tukey HSD multiple comparisons followed ANOVA runs to determine which combinations of the levels were significant. A

regression on log transformed data determined how larval size changed through time during the holding tank experiment in 1000 L hatchery tanks.

For calcein detection experiments, linear regressions were run with expected number of larvae as the independent variable and observed number of larvae as the dependent variable to determine if the microscope or FlowCam had better detection of calcein-stained larvae. Homogeneity of slopes tested if the regressions for the expected and observed microscope and FlowCam larval counts were different. Residuals ±2 were considered outliers and were removed from further analyses. A *t*-test determined if there was a difference between microscope and FlowCam detection for expected versus observed larvae. Normality and homogeneity of variances were tested to ensure assumptions of ANOVAs, regressions, and *t*-tests were met and an α of 0.05 was used for all tests. ANOVAs and regressions were conducted in XLSTAT Base version 19.6. and the general linear model (*MASS* R package: Venables and Ripley 2002) was conducted in RStudio Version 1.1.453 (R Core Team 2017). Error is presented as standard error.

Results

Calcein marking methods

Salinity treatments.

During the staining and post standing period, staining and salinity did not have a significant effect on larval size (salinity: $F_{2,45} = 0.001$, $p = 0.97$; staining: $F_{1,45} = 0.02$, $p = 0.88$), and larvae did not have significant growth during post staining (time: $F_{1,45} = 2.90$, $p = 0.10$). Salinity and staining did not have a significant effect on larval survival ($F_{3,8} =$

0.85, $p = 0.50$) during the staining period, and survival was variable among treatments (Table 1).

Manipulation of salinity, however, did affect larval size ($F_{2,25} = 17.08$, $p < 0.0001$) (Fig. 2a), such that larvae in salinity treatments using ambient water were significantly larger (108 ± 4 µm) than treatments modified using either DI water (83 ± 2 µm) or Instant Ocean® (79 ± 4 µm) (Tukey's HSD: $p < 0.001$ for all significant comparisons).

Holding tank effects.

Tank size had an effect on larval growth and survival during the post-staining process. Larvae in 1000 L conical hatchery tanks showed faster growth and better survival than those in smaller 37.6 L rectangular aquaria. The larval size at day 20 for the hatchery tanks was 480 ± 26 µm, while size at day 20 for the aquaria larvae were 170 ± 2 µm. Larvae in post-staining aquaria survived for 20 days and thus were not able to reach settlement size (~300 µm). Larvae in post-staining hatchery tanks lived until day 42 when the experiment was terminated, set on settlement plates, and continued to grow at an exponential rate to a maximum length of 22.5 mm ($F_{reg1,9} = 65.86$, $p < 0.001$) (Fig. 2b).

Calcein detection

Neither the microscope nor FlowCam enabled 100% detection of stained larvae. The microscope detected a greater proportion of larvae (73.3 ± 3.6%) compared to the FlowCam (31.2 ± 3.9%) (Fig. 3; $t = 2.09$, $p = 0.002$). The microscopy method was also less variable, with detection efficiency ranging from 58 to 98% among samples. FlowCam detection ranged from 16 to 57% (data not shown), suggesting both methods

have nearly equal variance, but manual microscopy was more efficient overall ($t = 2.09$, $p = 0.002$) (Fig. 3). However, the FlowCam had a throughput advantage, being capable of analyzing two orders of magnitude more sample (e.g., 250 mL) than the microscope (e.g., 1 mL).

Field mark-recapture and model simulations

Two stained larvae were recaptured at site 4, farthest west in eastern Mississippi Sound, with each at 2 and 5 days after the second release in July. Stained-released and wild stock (naturally occurring) larvae were found in the 150–419 µm size class Niskin samples. Recovered stained larvae were 190 and 220 µm, respectively (Fig. A1), consistent with the expected size range for larvae at this age (8 and 11 days; Rikard and Walton 2010). Naturally occurring, unstained larvae were also captured following the second release, with 2–4 larvae captured every day at site 4 and one larva captured at site 3 on day 3 (Table A1). A lower abundance of larvae (three naturally occurring larvae and no stained larvae) were captured during the first release (May 19). Overall, larvae (stained and naturally occurring) found in Niskin samples at sampling locations were most abundant at site 4 during the second field release on July 28 (Table A1). Hence, subsequent comparisons to model simulations of larval flow patterns were only made for the second release (Fig. 4).

The model results based on physical transport alone (Fig. 4a) showed that it should take 3 to 5 days for larvae to move from the release sites to the area near site 4 during the second release, while the stained larvae were recaptured on days 2 and 5, indicating a time lag of 1–2 days between data and the model. When the model was run to additionally include biological movement of larvae (swimming and settling) (Fig. 4b),

22

there was still a time lag of 1–2 days. Inclusion of biological movement, however,

resulted in higher larval concentration, particularly in the southern part of the borderline

between Mobile Bay and eastern Mississippi Sound (Fig. 4b). However, there was no

sampling site in this area and the model results indicated the possibility of about two

larvae in the area. The modeled salinity agreed well with salinity observed in the field

during the sampling period (Fig. 4c; Table A1).

   Differences in freshwater discharge and wind resulted in different modeled flow

patterns between the two releases (Fig. A2). River discharges were higher during the first

release (900–2000 m^3 s^{-1}) than those during the second release (300–500 m^3 s^{-1}). Winds

also were stronger during the second release (maximum of 15 m s^{-1}) than those during the

first release (maximum of 5 m s^{-1}). During the second release, strong south winds

prevailed on the first day after release, switched to northeast winds on the second and

third days, and then died down.

Discussion

Calcein marking methods

   Oysters were successfully calcein marked using methods similar to those used for

other species and under salinity conditions typical to native habitat for oysters, showing

promise for field application. A calcein concentration of 100 mg L^{-1} was adequate to

stain oyster larvae, consistent with the previous studies for other mollusk larval species,

e.g., *Perna canaliculus* (Fitzpatrick et al. 2013), *Nucella ostrina* (Moran 2000), and

Haliotis rubra (Chick 2010), and the calcein concentration could be prepared using lower

or super concentrated dissolution methods. Calcein staining and salinity did not affect larval growth, but growth after staining was influenced by water salinity manipulations and tank type. Lower growth in the treatments using Instant Ocean® and DI water suggests that staining in ambient water near the salinity of release locations is preferable. Potentially, the use of DI water in salinity manipulations (including Instant Ocean® that was mixed with DI water) diluted dissolve organic nitrogen, a known food source of larvae, which in turn decreased available food for larvae compared to the unaltered hatchery control (Manahan and Crisp 1982). If salinity manipulations are needed, as may be the case for controlled laboratory experiments, reducing salinity (e.g., adding DI water) is likely a superior approach to adding Instant Ocean®, which has also been observed to negatively affect bivalve growth in culture (Scott Rikard, personal communication; Supan 2014). Some variation in survival among treatments was likely due to high stocking density used in calcein staining (13 larvae mL^{-1}). Stocking densities between 4–10 larvae mL^{-1} are typical for culture applications (Utting and Spencer 1991; Reiner 2011). Also, other bivalve larval calcein staining studies have found survival rates of 75 to 98% (higher than this study) when a 1 larva mL^{-1} stocking density was used (Fitzpatrick et al. 2013). Overall, growth and survival differences were not attributable to the staining process, indicating that my calcein staining protocol was effective for eastern oyster larvae at a range of typical estuarine salinities and making this study the first to demonstrate effective calcein marking of *Crassostrea virginica* larvae for estuarine applications.

Holding tanks had a significant effect on oyster size and survival, but only during the post-staining process and when held for longer periods (>20 days), which would not

24

be relevant to field applications where larvae would be released within 3 days. Better

long-term larval growth, survival, and settlement was observed in larvae grown out in

1000 L hatchery tanks compared to smaller aquaria, which reinforces the utility of typical

(>946 L) fiberglass or polyethylene tanks used in larval rearing (Wallace et al. 2008;

Supan 2014), which allow lower stocking densities and lower surface area to volume

ratios, and thus better grow-out conditions (Supan 2014). Conversely, tank type did not

affect oyster growth and survival during the staining period, which is likely due to larvae

being held for only 48 hours in their respective holding tanks (buckets or hatchery tanks).

These results demonstrate that larvae can be stained in any tank suitably sized for a given

target density during the 48-hour staining period, prior to transfer into larger tanks post-

staining to ensure longer-term growth and survival. Hence, tank type used in calcein

studies with oyster larvae can be selected based on logistics and to meet the minimum

requirements for most suitable densities (I recommend <13 larvae mL^{-1}).

Calcein detection

The manual fluorescent microscope and the FlowCam have strengths and

weaknesses that potentially affect their usefulness for particular applications. The

manual microscope method, on average, had twice the detection efficiency, similar to

results in Kydd et al. (2018); however, its use was limited for conditions with high

particulate background and large sample volume (i.e., the conditions for which FlowCam

is superior). Despite lower detection capability, I recommend the FlowCam to validate

larval movements in the field because validation studies do not rely on accurate

abundance of recaptured larvae, but rather, relative abundance of larvae recaptured

among sites (Álvarez et al. 2014; Kydd et al. 2018). Hence, the tradeoff in accuracy

(microscope) for increased throughput (FlowCam) can be highly worthwhile to increase

capacity for quickly analyzing large sample volumes (200 times faster for 250 mL field

samples) and reduce error associated with prolonged processing time (e.g., loss of

fluorescence, researcher fatigue: First and Drake 2012). Furthermore, FlowCam allows

for site-specific improvements to detection based on background conditions in local

waters by developing and optimizing image libraries of stained oysters under a variety of

orientations (e.g., Fig. A1) to more reliably identify particles of interest based on the

metrics for each image library. Such development has potential to speed up post-

processing and increase the utility of FlowCam in estimating larval abundance for longer-

term studies.

While this study found lower detection of larvae on the FlowCam compared to

traditional microscopy, my findings also suggest that detection can be refined for future

applications. Using a shallower flow cell (<2 mm) and higher magnification (>2X

objective) may improve detection and image resolution (Ide et al. 2008; Fig. A1).

Increased fluorescence level (i.e., calcein concentration) has also been shown to improve

detection by producing brighter marks in stained scallop (150-500 mg L^{-1}: Crocker et al.

1998) and mussel larvae (200 mg L^{-1}: Fitzpatrick et al. 2013). Higher calcein

concentrations would need to be tested with eastern oyster larvae to determine mortality

and growth effects, but my findings suggest higher dosing is possible. Further study is

also needed to explore the effects of preservation methods (e.g., formalin vs.

glutaraldehyde) on fluorescence when using FlowCam applications. Lastly, I found that

extended use of the FlowCam by multiple users with distinctly adjusted settings added

time and complexity to the analysis that may be avoided with a dedicated instrument.

These considerations may improve detection of calcein-stained larvae or other similarly sized particles and increase the utility of FlowCam (especially for application on new and improved models) for a variety of mark-recapture studies in the future.

Field mark-recapture and model simulations

Larval transport encompasses physical transport (i.e., advection and diffusion) and biological processes (i.e., larval behavior) (Pineda et al. 2007), and knowledge of transport is important to effectively manage species with pelagic life stages. To date, there have been only two successful mark-recapture studies of free-released pelagic bivalve larvae (Millar 1961; Crocker 1998), with the latter the only one using calcein (Table 2). This study using calcein-stained eastern oyster larvae free-released in the field is currently the largest scale (~40 km) mark-recapture experiment. Recovery of two oyster larvae over a large release area in a freshwater-dominated estuarine system is a major advance in demonstrating that calcein-based mark-recapture studies have potential to be used to track movements of larvae for any species in the future. Applications of this approach, particularly for commercial species, extend broadly from model validation to assessment of propagation and restoration efforts.

This mark-recapture field validation study found larval oysters at sites predicted by an existing flow model, with a 1–2 day time lag between model and field data. The lag was present for model simulations regardless of the inclusion of biological movement (swimming and settling). Oyster larval transport and distribution are influenced by many biological and physical processes. Variation in transport patterns, salinity, DO, physiological tolerance, presence of competition and predators, and larval abundance may result in dramatic changes in transport and settlement intensity within a small spatial

27

and short time scale (reviewed by Kennedy 1996). While a model does not yet exist to include all of these complex and interacting processes, the model I validated is based on necessarily simplified biological conditions. For example, the model assumes a constant linear growth rate and no mortality of oyster larvae. Such simplifications may account for the time lag between model and recapture data. Additional study is required to determine the biological factors that are most important for model parameterizing in the future. If flow pathways are well-defined, future model validation studies could release larvae from a single location to more precisely define potential time-lags between expected and actual locations of larvae following release. The presence of stained and naturally produced larvae in higher numbers at sampling sites indicated by the model, demonstrate the effectiveness of the model to simulate larval transport and the utility of calcein staining to help validate model outputs.

While detection of marked larvae was low during this study, my findings were not unexpected given the constraints typical to large-scale natural mark-recapture experiments. The recapture of two larvae during the second, lower discharge and higher salinity release (July 28) represents a recapture success of 0.000009%. Although this number is low, recapture of two 8–10 day old larvae at ~200 μm size, using two 10-L Niskin samples (i.e., 0.66% of the volume of a $1 \text{ m}^2 \times 3$ m water column) is a promising success in the field of mark-recapture techniques. The ~30% detection rate for FlowCam in the lab studies suggests 4–5 additional larvae could have been present in the samples where larvae were detected (suggesting a best expected recovery rate of ~0.00002%). Most mark-recapture studies have been done with larger organisms such as juvenile and adult fish, 700 to 2000 times larger than bivalve larvae. Mark-recapture success of

28

invertebrate larvae and larger fish larvae free-released in the field has been much <1%

(Table 2). It also should be noted that most previous studies were conducted in rivers,

inlets, or other sheltered areas and used plankton tows, from which recapture success

should be higher. In contrast, I released larvae into a dynamic freshwater-dominated

estuarine system, where larval loss due to advection was likely higher compared to

sheltered systems. For example, although release and recapture sites were selected based

on previous model runs, during the first release oysters were likely lost due to salinity-

related mortality, and during the second release, relatively strong northeast winds may

have pushed larvae south of my sampling sites, lowering chances of recapture success

and implicating the importance of physical transport. Furthermore, Niskin sampling,

which captures a relatively smaller volume of water than a plankton tow, was chosen as

the most efficient method for sampling over the large study area given the demand for

capturing location-specific water samples during discrete time periods to support model

validation efforts. Future studies could use plankton tows and increased sampling

frequency (i.e., sampling as soon as 1–12 hours post release and multiple times a day:

Crocker 1998; Millar 1961) to increase chance of larvae recapture. However, plankton

tows will require sorting higher density plankton samples to find recaptured larvae that

are present in low numbers. Thus, techniques such as mechanical size separation,

polarized light identification (Tiwari and Gallager 2003), and chemical pre-treatment of

samples (e.g., hydrogen peroxide: Viitasalo et al. 2005) will be needed to separate

bivalve larvae from phytoplankton for rapid detection. Field sampling for fluorescently

stained particles also is inherently affected by photodegradation (Linard et al. 2011).

Photodegradation, however, is likely less important in turbid, low-light estuaries like

Mobile Bay because of lower light penetration (McCarthy et al. 2018). I found that

marked oyster larvae were detectable after 5 days (my longest sampling effort) in the

field and >42 days in the laboratory, indicating that photodegradation was not a major

concern. Despite the variety of potential constraints to performing a large-scale field-

based study, I was able to recapture marked larvae at rates within the range expected

based on previous study and model expectations. Future studies can build on this

approach to develop application and location-specific sampling approaches to optimize

recovery conditions.

Conclusion

Calcein shows promise as a marker for future mark-recapture studies on species

with pelagic larval stages and where there is interest in understanding larval movements,

such as for restoration and propagation efforts. Calcein demonstrated two of the four

qualities that constitute an effective marker for mark-recapture studies (Ricker 1956;

Thorrold et al. 2002). 1) Calcein had an appropriately long-lasting mark, visible

throughout the duration of the study and was resistant to photodegradation in the Mobile

Bay-eastern Mississippi Sound system. 2) Calcein staining did not affect growth or

survival of oyster larvae. 3) Markers should be low cost, and unfortunately the relatively

high cost of calcein ($4.70 g^{-1} in 2018; Fisher Scientific) could be a limiting factor for

large-scale field mark-recapture studies, but use will depend on end-user cost-benefit

assessments. 4) Importantly, the calcein mark is not readily detectable upon field

recapture in high particle background, high volume samples, and marked individuals are

likely to be present in low density, requiring a large number of samples and making

traditional microscopy impractical (e.g., researcher fatigue: First and Drake 2012).

Although not perfect, the FlowCam was the most viable option for detection of large-

volume, high-background field sampling. Calcein-based mark-recapture studies have

potential to be used to track movements of larvae for any species in the future and

applications of this approach, particularly for commercial species, extend broadly from

model validation to assessment of restoration and propagation efforts.

Table 1. Larval size (maximum linear dimension) and survival (percent of larvae alive as determined from ten 200 μL samples) immediately after the 48-hour staining period for salinity and holding tank experiments (± standard error). Larvae were stained in replicate 18.9 L buckets in the salinity experiments, while larvae were stained in 4000 L hatchery tanks in the holding tank experiments.

Experiment	Staining	Salinity	Oyster size (μm)		Survival (%)
			Pre-stain	Post-stain	
Salinity	Stained	15	75 ± 1	80 ± 3	39.6 ± 12.7
		20		80 ± 3	50.4 ± 25.4
		26		78 ± 1	50.7 ± 20.8
	Unstained	15		86 ± 1	37.3 ± 7.7
		20		81 ± 2	39.4 ± 6.0
		26		78 ± 1	16.0 ± 1.0
		Control		92 ± 2	39.8
Holding tank	Stained	15	72 ± 3	75 ± 4	63.0
		26	76 ± 2	87 ± 3	63.0

Table 2. Recapture success from mark-recapture studies with invertebrate and fish larvae free-released in the field: ALC = Alizarin complexone; TC = Tetracycline. "Study distance" indicates the longest distance between the locations of release and recapture and "Time frame" indicates the longest time period between release and recapture.

Species type	Species	Mark	Study location	Study distance (km)	Recovery technique	Time frame	n Released	Recaptured	Recapture rate (%)	Citation
Invertebrate	*Crassostrea virginica*	Calcein	Bay	40	Niskin	5 d	2.20×10^7	2	0.000009	This study
	Placopecten magellanicus	Calcein	Inlet	2	Plankton tows	69 d	1.73×10^7	99	0.00058	Crocker 1998
				2		69 d	1.50×10^7	11	0.000073	
				2		49 d	1.50×10^7	27	0.00018	
				2		49 d	2.70×10^7	12	0.000044	
	Ostrea edulis	Neutral red		2.2	Plankton tows	18 h	-	103	-	Millar 1961
Fish	*Morone saxatilis*	ALC	River	20	Plankton tows	34 d	6.50×10^6	4	0.00006	Secor et al. 1995
		ALC, TC		30	Plankton tows	21 d	2.51×10^7	130	0.00052	Secor et al. 2017
		TC		-	Electrofishing	3 y	4.23×10^5	80	0.02	Reinert et al. 1998
	Thymallus thymallus	ALC		10	Electrofishing	1 m	3.00×10^4	19	0.06	Nagieć et al. 1995
	Plecoglossus altivelis	TC		-	-	6 d	3.00×10^6	500	0.02	Tsukamoto and Kajihara 1987
	Coregonus lavaretus	^{85}Sr		22	Seine	3 m	1.20×10^5	1,342	1.1	Lehtonen et al. 1992
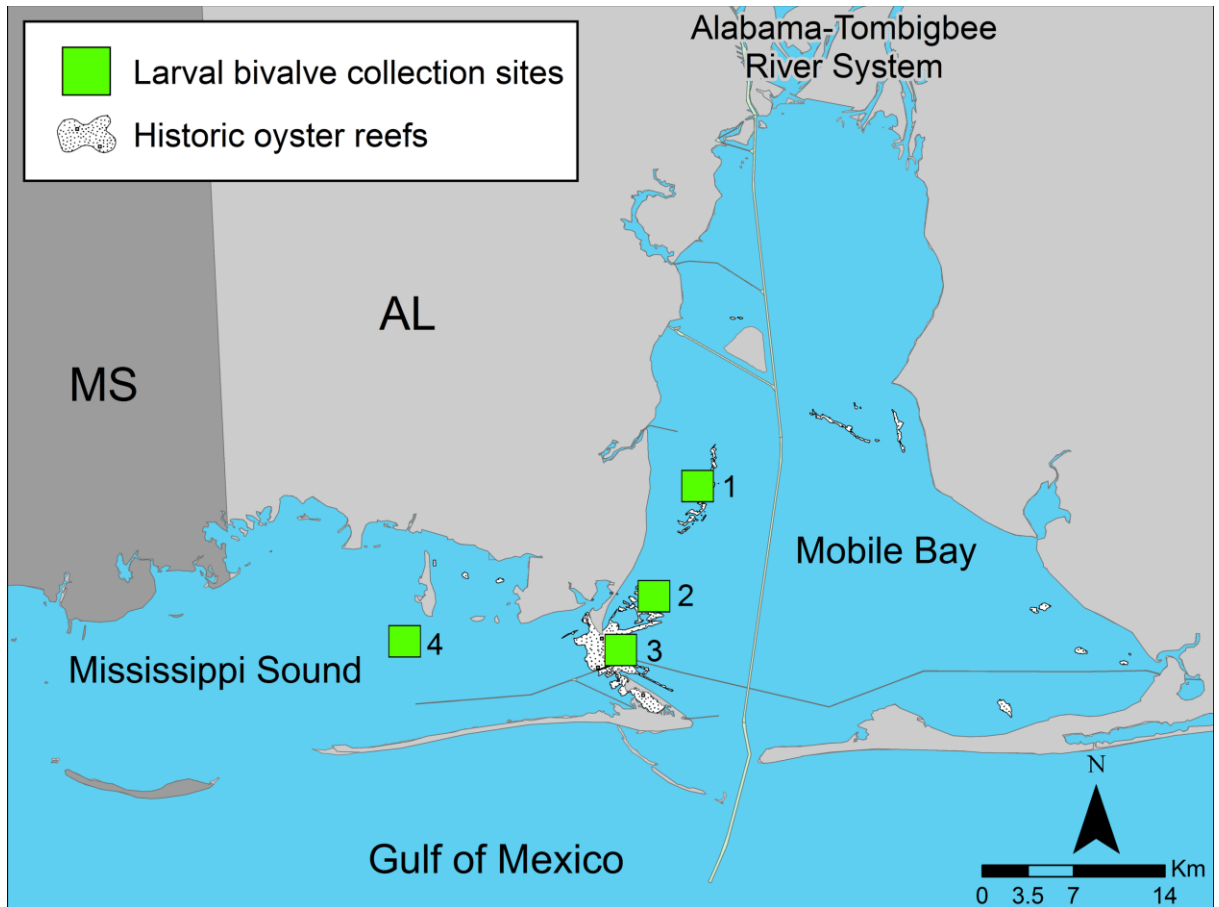
Figure 1. Larval oyster sampling sites in the Mobile Bay-eastern Mississippi Sound system, AL for the field study in 2014. For each of lower (May 19) and higher (July 28) salinity releases, 22 million calcein stained oyster larvae were released at sites 1 and 2, and larval recapture sampling was conducted at sites 1–4 on days 1, 2, 3, and 5 after release. Site GPS coordinates are: 1: 30.412°N, 88.071°W; 2: 30.336°N, 88.101°W; 3: 30.299°N, 88.124°W; 4: 30.305°N, 88.273°W. White shapes indicate known historic and present native oyster reef locations (layer citations: May 1971; Tatum et al. 1995; Alabama Department of Conservation and Natural Resources 2001).
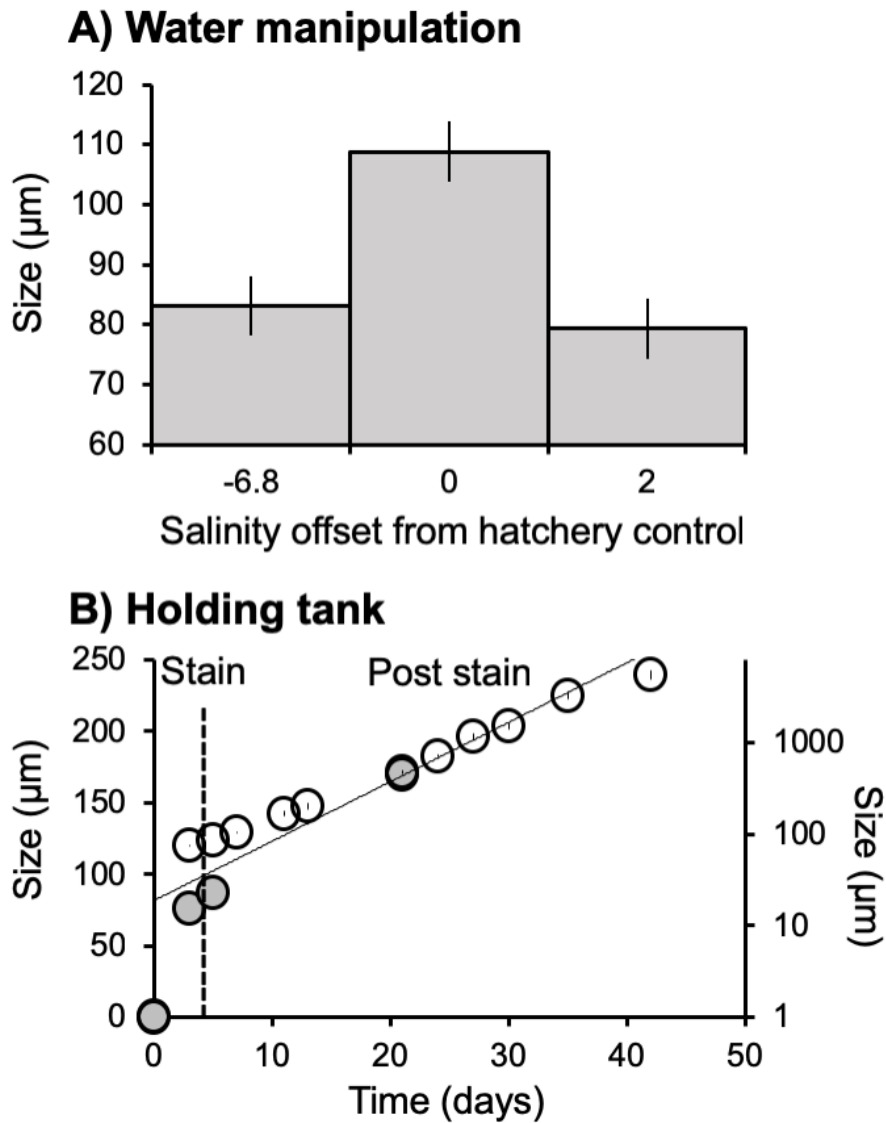
Figure 2. Mean changes in maximum linear length (± SE) of larval oysters compared to (a) water manipulations (salinity offset from hatchery control conditions) and (b) holding tank effects through time. Salinity offset refers to the mean salinity differences between hatchery control water and treatment salinities for all water changes during the salinity experiments, due to the addition of Instant Ocean® to increase salinity (+2) or the addition of DI water to lower salinity (-6.8) (a). Oysters held in larger hatchery tanks are represented by open circles on the right y-axis in a log scale ($y = 18.71e^{0.15x}$, $R^2 = 0.80$, $F_{reg1,9} = 65.86$, $p < 0.001$), and oysters held in smaller aquaria are represented by filled circles on the left y-axis (b). The dashed vertical line marks the end of the 48-hour staining period (5-day old larvae).
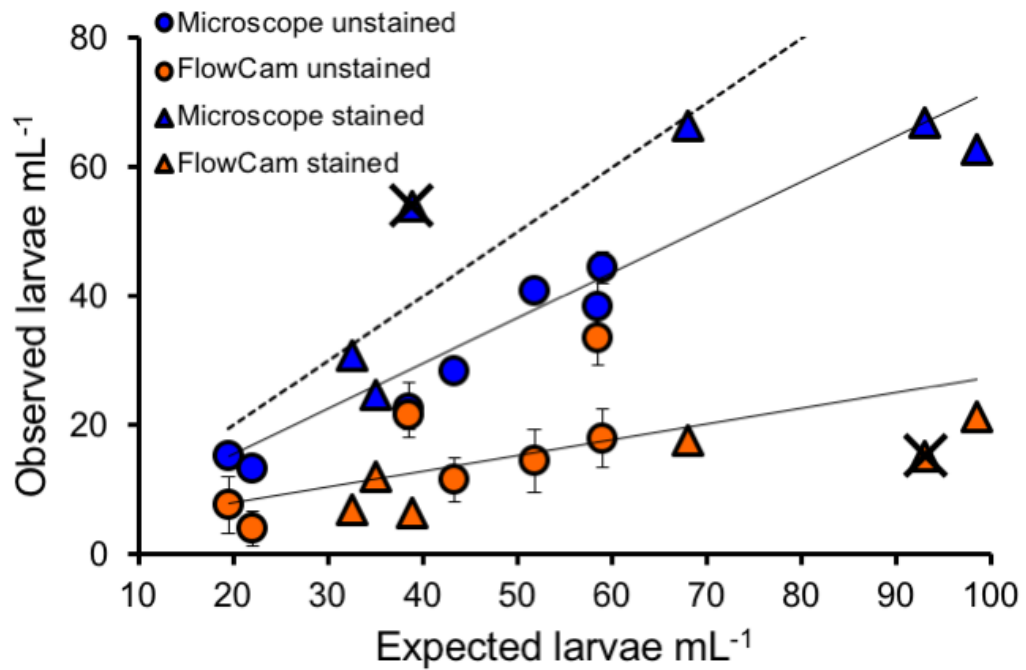
Figure 3. Observed versus expected number of larvae detected using an Olympus BH2-RFCA fluorescent microscope and a FlowCam®VS series. Dashed line indicates a one-to-one line of perfect fit, and solid lines are linear regression lines: $y = 0.70x + 1.5$ ($R^2 = 0.88$, $F_{reg1,10} = 71.06$, $p < 0.001$) for microscope and $y = 0.24x + 3.12$ ($R^2 = 0.40$, $F_{reg1,10} = 6.66$, $p = 0.03$) for FlowCam. Outliers not included for regression analysis are marked with "X."
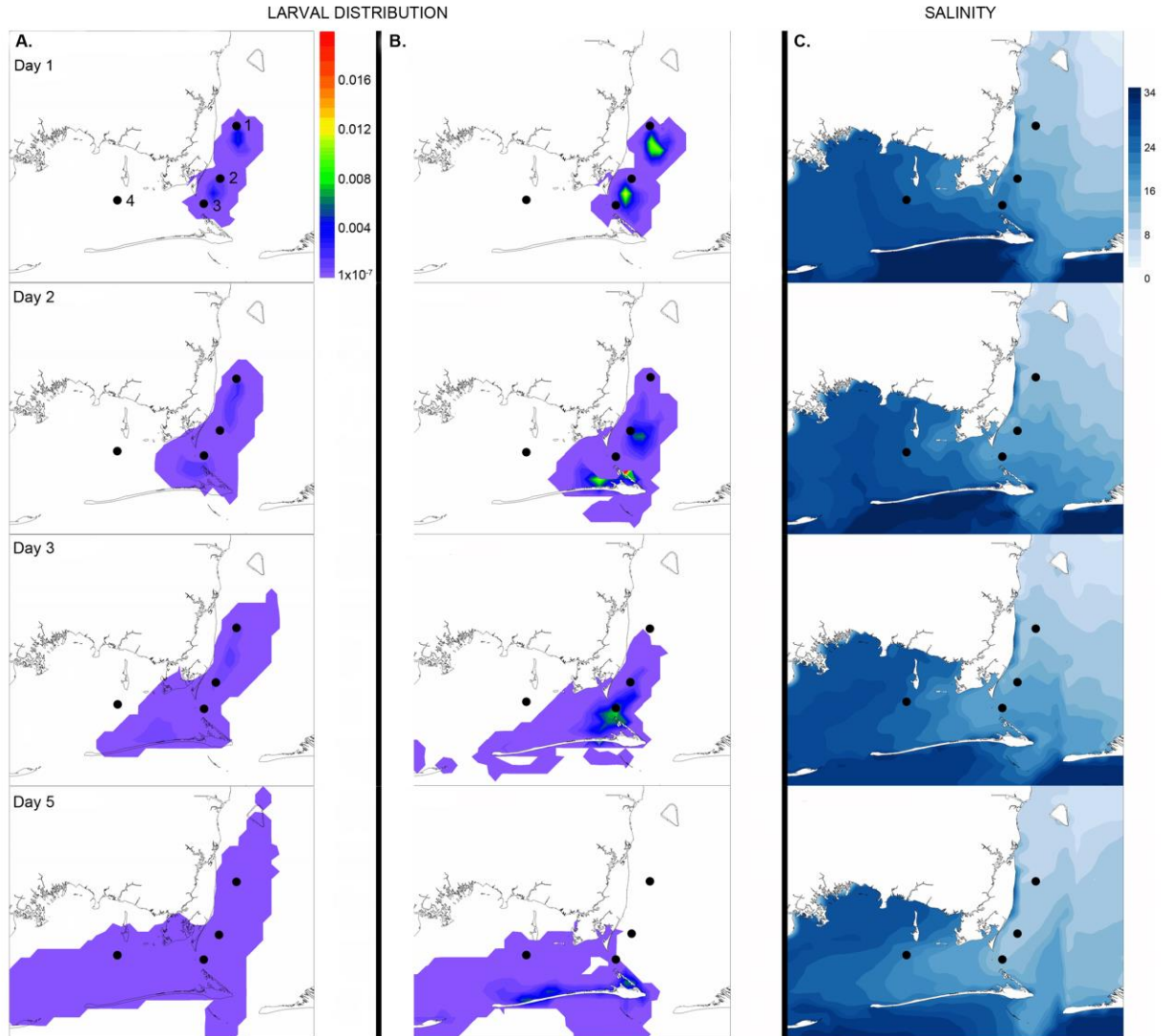
Figure 4. Model results for larval distribution with physical transport processes only (a) and with biological movement as well as physical transport processes (b), and salinity (c) on days 1, 2, 3, and 5 for the second release on July 28, 2014.

CHAPTER 2

USE OF SETTLEMENT PATTERNS AND GEOCHEMICAL TAGGING TO TEST POPULATION CONNECTIVITY OF EASTERN OYSTERS (*CRASSOSTREA VIRGINICA*) IN A FRESHWATER-INFLUENCED ESTUARY

Abstract

Freshwater-dominated estuaries experience large fluctuations in their physical and chemical environments, which may influence larval dispersal processes and connectivity of populations with pelagic larval stages. I used a combined settlement and natural tagging approach to trace and define connectivity among oysters across the freshwater-dominated Mobile Bay-eastern Mississippi Sound (MB-EMS) system. Specifically, I 1) tested how freshwater inputs and associated environmental attributes influenced settlement patterns during high and low discharge conditions in 2014 and 2016, respectively, 2) assessed the utility of natural tags, i.e., trace element (TE) ratios incorporated into shells, to define natal-site reference signatures and link spat to those natal sites to infer connectivity, and 3) determined the temporal variability of those site-specific TE signatures. During low discharge, settlement was 4x higher than during high discharge, when oysters only settled in higher salinity regions (EMS). Salinity and

temperature likely influenced the timing, magnitude, and location of settlement and spawning events, in turn, influencing connectivity between years. Adult shell showed promise as a proxy for natal-site reference signatures due to high spatial resolution (~2.5 km) in discriminating among potential natal sites. Although TE ratios were colinear and temporally variable, larval shells could be assigned to natal sites. Results suggest that EMS is an important larval source. Biological and geochemical data demonstrate potential to identify environmental attributes that spatiotemporally mediate connectivity in dynamic systems, and results provide a baseline for measuring future larval connectivity and adult distribution changes in the MB-EMS system.

Introduction

Many marine species have pelagic larval stages, and knowledge of larval dispersal and subsequent population connectivity (i.e., from larval origins to recruitment) is imperative to better understand population dynamics and manage populations (Thorrold et al. 2007). Larval dispersal and transport are difficult to quantify due to: 1) uncertainty in larval sources and 2) difficulty of tracking microscopic larval movements *in situ* due to advection and high larval mortality (Levin 2006). Many species, including bivalves, also inhabit dynamic habitats often dominated by freshwater inputs (Pollack et al. 2011), which can modify larval transport and delivery of new recruits for settlement (Dong et al. 2012; Kim et al. 2013). Freshwater discharge alters the chemical and physical environment and interacts with environmental factors such as surface heat exchange, winds, and tides to affect salinity, water temperature and water circulation patterns that mediate reproduction, survival, growth, distribution and settlement processes (Wilber

39

1992; Kennedy 1996; O'Connor et al. 2007; Kim et al. 2010, 2013). While it is well-established that freshwater inputs affect the distribution and abundance of bivalves, with lower flows resulting in more abundant adult bivalve populations (Wilber 1992; Soniat et al. 2012), how changes in freshwater discharge influence dispersal of larvae, settlement of recruits, and ultimately population connectivity has been less studied.

Natural tags (i.e., geochemical tracers) have been used to indirectly track larvae to determine larval sources, define transport, and infer population connectivity (Thorrold et al. 2002; Becker et al. 2005; Bradbury et al. 2011). Geochemical tracers such as trace elements (TE) are incorporated into larval shells from the natal environment and retained throughout early development and settlement (Levin et al. 1993; Anastasia et al. 1998; DiBacco and Levin 2000). The ratios of these elements can be location-specific and thus are useful to determine larval origins by comparing larvae of unknown origin to natal reference signatures. Reference TE signatures need to be spatially distinct, encompass the potential dispersal distance (Miller et al. 2013a), and have low temporal variation during the pelagic period (Campana et al. 2000). Adult bivalves are sedentary and can integrate TE signatures over longer time periods (i.e., weeks to years) than larvae, reflecting TE ratios of multiple larval cohorts. Therefore, site-specific TE ratios in adult bivalve shell can serve as a time-integrated proxy for natal site reference TE signatures.

To determine the utility of geochemical tracers to track larval origins and movements within a system, the spatial and temporal variation of TE ratios needs to be defined. Elemental spatiotemporal variability is determined by differences in environmental (physical and chemical) and biological factors (Lorens and Bender 1980; Vander Putten et al. 2000). Estuaries are ideal areas to study variation in TE ratios

because they have high spatiotemporal environmental variability due to different geomorphologies, pollution sources, and freshwater inputs (Swearer et al. 2003; Thorrold et al. 2007). Previous estuarine-based studies have found spatial variation in TE ratios in bivalve shells across 1 to 10s km (Norrie et al. 2016) and temporal variation on a scale of weeks to months in bivalve shells (Becker et al. 2005) and years in gastropod shells (Zacherl 2005). These findings suggest that spatiotemporal variation within estuaries should be adequate to distinguish larvae among natal sites using TE ratios. The ability to define spatial and temporal variation in TE ratios is of particular concern in freshwater-dominated systems where large-scale mixing may affect larval dispersal processes and reduce the spatial distinction of TE ratios among sites through time.

Knowledge about larval origins and connectivity are needed to better understand larval biology and ultimately conserve bivalve stocks. Oysters are commercially, ecologically, and biogeochemically important, particularly in the north-central Gulf of Mexico (nGoM), which is home to a few of the remaining commercially harvestable oyster populations worldwide (Beck et al. 2011). Eastern oysters are a spawning species that produce a planktonic larval stage lasting ~2–3 weeks depending on environmental conditions (Medcof 1939). Larvae can disperse 0.1–100s of km (North et al. 2008; Haase et al. 2012; Puckett and Eggleton 2016), during which a larval calcite shell develops (Stenzel 1964). In the nGoM, eastern oysters are capable of spawning multiple larval cohorts throughout the year, depending on temperature, with spawning typically occurring between April and October (Ingle 1951; Butler 1965; Hayes and Menzel 1981). Spawning is induced when temperatures reach >25°C or following a rapid increase or decrease in temperature (Nelson 1928; Hayes and Menzel 1981; Saoud et al. 2000).

41

Freshwater discharge can influence connectivity by affecting the growth and survival of early life stages, which are salinity dependent, with optimum salinities for larval development and spat settlement between 7.5–22.5 and 10–30, respectively (Carriker 1951; Davis 1958; Calabrese and Davis 1970; Chatry et al. 1983). Following the pelagic larval period, oysters settle under suitable conditions and remain in the settlement location throughout juvenile and adult life stages, incorporating TE ratios of settlement locations into an aragonite shell (Stenzel 1964) representing long-term temporal scales. Thus, oysters are promising model organisms to understand how changes in freshwater discharge and associated environmental attributes mediate larval connectivity on different spatial and temporal scales.

To determine how changes in freshwater discharge influence connectivity of oyster populations, I conducted a two-part study to define connectivity using a novel approach that combined larval oyster settlement patterns and geochemical tags. I used the Mobile Bay-eastern Mississippi Sound (MB-EMS) system, a nGoM estuary system with the sixth largest freshwater drainage basin in the U.S. (Isphording and Flowers 1987), as a model system. Previous studies have found oyster settlement to be highest in the southwest side of MB and EMS, following an increasing salinity gradient from northern to southern MB and westward into eastern MS, with negligible settlement in the middle, east, and upper portion of MB (Hoese et al. 1972; Lee 1979; Saoud et al. 2000; Kim et al. 2010). Thus, in the first part of the study, oyster spat were collected from areas of known oyster settlement in two different years with low and high discharge conditions to determine whether the flow patterns and associated environmental attributes (salinity and temperature) determined by freshwater discharge, winds, and tides defined

where eastern oysters settled and how they grew in the MB-EMS system. In the second part of the study, geochemical tags (i.e., TE ratios) were used to: 1) define possible natal (i.e., spawning) site-specific TE ratios integrated into native adult oyster shells that represent potential brood stock and 2) compare spatially distinct natal site TE ratios with ratios in the larval component of shell from newly settled spat to determine larval origins. Because connectivity studies using TE ratios have not been conducted in freshwater-dominated systems, I first had to verify methods to ensure larval origins could be predicted. To do this, I tested: 1) if the larval and post settlement components of spat shell could be distinguished from each other, to distinguish between natal origins and settlement locations, 2) if the larval and settled shells of spat were different among sites, confirming sufficient variability in the physiochemical environment to determine spatial distinctions among sites, and 3) if TE ratios in larval, settled, and adult shells were temporally stable on seasonal or annual scales to determine use of singular or multiple time points to adequately represent TE ratios in the MB-EMS system. These data may have important implications for understanding larval connectivity in freshwater-dominated systems and under changing discharge regimes.

Methods

Settlement sampling

Sampling scheme.

To determine spat settlement patterns, settlement plates were deployed at settlement sites (Fig. 5; Table A2) in the freshwater-dominated MB-EMS system

throughout a region of historically known oyster habitat (Hoese et al. 1972; Lee 1979; Saoud et al. 2000) with sites 1–3 located west to east in EMS and 4–8 located south to north along a salinity gradient in MB. In 2016, S3, S6, and S8 settlement plate sites were added to include a natural reef site (S3) and historically productive oyster areas that have been unproductive in recent years (S6 and S8) (Stout et al. 1998). Plates were changed bimonthly from May to mid-September of 2014 and 2016.

Settlement plate moorings.

Settlement plate moorings were attached to existing pilings, below the water surface to reduce potential vandalism. Moorings consisted of an 18.9 L bucket with a steel pole (25.4 mm × 2.1 m) cemented in the center with 18 kg of concrete, ratchet strapped to a piling. A PVC sheath holding four settlement plates was bolted in place 1 m above the bottom and accessible via snorkeling to allow easy access to plates without removing the mooring. Settlement plates (17 × 17 cm) made of HardieBacker®
Cement Board were deployed at a 45˚ angle (Carleton and Sammarco 1987; Dayton et al. 1989). Plates were pre-soaked in 0.7 μm filtered seawater for ~24 hours to promote biofilm development *in situ* to increase settlement (Quayle and Newkirk 1989; Tamburri et al. 2008). Seawater was prefiltered to remove organisms that could potentially affect settlement. To reduce predation while allowing adequate water flow, a half-caging method was used by placing 3.5 mm plastic mesh with two sides open with the top and bottom closed (Kim et al. 2010).

Spat abundance and heights.

Two settlement plates were analyzed per site, and only the inner 16 × 16 cm of the plate was analyzed (outer 1 cm excluded) to reduce handling effects. Spat on

settlement plates were examined with a Fisher Stereomaster zoom dissecting microscope (10–60x magnification). All spat were counted and distinguished as live (non-gaping and/or tissue present) or dead (spat scars or gaping oysters with no visible tissue; only used for mortality analyses). Percent mortality was calculated as the number dead divided by the total spat that had settled. Height of spat were measured as longest length from umbo to outer edge, using AxioVision software with a SteREO Discovery V12 Zeiss microscope to the nearest 0.01 µm. Because it was not feasible to measure all oysters, a representative number of spat were measured, such that on plates with <200 spat settled, all spat were measured and when >200 spat settled, a minimum of 200 haphazardly selected spat were measured. Spat too large to be measured under the microscope were measured with Vernier calipers to the nearest 0.01 mm. Some spat (<300 µm) were too small to be accurately measured and were not included in height analyses.

Environmental attributes.

To determine freshwater discharge, daily discharge data in 2014 and 2016 were downloaded from United States Geological Survey gauging stations 02428400 (Alabama River at Claiborne near Monroe) and 02469761 (Tombigbee River at Coffeeville) (last accessed 3 February 2017) and summed to equal the total discharge into the MB-EMS system (Park et al. 2007). To determine environmental attributes at the time of sampling, temperature, salinity, and dissolved oxygen were measured when changing plates bimonthly at settlement sites (at the depth of plates) using a YSI pro 2030 handheld data sonde. To determine wind (direction and velocity) and water temperature, hourly data were downloaded from Dauphin Island station DPIA1 (NOAA Tides and Currents; last

accessed 15 July 2019). Spatially uniform wind and temperature were used following the

previous studies in the MB-EMS system (e.g., Kim and Park 2012; Park et al. 2014). A

well-validated three-dimensional hydrodynamic model was used to simulate salinity at

finer spatial and temporal resolution through the study area in 2014 and 2016. Detailed

information of the model configuration and its application and validation can be found in

Kim and Park (2012) and Park et al. (2014).

Settlement sampling statistical analyses.

To determine spatial variability in spat settlement, regression analysis was used to

compare average numbers of spat settled to longitude. To compare settlement patterns

found in this study to previous studies conducted in the MB-EMS system, literature data

were collected from Hoese et al. (1972), Lee (1979), Saoud et al. (2000), and Kim et al.

(2010), and average settlement trends versus longitude were compared to results from

this study. Data collected from Lee (1979) and Saoud et al. (2000) were not included in

regression analyses due to having too few sites where spat settlement was measured. To

determine spatial and temporal variability in spat settlement, growth, and mortality,

general linear models (GLMs) were used with settlement site and week as factors.

Negative binomial GLMs with log-links were run for 2014 spat settlement. To account

for over-dispersed count data with zero inflation, 2016 spat settlement data were analyzed

using a zero-altered negative binomial GLM with a log-link using the *pscl* package in R

(Jackman 2008). To determine break-points in settlement GLMs to indicate time points

where settlement was different from zero and representative of consistent settlement at all

sites, the *segmented* package in R was used (Muggeo 2019).

To determine if discharge differed between years, a generalized additive model was run with a reduced maximum likelihood smoothing function using the *mgcv* package in R (Wood 2012). To determine spatial and temporal variability in salinity and temperature, GLMs were run with settlement site and week as factors for sites and time periods that had appreciable settlement. For comparisons between years, GLMs with year, week, and settlement site as factors were run with salinity data for the same sites and time periods and a *t*-test was performed for temperature comparisons. Because environmental variables measured at the time of plate collection represented a single time point that is not necessarily representative of conditions in the MB-EMS system during settlement in the days prior to collection, settlement data were not directly compared to environmental data. Rather, temperature and salinity patterns throughout the settlement season were analyzed, and time points where break-points were identified (*segmented* package in R: Muggeo 2019) were considered "settlement events." To determine environmental conditions potentially indicative of spawning or optimal conditions for settlement, temperature and salinity changes two and four weeks prior to the settlement event were assessed. Two and four weeks prior to the settlement event were chosen based on an average 2–3 week pelagic larval duration where spawning and subsequent settlement could potentially be explained by environmental conditions during these time periods. For example, previous studies have indicated that settlement events commence ~three weeks after a decline in temperature triggers spawning (Saoud et al. 2000). Two weeks prior to the settlement events were termed "spawning events" and four weeks before were termed "prior to spawning."

Data were statistically modeled independently for 2014 and 2016 due to large

differences in settlement between years and the addition of settlement plate sites in 2016.

Due to overfitting of models, settlement sites and sampling periods with few ($n \leq 3$) spat

settled were removed from models, such that data collected from S6 were removed from

2016 spatial and temporal settlement models, data collected from S5 and S7 were

removed from 2014 temporal settlement models, and data collected from S8 were

removed from 2016 temporal settlement models. Additionally, data collected from S4 in

2014 were removed from the growth analysis due to having few heights measured. For

comparison between years, spatial and temporal settlement and growth models were run

from mid-May through mid-August and from the beginning-June through mid-August,

respectively, to cover periods of common spat settlement and data acquisition.

All models were checked for the assumptions of linearity, normality, and

heteroscedasticity of residuals. If assumptions were not met, appropriate model

relationships, i.e., polynomial relationships, were used or data were log transformed.

GLMs were re-run without significant factors and/or interactions in cases where factors

and/or interactions were not significant. Final models were chosen using partial

likelihood ratio tests. Week as a unit of time was used as a continuous variable in all

models. An α of 0.05 was used for all tests and error is presented as $\pm$ standard error.

GLMs and the negative binomial GLM were run using the *MASS* package in R (Venables

and Ripley 2002). All analyses were conducted in R Studio version 1.1.453 (R Core

Team 2017).

Trace element analysis

TE ratios in native adult oysters that are potential brood stock for larvae were used as a proxy for site-specific TE ratios to define natal origin (i.e., spawning sites). To assign larvae to sites of origin and distinguish spawning sites from settlement sites, the shells of settled spat were analyzed along a cross-section from umbo to margin to characterize TE ratios throughout life, including both the larval and settled portion of spat shells. These ratios in larval shells were then compared to site-specific TE ratios in the outer margin of adult shell. Within-season variation in site-specific signatures of larvae that might confound origin assignment was quantified by determining and comparing TE ratios in spat among the three time periods that spat were collected (May–June, July–August, late-August–September 2016). Similarly, variation with time in site-specific TE signatures recorded in adults was quantified by analyzing whole adult shell, representing multiple years, and comparing aggregate lifetime values to the most recent year of shell growth that was used to determine natal site signatures.

Shell collection.

Native adult oysters were collected from The Nature Conservancy (TNC) Mobile Bay Restoration Project intertidal oyster reefs (at sites A3a, A3b, A5, and A6) and opportunistically during field sampling from subtidal settlement plate sites (shell symbols in Fig. 5). Sample size ($n = 3$–5) at each site was limited by the number of available adult oysters. Only adult oysters collected after September 2016, which were in the water for the duration of spat settlement sampling, were used for analysis to ensure that the time period of TE ratio acquisition overlapped between adult and spat shell. Only spat shells collected from 2016 settlement plates were used for TE analysis due to low and

inconsistent spat settlement in 2014. Spat shells were collected at all settlement plate

sites in Fig. 5, except S8 due to inconsistent plate recovery.

Shell preparation.

Native adult oyster shells were radially sectioned (hinge to outer edge) using a

Buehler Isomet® 1000 Precision Saw using Isomet™ Diamond Wafering Blades (152.4

× 5.1 × 12.7 mm) to create a 2 mm thick section. Spat shells were collected off

settlement plates using a tungsten probe. To remove excess organic matter (i.e., mud and

bryozoans), spat shells underwent three cycles of rinsing with ultrapure water and drying

at 60°C. Additional chemical treatments were not used to avoid altering the elemental

composition of biogenic carbonate (Krause-Nehring et al. 2011) or degrading the fragile

larval shells (Kroll et al. 2016). For analysis, all shells (adult sections and whole spat)

were mounted to slides using Scotch™ double-sided tape.

Laser ablation inductively coupled plasma mass spectrometry.

Shells were ablated with an Nd: YAG NWR213 (Electro Scientific Industries,

Portland, OR) laser ablation system coupled with Agilent Technologies (Santa Clara, CA,

USA) 7700x inductively coupled plasma mass spectrometry (ICP-MS). Adult shells

were ablated on a transect from inner to outer surface, perpendicular to internal lines of

growth at a 25 μm spot size, scan speed of 15 μm s^{-1}, 45% intensity, and 10 Hz following

pre-ablation at 40 μm spot size, 50 μm s^{-1} scan speed, and 40% intensity. Spat were

ablated across the whole shell (umbo to outer edge) with a 10 μm spot size, scan speed of

10 μm s^{-1}, 25% intensity, and 10 Hz following pre-ablation at 20 μm spot size, 50 μm s^{-1}

scan speed, and 20% intensity. Laser intensities and scan speeds were chosen to ensure

that the laser did not burn through the entire depth of spat shell, and all spat were checked

under the microscope post-ablation. Three transects were run per shell, with a laser warm

up and washout delay of 30 seconds between transects. NIST 612 glass (National

Institute of Standards and Technology, Maryland) and MACS-3 calcium carbonate

(United States Geological Survey) reference standards (two transects with identical

parameters to shells) were run every hour and at the beginning and end of sampling.

Shells were sampled for ^{24}Mg, ^{88}Sr, ^{137}Ba, ^{208}Pb, ^{57}Fe, ^{111}Cd, ^{63}Cu, ^{55}Mn, ^{66}Zn,

^{75}As, ^{60}Ni, ^{51}V, ^{52}Cr, ^{59}Co with ^{43}Ca as the internal standard. Elements were chosen

based on previous geochemical tracking studies done in estuarine environments (Becker

et al. 2005; Kroll et al. 2018). Data reduction and limits of detection were calculated in

Iolite software (version 3.63) using MACS-3 as the reference material and

Trace_Elements as the data reduction scheme. Elements are reported as metal (Me):Ca in

mmol mol^{-1}. Concentrations in adult shells were averaged for whole transect (multi-year

average) and for 300 μm of most recent growth (single year). Spat transects were

averaged along the first 150 μm from the umbo and the last 150 μm near the shell margin,

representing larval and settled shell, respectively. Distance stratification along the shell

was based on known growth relationships for adult and larval oysters in the region

(Gallager et al. 1986; Kirby et al. 1998; Rikard and Walton 2010).

Trace element statistical analyses.

To determine if elemental composition in adult shell differed among potential

natal sites, linear discriminant function analysis (LDA) was used with TE ratios measured

in adult shell grown during the study (most recent 300 μm). To distinguish spawning

sites from settlement sites, TE ratios of the larval and settled shell were directly

compared using two-way MANOVAs (multi-elemental comparisons; Pillai's trace test

statistic) with site and shell type as factors, followed by univariate ANOVAs (individual elemental comparisons). To determine if the elemental composition in larval and settled shells differed among potential natal and settlement sites, LDAs were run for larval and settled shells separately. To predict larval origins, larvae were classified to sites using most recent adult shell TE ratio LDAs that were run with 1) TE ratios chosen from larval shell LDA results (except V because it was not present in adult shell) and 2) without the northernmost MB site (S8) from where larvae were unlikely to originate. Larval predictions were also attempted with whole shell TE ratios, but differences among sites were greater for the recent shell LDA, and thus the whole shell LDA was not used.

To determine if the elemental composition in larval and settled shell grown during the study was similar within the spawning season, separate LDAs were run for larval and settled shells sampled during the three spat collection time periods and compared to determine variability in site separation. To determine if the elemental composition in adult shell grown during the study (most recent 300 μm) was similar to all previous years of shell growth, separate LDAs were run for the recent shell (~single year) and whole shell (~multiple years) and compared to determine variability in site separation.

For all statistical tests, TE ratios were Box-Cox transformed. Multivariate outliers were identified by plotting robust squared Mahalanobis distances of the residuals against the corresponding quantiles (Q-Q plot) of chi-square distribution. Multivariate normality was tested using a multivariate Shapiro Wilks test. I had equal number of groups and small sample sizes, and thus homogeneity of variance-covariance (Box M test) was not tested and LDAs (*MASS* R package: Venables and Ripley 2002) were chosen over quadratic discriminate function analysis. Adult shell LDAs were run in

backward stepwise fashion using the stepclass function in *klaR* package in R (Roever et al. 2018) to determine the suite of elements to include in the final models. Larval and settled shell of spat LDAs were run in a forward stepwise fashion using the Wilks Lambda statistic to determine the order of variable entry, and *F* statistic probabilities were used to evaluate model improvement using the *klaR* package in R (Roever et al. 2018). Backward LDAs did not perform well in spat analyses because of high collinearity among most TE ratios. Prior to running final LDAs, MANOVAs were run using Pillai's trace test statistic to ensure site separation in multi-elemental TE ratios to validate the use of an LDA. Prior probabilities were computed with equal group sample sizes for all LDAs. Jack-knife reclassification success was used to determine classification accuracy (i.e., the success rate of the LDA to assign shells to a site). Standardized coefficients were used to assess the relative contribution of each TE ratio in contributing to site separation. Because the LDA model is forced to predict all larvae to a potential sampled spawning site, of which not all potential spawning sites in the system were sampled, when I assigned larvae to a natal source (i.e., adult shell proxy source), any larvae with a group probability >0.9 had a strong likelihood of originating from the predicted site (Gomes et al. 2016). All analyses were conducted in R Studio version 1.1.453 (R Core Team 2017).

Results

Spat settlement

Spatial and temporal variation.

In both years, settlement was higher in EMS compared to MB. Settlement was higher in 2016 with a mean and maximum settlement of 70 ± 19 and 1137 spat plate^{-1}, respectively, compared to 2014 mean and maximum settlement of 18 ± 6 and 174 spat plate^{-1}, respectively. In 2014, MB sites had up to 1 ± 1 spat plate^{-1}, while in 2016 MB sites had up to 25 ± 11 spat plate^{-1}. In 2014, spat settlement exponentially increased westward from S7 to S1 (EXP(y) = $17.47x - 1539.56$, $R^2 = 0.94$, $F_{1,3} = 43.69$, $p = 0.007$; Fig. 6a) with the highest settlement at the westernmost site, S1 (34 ± 14 spat plate^{-1}). In 2016, spat settlement had higher settlement at S4 (56 ± 23 spat plate^{-1}) compared to S1 (54 ± 23 spat plate^{-1}), and thus settlement did not increase westward in 2016 among sites that were sampled in both years (Fig. 6a). The native site sampled only in 2016 (S3) had the highest settlement (200 ± 91 spat plate^{-1}), and spat settlement increased linearly westward from S8 to S3 ($y = -1225.10x - 107890$, $R^2 = 0.99$, $F_{1,3} = 213.80$, $p < 0.001$), shifting peak settlement from west to east EMS in 2016 compared to 2014 (Fig. 6a). Previous studies conducted in the MB-EMS system reported higher maximum settlement than found in this study and found patterns of increasing settlement westward during 1967 (Hoese et al. 1972: EXP(y) = $-10.17x - 892.71$, $R^2 = 0.59$, $F_{1,9} = 21.81$, $p = 0.01$), 1977 (Lee 1979), 1999 (Saoud et al. 2000), and 2006 (Kim et al. 2010: EXP(y) = $-8.18x - 715.78$, $R^2 = 0.65$, $F_{1,16} = 29.92$, $p < 0.0001$) (Fig. 6b).

An exponential increase in spat settlement began in mid-July 2014 (day 192 ± 7 days) and 2016 (day 206 ± 7 days) (break-point estimation; dashed lines in Fig. 7). Settlement models showed that in 2014 site and week together explained 49% of the deviance with a dispersion parameter of 0.58 (negative binomial GLM). In 2016, the settlement model had a McFadden's pseudo R^2 of 0.13 and a dispersion parameter of 0.62 (zero-altered negative binomial GLM). In 2014 and 2016, oyster settlement increased exponentially at a similar rate (slope $= 0.38$ in 2014; 0.34 in 2016) with time at all sites (2014: $z = 5.19$, $p < 0.0001$; 2016: $z = 10.59$, $p < 0.0001$), but intercepts differed among sites (Fig. 7; Table A3). In 2014, the intercept for S4 was lower than S1 and S2 (Fig. 7a; Table A3), and in 2016, S7 had the largest intercept (Fig. 7b; Table A3). In 2016, the probability of measuring a non-zero increased with sampling time ($z = 4.50$, $p < 0.0001$).

Growth and mortality.

In 2014, spat shell height, a metric of growth, varied during sampling ($F_{2,379} = 20.93$, $p < 0.0001$) and peaked in mid-July (day 192) (Fig. 8a). In 2016 (Fig. 8b), there was a significant interaction between site and week ($F_{10,2770} = 18.48$, $p < 0.0001$), showing different polynomial regression lines for S1 and S2. Spat shell heights were larger in the latter part of sampling (days 234–262; late August–September) and S3 spat had the largest shell heights (7.5–11.5 mm, day 248; early September). Mortality increased with time in 2016 (data not shown: $y = 0.29x - 0.80$, $R^2 = 0.26$, $F_{1,67} = 23.64$, $p < 0.001$) but was not statistically different in 2014, and mortality did not have any significant relationships with environmental variables measured during this study.

Environmental attributes.

Freshwater discharge differed between years ($F_{1,303} = 93.03$, $p < 0.0001$, effective degrees of freedom: 8.29, gaussian process smoother). In 2014 and 2016, discharge was highest at the beginning of sampling with discharges of 3000–5000 (May–June) and ~2500 $m^3 s^{-1}$ (early-May), respectively, and discharges for the remaining sampling periods were <1500 and <1000 $m^3 s^{-1}$, respectively (Fig. 9a). Winds during both years were primarily SW and SE with speeds of 3–6 $m s^{-1}$, and leading up to the settlement event, winds were primarily SW during 2014 and 2016 (Fig. A3).

Because salinity (2014 only) and temperature did not vary with time among sites that had appreciable settlement (Salinity$_{2014}$: $F_{2,14} = 2.42$, $p = 0.13$; Temperature$_{2014}$: $F_{2,14} = 0.20$, $p = 0.82$; Temperature$_{2016}$: $F_{5,47} = 0.11$, $p = 0.99$), sites were averaged. In 2014, salinity increased with time ($y = 1.83x + 2.58$, $R^2 = 0.86$, $F_{reg1,4} = 25.50$, $p = 0.007$; Fig. 9a, top panel) similarly at all sites, while in 2016, salinity increased linearly through time with the same slope (0.34) at all sites with appreciable settlement, but intercepts varied among sites (Fig. 9a, bottom panel; Table A4). Among the sites tested (S1, S2, S4) when comparing 2014 and 2016 salinity data, there was a significant interaction between year and week ($F_{1,32} = 25.17$, $p < 0.0001$) and for every 2-week period, there was a 1.4x greater increase in salinity in 2014 compared to 2016, indicating that salinity rose quicker in 2014 (Fig. A4; Table A5) due in part to differences in freshwater discharge between years. Additionally, modelled salinities were higher in the MB-EMS system in 2016 than in 2014, when salinities within MB were rarely >10. Temperature differed between years ($t = 2.36$, $p = 0.01$) and was lower (25 vs 28) at the beginning of 2014 than in 2016 (Fig. 9b).

Two weeks prior to beginning of the 2014 exponential increase in settlement, i.e., settlement event, salinity increased 4.2 units and temperature dropped 1°C during a two-week period in late June to mid-July (days 178 to 192). Two weeks prior to the potential spawning event in 2014, salinity rose 9.5 units and temperature rose 1.8°C during a two-week period in mid to late June (days 164 to 178) (Fig. 9). Modelled results also indicated a salinity increase in 2014 prior to the settlement event, with salinities throughout MB and EMS <10 and <15, respectively, prior to the event but ~20 in EMS during the settlement period (Fig. 10a). Two weeks prior to the 2016 settlement event, salinity decreased 2.5 units at all sites except for the two westernmost sites in EMS, S1 and S2, where salinity increased 3.4 units; temperature increased 0.6°C during a two-week period in mid to late July (days 192 to 206). Two weeks prior to the potential spawning event in 2016, salinity increased 3.4 units among all settlement sites except for the two westernmost sites in EMS, S1 and S2, where salinity decreased 0.9 units; temperature was stable within 0.2°C during a two-week period in late June to early July (days 178 to 192) (Fig. 9). Modelled salinities in 2016 rose leading up to the settlement event on day 206, with salinities between 10–25 in lower MB and 25–30 in EMS during this time (Fig. 10b). Finer resolution hourly buoy temperature data showed a 3°C and 2°C decrease in 2014 and 2016, respectively, during the 2 weeks prior to settlement events, and a 3.5°C and 1°C temperature increase in 2014 and 2016, respectively, during the 2-weeks prior to the potential spawning event (Fig. A5).

Trace elements

Adult shell.

TE ratios in shells of adult oysters differed among sites (MANOVAs: $p < 0.001$; Table A6; Fig. 11a). Recent shell site differences were driven by differences in Sr and Fe (first linear discriminate explained 69.1% of site variation), while whole shell site differences were driven by Sr and Mg (first linear discriminate explained 78.6% of site variation; Table A7). Recent and whole shell TE ratios were temporally variable (classification [100 and 96%, respectively] and jack-knifed reclassification [74 and 63%, respectively] success; Table A8). Among elements tested, Cd, As, and V were not detected in adult shells.

Spat shell.

TE ratios differed between larval and settled shells (i.e., natal origins vs. settlement locations) of spat and among sites for all three time periods tested (all MANOVAs: $p < 0.001$; Table A9), with Sr being the only element to differ among sites for all time periods tested (Table A10). Accordingly, TE ratios differed between larval and settled shells for all elements except Cu in May–June, Mg and Sr in July–August, and all elements except Mn, Cu, and Sr in August–September (Table A10). TE ratios differed among sites for Mg, Mn, Co, and Sr in May–June, all elements in July–August, and Sr in August–September (Table A10). Sites that drove the spatial elemental differences were S4 in May–June and July–August, S3 in July–August (Sr), and S2 in August–September (Sr).

TE ratios in larval shells differed among sites (i.e., natal sites were distinct) in May–June (MANOVA: $p < 0.001$) and August–September (MANOVA: $p = 0.02$; Table

A10). TE ratios in settled shells differed among sites (i.e., settlement locations were distinct) in July–August and August–September (MANOVAs: $p < 0.001$; Table A11). Larval shell site differences in May–June and August–September were driven by differences in Sr and Ni (first linear discriminate explained 69.6% of site variation) and Mn and Sr (first linear discriminate explained 61.5% of site variation), respectively, while settled shell site differences in July–August and August–September were driven by differences in Sr and Cu (first linear discriminate explained 60.0% of site variation) and Sr and V (first linear discriminate explained 75.4% of site variation), respectively (Table A12). Larval May–June and settled August–September shell differed in site separation (Fig. 11b) and were temporally variable (classification [100 and 89%, respectively] and jack-knifed reclassification [73 and 67%, respectively] success; Table A13). Among elements tested, Cd and As were not detected in spat (larval and settled) shells, and except for Sr, there was high collinearity among TE ratios in spat shells. Sr in settled shells had a weak positive relationship to salinity, but larval shells did not ($R^2 = 0.10$, $p = 0.05$).

Larval predictions.

Larval origins were only predicted for the May–June time period because TE ratios had the most differentiation among sites for this time period. In recent adult shells, TE ratios used for larval predictions differed among sites (MANOVA: $p < 0.001$; Table A14) (classification [92%]; jack-knifed reclassification [54%]; Table A15; Fig. A6), indicating that adult shells could be used as a proxy for natal site TE ratios. Recent shell site differences were driven by differences in Sr (first linear discriminate explained 70.9% of site variation; Table A16). All larvae that settled at site S1 were predicted to

originate from site A1 (probability >0.9; Table 3). Additionally, some larvae from sites

S3, S5, and S6 were predicted to originate from site A1 (probability >0.8) (Table 3).

Discussion

Spat settlement and connectivity

Larval transport processes are inherently stochastic (Pineda et al. 2007) and result

in variable spatial and temporal larval settlement patterns and subsequently

heterogeneous larval connectivity patterns (Siegel et al. 2008). Accordingly, oyster

settlement in the MB-EMS system was variable among sites, through sampling seasons,

and between years, showing overall patterns similar to other studies (Hoese et al. 1972;

Lee 1979; Saoud et al. 2000; Kim et al. 2010). Collectively this study and others indicate

a persistent gradient of increasing spat settlement westward from MB into EMS during

the past ~40 years (Hoese et al. 1972; Lee 1979; Saoud et al. 2000; Kim et al. 2010) (Fig.

6b). In this study, however, peak settlement was overall lower than in previous studies,

with the highest settlement within EMS in a known productive commercial harvesting

area in Alabama (S3; Gulf States Marine Fisheries Commission 2012). Kim et al. (2010)

also observed highest settlement in this commercial harvesting area during one yearly

survey, while the remaining surveys had highest settlement in western EMS. Similarly,

Saoud et al. (2000) found 7x greater spat settlement in this harvesting area in 1999

compared to 1998 but did not measure settlement in EMS, limiting conclusions about

EMS settlement during 1998–1999 (Fig. 6b).

Settlement timing (June–October) also occurred within the range reported in other studies in the MB-EMS system (Hoese et al. 1972; Lee 1979; Saoud et al. 2000). Observed peak settlement coincided with published summer peaks (late July–early August) in settlement (Hoese et al. 1972; Lee 1979; Saoud et al. 2000). Other published studies have reported summer and fall peaks in settlement, but this study did not assess fall settlement. However, I did find peak settlement occurring in late July and late September in 2014 and 2016, respectively. Due to missing settlement data from the later part of 2014 and the fact that settlement did not taper off during the sampling period in both years suggests that additional settlement could have occurred later in the season. While variability in the number of larvae, timing and location of settlement may influence interannual variation in connectivity, my data along with previous studies suggest that spatial and temporal settlement within the MB-EMS system is largely consistent across decades, and overall connectivity is likely to be similarly consistent on this time scale.

Yearly changes in salinity in response to varying freshwater discharge conditions, and to a lesser extent temperature, were responsible for differences in spawning, settlement, and growth patterns during this study (Fig. 9). Changes in salinity and temperature two to four weeks prior to peak settlement (i.e., break-points in regressions) likely triggered spawning events such that settlement occurred at higher salinity and lower temperature (2014 only) than spawning, consistent with findings in previous studies (Hoese et al. 1972; Hayes and Menzel 1981; Kenny et al. 1990; Ortega and Sutherland 1992). Specifically, a salinity increase of 4 to 10 units in both years and a 2°C increase in temperature in 2014 prior to the potential spawning event, likely

triggered spawning in the MB-EMS system (Fig. 9). Furthermore, settlement in the high

discharge year (2014) was only seen in EMS when high discharge potentially transported

larvae westward in EMS (Kim et al. 2013) or conversely, spawning only occurred in this

higher salinity region of EMS. In contrast, during the low discharge year (2016)

settlement was higher and more spatially wide-spread. Consequently, higher discharge in

2014 likely reduced the spatial scale of connectivity among oysters throughout the MB-

EMS system by limiting the magnitude and spatial scale of settlement. In this study,

maximum oyster growth also coincided with peak settlement and salinities higher than 20

(Figs. 7–9), which are known to be most favorable for settlement and growth (~15–23:

Davis 1958; Calabrese and Davis 1970; Chatry et al. 1983). It is important to note that

the discharge rates, salinities, and corresponding temperatures measured in 2014 and

2016 do not represent historical extremes. Environmental data were within the ranges

reported in previous settlement studies in the MB-EMS system (Hoese et al. 1972; Lee

1979; Saoud et al. 2000; Kim et al. 2010; discharge data not shown), further suggesting

longer-term consistency in environmental variation. Future studies could consider other

environmental factors, such as pH and DO, that may also be linked to freshwater

discharge and are of growing importance to larval demographics in global oceans

(Peguero-Icaza et al. 2011; Gerber et al. 2014).

Trace elements and connectivity

The use of adult shell as a proxy for natal site reference signatures enabled

assignment of larval origins and provided evidence of connectivity patterns between

adults and larvae in the MB-EMS system. There was high self-recruitment and

recruitment to nearby locations among larvae collected from EMS, where larval retention

is high (this study; Kim et al. 2010) and more than 90% of oysters from AL are historically harvested (May 1971). Although self- and nearby-recruitment was seen among EMS sites, probabilities were highest (>0.9) for the site farthest west in EMS, and other predicted sites had probabilities of (>0.5), indicating potentially high larval mixing in EMS or larvae originated from natal locations outside the study area (Table 3; Fig. 12). Interestingly, larval shells collected from lower and lower-mid MB near the MB ship channel had some larvae predicted to originate from the site farthest west in EMS, suggesting that oysters in EMS are important larval sources to this system and may be the primary source of larval oysters to some of the most productive harvest areas in the Gulf of Mexico (Zu Ermgassen et al. 2012).

Other studies have concluded that larvae are unlikely to pass from west to east MB due to flushing at the mouth. Under certain physical conditions (i.e., low river discharge (<500 m^3 s^{-1}), south to southwest winds, and tropic tides), however, small numbers of larvae may be transported to the lower-mid MB region against the expected dominant flow pathway (Kim et al. 2013). Conditions during May–June 2016 were conducive for larval transport from EMS to lower-mid MB (discharge: <298 m^3 s^{-1}; winds: southwest 4–8 m^3 s^{-1}). Additionally, when discharge conditions are <1715 m^3 s^{-1}, MB-EMS is a tidally-dominated system (Webb and Marr 2016) and larvae may use selective tidal stream (i.e., biological) transport to move from EMS to MB across multiple tidal cycles (Wood and Hargis 1971; Newell, Kennedy et al. 2005). Previous studies concluded that although biological transport is negligible to the overall pattern of larval transport in MB-EMS it does contribute to larval retention in EMS (Kim et al. 2010), which is in line with the results of this study. Thus, a combination of low river

discharge, wind-driven circulation, and tidal currents could transport larvae from EMS to lower-mid MB according to TE-based model predictions. It also is possible that similarities in the physiochemical environment, such as salinity and temperature, among sites led to difficulty discriminating sites using the LDA model. Overall, larval predictions showed self-recruitment and major connectivity to the EMS region.

Adult shells provided superior site separation compared to larval and settled shells of spat and had a high spatial resolution (adult and spat sites separated by ~2.5 km and ~11 km, respectively; Table 4). TE ratios in larval and settled shells were highly collinear, possibly due to high freshwater input into the system, which is known to increase variation in TE ratios due to mixing of environmental gradients (Miller et al. 2013a; Kroll et al. 2016). Spat shells likely were more affected by changes in freshwater input compared to adults due to: 1) shorter time spent (~2–3 week larval period) in the environment resulting in less reliable incorporation of elements into the shell and 2) a larval stage that experiences multiple water masses during transport, increasing the likelihood of encountering freshwater and potentially homogenizing TE signatures (Miller et al. 2013b). Other factors that affect TE resolution among sites in spat shells include growth rate and physiological state (higher elemental incorporation at faster growth rates: Carré et al. 2006; no elemental uptake during growth cessation: Schöne 2008), food composition (phytoplankton blooms increase elemental incorporation into shell: Thébault et al. 2009), and shell matrix composition (elements incorporated differently between calcite and aragonite: Lorens and Bender 1980; Weiss et al. 2002), all of which affect intake, assimilation, and retention of elements. High variability in spat TE ratios suggests that traditional larval outplant studies that do not provide time- and

spatially-integrated natal signatures such as via analysis of adult oysters, would be less useful (Becker et al. 2007; Carson et al. 2010; Kroll et al. 2018). I suggest the use of adult shells as a promising novel proxy for natal site TE reference signatures in highly dynamic environments. Future studies would benefit from validating adult TE ratios with *in situ* adult transplants to more accurately define location-specific time periods of TE incorporation.

Sr concentration, which has been documented to vary with salinity in taxa in many systems, consistently contributed to site separation in this study (Fig. 11). Sr was the most important TE ratio in larval and settled shells of spat to discriminate among sites in this study, and Sr was not correlated with other TE ratios. No collinearity suggests Sr was likely incorporated differently than other TE ratios (Lazareth et al. 2003). Sr is a commonly used salinity indicator (Dodd and Crisp 1982) despite some contradicting relationships depending on the study system and/or organism (e.g., positive relationship in fish otoliths [Secor et al. 1995]; negative relationship in *Crassostrea virginica* shells [Kroll et al. 2016]). Here, I found that Sr in settled shells had a weak positive relationship to salinity, but larval shells did not, which is not surprising given the potential movement of larvae across a highly variable salinity gradient in the freshwater-dominated MB-EMS system. Although understanding the cause of TE variation is not a requirement for use of elemental signatures in larval connectivity studies (Gillanders 2002; Carson 2010; Cook et al. 2014), more study on factors controlling Sr incorporation into eastern oyster shells, especially in freshwater-dominated systems would benefit application of TE for this and other indicator studies (see Lazareth et al. 2003). Localized sources of TE ratios, such as from industry, agriculture, groundwater, and river

discharge, may also contribute to among site variation (Charette and Sholkovitz 2002; Cordi et al. 2003; Carson et al. 2013). Overall, the potential for relatively high variation in TE ratios in larval and settled oyster shells within sites on short timescales (weeks) suggest the need to determine site- and temporally-specific elemental signatures for each study. This need may be particularly great in freshwater-dominated and urbanized estuaries like the MB-EMS system, which receive elements from multiple and poorly defined upstream sources.

Conclusion

Settlement data in conjunction with geochemical tagging data can provide information on larval origins and population connectivity that are critical to define priority areas for settlement and recruitment in freshwater-dominated systems. Together, a novel approach using settlement patterns and TE analyses indicated: 1) environmental attributes, particularly salinity and temperature, mediated connectivity because they affected magnitude, timing, and location of spawning and settlement (Fig. 9) 2) despite seasonal or interannual variation seen in this study and previous studies in the MB-EMS system, long-term connectivity is likely to be stable in the study area during the past several decades and this study provides a baseline and approach for measuring future change; and 3) higher spat settlement in conjunction with larvae predicted to originate from EMS indicate that the EMS could be an important source of larvae to the region (Fig. 8). Elemental tagging was able to use adult shell as a novel method to determine natal site reference signatures because the temporally integrated adult signature provided superior site separation (~2.5 km; Fig. 11) and TE ratios were not colinear. Higher TE

66

variation was recorded in spat shells during the ~2–3 week pelagic larval period likely

due to spatiotemporal variation in the physiochemical environment in the freshwater-

dominated MB-EMS system. Application to other systems will require similar study to

define site- and time-scale specific environmental attributes that mediate settlement and

TE ratios that can be used to determine connectivity. Overall, results indicate that

connectivity was largely mediated by freshwater discharge, winds, and tides, and

associated salinity changes, and these data can be applied to other regions of the world

where freshwater inputs are high or increasing due to habitat alteration or climate change.

This work highlights that a combined biological and geochemical approach can help

identify and predict how larval connectivity and subsequent adult distributions may

change through time in highly dynamic environments.

Tables

Table 3. Predictions of larval origins (May–June 2016) from the larval origin prediction linear discriminant function analysis using trace element (TE) ratios in recent adult shell (i.e., proxy for natal site TE ratios). Site indicates spat collection site and predicted site indicates adult shell collection site where larvae were predicted to originate from. Probability of group classification is the probability of larvae correctly originating from a site. Bold indicates the highest probability of site origination and thus indicates the predicted site. Each row represents an individual larva shell.

Site	Predicted site	Probability of group classification							
		A1	A2	A3	A3a	A3b	A4	A5	A6
S1	A1	**0.99**	0	0	0	0	0	0	0.01
S1	A1	**0.97**	0	0	0.01	0	0	0	0.02
S1	A1	**0.96**	0	0	0.01	0	0	0	0.03
S3	A3a	0.02	0	0	**0.47**	0	0	0.12	0.39
S3	A3a	0.05	0	0	**0.48**	0	0	0.1	0.36
S3	A1	**0.87**	0	0	0.03	0	0	0	0.1
S4	A5	0.02	0	0	0.15	0	0	**0.76**	0.06
S4	A5	0.03	0	0	0.19	0	0	**0.65**	0.13
S4	A4	0	0	0.22	0	0	**0.58**	0.2	0
S5	A1	**0.8**	0	0	0.08	0	0	0	0.12
S5	A1	**0.67**	0	0	0.17	0	0	0.01	0.15
S5	A6	0.2	0	0	0.33	0	0	0.03	**0.45**
S6	A6	0.06	0	0	0.34	0	0	0	**0.6**
S6	A1	**0.58**	0	0	0.12	0	0	0	0.3
S6	A1	**0.98**	0	0	0	0	0	0	0.02

Table 4. Field studies done in open coast and estuarine environments that determined spatial and temporal variability of trace element (TE) ratios in bivalve shells for use in larval connectivity studies. Spatial scale indicates the highest spatial resolution (i.e., the shortest spatial scale) that TE ratios provided within a continuous body of water (i.e., no bay to bay comparisons). Temporal scale indicates temporally variable (non-bold) and temporally non-variable (bold) time periods tested. Predicted larval origins refers to studies that classified larval origins from natal reference locations.

System type	Location	Species	Spatial scale (~km)	Temporal scale	Trace element ratios	Predicted larval origins	Reference
Open coast	Southern California	*Ostrea lurida*	25	Yearly	Cu, Ba, Pb, U	X	Carson 2010
Open coast	New Zealand	*Perna canaliculus*	> 11	**monthly**	Zn, Mn, B, Sr, Mg, Ba, Cu	-	Dunphy et al. 2011
Open coast	Portugal	*Mytilus galloprovincialis*	25	-	B, P, Co, Cu, Zn, Ce, Pb, U	X	Gomes et al. 2016
Open coast/Bays	Southern California	*Mytilus californianus, Mytilus galloprovincialis*	20	Weekly, monthly	Mg, Ca, Cr, Mn, Zn, Sr, Ba, Pb, U	-	Becker et al. 2005
Open coast/Bays	Southern California	*Mytilus californianus, Mytilus galloprovincialis*	20-30	-	Ca, Mn, Co, Sr, Ba, Pb, U	X	Becker et al. 2007
Open coast/Bays	New Zealand	*Austrovenus stutchburyi*	10	**> monthly**	Ca, Sr, Mn, Mg, Ba, Zn	-	Niemand 2009
Open coast/Bays	Southern California	*Mytilus californianus, Mytilus galloprovincialis*	-	-	Mn, Mg, Cu, U, Ba, Sr, Pb, Co	X	Carson et al. 2010
Open coast/Bays	Southern California	*Mytilus californianus, Mytilus galloprovincialis*	-	Weekly	Mg, Mn, Cu, Sr, Cd, Ba, Pb, U	-	Fodrie et al. 2011

69

Table 4 cont.

System type	Location	Species	Spatial scale (~km)	Temporal scale	Trace element ratios	Predicted larval origins	Reference
Estuary	Whangarei Harbour, New Zealand	*Austrovenus stutchburyi*	1.2 - 35	-	Li, B, Mg, Al, Ca, Ti, V, Mn, Fe, Co, Ni, Cu, Zn, Sr, Y, Ba, La, Ce, Pb, U	-	Norrie et al. 2016
Estuary	Pamlico Sound, NC	*Crassostrea virginica*	35	-	Mg, Ca, Mn, Cu, Sr, Sn, Ba, Pb	-	Kroll et al. 2016
Estuary	Pamlico Sound, NC	*Crassostrea virginica*	-	Monthly, yearly	Mg, Ca, Mn, Co, Cu, Sr, Cd, Sn, Ba, Pb	X	Kroll et al. 2018
Estuary	Mobile Bay, AL	*Crassostrea virginica*	2.5	Monthly, yearly	Mg, Sr, Ba, Pb, Fe, Cu, Mn, Zn, Ni, V, Cr, Co	X	This study
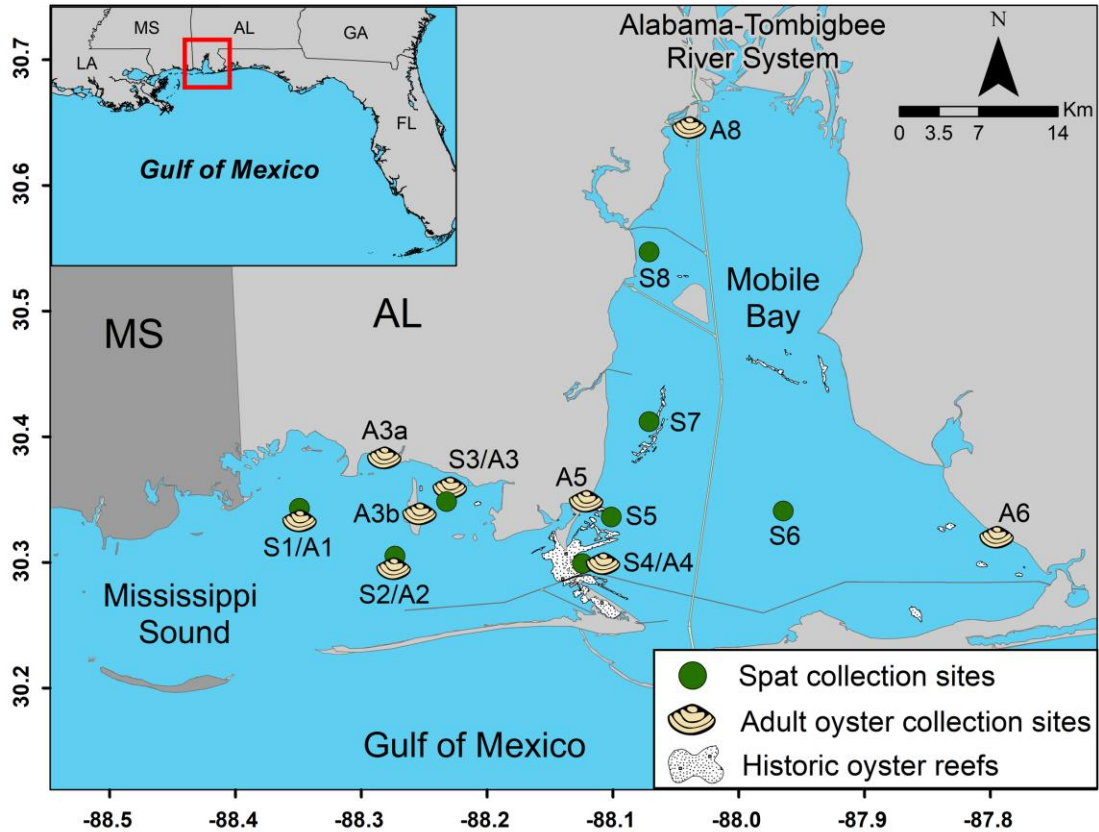
Figure 5. A site map showing settlement plate (green circles with "S") and native adult oyster collection (shell symbols with "A") sites in the Mobile Bay-eastern Mississippi Sound system. White shapes indicate known historic and present native oyster reef locations (layer citations: May 1971; Tatum et al. 1995; Alabama Department of Conservation and Natural Resources 2001).
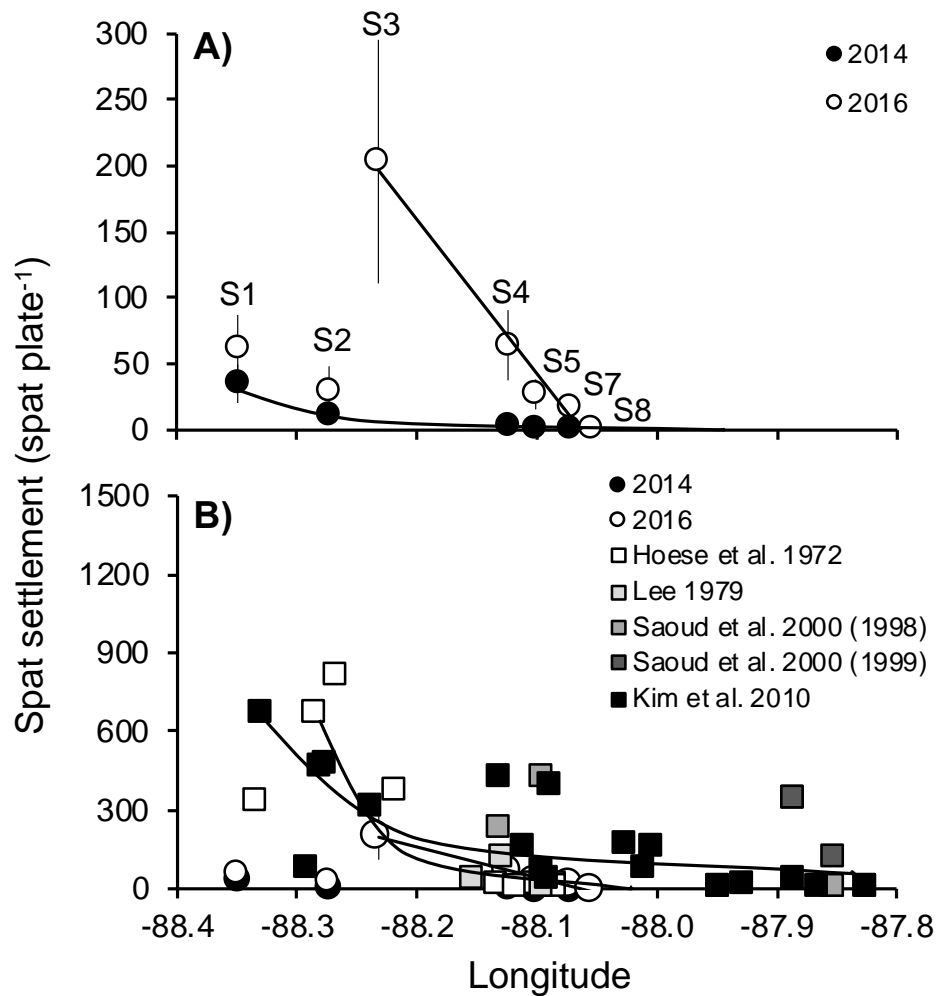
Figure 6. a) Average spat settlement per settlement plate for 2014 and 2016 collected from mid-May (day 150) to mid-August (day 234) in 2014 and from mid-May to mid-September (day 262) in 2016. Settlement increased westward in both years showing different patterns of increasing settlement between years. In 2014 settlement increased from S7 to S1 (EXP(y) = 17.47x – 1539.56, R^2 = 0.94, $F_{1,3}$ = 43.69, p = 0.007) and in 2016 settlement increased from S8 to S3 (y = -1225.10x – 107890, R^2 = 0.99, $F_{1,3}$ = 213.80, $p < 0.001$). b) Average spat settlement from previous studies conducted in the Mobile Bay-eastern Mississippi Sound system (square symbols) and from the current study (circles). One point (-88.1, 1541) in Saoud et al. 2000 (1999) not shown. Settlement increased westward in the Hoese et al. (1972) (EXP(y) = -10.17x – 892.71, R^2 = 0.59, $F_{1,9}$ = 21.81, p = 0.01) and Kim et al. (2010) (EXP(y) = -8.18x – 715.78, R^2 = 0.65, $F_{1,16}$ = 29.92, $p < 0.0001$) study.
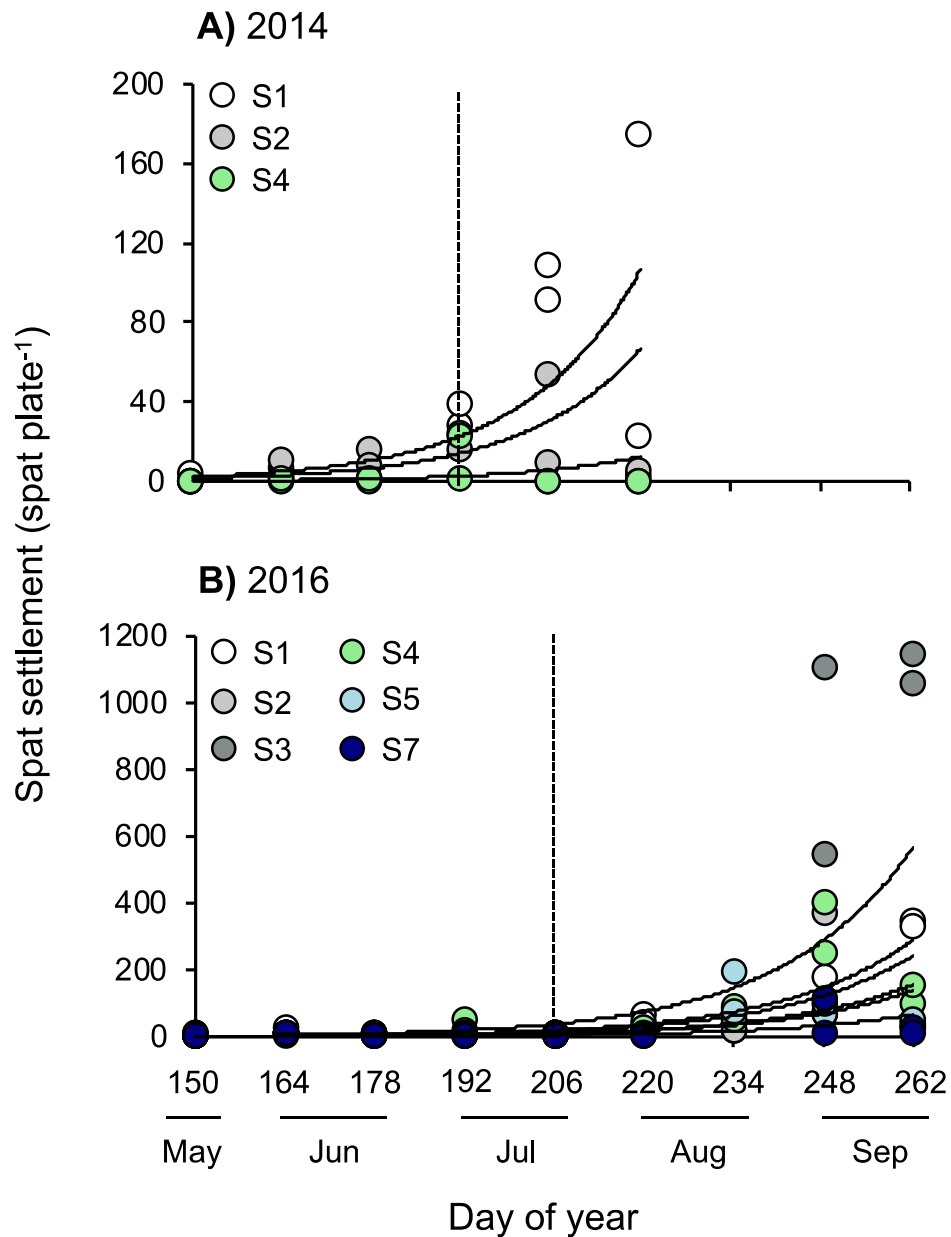
Figure 7. Spat settlement per settlement plate with time for 2014 (a) and 2016 (b), showing only the sites that had appreciable settlement. Dashed lines indicate a break-point from a slope of zero and represent the beginning of consistent settlement at all sites. Settlement increased exponentially with time at all sites with similar slopes (2014 negative binomial regression: slope = 0.38, $z = 5.19$, $p < 0.0001$; 2016 zero-altered negative binomial regression: slope = 0.34, $z = 10.59$, $p < 0.0001$), but different intercepts among sites (cf. intercept statistics Table A3).
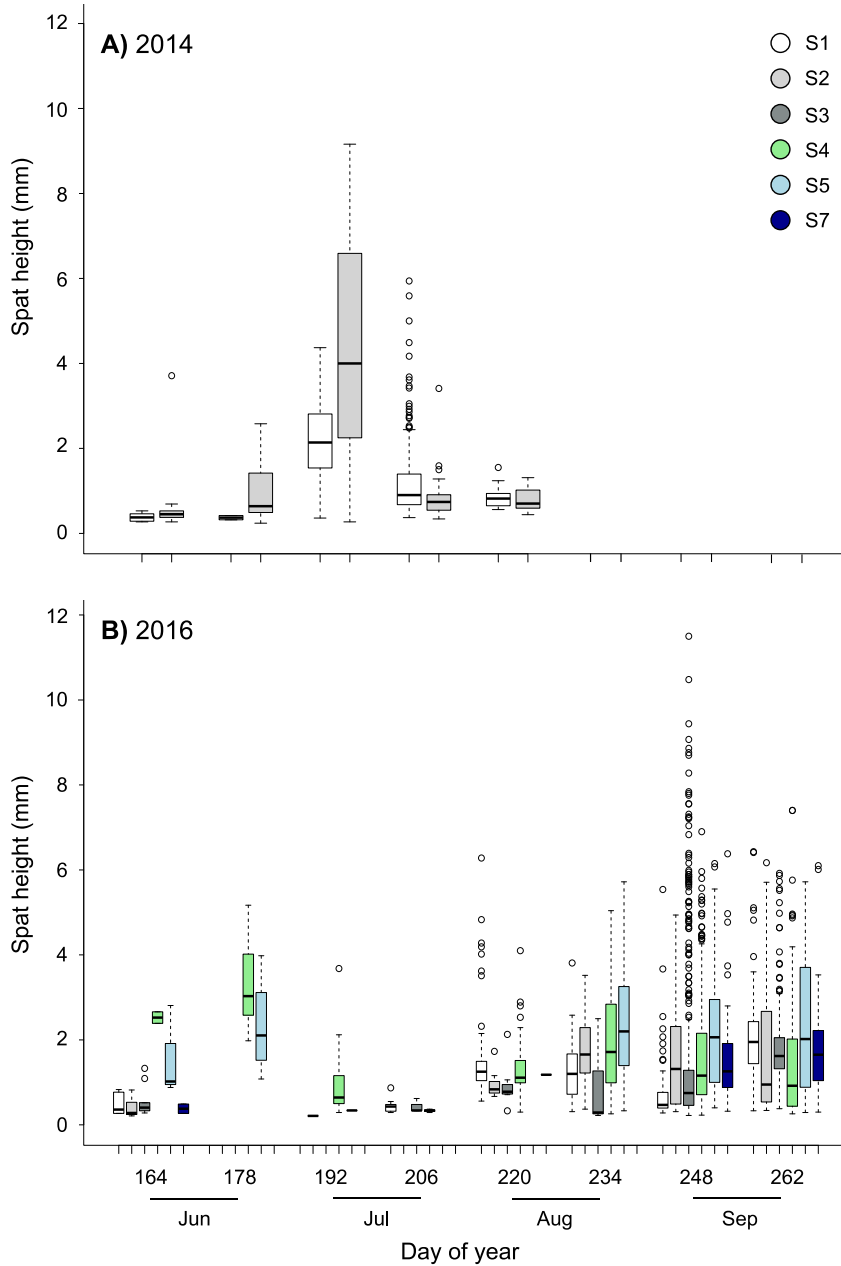
Figure 8. Boxplots of settled spat shell height (mm) measured from settlement plate spat separated by settlement site and sampling period for 2014 (a) and 2016 (b) data. Data collected from S4 in 2014 were removed due to low settlement limiting number of heights measured. The midline is the median of the data with the upper and lower limits being the first (25th) and third (75th) quantile. Whiskers are 1.5 times the interquartile range and circles are outliers. Measurable spat were observed starting from day 164 (early June).

74
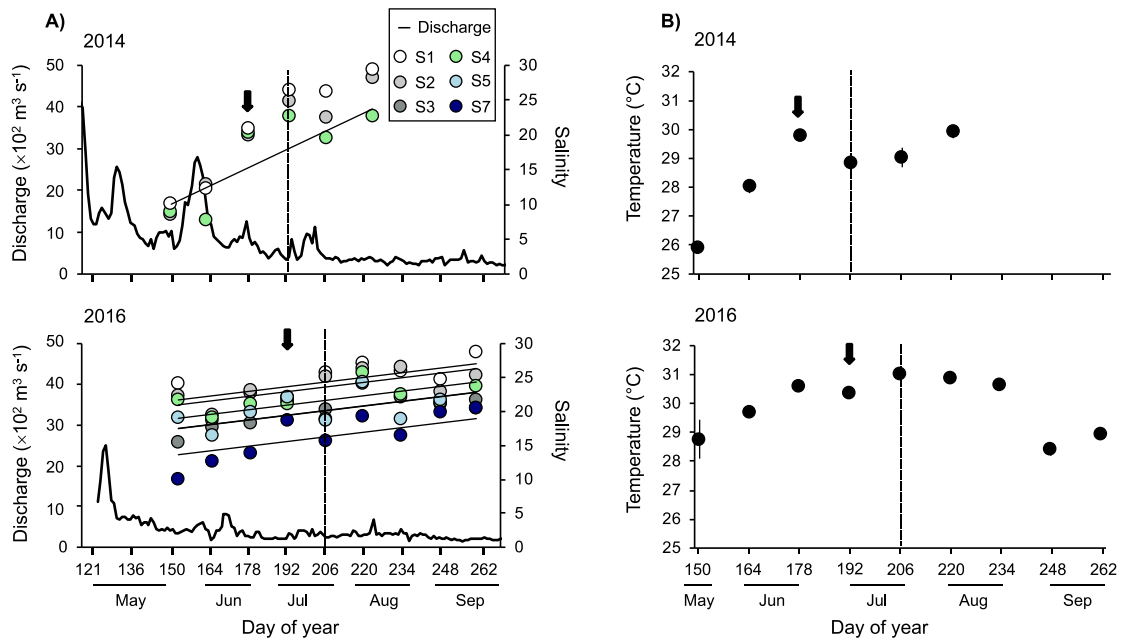
Figure 9. a) Freshwater discharge input and salinity (a) and temperature (b) for 2014 and 2016. For temperature each data point represents an average for all sites shown in Fig. 7 (averages were used because of no statistical differences among sites with time). Salinity in 2014 increased similarly at all sites with time ($y = 1.83x + 4.36$, $F_{3,14} = 25.85$, $p < 0.0001$). Salinity in 2016 varied among sites with time with the same slope (0.34) but different intercepts (cf. intercept statistics Table A4). Dashed lines indicate the beginning of an exponential increase in spat settlement. Arrows indicate possible brood stock spawning events.
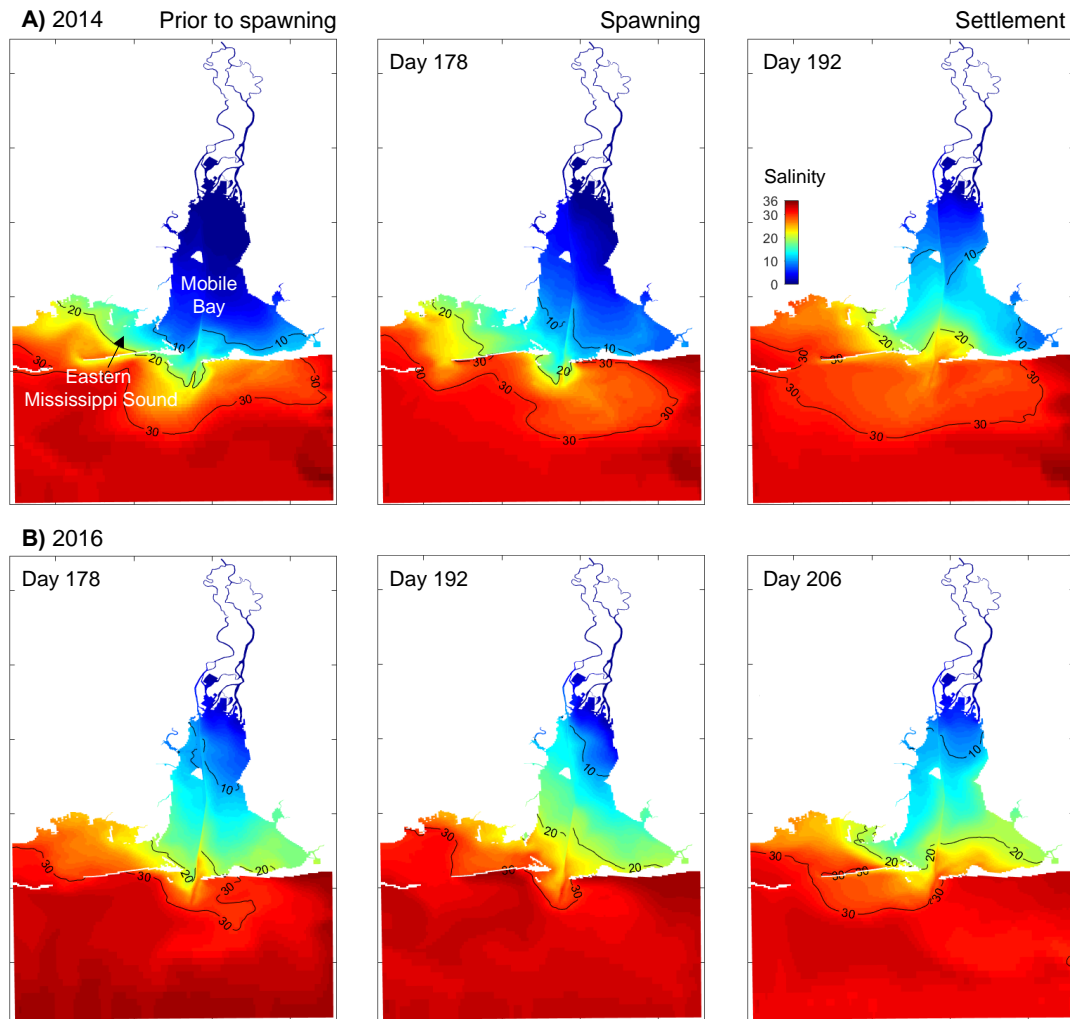
Figure 10. Model results for salinity conditions of the Mobile Bay-eastern Mississippi Sound system leading up to the beginning of an exponential increase in spat settlement for 2014 (a) and 2016 (b). The left panels show salinity conditions 2-weeks prior to the potential spawning event and 4-weeks prior to the increase in settlement. The middle panels show salinity conditions during the potential spawning event. The right panels show the salinity conditions during the increase in settlement. In both years peak settlement was in eastern Mississippi Sound (cf. Fig. 6).
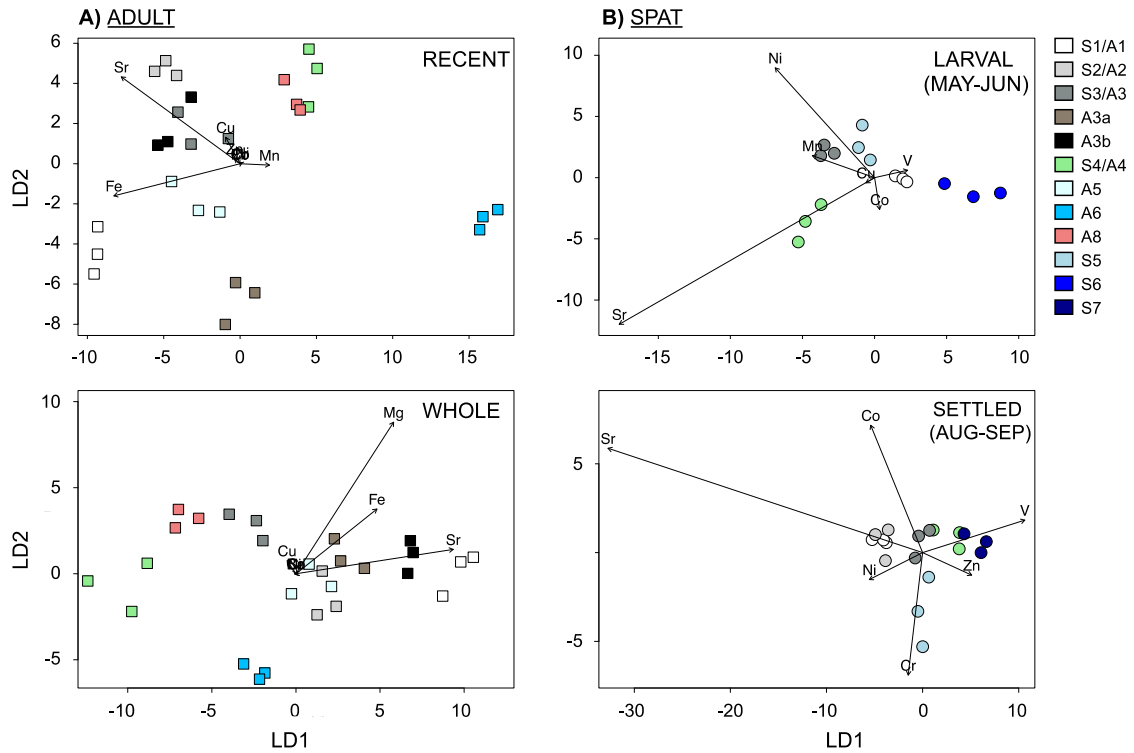
Figure 11. Biplots showing the first two linear discriminates of adult (a) and spat (b) shell linear discriminate function analyses. Adult shell panels show recent shell (top panel) representing ~single year and whole shell (bottom panel) representing multiple years. Spat panels show larval (top panel) and settled (bottom panel) shells for time periods that had different trace element (TE) ratios among sites (i.e., significant MANOVAs); May–June and August–September, respectively. Arrows indicate TE ratios causing site differences. Squares indicate adult shell sites (A1–6, A8) and circles indicate spat shell sites (S1–7).

77
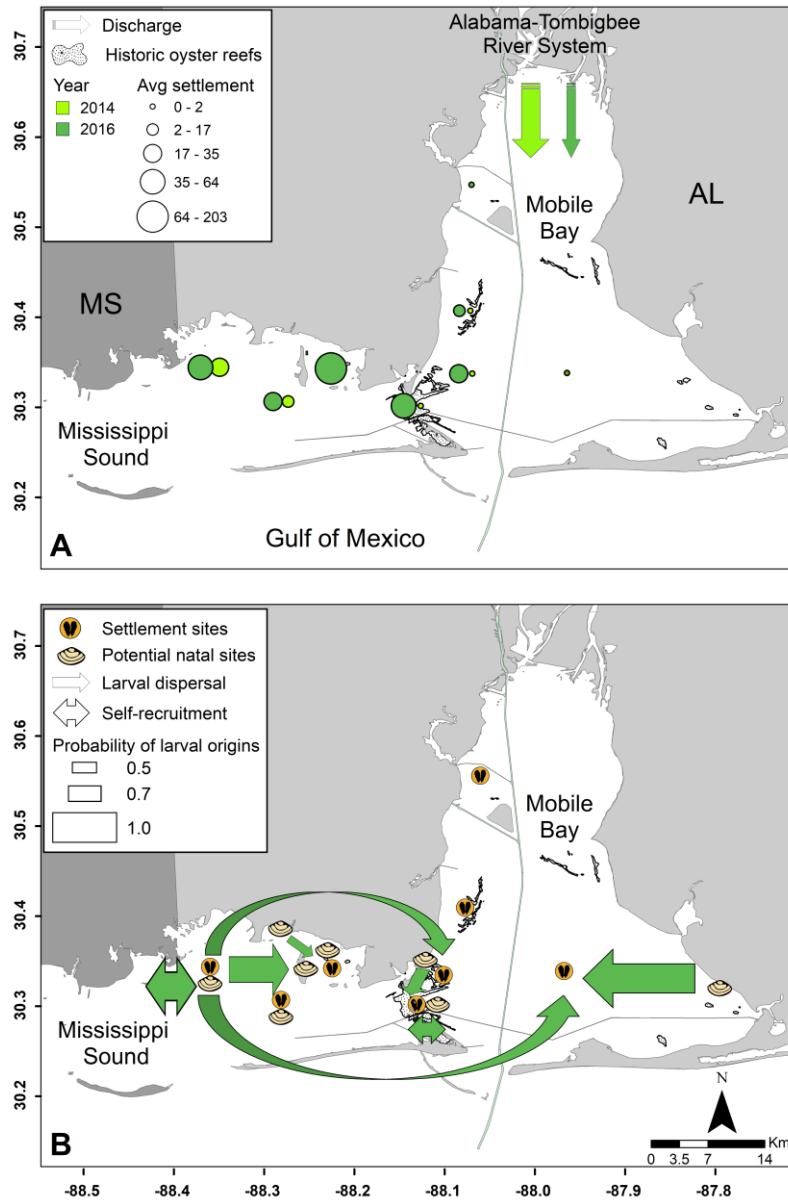
Figure 12. Average spat settlement (circles) and freshwater discharge (hatched arrows) in 2014 and 2016 (a). Larger circles indicate higher average spat settlement and thicker hatched arrows indicate higher freshwater discharge. Connectivity patterns (i.e., arrows from predicted larval origins to settlement sites) for the May-June 2016 time period when TE ratios were distinct among sites (b). Thicker arrows indicate higher probability of correctly predicting larval origins from a natal site. White shapes indicate known historic and present native oyster reef locations (layer citations: May 1971; Tatum et al. 1995; Alabama Department of Conservation and Natural Resources 2001).

CHAPTER 3

STRAIGHT TO THE SOURCE: UNDERSTANDING WASTEWATER INPUTS IN A FRESHWATER-DOMINATED SYSTEM

<u>Abstract</u>

Freshwater-dominated coastal systems often have high wastewater loads, but wastewater inputs to these fluvially-fed systems are under-studied. To define and quantify the relative influence of different wastewater sources to these systems, I determined 1) if point (wastewater treatment plants [WTPs]) or non-point (rivers: aggregation of non-point sources) inputs were primary wastewater sources and 2) the extent of wastewater influence (nutrient and microbial inputs) downstream. Nutrient (N, P) and microbial (bacteria, virus) wastewater indicators were sampled seasonally under high and low flow conditions from WTPs and rivers discharging into a freshwater-dominated north-central Gulf of Mexico estuary. Wastewater indicators were higher in a high flow subsystem, where source flow rates were 26x (WTP) and 253x (river) larger than those in a low flow subsystem. WTP effluent had higher nutrient but lower microbial concentrations compared to rivers, in line with removal of indicator microbes via WTP disinfection. When flow volume was considered, however, wastewater

indicator loads were higher from the river within the high flow subsystem, but nutrient

load dominance within the low flow subsystem depended on the nutrient species. Both

WTPs and rivers delivered wastewater indicators to downstream sites, but overall, rivers

were larger nutrient sources, except during high WTP flow. Rivers influenced indicator

bacteria directly by delivering bacteria and indirectly by providing nutrients for bacterial

growth. Additionally, seasonal variation in flow and temperature affected load influence

at downstream sites. These data provide critical information for understanding how flow

conditions influence wastewater pollution in freshwater-dominated systems and may be

applied to mitigate water quality declines and human health effects.

Introduction

Nutrients and microbial pollutants from human and animal waste are delivered to

estuaries from point (e.g., wastewater treatment plants [WTPs]) and distributed non-point

(e.g., watershed inputs via rivers, surface runoff, atmospheric deposition) sources.

Nutrient pollution is a major problem in estuarine environments (National Research

Council 2000; Howarth et al. 2002; Barbier et al. 2011), where it is known to increase

eutrophication and lead to ecosystem degradation (Nixon 1995; Cloern 2001; Rabalais

2002; Kennish 2002). Wastewater associated microbial pollution additionally is a public

health concern and can result in shellfish harvest area closures due to risks from

consumption of contaminated shellfish (Rippey 1994). Increased precipitation and

population density can lead to changes in WTP and riverine flows, which in turn, affect

nutrient and microbial delivery to a system (El-Din and Smith 2002; Borsuk et al. 2004).

Due to high surface flows, freshwater-dominated and urbanized systems have potential

for higher nutrient and microbial loads and greater interaction between point and non-point sources (Vollenweider 1976; Bertrand-Krajewski et al. 1995; Dorioz et al. 1998; Edwards and Withers 2008). Although freshwater-dominated estuarine systems exist in coastal areas globally, studies quantifying wastewater loads have largely overlooked local fluvial hydrology or were mostly done in groundwater fed systems (e.g.; Valiela et al. 1992; Capone and Bautista 1995; Seitzinger and Harrison 2008).

The downstream influence of point and non-point wastewater sources can be mediated by seasonal differences in freshwater flow and associated changes in environmental conditions. Globally, seasonal flows from rainfall and runoff are highest from May to September (Dai and Trenberth 2002), but vary regionally, with flows in some temperate estuaries higher in colder periods due to upstream runoff (Billen et al. 2001; Brown and Ozretich 2009; Novick and Senn 2014). During warmer periods, nutrient uptake can increase due to increased phytoplankton productivity, resulting in lower nutrient concentrations in some areas (Dugdale et al. 2007). In contrast, during colder periods, nutrient concentrations may be higher due to both higher nutrient delivery and lower biological activity (Kemp and Boynton 1984). Microbes are similarly affected by seasonal changes in environmental conditions, such as temperature and salinity; bacteria proliferate in warmer periods, but viruses persist longer in colder periods (Lipp et al. 2001; Fong and Lipp 2005). Coliform bacteria, for example, are also known to survive better at lower salinities (Anderson et al. 1979). While individual studies have considered the relative contribution of point and non-point inputs, no study has investigated the relative importance of these sources in a single system, under different flow regimes.

Nutrient and microbial inputs provide key evidence for routes of wastewater

exposure to a system. Nutrients increase with proximity to sources, and nutrient species

can be source specific. For example, NO_3^- often dominates from septic tanks and

urbanized rivers, while NH_4^+ can dominate agriculturally-influenced rivers (Weiskel and

Howes 1992; Carpenter et al. 1998; Tao et al. 2008). Different treatment methods or

levels of treatment employed by WTPs (i.e., biological nutrient removal, activated

sludge, etc.) can also affect the quantities and forms of nutrients discharged (Carey and

Migliaccio 2009). Similarly, indicator microbes are used to assess the sanitary quality of

a waterbody by indicating presence of pathogenic microbes (bacteria and viruses)

associated with human sewage and wildlife feces (United States Environmental

Protection Agency 2003, 2006). Indicator bacteria, such as fecal coliforms and

Escherichia coli, are typically used to assess fecal contamination in estuarine and

shellfish waters (United States Environmental Protection Agency 1986, 2012; National

Shellfish Sanitation Program 2015); however, indicator bacteria are poor indicators of

viral presence, which are more directly associated with human health risks (Doré and

Lees 1995; Wetz et al. 2004; Flannery et al. 2009). Thus, indicator viruses, such as male-

specific coliphage (MSC), which are also present in wastewater, have been used as

surrogates for human enteric viruses and have been used to monitor shellfish for viral

contamination (Doré et al. 2000; Sinton et al. 2002; Flannery et al. 2009). Current

regulations allow the use of MSC in conjunction with fecal coliforms to assess the

sanitary quality of shellfish waters near WTP discharges (National Shellfish Sanitation

Program 2015). Because indicator microbes are not always correlated with pathogenic

microbes, especially under varying environmental conditions (Winfield and Groisman

2003; Biancani et al. 2011), the use of multiple wastewater indicators (i.e., nutrients and indicator microbes) can better detect and help mitigate effects of wastewater contamination (Vant 2001; Schindler 2006).

To determine the relative contribution of point and non-point wastewater sources in higher and lower flow regions (referred to as "subsystems") of the freshwater-dominated Mobile Bay-eastern Mississippi Sound (MB-EMS) system, wastewater indicator (nutrients and indicator microbes) concentrations and loads (source flow rate × concentration) were measured seasonally over two years at WTPs (point) and riverine discharge (non-point) locations. Rivers in this study are considered non-point sources because they represent an aggregation of non-point sources including agricultural activities, runoff, sewer overflows, atmospheric deposition, and other sources that are introduced in a diffuse manner (Duda 1993; Van Drecht et al. 2003), resulting in unknown pollution sources in river samples. Furthermore, high and low flow subsystems were sampled, representing two differing regions of the MB-EMS system where a high flow subsystem included a paired high flow WTP and river and a low flow subsystem included a paired low flow WTP and river. Specifically, to determine which wastewater source (WTP or river) was larger within each subsystem, which subsystem had higher wastewater inputs, and downstream effects, I compared indicator concentrations and loads between sources and subsystems and to environmental attributes in receiving waters. Overall, to better understand system-wide wastewater inputs I combined data for all major WTP and river sources. These data may have important implications for understanding the fate of wastewater pollution and subsequent water quality degradation

in freshwater-dominated systems that have a mosaic of different fluvial and anthropogenic influences.

Methods

Study sites and sampling scheme

The Mobile Bay-eastern Mississippi Sound (MB-EMS) system (Fig. 13) located in the north-central Gulf of Mexico, has the highest freshwater inflow per estuary area of all U.S. estuaries (Ward 1980) and, like many other urbanized estuaries, is experiencing population growth and land-use changes, with higher population growth and urbanization occurring along northern MB compared to EMS (Ellis et al. 2011). This freshwater-dominated estuary was selected to study point (WTPs) and non-point (rivers) wastewater sources because there is a gradient of high to low river and WTP effluent discharges coinciding with urbanization in the watershed (Table 5), such that within a single system I could measure and compare a paired high flow WTP and river to a paired low flow WTP and river. I sampled a known high flow WTP (Clifton C. Williams WTP in Mobile, AL) and river (Mobile River) in close proximity in northern MB (high flow subsystem) and a known low flow WTP (Buford L. Bryant WTP in Bayou La Batre) and rivers (Bayou La Batre River and West Fowl River) in close proximity in EMS (low flow subsystem) (Fig. 13; Table 5). To determine the potential influence of a smaller river to the high flow site, I also sampled adjacent Dog River, a tributary of MB. To define downstream effects, I sampled potential receiving sites, MB1 and MB2 in northern MB (high flow subsystem) and BLB1, BLB2, and BLB3 in EMS (low flow subsystem). To

quantify system-wide wastewater input, an additional WTP (Fairhope) and river (East Fowl River) site were sampled for wastewater indicators (Fig. 13; Table A17). WTPs sampled were secondary removal systems (using physical and biological methods) and did not have advanced nutrient removal.

To account for seasonal variation, sampling was conducted during warm (May–September) and cold (November–January) seasons. Accordingly, sites were sampled monthly from May–September 2015, June–September 2016, November 2015–January 2016, and November 2016–January 2017, except BLB3 and Fairhope WTP, which were sampled only during the latter two warm and cold seasons.

Effluent and water sampling

Treated effluent from WTPs was directly collected from the dechlorination (Mobile WTP) or ultraviolet (UV: Bayou La Batre and Fairhope WTP) chamber prior to release into the outfall pipe using a 1 L Nalgene bottle stick sampler. Water samples were collected for wastewater indicators at the surface of dredged river mouths (total depth >3 m) and 1 m off the bottom at receiving sites, using a horizontal water sampler (Wilco). Samples from river mouths were collected 2–4 hours after high tide to maximize capture of wastewater indicators discharging from rivers, representing a potential multitude of non-point sources. Samples collected for nutrients were pre-filtered through a 150 μm mesh and collected in 1 L acid-washed opaque Nalgene bottles. Samples for indicator microbes were collected in sterilized 500 mL Nalgene bottles (not pre-filtered); samples directly collected from the dechlorination chamber (Mobile WTP) had sodium thiosulfate added as a dechlorinating agent to prohibit bactericide during

sample transit (American Public Health Association 1999). All samples were kept on ice

and processed within 24 hours.

Wastewater indicators

Nutrients.

To determine nutrient concentrations in effluent and water samples, samples were

vacuum filtered through pre-ashed 25 mm 0.7 μm pore-size glass fiber filters (GF/F)

(EMD Millipore). Filtrate was collected and frozen at -20°C until analysis. Inorganic

nutrients (NO_3^-, NO_2^-, NH_4^+, PO_4^{3-}, TDN) were measured on a Skalar San+ Autoanalyzer

according to Strickland and Parsons (1972). DIN was calculated as the sum of NO_3^-,

NO_2^-, and NH_4^+. DON was calculated as DIN subtracted from TDN.

Indicator microbes.

To determine indicator microbes in effluent and water samples, bacterial (fecal

coliforms [FC] and *Escherichia coli* [EC]) and viral (male-specific coliphage [MSC])

indicator concentrations were enumerated. FC and EC were determined using membrane

filtration (Dufour et al. 1981). Samples were vacuum filtered through 47 mm, 0.45 μm

pore-size mixed cellulose ester filters (EMD Millipore), transferred to membrane

thermotolerant *E. coli* (m-TEC) media plates, inverted, and incubated at 35.0°C for 2

hours for resuscitation. Samples were then incubated at 44.5°C for 18–24 hours (Rippey

et al. 1987). FC were enumerated as colonies that were yellow, yellow-green, or yellow-

brown; EC were enumerated as colonies that remained yellow after adding of 1 mL of

urease reagent to membrane filters for 2–15 minutes of incubation at room temperature

(urease negative). MSC was determined using a double-agar overlay method according

to Cabelli (1990). Tryptone broth was used as the growth media for Famp *E. coli* (host *E.*

coli resistant to streptomycin and ampicillin) and incubated at 35°C for 3–4 hours until turbid. After incubation, 0.2 mL of the bacterial suspension and 2.5 mL of sample was added to tempered agar and poured over Famp media plates. Once solidified, plates were inverted and incubated at 35°C for 18–24 hours and MSC plaques were enumerated.

Environmental attributes

To determine if environmental attributes contributed to variation in wastewater indicator concentrations at receiving sites, data were collected for salinity, temperature, dissolved oxygen (DO), chlorophyll *a*, wind direction (which may affect surface flow and water level in the study area; Kim and Park 2012), tidal amplitude, and rainfall. Salinity, temperature, and DO were measured using a YSI Pro 2030 handheld data sonde. To determine chlorophyll *a* (proxy of phytoplankton concentration), water samples were collected as described above for nutrient analyses and 15–40 mL of water was filtered through 25 mm, 0.7 μm pore-size GF/F (EMD Millipore). Chlorophyll *a* was extracted using a 2:3 DMSO:90% acetone solution (MacIntyre and Cullen 2005) and analyzed on a Turner Designs TD700 fluorometer. To determine wind direction at the time of sampling, wind data were collected from NOAA National Data Buoy Center (ndbc.noaa.gov; last accessed 2 February 2019) and averaged over 24 hours prior to sampling. Stations used for high flow sites were Meaher Park (MHPA1) and Middle Bay Lighthouse (MBLA1); stations used for low flow sites were Cedar Point (CRTA1) and Katrina Cut (KATA1). To determine tidal amplitude at the time of sampling, mean sea level tide data were collected from NOAA Tides and Currents (tidesandcurrents.noaa.gov; last accessed 2 February 2019) and averaged over 24 hours prior to sampling. Stations used for high flow sites were Mobile State Docks (8737048)

and Dog River Bridge (8735391); stations used for low flow sites were West Fowl River

Bridge (8738043) and Bayou La Batre Bridge (8739803). Rainfall data for high flow

sites were collected from the Mobile downtown airport (ndbc.noaa.gov; station ID:

GHCND:USW00013838), and rainfall data for low flow sites were collected from the

Garland Street Pump Station rain gauge (Bayou La Batre Utilities Board). Because

wastewater indicators are known to increase hours to days after a rain event (Hubertz and

Cahoon 1999, He and He 2008), rainfall accumulations over 24, 48, and 72 hours were

calculated and compared to wastewater indicator concentrations at sites using regression

analysis. The 72-hour accumulation data had the best relationships to wastewater

indicators and were used in all subsequent analyses.

Source loads

Loading rates.

To determine source (WTP, river) nutrient and indicator microbial loading rates

(i.e., loads), source flow rates were multiplied by wastewater indicator concentrations.

To determine if chlorophyll *a* from river sources had an effect on nutrient concentrations

at receiving sites, chlorophyll *a* river loads were calculated. Flow rates used for

calculations corresponded to the day the effluent or water sample was taken because

relationships were best for the day of sample collection compared to a day before and two

weeks before sample collection.

Effluent and river flow rates.

Effluent flow rates were obtained from individual WTP and Utility Board

facilities. To determine river flow, flow rates were downloaded from United States

Geological Survey (USGS) (waterdata.usgs.gov; last accessed 18 November 2018)

gauging stations 02470629 (Mobile River [MR] at Bucks) and 2471078 (Fowl River).

West Fowl River (WFR) and East Fowl River flow were taken directly from Fowl River

flow. Because Dog River (DR), Fowl Rivers (FR), and Bayou La Batre River (BBR) are

similar in size, flow for DR and BBR were derived from the FR flow using:

$$\text{DR or BBR flow } (\text{m}^3\text{s}^{-1}) = \text{FR flow } (\text{m}^3\text{s}^{-1}) \times \frac{\text{DR or BBR drainage basin } (\text{km}^2)}{\text{FR drainage basin } (\text{km}^2)} \qquad (1)$$

FR, DR, and BBR drainage basins are 42.73 (waterdata.usgs.gov), 241.62 (United States

Geological Survey 2017), and 78.14 km^2 (Alabama Department of Environmental

Management 2009), respectively. MR data were tidally influenced, and data were tidally

filtered using a 40–hour Lanczos filter prior to use. After filtering, flooding discharge

(i.e., overbank flow) was not seen according to USGS flooding levels indicating

discharge did not exceed measurable limits.

Relative influence of sources

To determine the relative subsystem influence of WTPs compared to river

sources, ratios of WTP load to river load were calculated for high (Mobile WTP:Mobile

River) and low (Bayou La Batre WTP:Bayou La Batre River) flow subsystems such that

WTP:river load >1 indicated the WTP source was larger and <1 indicated the river source

was larger.

Wastewater influence on the system

To determine if source wastewater loads (i.e., wastewater influence) or

environmental attributes explained wastewater indicator concentrations at receiving sites,

information theoretic multivariable model selection (Johnson and Omland 2004;

Anderson and Burnham 2004) was performed on high and low flow subsystems. Each

receiving site was modelled separately (high flow: $n = 2$; low flow: $n = 3$) for all

wastewater indicators (nutrients: $NO_3^- + NO_2^-$, NH_4^+, PO_4^{3-}, TDN, DIN, DON; indicator

microbes: FC, EC), except MSC in each flow subsystem and FC and EC in the low flow

subsystem due to low indicator microbe detection, resulting in 34 global models

(inclusive of 6 nutrients at 5 sites and 2 indicator microbes at 2 sites; explanatory

variables: Table A18).

To avoid overfitting of the models due to small sample size compared to the

number of possible explanatory variables, only explanatory variables that had a potential

predictable relationship to the dependent variable were included at the beginning of

model selection. Only independent explanatory variables were included in models, and

due to non-independence of some variables, the inclusion of variables differed among

models. Collinearity was defined among explanatory variables via variance inflation

factors (VIFs) and individual Pearson correlations. A VIF >3 (Zuur et al. 2007) and

significant correlations with an r >0.6 (Zuur et al. 2009) indicated collinearity. Collinear

explanatory variables were either 1) included in the model with an interaction term if

there was an ecologically relevant reason (e.g., variables with potential additive effects,

such as source loads in close proximity) or 2) dropped from the model. To determine the

global model, i.e., the most complex candidate model without collinearity, full models

were run, and variables were dropped until all VIFs <3 (Zuur et al. 2007). Variables

were dropped from the global model in a stepwise fashion and variable inclusion or

exclusion was determined via Akaike information criterion for small sample size (AICc).

Model selection ended with a set of candidate models and a null model (y = data ~

1). Akaike weights (w) were then calculated for each candidate model and unless there

was a candidate model with *w* >0.9, indicating best model fit for a single candidate

model, parameter estimates were weighted by *w* for model averaging to make an

inference about the model set (Burnham and Anderson 2002; Burnham et al. 2011). *P*-

values were recalculated from the averaged parameter estimates. Homogeneity of

variances and normality of residuals were checked using Bartlett's and Shapiro-Wilk's

tests, respectively. Log transformations were applied to the dependent variable if

heterogeneity and normality assumptions were violated. Outliers were determined as two

standard deviations from the mean. Models with outliers that could be explained as

important system processes (i.e., high source flows and/or concentrations) were run with

and without outliers. Model selection was performed in RStudio Version 1.1.453 (R

Core Team 2017) and an α of 0.05 was used.

Estuarine-scale wastewater inputs

To determine if WTPs or rivers input more wastewater indicators system-wide, a

combined nutrient and indicator microbial load was calculated. Average nutrient and

indicator microbial loads for each WTP and river for all sampling periods (Fairhope: *n* =

6; all other sampling sites: *n* = 13) were calculated, and average WTP loads (3 WTPs)

and average river loads (5 rivers) were summed to directly compare which source was

larger to the system.

Other statistical analyses

To determine if nutrient and indicator microbial concentrations and loads and

source flow rates were different in the WTP versus the river within each subsystem

through time, three-way ANOVAs with source (WTP, river), season (warm, cold), and

year (2015, 2016) as factors were conducted with high and low flow subsystems

modelled separately. To determine if nutrient and indicator microbial concentrations and loads and source flow rates were different between sources in high and low flow subsystems (WTPs, rivers) through time, three-way ANOVAs with flow (high, low), season (warm, cold), and year (2015, 2016) as factors were conducted with WTPs and rivers modelled separately. To determine if receiving sites had different nutrient and indicator microbial concentrations and environmental attributes, three-way ANOVAs with site (MB1, MB2, BLB1, BLB2), season (warm, cold), and year (2015, 2016) were conducted. Receiving site BLB3 was not included in statistical analyses because only one year of data was collected.

To determine if nutrient and indicator microbial load ratios (WTP:river) differed within each subsystem, two-way ANOVAs were conducted with season (warm, cold) and year (2015, 2016) as factors with high and low flow subsystems modelled separately. To determine if nutrient and indicator microbial load ratios (WTP:river) differed between subsystems, a three-way ANOVA was conducted with flow (high, low), season (warm, cold), and year (2015, 2016) as factors.

When applicable, nutrient and indicator microbes were log transformed to ensure homoscedasticity and normality of residuals and tested with Bartlett's and Shapiro-Wilk's tests, respectively. When data had unequal variances, but normally distributed residuals, a white-adjusted ANOVA for heteroscedasticity was performed. For all cases where interactions were not significant, ANOVAs were re-run without interactions. Tests were performed in RStudio Version 1.1.453 (R Core Team 2017). All α were set at 0.05 and error is presented as standard error.

Wastewater indicator concentrations

Nutrients.

Within each high and low flow subsystem, nutrient concentrations were higher at the WTP compared to the river (Tables 6 and A19). When comparing sources (WTPs and rivers) between high and low flow subsystems, differences in nutrient concentrations were dependent on nutrient forms. The high flow WTP had lower $NO_3^- + NO_2^-$ and PO_4^{3-}, but higher NH_4^+ concentrations compared to the low flow WTP, while the high flow river had higher DIN concentrations (driven by $NO_3^- + NO_2^-$) compared to the low flow river (Tables 7 and A19). At receiving sites, inorganic nutrients were higher at high flow sites compared to low flow sites. For example, high flow receiving sites (MB1, MB2) had higher $NO_3^- + NO_2^-$ and TDN concentrations compared to low flow receiving sites (BLB1, BLB2). Receiving site MB1, nearest to the high flow WTP and river, had the highest nutrient concentrations for all nutrients (Tukey HSD: $p < 0.02$ for all comparisons) except DON (Tukey HSD: $p = 0.08$) (Tables 8 and A19).

Comparing between seasons, high flow subsystem DIN concentrations (driven by $NO_3^- + NO_2^-$) decreased and low flow subsystem DON concentrations increased during the warm season vs. the cold season (Tables 6 and A19). Results were driven by lower DIN (driven by $NO_3^- + NO_2^-$) in the high and low flow rivers and higher DON in the high and low flow WTPs in the warm season compared to the cold season (Tables 7 and A19). Nutrient concentrations at receiving sites followed river concentrations with lower DIN (driven by $NO_3^- + NO_2^-$) in the warm season compared to the cold season (Tables 8 and

A19). Comparing between years, source nutrient concentrations within the high flow subsystem did not differ between years, but sources within the low flow subsystem had higher TDN (driven by $NO_3^- + NO_2^-$ and DIN) in 2015 compared to 2016 (Tables 6 and A19). Similarly, higher DIN concentrations (driven by $NO_3^- + NO_2^-$) were found in the high and low flow WTPs in 2015 (Tables 7 and A19). High and low flow rivers had higher TDN concentrations (driven by both DIN and DON) in 2015 (Tables 7 and A19). Receiving sites followed river concentration patterns, and all N forms were higher in 2015 (Tables 8 and A19).

Indicator microbes.

Within the high flow subsystem, indicator bacterial (FC and EC) concentrations were not statistically different between the WTP and the river, but the indicator virus, MSC, was higher in the WTP compared to the river (Tables 6 and A20). Due to many non-detect measurements (FC and EC: <5 CFU 100 mL^{-1}; MSC: <10 PFU 100 mL^{-1}) in the low flow subsystem, statistical comparisons of the WTP versus the river within the low flow subsystem, and comparisons between high and low flow WTPs and receiving sites were not performed. Although statistical comparisons could not be made, FC and EC concentrations were lower in the WTP compared to the river, and MSC was only measured above detection in one river sample within the low flow subsystem (Tables 6 and A20). As expected, the high flow WTP had higher concentrations of all indicator microbes compared to the low flow WTP, while the high flow river had lower FC, but higher MSC concentrations compared to the low flow river (Tables 7 and A20). Accordingly, receiving sites in the high flow subsystem had higher indicator microbial concentrations compared to low flow sites (Tables 8 and A20).

Seasonal comparisons showed that within each high (significant comparisons) and low (no statistical comparisons) flow subsystem, FC and EC concentrations were lower in the warm season compared to the cold season, and MSC did not have seasonal differences (Tables 6 and A20). Results were driven by lower FC and EC concentrations in the warm season compared to the cold season in both the high and low flow rivers (Tables 7 and A20). All indicator microbial concentrations at the high and low flow WTPs were not different between seasons (no statistical comparisons) (Tables 7 and A20). Similarly, indicator microbial concentrations at receiving sites were not different between seasons (no statistical comparisons) in either subsystem (Tables 8 and A20), and low flow receiving sites had only one FC and EC measurement (December 2016: FC: BLB1: 2950, BLB2: 50, BLB3: 195 CFU 100 mL^{-1}; EC: BLB1: 2900, BLB2: 50, BLB3: 195 CFU 100 mL^{-1}) and no MSC measurements above detection limits (Table A20). Yearly comparisons showed no differences in indicator microbial concentrations within subsystems, between high and low flow sources, nor among receiving sites.

Environmental attributes

During the study period, I confirmed that the WTP ($F_{1,22} = 146.72$, $p < 0.001$) and river ($F_{1,22} = 32.31$, $p < 0.001$) in the high flow subsystem had higher flow rates compared to the low flow WTP and river. Within each high and low flow subsystem, the WTP flow rate was lower than the river flow rate (high flow: $F_{1,22} = 32.39$, $p < 0.0001$; low flow: $F_{1,22} = 66.96$, $p < 0.001$; Fig. 14). Seasonal comparisons showed that within the high flow subsystem, the river flow rate was lower in the warm season compared to the cold season ($F_{1,18} = 7.01$, $p = 0.02$), but there were no seasonal differences within the low flow subsystem. Similarly, high and low flow river flow rates were lower in the

warm season compared to the cold season ($F_{1,22} = 4.96$, $p = 0.04$), with the high flow river having double the flow rate in the cold season; WTP flow rates were not different between seasons (Fig. 14). Flow rates were not different between years within either subsystem or between high and low flow sources.

When comparing environmental attributes at receiving sites, salinity was lower at high flow sites ($F_{3,46} = 13.85$, $p < 0.001$) and not statistically different between seasons or years (Table A21). Temperature was higher during the warm season ($F_{1,48} = 534.05$, $p < 0.001$), but not statistically different among receiving sites or between years (Table A21). DO and chlorophyll a were lowest at receiving site MB1 (DO: $F_{3,46} = 5.10$, $p < 0.01$; chlorophyll a: $F_{3,46} = 7.15$, $p < 0.001$) within the high flow subsystem. Seasonally, DO was lower ($F_{1,46} = 17.25$, $p < 0.001$) and chlorophyll a was higher ($F_{3,46} = 9.10$, $p < 0.01$) at all sites during the warm season compared to the cold season (Table A21). Winds were primarily S (133°) in the warm season and N (7°) in the cold season. Rainfall was higher in the high flow subsystem ($F_{1,24} = 11.03$, $p < 0.01$) (Table A21). Tidal amplitude was not different among sites or between season or years (Table A21).

<div align="center">

Subsystem loads

</div>

Nutrients.

Consistent with higher flow rates, nutrient loads were higher from high flow sources (~7–400x higher for the high flow WTP and ~200–1300x higher for the high flow river) compared to low flow sources (Tables 7 and A22). As a result, although nutrient concentrations were always higher in WTP effluent than river water, nutrient loads within the high flow subsystem were lower from the WTP compared to the river due to higher river flow (Tables 6 and A22). Within the low flow subsystem, nutrient

load dominance varied between sources, where $NO_3^- + NO_2^-$ and PO_4^{3-} loads were higher from the WTP than the river, while NH_4^+ and DON loads were higher from the river than the WTP (Tables 6 and A22).

Nutrient loads followed similar seasonal patterns to nutrient concentrations. Within the high flow subsystem, DIN loads (driven by $NO_3^- + NO_2^-$) were lower in the warm season compared to the cold season, and within the low flow subsystem, DON loads were higher in the warm vs. cold season (Tables 6 and A22). Similarly, the high and low flow WTPs had higher TDN loads (driven by DON) and the high and low flow rivers had lower DIN loads (driven by $NO_3^- + NO_2^-$) in the warm season compared to the cold season (Tables 7 and A22). Nutrient loads within the high flow subsystem differed between years, with higher TDN loads (driven by both DIN and DON) in 2015 compared to 2016, while nutrient loads within the low flow subsystem were not different between years (Tables 6 and A22). Similarly, the high and low flow WTPs and rivers had higher TDN loads in 2015 compared to 2016 (Tables 7 and A22).

Indicator microbes.

As with nutrients, indicator microbial loads (FC, EC, MSC) were higher where flow rates were higher. Within each subsystem, indicator microbial loads were lower in the WTP compared to the river (Tables 6 and A23). Between high and low flow sources, the high flow WTP and river had higher loads of all indicator microbes compared to the low flow WTP and river (Tables 7 and A23). Consistent with results for indicator microbial concentrations, indicator bacterial loads (FC and EC) within the high flow subsystem and only FC loads within the low flow subsystem were lower in the warm vs. cold season (Tables 6 and A23). High and low flow WTP indicator microbial loads were

not different between seasons, but the high and low flow rivers had lower indicator

microbial loads in the warm vs. cold season (Tables 7 and A23). Comparing between

years, there were no differences in indicator microbial loads within the high flow

subsystem, but FC and EC loads within the low flow subsystem were higher in 2015 than

in 2016 (Tables 6 and A23).

Relative influence of sources

Nutrients.

Within the high flow subsystem, all nutrient load ratios (WTP:river) were <1,

except for NH_4^+ during July 2015 and 2016 (data not shown), indicating that the WTP

was a smaller source for all nutrients when compared to the river (Figs. 15 and A7, left

panels). Within the low flow subsystem, the load ratios were >1 for $NO_3^- + NO_2^-$, PO_4^{3-},

and DIN (WTP was larger source), but <1 for NH_4^+ and DON (river was larger source),

and TDN was conveyed equally between the WTP and river (~1) (Figs. 15 and A7, right

panels). The load ratios (WTP:river) for all nutrients were lower from the high flow

subsystem than the low flow subsystem ($p < 0.0001$ for all significant ANOVAs), except

for NH_4^+, which was not statistically different between subsystems. Seasonally, the

relative contribution of $NO_3^- + NO_2^-$ from the WTP within the high flow subsystem and

DIN load ratios within both subsystems were higher in the warm vs. cold season ($NO_3^- +$

NO_2^-: $F_{1,9} = 7.54$, $p = 0.02$; DIN: $F_{1,22} = 5.01$, $p = 0.04$). Yearly comparisons showed

$NO_3^- + NO_2^-$ load ratios in the high flow subsystem were lower in 2015 than in 2016 ($F_{1,9}$

$= 17.50$, $p < 0.01$).

Indicator microbes.

Within each subsystem, indicator microbial load ratios (WTP:river) were <1, indicating that WTPs were smaller sources of all indicator microbes (FC, EC, MSC) compared to rivers. Consistent with nutrient load ratios, MSC load ratios were lower in the high flow subsystem compared to the low flow system ($F_{1,22} = 29.08$, $p < 0.0001$), but FC and EC load ratios were not different between high and low flow subsystems (Fig. 16). There were no seasonal or yearly differences in indicator microbial load ratios within or between subsystems (Fig. 16).

Wastewater influence on the system

Nutrients.

Overall, nutrient concentrations at receiving sites depended on WTP and river nutrient loads, while other variables included in model selection (season, year, rainfall, wind direction, tidal amplitude, and chlorophyll a [load and concentration]) were less important in affecting nutrient concentrations. While season and year were important factors for flow rates and wastewater indicator loads, season and year were correlated with multiple variables that were likely important drivers of wastewater indicator concentrations. Therefore, season and year were removed from nutrient concentration models early in the model selection process.

Within the high flow subsystem at the receiving site MB1, all nutrient concentrations, except NH_4^+, increased with increasing river nutrient loads, and models that only included the river load variable had Akaike weights (w) >0.79, indicating that the Mobile River load was the main variable influencing nutrient concentrations at MB1 (Tables A24 and A25). Yet, PO_4^{3-}, DIN (driven by $NO_3^- + NO_2^-$), and DON

concentrations depended on both Mobile River and WTP loads, with $w = 0.1$, indicating that the WTP could not be discounted as a source of these nutrient forms to MB1 (Table A24). Furthermore, an outlier was identified during May 2015 when high source DON concentrations coupled with high WTP flow and average river flow resulted in high source loads to nearby receiving site MB1 (Fig. 17, left panels). When this outlier was included in model selection analysis, both the WTP and Mobile River contributed DON to MB1 during this sampling period (Tables 9 and 10; cf. full models results in Tables A26 and A27).

Within the high flow subsystem at the receiving site MB2, $NO_3^- + NO_2^-$, NH_4^+, and DIN concentrations increased with increasing Dog River nutrient loads (w for models with Dog River loads: >0.77), indicating that this smaller river influenced nutrient concentrations at this site. However, DIN (driven by $NO_3^- + NO_2^-$) also had models including Mobile River load with w >0.1 and therefore, Mobile River cannot be excluded as a DIN source to site MB2, further downstream (Tables A28 and A29). During May 2015, an outlier point driven by high DON concentrations in both river sources coupled with high Dog River flow and average Mobile River flow resulted in an interactive effect between Dog River and Mobile River loads contributing to higher DON concentrations at MB2 when this outlier point was included in model selection analysis (Fig. 18; Tables 9 and 10; cf. full models results in Tables A26 and A27). Overall, DON concentrations at MB2 were mainly driven by the Mobile River, while Dog River influenced DON concentrations only at the highest Dog River flows.

Within the low flow subsystem, the WTP and river were potential nutrient sources to the receiving site BLB1. For example, $NO_3^- + NO_2^-$ and TDN concentrations increased

with increasing WTP load (w for models with WTP loads: >0.77), NH_4^+ concentrations

depended on the Bayou La Batre River load ($w = 0.3$), and DIN concentrations depended

on both Bayou La Batre River and WTP loads ($w = 0.2$) (Tables A30 and A31). Similar

to high flow subsystem results, during May 2015 high source (WTP, river) DON

concentrations resulted in high source loads at site BLB1. Model selection analysis with

the outlier included indicated the WTP contributed to DON at BLB1, but the Bayou La

Batre River ($w = 0.3$) cannot be discounted as a DON source to BLB1 (Fig. 17, right

panels; Tables 9 and 10).

Within the low flow subsystem at receiving sites BLB2 and BLB3, NH_4^+

concentrations increased with increasing river NH_4^+ loads (best models only included

river load variable: w >0.86; Tables A32–A35). DIN concentrations at BLB2 depended

on both Bayou La Batre River and WTP loads, with $w = 0.2$, and thus the WTP could

also be a DIN source to nearby sites (Tables A32 and A33).

Indicator microbes.

Higher river loads and nutrient concentrations at high flow receiving sites resulted

in increased indicator microbial concentrations, while other variables included in model

selection (season, year, DO, salinity, rainfall, wind direction, and tidal amplitude) were

less important in affecting indicator microbial concentrations. While season and year

were important factors for flow rates and wastewater indicator loads, season and year

were correlated with multiple variables that were likely important drivers of wastewater

indicator concentrations. Therefore, season and year were removed from indicator

microbial concentration models early in the model selection process.

Within the high flow subsystem at the receiving site MB1, FC concentrations increased with increasing river nutrient loads and DON concentrations (w >0.95; Tables A36 and A37). At high flow receiving sites MB1 and MB2, FC and EC concentrations increased with increasing DON and $NO_3^- + NO_2^-$ concentrations, respectively (w >0.84; Tables A36–A39), which in turn were driven by Mobile River and Dog River nutrient loads, respectively.

In contrast to nutrients, outlier indicator microbial concentrations at receiving sites in either high or low flow subsystems were not directly related to flow or concentrations at sources (Fig. 17, both panels; Tables 9 and 10). In the low flow subsystem, model selection and relationships between source flow and concentration could not be discerned due to low detection, however, indicator bacteria at receiving sites were only above detection when the WTP malfunctioned (December 2016) (Fig. 17, right panels).

<div align="center">Estuarine-scale wastewater inputs</div>

When all WTP and river nutrient loads were summed together, WTPs were smaller sources of nutrients and indicator microbes to the MB-EMS system compared to rivers (Figs. 19, 20, A8; Tables A40 and A41). Results were driven by the high flow WTP and river, which were 16x and 178x larger than other WTP and river sources combined. When I excluded the high flow WTP and river from the analyses, WTPs were larger sources of $NO_3^- + NO_2^-$ and PO_4^{3-}; rivers were larger sources of NH_4^+, TDN, and DON; and WTPs and rivers were equal sources of DIN (Table A40). Results for indicator microbes did not change when the high flow WTP and river were excluded from analyses (Table A41).

mild**Discussion**

Globally, point and non-point sources need to be identified to manage and reduce

wastewater pollution to coastal systems. In the freshwater-dominated MB-EMS system

both WTPs and rivers were sources of nutrients and indicator microbes to nearby

receiving sites. In the high flow subsystem, the high flow river was the dominant source

of most nutrients (except NH_4^+) and indicator bacteria, and a smaller river (Dog River)

contributed additional DIN to nearby receiving sites. Conversely, in the low flow

subsystem, the WTP was a source of $NO_3^- + NO_2^-$ and the river was a source of NH_4^+ to

nearby receiving sites. Thus, different flow regimes within the same estuarine system

can mediate the influence of wastewater sources, indicating that the combination of local

hydrology and source volume is important to consider when identifying and quantifying

wastewater inputs to a system.

Influence of flow on subsystem loads

Wastewater loads in high and low flow subsystems were largely dependent on the

flow component of the load relationships. Previous study concluded that the freshwater-

influenced MB-EMS system had lower nutrient concentrations, but higher riverine loads

compared to other nutrient-rich estuaries due to the large flow component (Pennock et al.

1994). Accordingly, despite higher nutrient ($NO_3^- + NO_2^-$, PO_4^{3-}) concentrations at the

low flow WTP compared to the high flow WTP, nutrient loads from the low flow WTP

were lower because the flow rate was 26x lower than from the high flow WTP.

Similarly, indicator microbial loads in the low flow subsystem were dominated by the

flow component due to non-detect measurements in the WTP. Furthermore, differences

in flow likely explain temporal variation during this study, with higher river flow and

associated runoff from the watershed during the cold season leading to higher DIN and indicator bacterial concentrations and loads in the high flow subsystem (Mallin et al. 1993; Qu and Kroeze 2010; Reeves et al. 2004). Other studies have found similar results, where rivers were larger sources of nutrients during high flow periods (Baltic: Laznik et al. 1999; Yaquina Estuary: Brown and Ozretich 2009) and WTPs were larger sources during low flow periods (River Avon catchment in Southern England: Bowes et al. 2005; Cachoeira River estuary in northern Brazil: Silva et al. 2013). Cold season discharges during this study were higher than average discharges in each subsystem (USGS data from 2003–2014), indicating cold season results may represent higher loads than typically encountered in this system. Regardless of departure from average measured discharges, differences between high and low flow source loads and seasonal differences were largely regulated by source flow rates in this freshwater-dominated system.

These data suggest that point sources, like WTPs, can be small relative to riverine inputs, especially in a high flow subsystem, but both WTPs and rivers can be important sources. For example, while river loads in the high flow subsystem and river (NH_4^+) and WTP ($NO_3^- + NO_2^-$) loads in the low flow subsystem delivered nutrients to nearby sites, the WTP was also a possible source of DIN delivery to both high and low flow receiving sites ($w > 0.1$). In addition, under certain flow conditions the relative influence of point and non-point sources shifted. During above average WTP flow simultaneous with average river flow in the high flow subsystem, the WTP had the largest relative influence during the study (i.e., DON May 2015; Fig. 16). In addition to differences in flow, high system-wide DON in May could have been the result of spring surface runoff increasing DON (Stepanauskas et al. 2000). While rivers were overall larger sources of $NO_3^- + NO_2^-$

in the high flow subsystem, seasonal differences in flow resulted in a larger relative

influence of the river in the higher flow cold season and a larger relative influence of the

WTP in the lower flow warm season (e.g.; $NO_3^- + NO_2^-$ WTP:river loads, Fig. 15).

Additionally, the WTP in the low flow subsystem had a higher relative influence due to

1) lower river flow and 2) the WTP flow representing a larger percentage of the river

flow (3.4%) compared to the high flow subsystem (0.4%) (e.g.; WTP:river loads, Fig.

16). A similar pattern has been reported in San Francisco Bay, where higher WTP

influence occurs in low flow regions than in high flow regions, with WTP inputs

comprising 13% and 33% of the river flow in high and low flow regions, respectively

(Conomos 1979; Novick and Senn 2014). Furthermore, WTPs can comprise most of the

river flow when WTPs are discharged into low flow or confined regions (e.g.; effluent-

dominated streams: Brooks et al. 2006) and during drought conditions when river flow

may become negligible (Andersen et al. 2004). While point and non-point sources were

important contributors of wastewater indicators in high and low flow subsystems, the

relative influence of a source will shift based on flow conditions.

Use of wastewater indicators

Nutrients and indicator microbes functioned differently as wastewater indicators

during this study. Consistent with previous studies, nutrients persisted longer than

indicator microbes (Peeler et al. 2006) at all receiving sites in each subsystem.

Consequently, rivers in the high flow subsystem provided nutrients to nearby sites and

perhaps provided nutrients for the growth and survival of indicator bacteria (Seitzinger et

al. 2002; Malham et al. 2014). Indicator bacteria in the low flow subsystem, however,

were not above detection limits at nearby sites even though indicator bacterial

concentrations were high in the river. This finding suggests that microbes did not survive long enough to reach downstream sites, potentially due to reduced flow limiting dispersal (Lipp et al. 2001; Steets and Holden 2003) or other site-specific environmental differences that affected survival. For example, indicator microbes may survive poorly in high salinity waters (>15) of the low flow subsystem (Anderson et al. 1979; Hood and Ness 1982). Interestingly, indicator bacteria were more prevalent in the cold season, which contradicts the typical pattern of higher indicator bacteria in warm seasons (Flint 1987; Šolić et al. 1999). It is possible that increased surface runoff associated with higher river flows and lower infiltration during the cold season delivered higher indicator bacterial concentrations and thus loads to my study sites despite colder temperatures that limit growth (Cohen and Shuval 1972; Frith et al. unpublished data) or decreased predation during colder periods may have allowed bacteria to persist (Rhodes and Kator 1988). Additionally, use of multiple nutrients and indicator microbes, e.g., rather than use of total N only, was important to assess nutrient sources (Table 11; reviewed in Statham 2012). For example, in the low flow subsystem, the WTP and river had high $NO_3^- + NO_2^-$ and NH_4^+ loads, respectively, while TDN loads were similar between sources, confirming the utility of monitoring multiple nutrient forms. Furthermore, while indicator bacteria were above detection in each flow subsystem, the indicator virus was above detection limits only in the high flow subsystem, limiting its utility as a wastewater indicator. Therefore, the utility of either nutrients or indicator microbes as wastewater indicators depended on the combination of hydrology and biogeochemical processes, emphasizing the value of multiple indicators to provide a more holistic view of wastewater influence.

The specificity of wastewater indicators is also affected by the specific technology and treatment processes used by WTPs (Dueñas et al. 2003). Wastewater treatment plants in this study were secondary removal systems (using physical and biological methods) and did not have advanced nutrient removal, resulting in higher nutrient concentrations in the WTPs compared to rivers. Furthermore, activities within rivers, such as, urban runoff, wildlife, septic tanks, boating activity, etc. can promote high indicator microbial concentrations in rivers compared to WTPs that specifically treat effluent to remove indicator microbes (Weiskel et al. 1996; Malham et al. 2014). Accordingly, WTP indicator microbial concentrations and loads were lower than rivers, and indicator bacteria at low flow receiving sites were above detection limits only when the WTP UV disinfection system malfunctioned in December 2016. This observation confirms that the disinfection processes employed by the WTPs were effective at removing indicator microbes. Previous study in a nearby system also found WTPs were effective at indicator microbe removal when properly maintained (Darrow et al. 2017). Furthermore, the low flow WTP had higher influent indicator bacterial concentrations (data not shown), but lower effluent indicator microbial concentrations than the high flow WTP, suggesting that UV disinfection was more effective than chlorine at removing indicator microbes, as has been found elsewhere (Burkhardt et al. 1992; Havelaar et al. 1991). Hence, WTPs that successfully remove microbial or other wastewater indicators, can reduce WTP influence on receiving waters, resulting in greater relative influence from other sources such as rivers, especially in freshwater-influenced systems.

Estuarine-scale wastewater inputs

Similar to other systems world-wide, riverine non-point sources were larger contributors of wastewater indicators to the overall MB-EMS system (Table 12). Compared to other estuaries in the U.S., nutrient loads were lower from WTPs (e.g.; Narragansett Bay, DIN and PO_4^{3-}) and higher from rivers (e.g.; Yaquina Estuary, DIN, Table 11) in this study, but compared to U.K. systems, such as the Severn and Thames, WTP and river nutrient loads were lower (Table 11). The variation in relative influence of different indicator microbial sources among systems depends, in part, on whether point sources are regulated and treated, i.e., WTP disinfection (Malik et al. 1994). For example, previous study in the Seine River watershed showed that non-disinfected WTP effluent caused point sources to be larger FC sources, but if WTP effluents were disinfected as they were in this study, non-point sources would dominate FC inputs (Garcia-Armisen and Servais 2007). Furthermore, indicator bacterial loads to the MB-EMS system are 2 orders of magnitude lower than found in the microbiologically impaired Seine River (Garcia-Armisen et al. 2005). Overall, WTP and riverine wastewater loads into the MB-EMS system were typically lower compared to other systems, but increasing urbanization and long-term environmental change have potential to increase wastewater loads. Increasing climate change, for example, may increase precipitation and thus freshwater inputs in the southeastern U.S. (Mulholland et al. 1997), further increasing the relative influence of non-point riverine sources compared to point sources and potentially increase system-wide loads. Atmospheric deposition and groundwater discharge are potentially important wastewater sources not directly measured in this study. Atmospheric deposition accounts for ~38% of total N inputs in

the MB watershed (Harned et al. 2004) and while groundwater discharge is thought to represent only ~5% of the total freshwater input into MB, 80% of total groundwater discharge occurs on the eastern side of MB (Montiel et al. 2019). Thus, future studies should consider the relative influence of atmospheric deposition and groundwater wastewater inputs when defining and quantify wastewater sources.

Conclusion

Wastewater sources to estuarine environments need to be identified to mitigate water quality degradation and protect marine resources. Flow regulated wastewater inputs in the MB-EMS system, with rivers (i.e., non-point sources) dominant under most conditions and higher flows during the colder season. Accordingly, the high flow river was an overwhelmingly larger source of nutrient and indicator microbes than all other sources measured because 1) the flow rate of the river was much larger than other sources (WTP point source input was 0.4% of the river flow), 2) WTPs successfully removed indicator microbes via disinfection, and 3) rivers conveyed indicator microbes from a wider variety of ultimate non-point sources such as untreated runoff and wildlife activity. Furthermore, rivers were direct and indirect sources for indicator microbes due to rivers providing indicator bacteria and nutrients for bacterial growth to downstream receiving sites. These data suggest that regions with different flow regimes, even within a single larger system, may require different wastewater management strategies.

While wastewater loads to this system were not as high as other systems world-wide, attempts should be made to reduce wastewater pollution, preserve water quality and future ecosystem function, and protect natural resources. This study suggests that

managers should focus on reducing non-point source pollution discharged locally (e.g.,

through implementing best management practices for agricultural runoff and other

contributors to non-point source pollution upstream) while also maintaining and

upgrading wastewater infrastructure to reduce sewer overflows (Abraham 2003).

Furthermore, this study suggests choosing the proper wastewater indicator for a system or

study is paramount. For example, higher salinity regions would benefit from use of

nutrients or indicators that have superior survival to ensure their utility as wastewater

indicators in these dynamic regions. Additionally, if managers are interested solely in

reducing wastewater pollution to coastal environments (i.e., compared to source

identification), monetary expenses could be reduced by sampling only DIN instead of

multiple individual N fractions. Results will aid in understanding and managing

anthropogenic pollutant delivery to freshwater-dominated systems under different flow

conditions to help mitigate water quality declines and protect human and ecological

health.

Tables

Table 5. Characteristics of wastewater treatment plant (WTP) and river sources sampled at high and low flow subsystems and at additional sites sampled for estuarine-scale analyses. Flow rates are 3-year averages except Fairhope WTP, which is a 1-year average. Major nutrient refers to the largest nutrient species discharged from WTPs. Disinfection refers to the type of disinfection employed by WTPs to remove microbes. Sewer customers is the number of customers served by the WTP and is an index of human population density and thus urbanization in the watershed. All data compiled from the United States Geological Survey (rivers) and utility boards (WTPs): Mobile Area Water and Sewage System, City of Fairhope Public Utilities, and Bayou La Batre Utilities Board. Error ± SE.

Source	Site type	Name	Flow (m^3 s^{-1})	Major nutrient	Disinfection	Sewer customers
WTP	High	Mobile	1.1 ± 0.01	NH_4^+	Chlorine	82203
	Low	Bayou La Batre	0.1 ± 0.0	$NO_3^- + NO_2^-$	UV	750
	Additional system site	Fairhope	0.1 ± 0.0	$NO_3^- + NO_2^-$	UV	17372
River	High	Mobile	502.0 ± 15.8	-	-	-
		Dog	5.4 ± 0.4	-	-	-
	Low	Bayou La Batre	2.0 ± 0.1	-	-	-
		West Fowl	1.1 ± 0.1	-	-	-
	Additional system site	East Fowl	1.1 ± 0.1	-	-	-

Table 6. Results of three-way ANOVAs used to determine if wastewater indicator (nutrient and indicator microbe) concentrations and loads were different in the WTP versus the river within each high and low flow subsystem through time using sources (WTP, river), seasons (warm, cold), and years (2015, 2016) as factors. Factors with bold p-values are statistically significant. Species indicates the nutrient or indicator microbe species. FC = fecal coliforms, EC = *E. coli*, MSC = male-specific coliphage. "–" indicates statistical test was not run. Superscripts indicate which level of each factor had higher concentrations or loads: WTP = WTP, R = river, W = warm, C = cold, 1 = 2015, 2 = 2016.

Flow	Indicator	Species	Factor	Concentrations				Loads			
				Sum sq	df	F	p	Sum sq	df	F	p
High	Nutrient	NO$_3^-$ + NO$_2^-$	WTP/River	40.69	1	60.05	**<0.0001**^{WTP}	66.54	1	36.91	**<0.0001**^{R}
			Season	5.89	1	8.70	**0.01**^{C}	12.71	1	7.05	**0.01**^{C}
			Year	0.24	1	0.35	0.56	5.25	1	2.91	0.10
			Residuals	14.91	22			39.66	22		
		NH$_4^+$	WTP/River	110.42	1	184.37	**<0.0001**^{WTP}	14.48	1	18.62	**<0.001**^{R}
			Season	0.15	1	0.24	0.63	1.18	1	1.52	0.23
			Year	0.04	1	0.07	0.79	1.83	1	2.36	0.14
			Residuals	13.18	22			17.11	22		
		PO$_4^{3-}$	WTP/River	71.96	1	183.36	**<0.0001**^{WTP}	17.29	1	35.66	**<0.0001**^{R}
			Season	0.04	1	0.09	0.77	0.55	1	1.13	0.30
			Year	0.01	1	0.02	0.90	0.85	1	1.76	0.20
			Residuals	8.63	22			10.66	22		
		TDN	WTP/River	64.09	1	627.70	**<0.0001**^{WTP}	52.40	1	119.33	**<0.0001**^{R}
			Season	0.00	1	0.00	0.99	0.24	1	0.55	0.47
			Year	0.45	1	4.36	0.05	3.50	1	7.96	**0.01**^{1}
			Residuals	2.25	22			9.66	22		
		DIN	WTP/River	77.61	1	176.24	**<0.0001**^{WTP}	38.12	1	47.20	**<0.0001**^{R}
			Season	2.37	1	5.38	**0.03**^{C}	4.90	1	6.07	**0.02**^{C}
			Year	0.71	1	1.60	0.22	4.82	1	5.97	**0.02**^{1}
			Residuals	9.69	22			17.77	22		

Table 6 cont.

Flow	Indicator	Species	Factor	Concentrations				Loads			
				Sum sq	df	F	p	Sum sq	df	F	p
High	Nutrient	DON	WTP/River	51.27	1	301.04	**<0.0001**[WTP]	65.11	1	115.23	**<0.0001**[R]
			Season	0.57	1	3.36	0.08	0.09	1	0.15	0.70
			Year	0.23	1	1.35	0.26	2.82	1	4.98	**0.04**[1]
			Residuals	3.75	22			12.43	22		
	Microbe	FC	WTP/River	2.39	1	1.48	0.24	286.54	1	133.81	**<0.0001**[R]
			Season	7.97	1	4.92	**0.04**[C]	11.74	1	5.48	**0.03**[C]
			Year	0.35	1	0.22	0.65	3.36	1	1.57	0.22
			Residuals	35.60	22			47.11	22		
		EC	WTP/River	1.77	1	1.27	0.27	279.29	1	140.50	**<0.0001**[R]
			Season	7.99	1	5.71	**0.03**[C]	11.77	1	5.92	**0.02**[C]
			Year	0.30	1	0.21	0.65	3.20	1	1.61	0.22
			Residuals	30.78	22			43.73	22		
		MSC	WTP/River	3.80	1	4.84	**0.04**[WTP]	177.15	1	165.76	**<0.0001**[R]
			Season	0.57	1	0.72	0.40	0.01	1	0.01	0.91
			Year	0.30	1	0.38	0.54	3.84	1	3.59	0.07
			Residuals	17.28	22			23.51	22		
Low	Nutrient	$NO_3^- + NO_2^-$	WTP/River	2.11×10^6	1	19.11	**<0.001**[WTP]	27.87	1	9.69	**0.01**[WTP]
			Season	5.28×10^3	1	0.05	0.83	6.86	1	2.38	0.14
			Year	8.40×10^5	1	7.60	**0.01**[1]	7.65	1	2.66	0.12
			Residuals	2.43×10^6	22			63.28	22		
		NH_4^+	WTP/River	5.15	1	5.36	**0.03**[WTP]	32.85	1	11.17	**<0.01**[R]
			Season	0.00	1	0.00	0.97	0.27	1	0.09	0.76
			Year	1.64	1	1.71	0.21	0.30	1	0.10	0.75
			Residuals	20.16	21			61.76	21		

Table 6 cont.

Flow	Indicator	Species	Factor	Concentrations				Loads			
				Sum sq	df	F	p	Sum	df	F	p
Low	Nutrient	PO_4^{3-}	WTP/River	141.36	1	1069.41	**<0.0001**[WTP]	28.96	1	93.53	**<0.0001**[WTP]
			Season	0.07	1	0.47	0.50	0.01	1	0.03	0.86
			Year	0.07	1	0.54	0.47	0.95	1	3.08	0.09
			Residuals	2.91	22			6.81	22		
		TDN	WTP/River	72.61	1	351.32	**<0.0001**[WTP]	0.49	1	1.50	0.23
			Season	0.83	1	4.04	0.06	1.11	1	3.40	0.08
			Year	1.28	1	6.18	**0.02**[1]	0.58	1	1.79	0.19
			Residuals	4.55	22			7.17	22		
		DIN	WTP/River	$2.21{\times}10^6$	1	20.19	**<0.001**[WTP]	5.43	1	2.28	0.15
			Season	$4.45{\times}10^3$	1	0.04	0.84	2.90	1	1.22	0.28
			Year	$8.43{\times}10^5$	1	7.69	**0.01**[1]	2.48	1	1.04	0.32
			Residuals	$2.41{\times}10^6$	22			52.37	22		
		DON	WTP/River	59.25	1	276.89	**<0.0001**[WTP]	1.76	1	5.48	**0.03**[R]
			Season	1.81	1	8.48	**0.01**[W]	2.32	1	7.25	**0.01**[W]
			Year	0.28	1	1.31	0.27	0.02	1	0.06	0.80
			Residuals	4.49	21			6.73	21		
	Microbe	FC	WTP/River	-	-	-	-	290.15	1	325.22	**<0.0001**[R]
			Season	-	-	-	-	4.14	1	4.64	**0.04**[C]
			Year	-	-	-	-	6.30	1	7.06	**0.01**[1]
			Residuals	-	-	-	-	19.63	22		
		EC	WTP/River	-	-	-	-	294.36	1	336.92	**<0.0001**[R]
			Season	-	-	-	-	3.65	1	4.18	0.05
			Year	-	-	-	-	5.69	1	6.51	**0.02**[1]
			Residuals	-	-	-	-	19.22	22		
		MSC	WTP/River	-	-	-	-	219.92	1	190.98	**<0.0001**[R]
			Season	-	-	-	-	3.37	1	2.93	0.10
			Year	-	-	-	-	3.42	1	2.97	0.10
			Residuals	-	-	-	-	25.33	22		

Table 7. Results of three-way ANOVAs used to determine if wastewater indicator (nutrient and indicator microbe) concentrations and loads in WTPs and rivers were different between subsystems (high, low), seasons (warm, cold), or years (2015, 2016). Factors with bold p-values are statistically significant. Species indicates the nutrient or indicator microbe species. FC = fecal coliforms, EC = *E. coli*, MSC = male-specific coliphage. "–" indicates statistical test was not run. Superscripts indicate which level of each factor had higher concentrations or loads: H = high flow, L = Low flow, W = warm, C = cold, 1 = 2015, 2 = 2016.

Source	Indicator	Species	Factor	Concentrations				Loads			
				Sum sq	df	F	p	Sum sq	df	F	p
WTP	Nutrient	$NO_3^- + NO_2^-$	Subsystem	1.13×10^6	1	9.69	**0.01**^{L}	9.52×10^8	1	18.32	**<0.001**^{H}
			Season	2.61×10^3	1	0.22	0.64	6.32×10^7	1	1.22	0.28
			Year	8.70×10^5	1	7.47	**0.01**^{1}	5.40×10^7	1	1.04	0.32
			Residuals	2.56×10^6	22			1.14×10^9	22		
		NH_4^+	Subsystem	55.80	1	50.04	**<0.0001**^{H}	254.94	1	201.90	**<0.0001**^{H}
			Season	0.61	1	0.55	0.47	1.10	1	0.87	0.36
			Year	1.15	1	1.03	0.32	1.55	1	1.23	0.28
			Residuals	23.42	21			26.52	21		
		PO_4^{3-}	Subsystem	11.66	1	24.15	**<0.0001**^{L}	21.88	1	47.03	**<0.0001**^{H}
			Season	0.26	1	0.55	0.47	0.30	1	0.65	0.43
			Year	0.04	1	0.08	0.77	0.11	1	0.24	0.63
			Residuals	10.63	22			10.24	22		
		TDN	Subsystem	0.08	1	0.42	0.53	62.86	1	315.68	**<0.0001**^{H}
			Season	0.92	1	4.92	**0.04**^{W}	0.91	1	4.58	**0.04**^{W}
			Year	0.80	1	4.33	0.05	0.96	1	4.80	**0.04**^{1}
			Residuals	4.09	22			4.38	22		
		DIN	Subsystem	9.53×10^4	1	0.72	0.41	9.79×10^9	1	42.86	**<0.0001**^{H}
			Season	4.4710^3	1	0.03	0.86	3.57×10^7	1	0.16	0.70
			Year	1.13×10^6	1	8.52	**0.01**^{1}	4.35×10^8	1	1.90	0.18
			Residuals	2.91×10^6	22			5.02×10^9	22		

Table 7 cont.

Source	Indicator	Species	Factor	Concentrations				Loads			
				Sum sq	df	*F*	*p*	Sum sq	df	*F*	*p*
WTP	Nutrient	DON	Subsystem	0.52	1	2.05	0.17	53.23	1	186.90	**<0.0001**[H]
			Season	2.08	1	8.27	**0.01**[W]	2.12	1	7.44	**0.01**[W]
			Year	0.04	1	0.15	0.70	0.07	1	0.24	0.63
			Residuals	5.29	21			5.98	21		
	Microbe	FC	Subsystem	-	-	-	-	124.78	1	112.01	**<0.0001**[H]
			Season	-	-	-	-	3.98	1	3.57	0.07
			Year	-	-	-	-	0.95	1	0.85	0.37
			Residuals	-	-	-	-	24.51	22		
		EC	Subsystem	-	-	-	-	122.27	1	122.70	**<0.0001**[H]
			Season	-	-	-	-	2.98	1	2.99	0.10
			Year	-	-	-	-	0.77	1	0.78	0.39
			Residuals	-	-	-	-	21.92	22		
		MSC	Subsystem	-	-	-	-	127.57	1	190.49	**<0.0001**[H]
			Season	-	-	-	-	0.36	1	0.54	0.47
			Year	-	-	-	-	1.45	1	2.16	0.16
			Residuals	-	-	-	-	14.73	22		
River	Nutrient	$NO_3^- + NO_2^-$	Subsystem	6.78	1	13.68	**<0.01**[H]	352.97	1	118.55	**<0.0001**[H]
			Season	5.51	1	11.12	**<0.01**[C]	24.80	1	8.33	**0.01**[C]
			Year	1.84	1	3.72	0.07	12.48	1	4.19	0.05
			Residuals	10.90	22			65.50	22		
		NH_4^+	Subsystem	14.79	1	2.25	0.15	204.56	1	99.10	**<0.0001**[H]
			Season	19.53	1	2.98	0.10	7.10	1	3.44	0.08
			Year	6.54	1	1.00	0.33	0.36	1	0.18	0.68
			Residuals	144.33	22			45.41	22		

Table 7 cont.

Source	Indicator	Species	Factor	Concentrations				Loads			
				Sum sq	df	F	p	Sum sq	df	F	p
River	Nutrient	PO_4^{3-}	Subsystem	0.00	1	0.03	0.87	3.39×10^9	1	34.44	**<0.0001**[H]
			Season	0.01	1	0.12	0.73	3.51×10^9	1	3.57	0.07
			Year	0.40	1	4.83	**0.04**[1]	2.76×10^8	1	2.81	0.11
			Residuals	1.84	22			2.16×10^9	22		
		TDN	Subsystem	0.06	1	0.45	0.51	209.35	1	352.77	**<0.0001**[H]
			Season	0.00	1	0.02	0.89	0.15	1	0.26	0.61
			Year	0.81	1	6.48	**0.02**[1]	2.75	1	4.63	**0.04**[1]
			Residuals	2.76	22			13.06	22		
		DIN	Subsystem	186.53	1	6.45	**0.02**[H]	284.26	1	135.45	**<0.0001**[H]
			Season	493.43	1	17.06	**<0.001**[C]	13.03	1	6.21	**0.02**[C]
			Year	144.68	1	5.00	**0.04**[1]	3.39	1	1.61	0.22
			Residuals	636.42	22			46.17	22		
		DON	Subsystem	0.00	1	0.01	0.91	201.15	1	324.87	**<0.0001**[H]
			Season	0.46	1	3.75	0.07	0.13	1	0.21	0.66
			Year	0.65	1	5.27	**0.03**[1]	2.44	1	3.94	0.06
			Residuals	2.70	22			13.62	22		
	Microbe	FC	Subsystem	9.29	1	5.94	**0.02**[L]	122.40	1	53.35	**<0.0001**[H]
			Season	9.17	1	5.86	**0.02**[C]	12.01	1	5.23	**0.03**[C]
			Year	0.24	1	0.15	0.70	0.09	1	0.04	0.84
			Residuals	34.44	22			50.47	22		
		EC	Subsystem	5.90	1	3.93	0.06	112.57	1	51.42	**<0.0001**[H]
			Season	13.02	1	8.67	**0.01**[C]	13.05	1	5.96	**0.02**[C]
			Year	0.24	1	0.16	0.69	0.08	1	0.04	0.85
			Residuals	33.03	22			48.16	22		

Table 7 cont.

Source	Indicator	Species	Factor	Concentrations				Loads			
				Sum sq	df	*F*	*p*	Sum sq	df	*F*	*p*
River	Microbe	MSC	Subsystem	-	-	-	-	95.56	1	57.76	**<0.0001**[H]
			Season	-	-	-	-	5.41	1	3.27	0.08
			Year	-	-	-	-	1.19	1	0.72	0.4
			Residuals	-	-	-	-	36.39	22		

Table 8. Results of three-way ANOVAs used to determine if wastewater indicator (nutrient and indicator microbe) concentrations were different among downstream receiving sites (MB1, MB2, BLB1, BLB2), seasons (warm, cold), or years (2015, 2016). Factors with bold p-values are statistically significant. Species indicates the nutrient or indicator microbe species. FC = fecal coliforms, EC = *E. coli*, MSC = male-specific coliphage. "–" indicates statistical test was not run. Superscripts indicate which level of each factor had higher concentrations: H = high flow, L = Low flow, W = warm, C = cold, 1 = 2015, 2 = 2016.

Indicator	Species	Factor	Sum sq	df	F	p
Nutrient	$NO_3^- + NO_2^-$	Site	23.35	3	25.32	**<0.0001**[H]
		Season	4.56	1	14.85	**<0.001**[C]
		Year	1.59	1	5.17	**0.03**[1]
		Residuals	14.14	46		
	NH_4^+	Site	7.40	3	5.48	**<0.01**[H]
		Season	0.43	1	0.96	0.33
		Year	4.48	1	9.96	**<0.01**[1]
		Residuals	20.70	46		
	PO_4^{3-}	Site	1.72	3	9.09	**<0.0001**[H]
		Season	0.03	1	0.41	0.53
		Year	0.10	1	1.60	0.21
		Residuals	2.90	46		
	TDN	Site	3.17	3	10.25	**<0.0001**[H]
		Season	0.35	1	3.43	0.07
		Year	1.30	1	12.57	**0.001**[1]
		Residuals	4.75	46		
	DIN	Site	17.42	3	15.32	**<0.0001**[H]
		Season	2.73	1	7.20	**0.01**[C]
		Year	5.88	1	15.51	**<0.001**[1]
		Residuals	17.43	46		

Table 8 cont.

Indicator	Species	Factor	Sum sq	df	F	p
Nutrient	DON	Site	1.44	3	2.43	0.08
		Season	0.21	1	1.05	0.31
		Year	1.35	1	6.83	**0.01**[1]
		Residuals	9.10	46		
Microbe	FC	Site	-	-	-	-
		Season	-	-	-	-
		Year	-	-	-	-
		Residuals	-	-	-	-
	EC	Site	-	-	-	-
		Season	-	-	-	-
		Year	-	-	-	-
		Residuals	-	-	-	-
	MSC	Site	-	-	-	-
		Season	-	-	-	-
		Year	-	-	-	-
		Residuals	-	-	-	-

Table 9. Candidate models for model selection to investigate nutrient and indicator microbial concentrations in high and low flow subsystems at the receiving sites MB1 and MB2 (high flow) and BLB1 (low flow), with outliers included and excluded from the models. Nutrient = DON with May 2015 outlier. Microbe = Fecal coliforms (FC) with August 2016 outlier. Models in bold indicate a model that had an Akaike weight >0.9, and model averaging was not carried out for that model. w = Akaike weights. Only w >0.1 are shown (cf. full models in Table A26). Models for indicator microbes in the high flow subsystem with the outlier included are not shown because data were not linear and thus model selection was not performed. In high flow, MR load = Mobile River DON or FC load, WTP load = Mobile wastewater treatment plant (WTP) DON load, Dog load = Dog River DON load. In low flow, BBR load = Bayou La Batre DON load, WTP load = Bayou La Batre WTP DON load.

Indicator	Flow	Receiving site	Outlier	Model	df	AIC_c	ΔAIC_c	w
Nutrient	High	MB1	Included	**y = MR load + WTP load + error**	**4**	**97.78**	**0.00**	**0.91**
			Excluded	y = MR load + error	3	87.29	0.00	0.79
				y = 1 + error	2	91.39	4.09	0.10
				y = MR load + WTP load + error	4	91.50	4.20	0.10
		MB2	Included	**y = MR load + Dog load + MR load*Dog load + error**	**5**	**94.28**	**0.00**	**0.97**
			Excluded	y = 1 + error	2	81.70	0.00	0.48
				y = MR load + error	3	81.79	0.09	0.46
	Low	BLB1	Included	y = WTP load + error	3	88.03	0.00	0.65
				y = BBR load + WTP load + error	4	89.83	1.79	0.27
			Excluded	y = 1 + error	2	79.33	0.00	0.66
				y = BBR load + error	3	81.07	1.75	0.28
Microbe	High	MB1	Excluded	**y = MR load + DON + error**	**4**	**147.82**	**0.00**	**0.95**

Table 10. Model averaging output for candidate models associated with Table 9 for model selection of nutrient and indicator microbial concentrations in high and low flow subsystems at the receiving sites MB1 and MB2 (high flow) and BLB1 (low flow), with outliers included and excluded from the models. Nutrient = DON with May 2015 outlier. Microbe = Fecal coliforms (FC) with August 2016 outlier. Variables with bold p-values are statistically significant. w = Akaike weights. "*" represent model that had a w >0.9 and therefore no model average (also shown by "-" in sum w column). In high flow, MR load = Mobile River DON or FC load, WTP load = Mobile wastewater treatment plant (WTP) DON load, Dog load = Dog River DON load. In low flow, BBR load = Bayou La Batre DON load, WTP load = Bayou La Batre WTP DON load.

Indicator	Flow	Receiving site	Outlier	Variable	Intercept	Std. error	t	p	Sum w
Nutrients	High	MB1	Included*	Intercept	5.72	3.71	1.54	0.15	-
				MR load	6.29×10^{-6}	1.40×10^{-6}	4.49	**0.001**	-
				WTP load	2.42×10^{-4}	5.80×10^{-5}	4.17	**0.002**	-
			Excluded	Intercept	15.57	3.13	5.13	**0.001**	1.00
				MR load	4.13×10^{-6}	1.38×10^{-6}	2.69	**0.03**	0.90
				WTP load	1.01×10^{-5}	1.68×10^{-5}	0.07	0.95	0.11
		MB2	Included*	Intercept	22.24	3.89	5.72	**0.0003**	-
				MR load	-5.26×10^{-6}	1.95×10^{-6}	-2.70	**0.02**	-
				Dog load	-1.00×10^{-4}	5.00×10^{-4}	-0.21	0.84	-
				MR load*Dog load	6.02×10^{-10}	1.32×0^{-10}	4.58	**0.001**	-
			Excluded	Intercept	10.00	1.25	4.26	**0.002**	1.00
				MR load	1.13×10^{-6}	6.33×10^{-7}	0.93	0.38	0.52
	Low	BLB1	Included	Intercept	5.16	2.56	2.05	0.07	1.00
				BBR load	4.00×10^{-4}	3.00×10^{-4}	0.69	0.51	0.35
				WTP load	5.00×10^{-3}	8.00×10^{-4}	5.67	**0.0003**	0.95
			Excluded	Intercept	3.69	1.25	1.06	0.32	1.00
				BBR load	3.00×10^{-4}	3.00×10^{-4}	0.42	0.68	0.34

Table 10 cont.

Indicator	Flow	Receiving site	Outlier	Variable	Intercept	Std. error	t	p	Sum w
Microbes	High	MB1	Excluded*	Intercept	-125.00	44.59	-2.80	**0.02**	-
				MR load	1.18×10^{-12}	4.28×10^{-13}	2.77	**0.02**	-
				DON	7.02	1.33	5.28	**0.0005**	-

Table 11. Nutrient loads (mol d^{-1}) from studies that compared WTP and river loads to estuaries for different nutrient species. "–" indicate data not collected. References: This study (1), Nixon and Pilson 1983 (2), Cloern and Jassby 2012 (3), Kurmholz 2012 (4), McKee and Gluchowski 2011 (5), Brown and Ozreitch 2009 (6), Nedwell et al. 2002 (7).

| Estuary | Nutrient load × 10^3 (mol d^{-1}) | | | | | | | |
| | $NO_3^- + NO_2^-$ | | NH_4^+ | | PO_4^{3-} | | DIN | |
	WTP	River	WTP	River	WTP	River	WTP	River
Mobile Bay, USA[1]	10	700	30	100	5	20	40	800
Mississippi Sound, USA[1]	2	1	0	1	1	0	2	1
Mobile Bay, USA[2,3]	-	-	-	-	-	-	200	-
Apalachicola Bay, USA[2,3]	-	-	-	-	-	-	20	-
Potomac, USA[2,3]	-	-	-	-	-	-	1300	-
Delaware Bay, USA[2,3]	-	-	-	-	-	-	3700	-
Narraganset Bay, USA[2,3]	-	-	-	-	-	-	400	-
Narraganset Bay, USA[4]	-	-	-	-	10	10	300	500
Long Island Sound, USA[2,3]	-	-	-	-	-	-	2400	-
San Francisco Bay, USA[3,5]	-	-	-	-	200	-	2500	-
Yaquina Bay, USA[6]	-	-	-	-	-	-	2	200
Severn, UK[7]	80	5500	700	800	70	300	-	-
Mersey, UK[7]	20	7300	200	3500	30	40	-	-
Morecambre Bay, UK[7]	4	600	100	200	20	30	-	-
Garnock, UK[7]	20	200	200	20	20	5	-	-
Tyne, UK[7]	20	800	300	600	40	60	-	-

Table 11 cont.

| Estuary | Nutrient load × 10³ (mol d⁻¹) | | | | | | | |
| | NO₃⁻ + NO₂⁻ | | NH₄⁺ | | PO₄³⁻ | | DIN | |
	WTP	River	WTP	River	WTP	River	WTP	River
Wear, UK[7]	3	300	30	60	4	30	-	-
Tees, UK[7]	20	600	200	300	20	40	-	-
Humber, UK[7]	3	8100	200	700	30	600	-	-
Wash, UK[7]	50	1200	200	200	20	60	-	-
Stour, UK[7]	1	100	2	1	0	10	-	-
Colne, UK[7]	10	100	50	60	20	20	-	-
Blackwater, UK[7]	3	500	0	5	1	30	-	-
Thames, UK[7]	2000	6300	1300	1300	400	700	-	-
Medway, UK[7]	50	600	200	200	70	90	-	-
Pegwell Bay, UK[7]	0	100	0	1	0	6	-	-
Rother, UK[7]	2	60	0	1	1	3	-	-
Arun, UK[7]	2	400	0	5	1	40	-	-
Southampton Water, UK[7]	50	600	200	20	40	10	-	-
Christchurch Harbour, UK[7]	40	1300	2	10	20	50	-	-
Plymouth Sound, UK[7]	20	400	300	10	60	4	-	-

Table 12. Percent N and P from WTP or sewage point sources and from direct riverine discharge or agricultural runoff into estuaries worldwide. Percentages are based on the most current literature. Estuarine characteristics (estuary area, watershed area, and discharge) for U.S. estuaries are from the National Estuarine Eutrophication Assessment (NEEA) database (http://ian.umces.edu/neea/siteinformation.php; last accessed 01 March 2019), except for watershed area for the Susquehanna River is from Moore et al. 2011 and discharge for Baltic proper is from De Jonge et al. 1994. N values indicate total nitrogen (TN) unless indicated by * = DIN or † = $NO_3^- + NO_2^-$ or NH_4^+. P values indicate PO_4^{3-}. References with (Ag) indicate citations for nutrient rivers/Ag runoff. "–" indicates data not collected. References: Castro et al. 2003 (1), Greening et al. 2014 (2), Whitall and Bricker 2006 (3), Whitall et al. 2007 (4), Moore et al. 2011 (5), Kauffman 2018 (6), Narragansett Bay Estuary Program 2017 (7), United States Environmental Protection Agency 2002 (8), Novick and Senn 2014 (9), Grimvall and Stålnacke 2001 (10), Murray et al. 2019 (11), Andersen et al. 2017 (12), Rask et al. 1999 (13), Nedwell et al. 2002 (14).

Region	Estuary	Estuary area (km²)	Watershed area (km²)	Flow (m³ s⁻¹)	N WTP	N Rivers/Ag runoff	P WTP	P Rivers/Ag runoff
Gulf of Mexico	Lower Laguna Madre, USA[1]	1300	1300	20	20	80	-	-
	Upper Laguna Madre, USA[1]	600	2000	1	10	70	-	-
	Corpus Christi Bay, USA[1]	600	45000	10	30	70	-	-
	Matagorda Bay, USA[1]	1100	120000	100	10	80	-	-
	Galveston Bay, USA[1]	1500	62000	700	40	50	-	-
	Sabine Lake, USA[1]	300	54000	500	20	70	-	-
	Calcasieu Lake, USA[1]	300	11000	100	20	50	-	-
	Terrebonne-Timbalier Bays, USA[1]	1300	2600	1	60	20	-	-
	Barataria Bay, USA[1]	900	4800	10	30	30	-	-
	Mississippi Sound, USA[1]	1600	4000	40	20	60	-	-
	Mobile Bay, USA[1]	1100	110000	1800	30	50	-	-
	Apalachicola Bay, USA[1]	600	52000	700	20	70	-	-
	Apalachee Bay, USA[1]	1800	14000	100	4	80	-	-

Table 12 cont.

Region	Estuary	Estuary area (km²)	Watershed area (km²)	Flow (m³ s⁻¹)	N WTP	N Rivers/Ag runoff	P WTP	P Rivers/Ag runoff
Gulf of Mexico	Tampa Bay, USA[2]	900	5700	40	20	60	-	-
Atlantic Coast	Charlotte Harbor, USA[1]	500	8100	60	6	90	-	-
	Indian River, USA[1]	900	3000	30	10	70	-	-
	Altamaha River, USA[1]	40	37000	400	10	70	-	-
	St. Catherine/Sapelo, USA[1]	200	2300	1	1	20	-	-
	St. Helena Sound, USA[1]	200	12000	90	1	80	-	-
	Charleston Harbor, USA[1]	90	41000	200	60	30	-	-
	Winyah Bay, USA[1]	90	47000	500	20	70	-	-
	Pamlico Sound, USA[3,4]	4700	2000	4	10	80	-	-
	Chesapeake Bay, USA[3,4]	7000	80000	1200	20	60	-	-
	James, USA[5]	600	26000	300	50	20	-	-
	Potomac, USA[5]	1300	37000	400	30	50	-	-
	Susquehanna, USA[5]	-	71000	-	9	60	-	-
	Delaware Bay, USA[3,4,6]	2100	3300	500	50	30	-	-
	Hudson/Raritan, USA[3,4,5]	800	42000	600	40	4	-	-
	Long Island Sound, USA[3,4,5]	3300	13000	200	30	6	-	-
	Narragansett Bay, USA[7]	400	4300	60	30	50*	50	20*
	Buzzards Bay, USA[3,4]	600	1600	5	60	20	-	-
	Waquoit Bay, USA[8]	5	50	0	40	20	-	-
	Massachusetts Bay, USA[3,4]	800	600	2	80	5	-	-
	Merrimack River, USA[3,4,5]	20	13000	200	40	5	-	-
	Great Bay, USA[3,4]	50	2600	20	40	20	-	-
	Casco Bay, USA[3,4]	400	2600	40	40	5	-	-

Table 12 cont.

Region	Estuary	Estuary area (km²)	Watershed area (km²)	Flow (m³ s⁻¹)	N WTP	N Rivers/Ag runoff	P WTP	P Rivers/Ag runoff
Pacific Coast	San Francisco Bay, USA[9*]	1300	120000	800	60	20	60	20
	North San Francisco Bay, USA[9*]	800	110000	800	20	70	20	60
	South San Francisco Bay, USA[9*]	500	4900	8	100	-	90	-
Baltic Area	Baltic proper, EUR[10,11,12]	150000	-	-	7	60	20	70
	Gulf of Riga, EUR[10,11,12]	19000	140000	-	4	80	20	70
	Funen, EUR[13]	-	-	-	8	30	30	50
United Kingdom[†]	Severn, UK[14]	560	16000	-	2 / 50	100 / 50	20	80
	Mersey, UK[14]	90	3400	-	0 / 6	100 / 90	6	90
	Morecambe Bay, UK[14]	500	2800	-	1 / 40	100 / 60	40	70
	Garnock, UK[14]	2	700	-	9 / 90	90 / 6	80	20
	Tyne, UK[14]	8	2900	-	3 / 30	100 / 70	40	60
	Wear, UK[14]	2	1200	-	1 / 30	100 / 70	10	90
	Tees, UK[14]	10	1900	-	3 / 40	100 / 60	30	70
	Humber, UK[14]	300	19000	-	0 / 30	100 / 70	4	10
	Wash, UK[14]	700	6500	-	4 / 50	100 / 60	20	80
	Stour, UK[14]	30	600	-	1 / 70	100 / 30	5	100
	Colne, UK[14]	20	300	-	10 / 50	100 / 50	50	60
	Blackwater, UK[14]	50	1200	-	1 / 5	100 / 100	4	100
	Thames, UK[14]	50	9900	-	20 / 50	80 / 50	40	60
	Medway, UK[14]	60	2400	-	8 / 50	90 / 50	40	60
	Pegwell Bay, UK[14]	9	300	-	0 / 20	100 / 80	0	100
	Rother, UK[14]	4	500	-	3 / 20	100 / 80	30	80
	Arun, UK[14]	2	533	-	1 / 6	100 / 90	2	100
	Southampton Water, UK[14]	40	1700	-	8 / 90	90 / 10	80	30

Table 12 cont.

Region	Estuary	Estuary area (km²)	Watershed area (km²)	Flow (m³ s⁻¹)	N WTP	N Rivers/Ag runoff	P WTP	P Rivers/Ag runoff
United Kingdom[†]	Christchurch Harbour, UK[14]	2	2800	-	3 / 11	100 / 90	20	80
	Plymouth Sound, UK[14]	40	1300	-	4 / 100	100 / 3	90	7
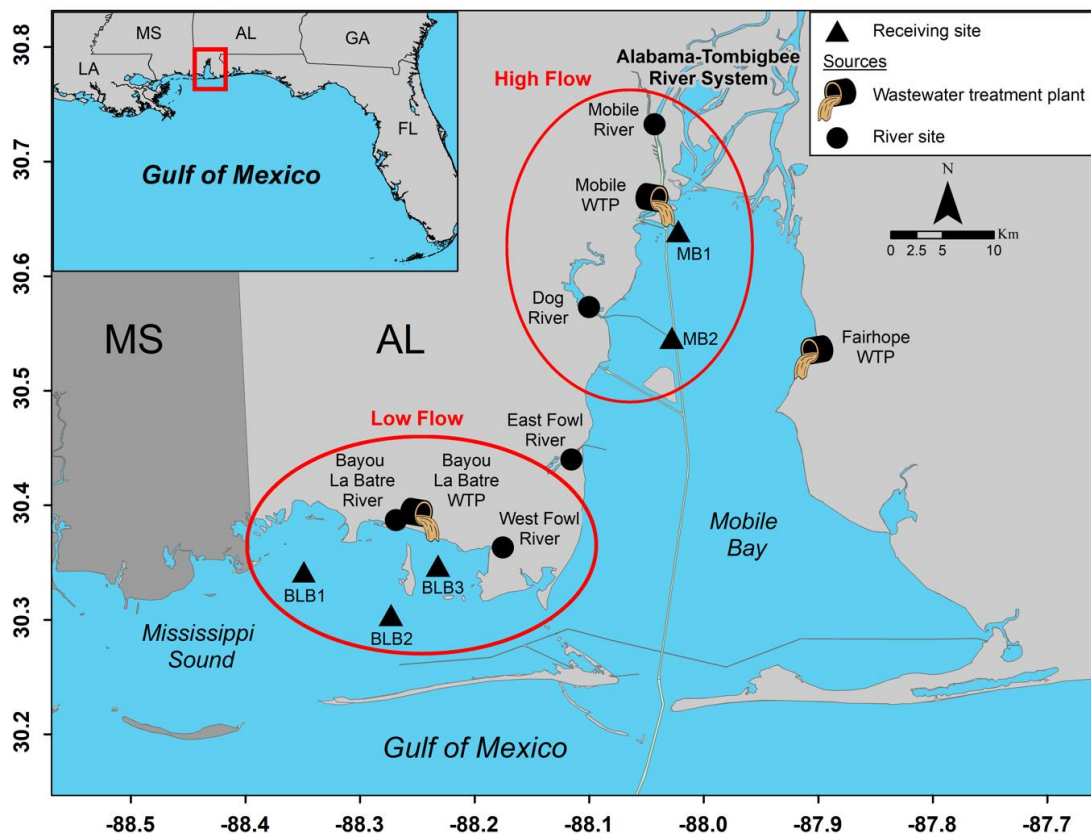
Figure 13. Wastewater source sites (wastewater treatment plants [WTP] and rivers) and downstream receiving sites sampled for wastewater indicators (nutrients and indicator microbes) in the Mobile Bay-eastern Mississippi Sound system (site GPS coordinates in Table A17). High flow subsystem sites include three sources (Mobile WTP, Mobile River, and Dog River) and two receiving sites (MB1 and MB2), while low flow subsystem sites include three sources (Bayou La Batre WTP, Bayou La Batre River, and West Fowl River) and three receiving sites (BLB1, BLB2, and BLB3). Estuarine-scale analyses also included two other sources (Fairhope WTP and East Fowl River).
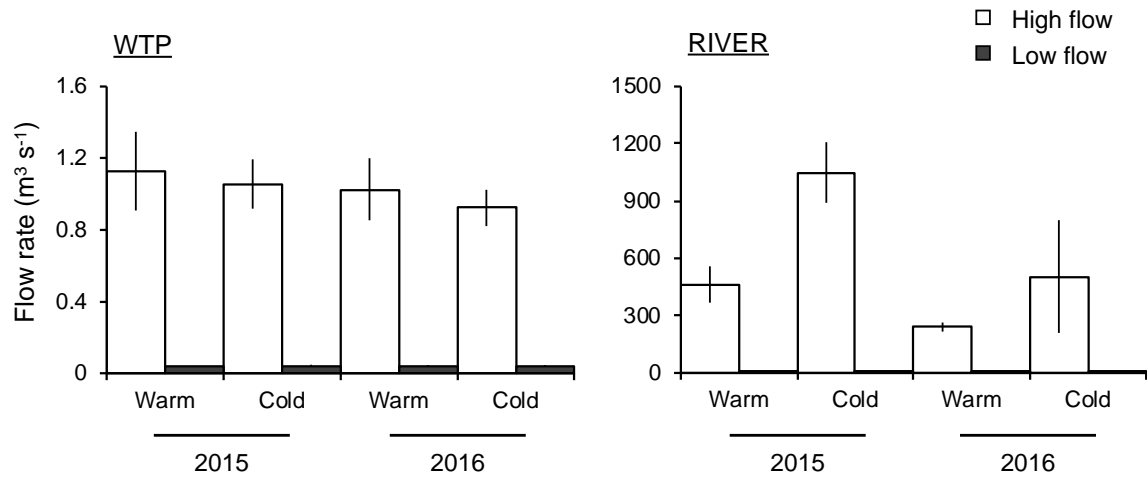
Figure 14. Flow rates (m^3 s^{-1}) of wastewater treatment plants (WTP) and rivers for high flow and low flow subsystems, separated by seasons and years. Error $\pm$ SE. Within each flow subsystem, river flow rates were higher than WTP flow rates ($p < 0.001$ for significant ANOVAs) and high flow source flow rates were larger than low flow source flow rates ($p < 0.001$ for significant ANOVAs). High and low flow river flow rates were higher in the cold season compared to the warm season ($p = 0.04$).
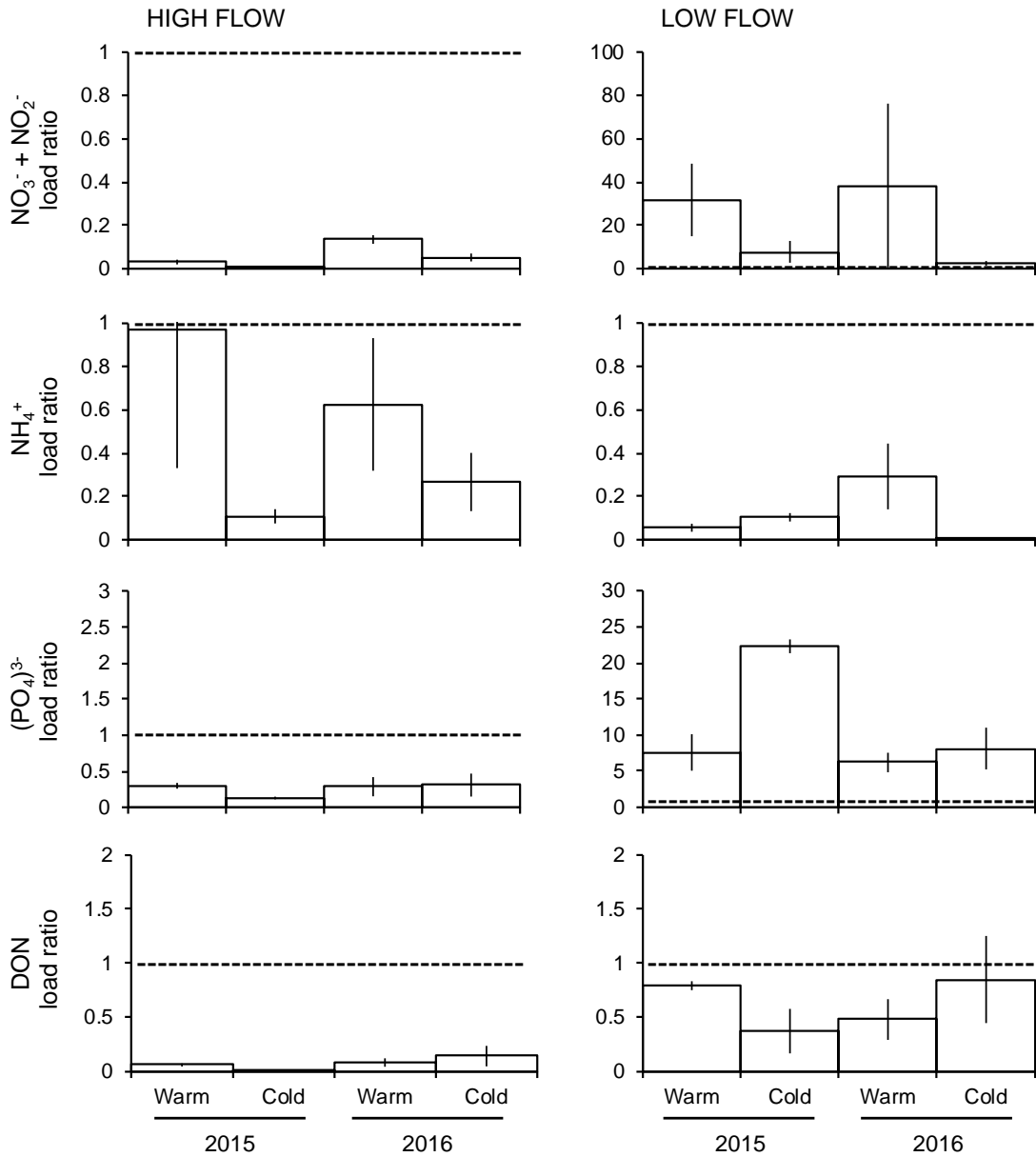
Figure 15. Ratio of wastewater treatment plant (WTP) to river nutrient loads for high flow and low flow subsystems (note the difference in scale), separated by seasons and years. Dashed line indicates where WTP:river load = 1; >1 indicates the WTP is a larger source and <1 indicates the river is a larger source. Error ± SE. Load ratios for all nutrients except NH_4^+ were lower from the high flow subsystem than the low flow subsystem ($p < 0.0001$ for all significant ANOVAs). $NO_3^- + NO_2^-$ load ratios within the high flow subsystem were higher in the warm vs. cold season ($p = 0.02$) and in 2016 vs. 2015 ($p < 0.01$). No other nutrient load ratios were different between seasons or years.
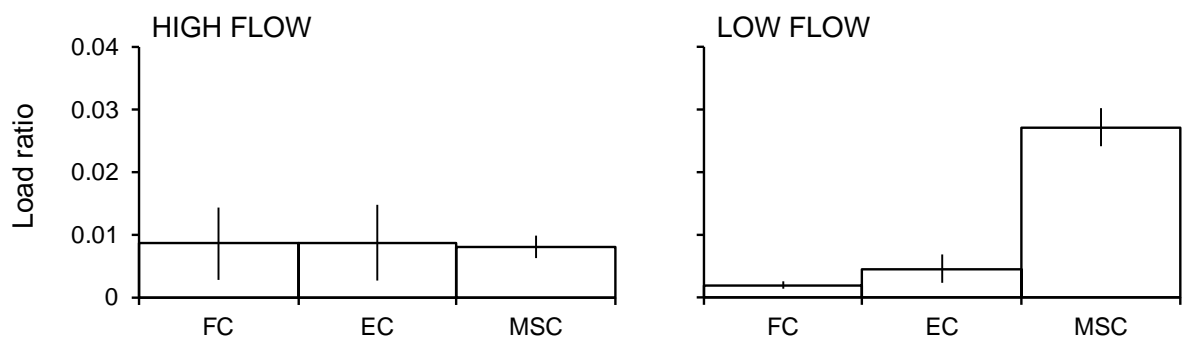
Figure 16. Ratio of wastewater treatment plant (WTP) to river indicator bacterial (fecal coliforms [FC] and *E. coli* [EC]) and viral (MSC) loads for high flow and low flow subsystems. Error ± SE. Data are presented as averages because there were no seasonal or yearly differences in indicator microbial load ratios. Indicator bacteria (FC and EC) load ratios were not different between high and low flow subsystems, but MSC was higher in the low flow subsystem compared to the high flow subsystem ($p < 0.0001$).
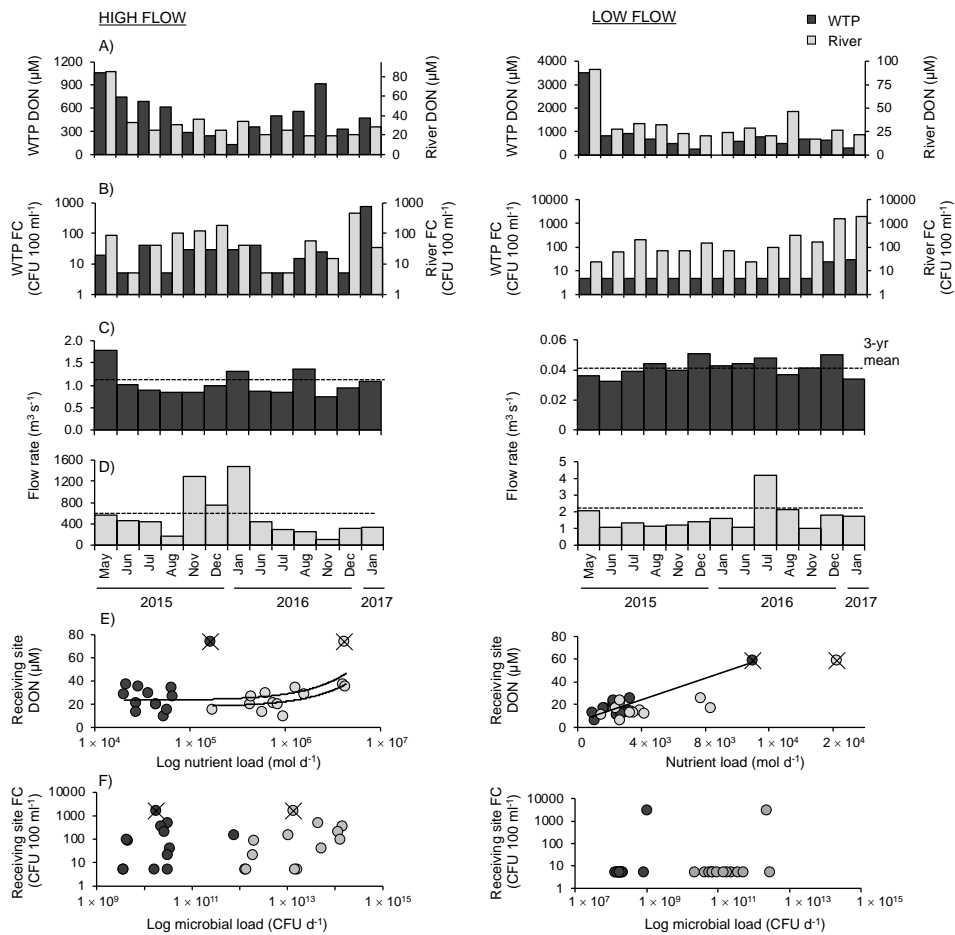
Figure 17. Data illustrating time points where high concentrations and/or flow rates resulted in high source loads to the system. DON (µM) and indicator microbial (log fecal coliform [FC]; CFU 100 ml^{-1}) concentrations in high and low flow subsystems measured at two sources (wastewater treatment plants [WTPs] and rivers) (A, B) and the corresponding flow rates (m^3 s^{-1}) measured in the high and low flow WTPs (C) and rivers (D) during each sampling period. Dashed line shows 3-year mean flow rate for each source. DON and indicator microbial (log fecal coliform [FC]) concentrations in high and low flow subsystems measured at receiving sites compared to WTP and river nutrient (mol d^{-1}) and indicator microbial (CFU d^{-1}) loading rates (source concentration × flow rate) (E, F). Solid lines indicate significant regressions as identified by information theoretic multivariable model selection (cf. corresponding model output results in Table 9 and 10). "X" indicates outliers to models (2 SD > mean). DON and FC outliers were May 2015 and August 2016, respectively. Points above detection in low flow FC are December 2016. In high flow, WTP = Mobile WTP, river = Mobile River, receiving site = MB1. In low flow, WTP = Bayou La Batre WTP, river = Bayou La Batre River, receiving site = BLB1.

134

Figure 18. Data illustrating time points where high concentrations and/or flow rates resulted in high source loads to the system. DON concentration (µM) in the high flow subsystem at two measured riverine sources (Dog River and Mobile River) (A) and corresponding flow rates (m³ s⁻¹) from Dog River (B) during each sampling period. Dashed line shows 3-year mean flow rate for each river. Mobile River flow rate cf. Fig. 17d (high flow). DON concentration measured at receiving site MB2 compared to WTP and river DON loading rate (source concentration × flow rate) (mol d⁻¹) (C). Solid lines indicate significant regressions as identified by information theoretic multivariable model selection (cf. corresponding model output results in Table 9 and 10). "X" indicates outliers to models (2 SD > mean) (May 2015).

Figure 19. Sum of sampled average ($n = 13$; $n_{Fairhope} = 6$) wastewater treatment plant (WTP) and river $NO_3^- + NO_2^-$, NH_4^+, PO_4^{3-}, and DON loads to the system. Error ± SE. Error was propagated as the square root of the sum of squares.
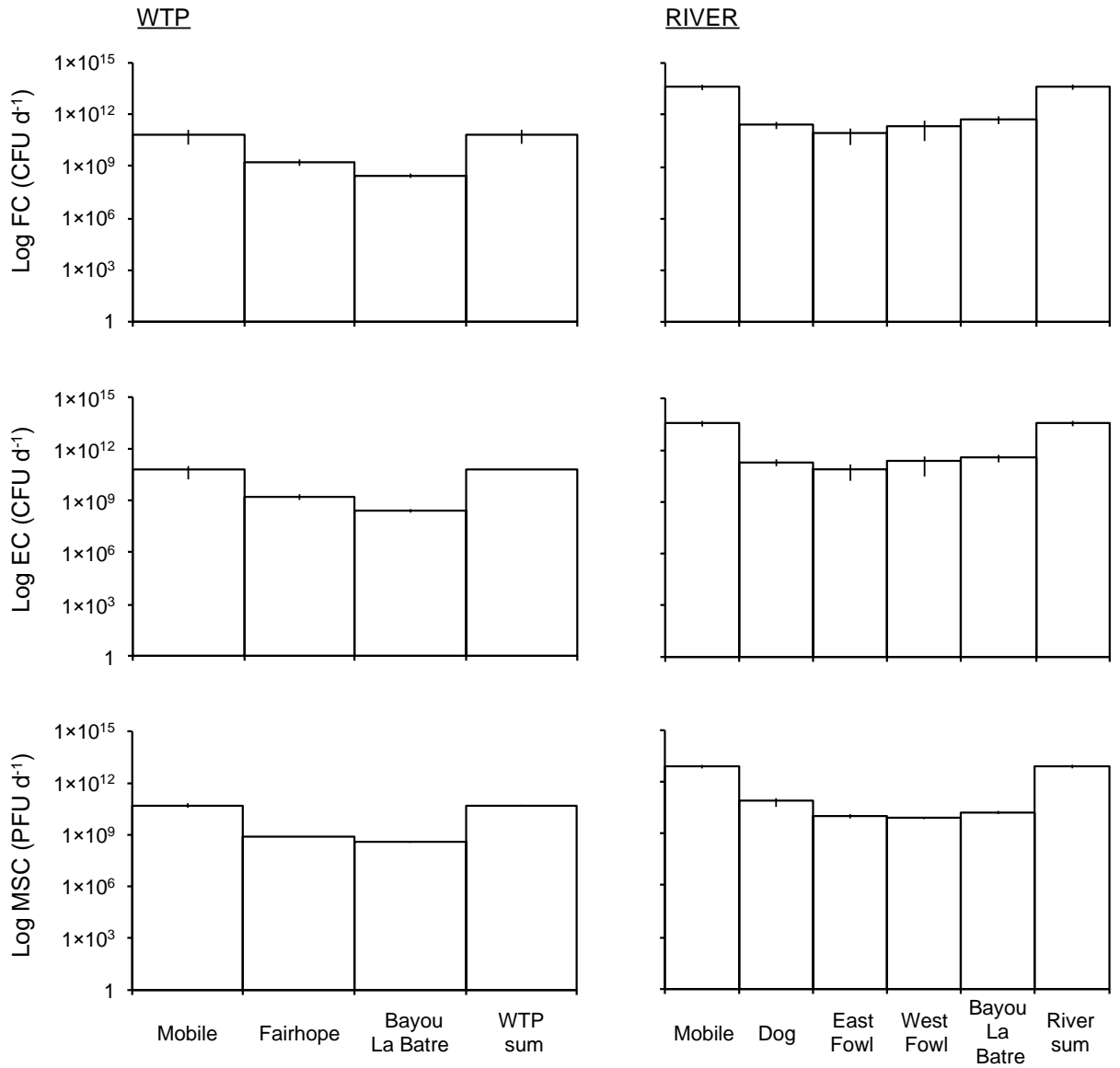
Figure 20. Sum of sampled average ($n = 13$; $n_{Fairhope} = 6$) wastewater treatment plant (WTP) and river fecal coliform (FC), *E. coli* (EC), and male-specific coliphage (MSC) loads to the system. Error ± SE. Error was propagated as the square root of the sum of squares.

SUMMARY

This study demonstrated that freshwater discharge along with winds and tides influenced larval transport and connectivity by mediating environmental attributes and water quality, which in turn affected the timing and location of oyster settlement and wastewater inputs. Specifically, differences largely in freshwater flows set up different salinity gradients within the Mobile Bay-eastern Mississippi Sound (MB-EMS) system, changing oyster transport, settlement, and connectivity patterns during differing flow regimes. Freshwater discharge also influenced point and non-point sources of wastewater inputs to the system and resulted in higher wastewater inputs where freshwater flows were higher. Wastewater inputs were lower, however, in regions of higher oyster settlement. These results suggest that 1) larvae do not survive well due to lowered salinities or are flushed out of areas where wastewater pollution inputs are high in the MB-EMS system due to higher freshwater inputs or 2) larval supply and available substrate for settlement are coincidently low in regions where wastewater inputs are higher. These data have implications for how changes in freshwater inputs and water quality conditions can influence the spatial and temporal scale of larval connectivity, the importance of freshwater controls on population dynamics of estuarine species with larval stages, and seafood safety.

Direct tracking of oyster larvae using a large-scale calcein-based mark-recapture method provided insight into larval transport pathways in the MB-EMS system. This study represents the first time that eastern oysters were successfully stained at a large scale (i.e., millions of larvae) with calcein at salinities representative of estuarine environments. The calcein mark was detectable from stained larvae free-released in the field. Although not perfect, the automated FlowCam was the most viable option to detect stained larvae in large-volume, high-particulate background field samples. Field validation of an existing larval transport model showed that larvae were transported through dominant flow paths set up by freshwater discharge and wind. Furthermore, calcein-stained larvae were only recaptured during the low discharge/high salinity release, suggesting that during the high discharge/low salinity release, larval survival was lowered due to lower salinity or higher freshwater input flushed larvae out of the system, lowering chances of recapture success and implicating the importance of physical transport. Future studies will benefit by optimizing methods to increase recapture success. For example, studies should 1) sampling sooner after release (hours) and at a higher sampling frequency and 2) use plankton tows instead of Niskin samples. These efforts will result in more samples with higher background densities to sort through, requiring methods development, i.e., mechanical size separation and chemical treatment of phytoplankton, to quickly and efficiently identify recaptured larvae. Calcein has potential to be a useful marker to track larval movement at large-scales needed for field-based studies, particularly in freshwater-dominated systems where larval movements are under-studied and can provide critical information to aid in assessment of biophysical models, restoration and management activities, and propagation or recovery efforts.

Settlement data in conjunction with geochemical tagging was able to provide information on larval origins and population connectivity in the MB-EMS system, which is critical to define priority areas for settlement and recruitment for oysters and other larval species in freshwater-dominated systems. Salinity and temperature were mediated by changes in freshwater discharge, winds, and tides, and in turn affected the magnitude, timing, and location of settlement and possible spawning events. Accordingly, differences in peak settlement in EMS were seen between high and low discharge years. Settlement was higher and observed over a larger spatial scale (i.e., settlement was measurable in lower MB) in the low discharge year when salinities were more favorable for settlement and growth. Consequently, there was potentially higher connectivity between EMS and lower MB oysters in the low compared to high discharge year, when larvae were present in both regions. These findings were confirmed by larval connectivity predictions using TE ratios, which showed self-recruitment and connectivity in the EMS region during the low discharge year, suggesting that oysters in EMS are important larval sources to this system. The importance of freshwater influence on larval connectivity was further evidenced by the consistent contribution of Sr, a salinity indicator, to site-specific differences in TE ratios. Therefore, Sr shows promise for future use in larval connectivity studies in freshwater-influenced systems. The seasonal and interannual variation seen in my study suggests the need to measure finer spatial and temporal scales of settlement within this system. Previous studies in the MB-EMS system (Hoese et al. 1972; Lee 1979; Saoud et al. 2000; Kim et al. 2010) similarly found high variation in settlement with consistent settlement in the EMS region, indicating this area is important for larval settlement. This study provides a baseline for measuring

future change of settlement and connectivity patterns in the MB-EMS system and provides an approach to measure connectivity in other freshwater-dominated systems world-wide.

Point and non-point wastewater inputs were largely controlled by freshwater discharge, with higher wastewater influence seen in the high flow subsystem where the majority of freshwater enters the MB-EMS system. In contrast to wastewater inputs, oyster settlement was higher in the low flow subsystem, and although the low flow WTP and river were nutrients sources, nutrient loads to downstream oyster settlement sites were low compared to other estuarine systems. Furthermore, indicator microbes were only above detection limits at downstream oyster settlement sites when the WTP disinfection system malfunction, indicating that with proper maintenance and operation, WTPs can protect water quality to downstream areas. Accordingly, wastewater inputs were better characterized by nutrients than indicator microbes, confirming the use of multiple indicators to examine wastewater exposure. These data suggest that wastewater loads to oyster settlement sites are relatively low and potentially represent incipient loads for water quality declines. Understanding how changing freshwater flow regimes influence point and non-point wastewater input and the conveyance of anthropogenic pollutants will help mitigate water quality declines that affect natural resources and ultimately commercial fishery harvest and human health.

This study showed the importance of freshwater discharge, winds, and tides in regulating larval transport, settlement, and population connectivity as well as water quality changes. These data provide a way to determine baselines from which to define how perturbations in freshwater inflow will influence population dynamics and

community resilience of species with pelagic larval stages and how these estuarine species will persist under changing freshwater flow regimes resulting from climatic (increased precipitation and runoff) or anthropogenic (e.g., spillway openings) changes. Point and non-point wastewater pollution is mediated by changes in flow conditions and should be considered when assessing and managing the effects of wastewater pollution on natural resources in highly dynamic estuaries. To this end, these data can inform restoration and management activities and propagation or recovery efforts by determining optimal restoration locations while reducing potential human health risks. These results are imperative to help protect and sustain the future of water-dependent economies that rely on harvestable marine populations with larval stages.

REFERENCES

REFERENCES

Abraham, D.M. 2003. Life cycle cost integration for the rehabilitation of wastewater infrastructure. In *Construction research congress: wind of change: integration and innovation*, 1–9. https://doi.org/10.1061/40671(2003)75

Alabama Department of Conservation and Natural Resources. 2001. Survey of oyster reefs in Portersville Bay, Alabama. Compiled by M. Van Hoose. Unpublished Report.

Alabama Department of Environmental Management. 2009. Total maximum daily load (TMDL) for Bayou La Batre assessment unit ID # AL03170009-0102-100 pathogens (enterococci).

Alabama Department of Public Health. 2012. Rules of Alabama state board of health bureau of environmental services chapter 420-3-18 for shellfish sanitation, 10–11.

Aleem, A.A. 1972. Effect of river outflow management on marine life. *Marine Biology* 15 (3): 200–208. https://doi.org/10.1007/BF00383550

Alexander, C. 1998. Classified shellfish growing waters. National Oceanic and Atmospheric Administration (NOAA). *NOAA's State of the Coast Report*. Silver Spring, MD.

Álvarez, E., Á López-Urrutia, E. Nogueira, and S. Fraga. 2011. How to effectively sample the plankton size spectrum? A case study using FlowCAM. *Journal of*

Plankton Research 33 (7): 1119–1133. https://doi.org/10.1093/plankt/fbr012

Álvarez, E., M. Moyano, Á. López-Urrutia, E. Nogueira, and R. Scharek. 2014. Routine determination of plankton community composition and size structure: a comparison between FlowCAM and light microscopy. *Journal of Plankton Research* 36 (1): 170–184. https://doi.org/10.1093/plankt/fbt069

American Public Health Association. 1999. Standard Methods for the Examination of Water and Wastewater. 9060 A.

Anastasia, J.R., S.G. Morgan, and N.S. Fisher. 1998. Tagging crustacean larvae: assimilation and retention of trace elements. *Limnology and oceanography* 43 (2): 362–368.

Andersen, C.B., G.P. Lewis, and K.A. Sargent. 2004. Influence of wastewater-treatment effluent on concentrations and fluxes of solutes in the Bush River, South Carolina, during extreme drought conditions. *Environmental Geosciences* 11 (1): 29–41.

Andersen, J.H., J. Carstensen, D.J. Conley, K. Dromph, V. Fleming-Lehtinen, B.G. Gustafsson, A.B. Josefson, A. Norkko, A. Villnäs, and C. Murray. 2017. Long-term temporal and spatial trends in eutrophication status of the Baltic Sea. *Biological Reviews* 92 (1): 135–149. https://doi.org/10.1111/brv.12221

Anderson, I.C., M. Rhodes, and H. Kator. 1979. Sublethal stress in *Escherichia coli*: a function of salinity. *Applied and Environmental Microbiology* 38: 1147–1152.

Anderson, D., and K. Burnham. 2004. Model selection and multi-model inference, 2nd ed. Springer-Verlag.

Andresen, H., I. Dorresteijn, and J. van der Meer. 2013. Growth and size-dependent loss of newly settled bivalves in two distant regions of the Wadden Sea. *Marine Ecology*

Progress Series 472: 141–154. https://doi.org/10.3354/meps10011

Anger, K. 2002. Salinity as a key parameter in the larval biology of decapod crustaceans. *Invertebrate Reproduction and Development* 43 (1): 29–45. https://doi.org/10.1080/-07924259.2003.9652520

Barbier, E.B., S.D Hacker, C. Kennedy, E.W. Koch, A.C. Stier, and B.R. Silliman. 2011. The value of estuarine and coastal ecosystem services. *Ecological Monographs* 81 (2): 169–193. https://doi.org/10.1890/10-1510.1

Beck, M.W., R.D. Brumbaugh, L. Airoldi, A. Charranza, L.D. Coen, C. Crawford, O. Defeo, G.J. Edgar, B. Hancock, M.C. Kay, H.S. Lenihan, M.W. Luckenbach, C.L. Toropova, G. Zhang, and X. Guo. 2011. Oyster reefs at risk and recommendations for conservation, restoration, and management. *BioScience* 61 (2): 107–116. https://doi.org/10.1525/bio.2011.61.2.5

Becker, B.J., F.J Fodrie, P.A. McMillan, and L.A. Levin. 2005. Spatial and temporal variation in trace elemental fingerprints of mytilid mussel shells: a precursor to invertebrate larval tracking. *Limnology and Oceanography* 50 (1): 48–61. https://doi.org/10.4319/lo.2005.50.1.0048

Becker, B.J., L.A. Levin, F.J. Fodrie, and P.A. McMillan. 2007. Complex larval connectivity patterns among marine invertebrate populations. *Proceedings of the National Academy of Sciences* 104 (9): 3267–3272. https://doi.org/10.1073/pnas.0611651104

Bellou, M., P. Kokkinos, and A. Vantarakis. 2013. Shellfish-borne viral outbreaks: a systematic review. *Food and Environmental Virology* 4 (4): 13–23. https://doi.org/-10.1007/s12560-012-9097-6

Bernhard, J.M., J.K. Blanks, C.J. Hintz, and G.T. Chandler. 2004. Use of the fluorescent

calcite marker calcein to label foraminiferal tests. *Journal of Foraminiferal

Research* 34 (2): 96–101. https://doi.org/10.2113/0340096

Bertrand-Krajewski, J.L., M. Lefebvre, B. Lefai, and J.M. Audic. 1995. Flow and

pollutant measurements in a combined sewer system to operate a wastewater

treatment plant and its storage tank during storm events. *Water Science and

Technology* 31 (7): 1–12. https://doi.org/10.1016/0273-1223(95)00317-G

Biancani, P.J., R.H. Carmichael, J.H. Daskin, W. Burkhardt III, and K.R. Calci. 2011.

Seasonal and spatial effects of wastewater effluent on growth, survival, and

accumulation of microbial contaminants by oysters in Mobile Bay, Alabama.

Estuaries and Coasts 35 (1): 121–131. https://doi.org/10.1007/s12237-011-9421-7

Billen, G., J. Garnier, A. Ficht, and C. Cun. 2001. Modeling the response of water quality

in the Seine River Estuary to human activity in its watershed over the last 50

Years. *Estuaries* 24 (6): 977–993.

Borsuk, M. E., C.A. Stow, and K.H. Reckhow. 2004. Confounding effect of flow on

estuarine response to nitrogen loading. *Journal of Environmental Engineering* 130

(6): 605–614. https://doi.org/10.1061/(ASCE)0733-9372(2004)130:6(605)

Bowes, M. J., J. Hilton, G.P. Irons, and D.D. Hornby. 2005. The relative contribution of

sewage and diffuse phosphorus sources in the River Avon Catchment, southern

England: implications for nutrient management. *Science of the Total

Environment* 344 (1–3): 67–81. https://doi.org/10.1016/j.scitotenv.2005.02.006

Bradbury, I.R., C. DiBacco, S.R. Thorrold, P.V.R. Snelgrove, and S.E. Campana. 2011.

Resolving natal tags using otolith geochemistry in an estuarine fish, rainbow

smelt *Osmerus mordax*. *Marine Ecology Progress Series* 433: 195–204.

https://doi.org/10.3354/meps09178

Brooks, B.W., T.M. Riley, and R.D. Taylor. 2006. Water quality of effluent-dominated ecosystems: ecotoxicological, hydrological, and management considerations. *Hydrobiologia* 556 (1): 365–379. https://doi.org/10.1007/s10750-004-0189-7

Brown, C.A., and R.J. Ozretich. 2009. Coupling between the coastal ocean and Yaquina Bay, Oregon: importance of oceanic inputs relative to other nitrogen sources. *Estuaries and Coasts* 32 (1): 219–237. https://doi.org/10.1007/s12237-008-9128-6

Burkhardt III, W., S.R. Rippey, and W.D. Watkins. 1992. Depuration rates of northern quahogs *Mercenaria mercenaria* (Linnaeus, 1758) and eastern oysters *Crassostrea virginica* (Gmelin, 1971) in ozone- and ultraviolet light-disinfected seawater systems. *Journal of Shellfish Reasearch* 11: 105–109.

Burkhardt III, W., and K.R. Calci. 2000. Selective accumulation may account for shellfish-associated viral illness. *Applied and Environmental Microbiology* 66 (4): 1375–1378. https://doi.org/10.1128/AEM.66.4.1375-1378.2000

Burnham K.P., and D.R. Anderson. 2002. *Model selection and inference: a practical information-theoretic approach*, 2nd edition, 150. New York: Springer-Verlag.

Burnham, K.P., D.R. Anderson, and K.P. Huyvaert. 2011. AIC model selection and multimodel inference in behavioral ecology: some background, observations, and comparisons. *Behavioral Ecology and Sociobiology* 65 (1): 23–35.

Buskey, E.J., and C.J. Hyatt. 2006. Use of the FlowCAM for semi-automated recognition and enumeration of red tide cells (*Karenia brevis*) in natural plankton samples. *Harmful Algae* 5 (6): 685–692. https://doi.org/10.1016/j.hal.2006.02.003

Butler, P.A. 1965. Reactions of estuarine mollusks to some environmental factors. In
Biological Problems in Water Pollution, U.S.H.E.W. Public Health Service, 92–
104.

Butt, A.A., K.E. Aldridge, and C.V. Sanders. 2004. Infections related to the ingestion of
seafood Part I: viral and bacterial infections. *The Lancet Infectious Diseases* 4 (4):
201–212.

Cabelli, R.J. 1990. Microbial indicator levels in shellfish, water, and sediments from the
upper Narragansett Bay conditional shellfish-growing area. *Report to the
Narragansett Bay Project.* Providence, RI: Narragansett Bay Project.

Calabrese, A., and H.C. Davis. 1970. Tolerances and requirements of embryos and larvae
of bivalve molluscs. *Helgoländer Wissenschaftliche Meeresuntersuchungen* 20:
553–564.

Calci, K.R., W. Burkhardt III, W.D. Watkins, and S.R. Rippey. 1998. Occurrence of
male-specific bacteriophage in feral and domestic animal wastes, human feces
and human-associated wastewaters. *Applied and Environmental Microbiology* 64
(12): 5027–5029.

Campana, S.E., G.A. Chouinard, J.M. Hanson, A. Fréchet, and J. Brattey. 2000. Otolith
elemental fingerprints as biological tracers of fish stocks. *Fisheries Research* 46
(1–3): 343–357. https://doi.org/10.1016/S0165-7836(00)00158-2

Capone, D.G., and M.F. Bautista. 1985. A groundwater source of nitrate in nearshore
marine sediments. *Nature* 313: 214–216.

Carey, R.O., and K.W. Migliaccio. 2009. Contribution of wastewater treatment plant
effluents to nutrient dynamics in aquatic systems: a review. *Environmental*

Management 44 (2): 205–217. https://doi.org/10.1007/s00267-009-9309-5

Carleton, J.H., and P.W. Sammarco. 1987. Effects of substratum irregularity on success

of coral settlement: quantification by comparative geomorphological techniques.

Bulletin of Marine Science 40 (1): 85–98.

Carmichael, R.H., A.C. Shriver, and I. Valiela. 2004. Changes in shell and soft tissue

growth, tissue composition, and survival of quahogs, *Mercenaria mercenaria*, and

softshell clams, *Mya arenaria*, in response to eutrophic-driven changes in food

supply and habitat. *Journal of Experimental Marine Biology and Ecology* 313 (1):

75–104. https://doi.org/10.1016/j.jembe.2004.08.006

Carpenter, S.R., N.F. Caraco, D.L. Correll, R.W. Howarth, A.N. Sharpley, and V. H.

Smith. 1998. Nonpoint pollution of surface waters with phosphorus and

nitrogen. *Ecological Applications* 8 (3): 559–568. https://doi.org/10.1890/1051-

0761(1998)008[0559:NPOSWW]2.0.CO;2

Carré, M., I. Bentaleb, O. Bruguier, E. Ordinola, N.T. Barrett, and M. Fontugne. 2006.

Calcification rate influence on trace element concentrations in aragonitic bivalve

shells: evidences and mechanisms. *Geochimica et Cosmochimica Acta* 70 (19):

4906–4920. https://doi.org/10.1016/j.gca.2006.07.019

Carriker, M.R. 1951. Ecological observations on the distribution of oyster larvae in New

Jersey estuaries. *Ecological Monographs* 21 (1): 19–38. https://doi.org/10.2307/-

1948644

Carson, H.S. 2010. Population connectivity of the Olympia oyster in southern California.

Limnology and Oceanography 55 (1): 134–148. https://doi.org/10.4319/lo.2010-

.55.1.0134

Carson, H.S., P.C. López-Duarte, L. Rasmussen, D. Wang, and L.A. Levin. 2010.
    Reproductive timing alters population connectivity in marine metapopulations.
    Current Biology 20 (21): 1926–1931. https://doi.org/10.1016/j.cub.2010.09.057

Carson, H.S., P.C. López-Duarte, G.S. Cool, F.J. Fodrie, B.J. Becker, C. DiBacco, and
    L.A. Levin. 2013. Temporal, spatial, and interspecific variation in geochemical
    signatures within fish otoliths, bivalve larval shells, and crustacean larvae. *Marine
    Ecolgy Progess Series* 473: 133–148. https://doi.org/10.3354/meps10078

Castro, M.S., C.T. Driscoll, T.E. Jordan, W.G. Reay, and W.R. Boynton. 2003. Sources
    of nitrogen to estuaries in the United States. *Estuaries* 26 (3): 803–814.

Cathey, A.M., N.R. Miller, and D.G. Kimmel. 2012. Microchemistry of juvenile
    Mercenaria mercenaria shell: implications for modeling larval dispersal. *Marine
    Ecology Progress Series* 465: 155–168. https://doi.org/10.3354/meps09895

Chalupnicki, M.A., G.E. Mackey, K. Nash, R. Chiavelli, J.H. Johnson, T. Kehler, and N.
    Ringler. 2016. Mark retention of calcein in Cisco and Bloater. *North American
    Journal of Aquaculture* 78 (2): 148–153.
    https://doi.org/10.1080/15222055.2016.1143-419

Charette, M.A., and E.R. Sholkovitz. 2002. Oxidative precipitation of groundwater-
    derived ferrous iron in the subterranean estuary of a coastal bay. *Geophysical
    Research Letters* 29 (10): 85–1. https://doi.org/10.1029/2001GL014512

Chatry, M., R.J. Dugas, and K.A. Easley. 1983. Optimum salinity regime for oyster
    production on Louisiana's state seed grounds. *Contributions in Marine Science*
    26: 81–94.

Chick, R.C. 2010. Batch-tagging Blacklip Abalone (*Haliotis rubra*) for identification of

hatchery-reared individuals on natural coastal reefs in New South Wales, Australia. *Journal of Shellfish Research* 29 (1): 209–215. https://doi.org/10.2983/035.029.0117

Clarke, A., E. Prothero-Thomas, J.C. Beaumont, A.L. Chapman, and T. Brey. 2004. Growth in the limpet *Nacella concinna* from contrasting sites in Antarctica. *Polar Biology* 28: 62–71. https://doi.org/10.1007/s00300-004-0647-8

Cloern, J.E. 2001. Our evolving conceptual model of the coastal eutrophication problem. *Marine Ecology Progress Series* 210: 223–253. https://doi.org/10.3354/meps-210223

Cloern, J.E., and A.D. Jassby. 2012. Drivers of change in estuarine-coastal ecosystems: discoveries from four decades of study in San Francisco Bay. *Reviews of Geophysics* 50 (4). https://doi.org/10.1029/2012RG000397

Cohen, J., and H.I. Shuval. 1972. Coliforms, fecal coliforms, and fecal streptococci as indicators of water pollution. *Water, Air, and Soil Pollution* 2 (1): 85–95.

Conomos, T.J. 1979. Properties and circulation of San Francisco Bay waters. In *Francisco Bay: the urbanized estuary*, ed T.J. Conomos, 47–84. San Francisco: S Pacific Division, AAAS.

Cook, G.S., P.E. Parnell, and L.A. Levin. 2014. Population connectivity shifts at high frequency within an open-coast marine protected area network. *PLoS ONE* 9 (7): e103654. https://doi.org/10.1371/journal.pone.0103654

Cordi, J.A., M.A. Meylan, and W.C. Isphording. 2003. Metal distribution and metal site partitioning, Mobile Bay surface sediments. *Gulf Coast Association of Geological Societies Transactions* 53: 145–159.

Cowen, R.K., G. Gawarkiewicz, J. Pineda, S.R. Thorrold, and F.E. Werner. 2007.

Population connectivity in marine systems an overview. *Oceanography* 20 (3): 14–21.

Cowen, R.K., and S. Sponaugle. 2009. Larval dispersal and marine population connectivity. *Annual review of marine science* 1: 443–466. https://doi.org/10.1146/annurev.marine.010908.163757

Crocker, E.G. 1998. Tracking and growth of larvae of the Giant Scallop*, Placopecten magellanicus* (Gmelin, 1791) on a scallop farm in Notre Dame Bay, Newfoundland. Memorial University of Newfoundland, MS thesis.

Dai, A. and K.E. Trenberth. 2002. Estimates of freshwater discharge from continents: latitudinal and seasonal variations. *Journal of hydrometeorology* 3 (6): 660**–**687. https://doi.org/10.1175/1525-7541(2002)003<0660:EOFDFC>2.0.CO;2

Dai, A., T. Qian, K.E. Trenberth, and J.D. Milliman. 2009. Changes in continental freshwater discharge from 1948 to 2004. *American Meteorological Society* 22: 2773–2792. https://doi.org/10.1175/2008JCLI2592.1

Darrow, E.S. 2015. Biogeochemical and microbial indicators of land-use change in a northern Gulf of Mexico estuary. University of South Alabama, Ph.D. Dissertation.

Darrow, E.S., R.H. Carmichael, K.R. Calci, and W. Burkhardt III. 2017. Land-use related changes to sedimentary organic matter in tidal creeks of the northern Gulf of Mexico. *Limnology and Oceanogrography* 62 (2): 686**–**705. https://doi.org/-10.1002/lno.10453

Day, R.W., M.C. Williams, and G.P. Hawkes. 1995. A comparison of fluorochromes for marking abalone shells. *Marine Freshwater Research* 46 (3): 599–605. https://-

doi.org/10.1071/MF9950599

Dayton, P.K., J.H. Carleton, A.G. Mackley, and P.W. Sammarco. 1989. Patterns of settlement, survival and growth of oysters across the Great Barrier Reef. *Marine Ecological Progress Series* 54: 75–90.

Davis, H.C. 1958. Survival and growth of clam and oyster larvae at different salinities. *The Biological Bulletin* 114 (3): 296–307.

De Jonge, V.N., W. Boynton, C.F. D'Elia, R. Elmgren, and R.L. Welsh. 1994. Responses to developments in eutrophication in four different North Atlantic estuarine systems, 179–196. Fredensborg, Denmark: Olsen and Olsen.

DeHaan, H., J. Stamper, and B. Walters. 2012. Mississippi River and tributaries system 2011 post-flood report. *US Army Corps of Engineers Mississippi Valley Division: Vicksburg, MS, USA*.

DiBacco, C., and L.A. Levin. 2000. Development and application of elemental fingerprinting to track the dispersal of marine invertebrate larvae. *Limnology and Oceanography* 45 (4): 871–880. https://doi.org/10.4319/lo.2000.45.4.0871

Dodd, J.R., and E.L. Crisp. 1982. Non-linear variation with salinity of Sr/Ca and Mg/Ca ratios in water and aragonitic bivalve shells and implications for paleosalinity studies. *Palaeogeography, Palaeoclimatology, Palaeoecology* 38 (1–2): 45–56. https://doi.org/10.1016/0031-0182(82)90063-3

Dong, Y.W., H.S. Wang, G.D. Han, C.H. Ke, X. Zhan, T. Nakano, and G.A. Williams. 2012. The impact of Yangtze River discharge, ocean currents and historical events on the biogeographic pattern of *Cellana toreuma* along the China coast. *PLoS One* 7:e36178.

Doré, W.J., and D.N. Lees. 1995. Behavior of *Escherichia coli* and male-specific

 bacteriophage in environmentally contaminated bivalve molluscs before and after

 depuration. *Applied and Environmental Microbiology* 61 (8): 2830–2834.

Doré, W.J., K. Henshilwood, and D.N. Lees. 2000. Evaluation of F-specific RNA

 bacteriophage as a candidate human enteric virus indicator for bivalve molluscan

 shellfish. *Applied and Environmental Microbiology* 66 (4): 1280–1285.

Dorioz, J.M., E.A. Cassell, A. Orand, and K.G. Eisenman. 1998. Phosphorus storage,

 transport and export dynamics in the Foron River watershed. *Hydrological*

 Processes 12 (2): 285–309. https://doi.org/10.1002/(SICI)1099-

 1085(199802)12:2<285::AID-HYP577>3.0.CO;2-H

Duda, A.M. 1993. Addressing nonpoint sources of water pollution must become an

 international priority. *Water Science and Technology* 28 (3–5): 1–11.

 https://doi.org/10.2166/wst.1993.0398

Dueñas, F.J., J.R. Alonso, À.F. Rey, and A.S. Ferrer. 2003. Characterisation of

 phosphorous forms in wastewater treatment plants. *Journal of Hazardous*

 Materials 97 (1–3): 193–205. https://doi.org/10.1016/S0304-3894(02)00260-1

Dufour, A.P., E.R. Strickland, and V.J. Cabelli. 1981. Membrane filter method for

 enumerating *Escherichia coli*. *Applied and Environmental Microbiology* 41 (5):

 1152–1158.

Dugdale, R.C., F.P. Wilkerson, V.E. Hogue, and A. Marchi. 2007. The role of

 ammonium and nitrate in spring bloom development in San Francisco Bay.

 Estuarine, Coastal and Shelf Science 73 (1–2): 17–29. https://doi.org/-

 10.1016/j.ecss.2006.12.008

Dunphy, B.J., M-A. Millet, and A.G. Jeffs. 2011. Elemental signatures in the shells of early juvenile green-lipped mussels (*Perna canaliculus*) and their potential use for larval tracking. *Aquaculture* 311 (1–4): 187–192. https://doi.org/10.1016/-j.aquaculture.2010.12.016

Edwards, A.C., and P.J.A. Withers. 2008. Transport and delivery of suspended solids, nitrogen and phosphorus from various sources to freshwaters in the U.K. *Journal of Hydrology* 350 (3–4): 144–153. https://doi.org/10.1016/j.jhydrol.2007.10.053

El-Din, A.G., and D.W. Smith. 2002. A neural network model to predict the wastewater inflow incorporating rainfall events. *Water Research* 36 (5): 1115–1126. https://-doi.org/10.1016/S0043-1354(01)00287-1

Ellis, J.T., J.P. Spruce, R.A. Swann, J.C. Smoot, and K.W. Hilbert. 2011. An assessment of coastal land-use and land-cover change from 1974–2008 in the vicinity of Mobile Bay, Alabama. *Journal of Coastal Conservation* 15 (1): 139–149. https://doi.org/10.1007/s11852-010-0127-y

First, M.R., and L.A. Drake. 2012. Performance of the human "counting machine": evaluation of manual microscopy for enumerating plankton. *Journal of Plankton Research* 34 (12): 1028–1041. https://doi.org/10.1093/plankt/fbs068

Fitzpatrick, M.P., A.G. Jeffs, and B.J. Dunphy. 2013. Efficacy of calcein as a chemical marker of green-lipped mussel (*Perna canaliculus*) larvae and its potential use for tracking larval dispersal. *Aquaculture Research* 44 (3): 345–353. https://doi.org/-10.1111/j.1365-2109.2011.03034.x

Flannery, J., A.D. Keaveney, and W.J. Doré. 2009. Use of FRNA bacteriophages to indicate the risk of norovirus contamination in Irish oysters. *Journal of Food*

Protection 72 (11): 2358–2362. https://doi.org/10.4315/0362-028X-72.11.2358

Flint, K.P. 1987. The long-term survival of *Escherichia coli* in river water. *Journal of Applied Bacteriology* 63 (3): 261–270. https://doi.org/10.1111/j.1365-2672.1987.tb04945.x

Fodrie, F.J., B.J. Becker, L.A. Levin, K. Gruenthal, and P.A. McMillan. 2011. Connectivity clues from short-term variability in settlement and geochemical tags of mytilid mussels. *Journal of Sea Research* 65 (1): 141–150. https://doi.org/-10.1016/j.seares.2010.09.001

Fogarty, M.J., and L.W. Botsford. 2007. Population connectivity and spatial management of marine fisheries. *Oceanography* 20 (3): 112–123.

Fong, T-T., and E.K. Lipp. 2005. Enteric viruses of humans and animals in aquatic environments: health risks, detection, and potential water quality assessment tools. *Microbiology and Molecular Biology Reviews* 69 (2): 357–371. https://doi.org/-10.1128/MMBR.69.2.357-371.2005

Galindo, H.M., A.S. Pfeiffer-Herbert, M.A. McManus, Y. Chao, F. Chai, and S.R. Palumbi. 2010. Seascape genetics along a steep cline: using genetic patterns to test predictions of marine larval dispersal. *Molecular Ecology* 19 (17): 3692–3707. https://doi.org/10.1111/j.1365-294X.2010.04694.x

Gallager, S.M., R. Mann, and G.C. Sasaki. 1986. Lipid as an index of growth and viability in three species of bivalve larvae. *Aquaculture* 56 (2): 81–103. https://doi.org/-10.1016/0044-8486(86)90020-7

Galtsoff, P.S. 1964. The American oyster *Crassostrea virginica. Fisheries Bulletin of the Fish and Wildlife Service* 64: 397–458.

Garcia-Armisen, T., A. Touron, F. Petit, and P. Servais. 2005. Sources of faecal
contamination in the Seine Estuary (France). *Estuaries* 28 (4): 627–633.

Garcia-Armisen, T., and P. Servais. 2007. Respective contributions of point and non-
point sources of *E. coli* and enterococci in a large urbanized watershed (the Seine
River, France). *Journal of Environmental Management* 82 (4): 512–518.
https://doi.org/10.1016/j.jenvman.2006.01.011

Gerber, L.R., M.D.M. Mancha-Cisneros, M.I. O'Connor, and E.R. Selig. 2014. Climate
change impacts on connectivity in the ocean: implications for
conservation. *Ecosphere* 5 (3): 1–18. https://doi.org/10.1890/ES13-00336.1

Gilg, M.R., and T.J. Hilbish. 2003. The geography of marine larval dispersal: coupling
genetics with fine-scale physical oceanography. *Ecology* 84 (11): 2989–2998.
https://doi.org/10.1890/02-0498

Gillanders, B.M. 2002. Temporal and spatial variability in elemental composition of
otoliths: implications for determining stock identity and connectivity of
populations. *Canadian Journal of Fisheries and Aquatic Sciences* 59 (4): 669–
679. https://doi.org/10.1139/f02-040

Gomes, I., L.G. Peteiro, R. Albuquerque, R. Nolasco, J. Dubert, S.E. Swearer, and H.
Queiroga. 2016. Wandering mussels: using natural tags to identify connectivity
patterns among marine protected areas. *Marine Ecology Progress Series* 552:
159–176. https://doi.org/10.3354/meps11753

Greening, H., A. Janicki, E.T. Sherwood, R. Pribble, and J.O.R. Johansson. 2014.
Ecosystem responses to long-term nutrient management in an urban estuary:
Tampa Bay, Florida, USA. *Estuarine, Coastal and Shelf Science* 151 (5): A1–A16.

https://doi.org/10.1016/j.ecss.2014.10.003

Grimes, C.B. 2001. Fishery production and the Mississippi River discharge. *Fisheries* 26

(8): 17–26. https://doi.org/10.1577/1548-8446(2001)026<0017:fpatmr>2.0.co;2

Grimvall A., and P. Stålnacke. 2001. Riverine inputs of nutrients to the Baltic Sea. In

A systems analysis of the Baltic Sea, ed. F.V. Wulff, L.A. Rahm, and P.

Larsson, 113–131. Berlin, Heidelberg: Springer.

Gulf States Marine Fisheries Commission. 2012. The oyster fishery of the Gulf of

Mexico United States: a regional management plan, ed. S.J. VanderKooy,

Number 202. Ocean Springs: Mississippi.

Gutiérrez, J.L., C.G. Jones, D.L. Strayer, and O.O. Iribarne. 2003. Mollusks as ecosystem

engineers: the role of shell production in aquatic habitats. *Oikos* 101 (1): 79–90.

Haase, A.T., D.B. Eggleston, R.A. Luettich, R.J. Weaver, and B.J. Puckett. 2012.

Estuarine circulation and predicted oyster larval dispersal among a network of

reserves. *Estuarine, Coastal and Shelf Science* 101: 33–43. https://doi.org/-

10.1016/j.ecss.2012.02.011

Harned, D.A., J.B. Atkins, and J.S. Harvill. 2004. Nutrient mass balance and trends,

Mobile River Basin, Alabama, Georgia, and Mississippi. *Journal of the American

Water Resources Association* 40 (3): 765–793. https://doi.org/10.1111/j.1752-

1688.2004.tb04458.x

Havelaar, A.H., T.J. Nieuwstad, C.C.E. Meulemans, and M. van Olphen. 1991. F-specific

RNA bacteriophages as model viruses in UV disinfection of wastewater. *Water

Science and Technology* 24 (2): 347–352. https://doi.org/10.2166/wst.1991.0088

Hayes, P.F., and R.W. Menzel. 1981. The reproductive cycle of early setting *Crassostrea virginica* (Gmelin) in the northern Gulf of Mexico, and its implications for population recruitment. *The Biological Bulletin* 160 (1): 80–88.

He, L. M.L., and Z.L. He. 2008. Water quality prediction of marine recreational beaches receiving watershed baseflow and stormwater runoff in southern California, USA. *Water Research* 42 (10–11): 2563–2573. https://doi.org/10.1016/j.watres.2008.01.002

Hoese, H.D., W.R. Nelson, and H. Beckert. 1972. Seasonal and spatial setting of fouling organisms in Mobile Bay and eastern Mississippi Sound, Alabama. *Alabama Marine Resource Bulletin* 8: 9–17.

Hood, M.A., and G.E. Ness. 1982. Survival of *Vibrio cholerae* and *Escherichia coli* in estuarine waters and sediments. *Applied and Environmental Microbiology* 43 (3): 578–584.

Howarth, R.W., A. Sharpley, and D. Walker. 2002. Sources of nutrient pollution to coastal waters in the United States: implications for achieving coastal water quality. *Estauries* 25 (4): 656–676.

Hubertz, E.D., and L.B. Cahoon. 1999. Short-term variability of water quality parameters in two shallow estuaries of North Carolina. *Estuaries* 22 (3): 814–823.

Huntington, T.G. 2006. Evidence for intensification of the global water cycle: review and synthesis. *Journal of Hydrology* 319 (1–4): 83–95. https://doi.org/10.1016/-j.jhydrol.2005.07.003

Ide, K., K. Takahashi, A. Kuwata, M. Nakamachi, and H. Saito. 2008. A rapid analysis of copepod feeding using FlowCAM. *Journal of Plankton Research* 30 (3): 275–

281. https://doi.org/10.1093/plankt/fbm108

Ingle, R.M. 1951. Spawning and setting of oysters in relation to seasonal environmental changes. *Bulletin of Marine Science* 1 (2): 111–135.

Isphording, W.C., and G.C. Flowers. 1987. Mobile Bay: the right estuary in the wrong place. In *Symposium on the Natural Resources of the Mobile Bay Estuary, Alabama*, ed. T.A. Lowery, 165–174. Alabama Sea Grant Extension Service, Auburn University. Mobile: Alabama.

Jackman, S. 2008. pscl: Classes and methods for R developed in the Political Science Computational Laboratory, Stanford University. Department of Political Science, Stanford University, Stanford, California. R package version 0.95, URL http://CRAN.R-project.org/ package=pscl

Jakobsen, H.H., and J. Carstensen. 2011. FlowCAM: Sizing cells and understanding the impact of size distributions on biovolume of planktonic community structure. *Aquatic Microbial Ecology* 65: 75–87. https://doi.org/10.3354/ame01539

Johnson, J.B., and K.S. Omland. 2004. Model selection in ecology and evolution. *Trends in Ecology and Evolution* 19 (2): 101–108. https://doi.org/10.1016/0006--3207(83)90068-x

Johnson, K.B., and A.L. Shanks. 2003. Low rates of predation on planktonic marine invertebrate larvae. *Marine Ecology Progress Series* 248: 125–139. https://doi.org/-10.3354/meps248125

Kaartvedt, S., and D.L. Aksnes. 1992. Does freshwater discharge cause mortality of fjord-living zooplankton? *Estuarine, Coastal and Shelf Science* 34 (3): 305–313.

Kaehler, S., and C.D. McQuaid. 1999. Use of the fluorochrome calcein as an *in situ*

growth marker in the brown mussel *Perna perna*. *Marine Biology* 133 (3): 455–460. https://doi.org/10.1007/s002270050485

Kauffman, G.J. 2018. The cost of clean water in the Delaware River Basin (USA). *Water* 10 (2): 95. https://doi.org/10.3390/w10020095

Kemp, M.W. and W.R. Boynton. 1984. Spatial and temporal coupling of nutrient inputs to estuarine primary production: the role of particulate transport and decomposition. *Bulletin of Marine Science* 35 (3): 522–535.

Kennedy, V.S. 1996. Biology of larvae and spat. In *The eastern oyster: Crassostrea virginica*, ed. V.S. Kennedy, R.I.E. Newell, and A.F. Eble, 371–421. College Park: Maryland Sea Grant College.

Kennish, M.J. 2002. Environmental threats and environmental future of estuaries. *Environmental Conservation* 29 (1): 78–107. https://doi.org/10.1017/S03768-92902000061

Kenny, P.D., W.K. Michener, and D.M. Allen. 1990. Spatial and temporal patterns of oyster settlement in a high salinity estuary. *Journal of Shellfish Research* 9 (2): 329–339.

Kim, C.-K., K. Park, S.P. Powers, W.M. Graham, and K.M. Bayha. 2010. Oyster larval transport in coastal Alabama: dominance of physical transport over biological behavior in a shallow estuary. *Journal of Geophysical Research* 115: C10019. https://doi.org/10.1029/2010JC006115

Kim, C.-K., and K. Park. 2012. A modeling study of water and salt exchange for a micro-tidal, stratified northern Gulf of Mexico estuary. *Journal of Marine Systems* 96–97: 103–115. https://doi.org/10.1016/j.jmarsys.2012.02.008

Kim, C.-K., K. Park, and S.P. Powers. 2013. Establishing restoration strategy of eastern oyster via a coupled biophysical transport model. *Restoration Ecology* 21 (3): 353–362. https://doi.org/10.1111/j.1526-100X.2012.00897.x

Kirby, M.X., T.M. Soniat, and H.J. Spero. 1998. Stable isotope sclerochronology of Pleistocene and recent oyster shells (*Crassostrea virginica*). *Palaios* 13 (6): 560–569. https://doi.org/10.2307/3515347

Kirby, M.X. 2004. Fishing down the coast: historical expansion and collapse of oyster fisheries along continental margins. *Proceedings of the National Academy of Sciences* 101 (35): 13096–13099. https://doi.org/10.1073/pnas.0405150101

Krause-Nehring, J., A. Klügel, G. Nehrke, B. Brellochs, and T. Brey. 2011. Impact of sample pretreatment on the measured element concentrations in the bivalve *Arctica islandica. Geochemistry, Geophysics, Geosystems* 12 (7): Q07015. https://doi.org/10.1029/2011GC003630

Kroll, I.R., A.K. Poray, B.J. Puckett, D.B. Eggleston, and F.J. Fodrie. 2016. Environmental effects on elemental signatures in eastern oyster *Crassostrea virginica* shells: using geochemical tagging to assess population connectivity. *Marine Ecology Progress Series* 543: 173–186. https://doi.org/10.3354/meps11549

Kroll, I.R., A.K. Poray, B.J. Puckett, D.B. Eggleston, and F.J. Fodrie. 2018. Quantifying estuarine-scale invertebrate larval connectivity: methodological and ecological insights. *Limnology and Oceanography* 63 (5): 1979–1991. https://doi.org/10.1-002/lno.10819

Kurmholz, J.S. 2012. Spatial and temporal patterns in nutrient standing stocks and mass-balance in response to load reductions in a temperate estuary. University of Rhode

Island, Ph.D. Dissertation.

Kydd, J., H. Rajakaruna, E. Briski, and S. Bailey. 2018. Examination of a high resolution laser optical plankton counter and FlowCAM for measuring plankton concentration and size. *Journal of Sea Research* 133: 2–10. https://doi.org/10.1016/j.seares.-2017.01.003

Lane, R.R., J.W. Day Jr, B.D. Marx, E. Reyes, E. Hyfield, and J.N. Day. 2007. The effects of riverine discharge on temperature, salinity, suspended sediment and chlorophyll *a* in a Mississippi delta estuary measured using a flow-through system. *Estuarine, Coastal and Shelf Science* 74 (1–2): 145–154. https://doi.org/10.1016/-j.ecss.2007.04.008

Landaeta, M.F., and L.R. Castro. 2006. Larval distribution and growth of the rockfish, *Sebastes capensis* (Sebastidae, Pisces), in the fjords of southern Chile. *ICES Journal of Marine Science* 63 (4): 714–724. https://doi.org/10.1016/-j.icesjms.2006.01.002

Landaeta, M.F., G. López, N. Suárez-Donoso, C.A. Bustos, and F. Balbontín. 2012. Larval fish distribution, growth and feeding in Patagonian fjords: potential effects of freshwater discharge. *Environmental Biology of Fishes* 93 (1): 73–87. https://-doi.org/10.1007/s10641-011-9891-2

Lazareth, C.E., E. Vander Putten, L. André, and F. Dehairs. 2003. High-resolution trace element profiles in shells of the mangrove bivalve *Isognomon ephippium*: a record of environmental spatio-temporal variations? *Estuarine, Coastal and Shelf Science* 57 (5–6): 1103–1114. https://doi.org/10.1016/S0272-7714(03)00013-1

Laznik, M., P. Stålnacke, A. Grimvall, and H.B. Wittgren. 1999. Riverine input of

nutrients to the Gulf of Riga — temporal and spatial variation. *Journal of Marine Systems* 23 (1–3): 11–25. https://doi.org/10.1016/S0924-7963(99)00048-2

Lee, C. 1979. Seasonal and spatial study of oyster spat in Mobile Bay and east Mississippi Sound. University of South Alabama, MS Thesis.

Lehtonen, H., K. Nyberg, P.J. Vuoronen, and A. Leskelä. 1992. Radioactive strontium ([85]Sr) in marking whitefish [*Coregonus lavaretus* (L.)] larvae and the dispersal of larvae from river to sea. *Journal of Fish Biology* 41 (3): 417–423. https://doi.org/-10.1111/j.1095-8649.1992.tb02670.x

Lenihan, H.S., C.H. Peterson, J.E. Byers, J.H. Grabowski, G.W. Thayer, and D.R. Colby. 2001. Cascading of habitat degradation: oyster reefs invaded by refugee fishes escaping stress. *Ecological Applications* 11 (3): 764–782.

Levin, L.A. 1990. A review of methods for labeling and tracking marine invertebrate larvae. *Ophelia* 32 (1–2): 115–144.

https://doi.org/10.1080/00785236.1990.10422028

Levin, L.A., D. Huggett, P. Myers, T. Bridges, and J. Weaver. 1993. Rare-earth tagging methods for the study of larval dispersal by marine invertebrates. *Limnology and Oceanography* 38 (2): 346–360. https://doi.org/10.4319/lo.1993.38.2.0346

Levin, L.A. 2006. Recent progress in understanding larval dispersal: new directions and digressions. *Integrative and Comparative Biology* 46 (3): 282–297. https://doi.org/-10.1093/icb/icj024

Linard, C., Y. Gueguen, J. Moriceau, C. Soyez, B. Hui, A. Raoux, J.P. Cuif, J.-C. Cochard, M. Le Pennec, and G. Le Moullac. 2011. Calcein staining of calcified structures in pearl oyster *Pinctada margaritifera* and the effect of food resource

level on shell growth. *Aquaculture* 313 (1–4): 149–155.
https://doi.org/10.1016/j.aquaculture.2011.01.008

Lipp, E.K., R. Kurz, R. Vincent, C. Rodriguez-Palacios, S.R. Farrah, and J.B. Rose.
2001. The effects of seasonal variability and weather on microbial fecal pollution
and enteric pathogens in a subtropical estuary. *Estuaries* 24 (2): 266–276.

Lorens, R.B., and M.L. Bender. 1980. The impact of solution chemistry on *Mytilus edulis*
calcite and aragonite. *Geochimica et Cosmochimica Acta* 44 (9): 1265–1278.
https://doi.org/10.1016/0016-7037(80)90087-3

MacIntyre, H.L., and J.J. Cullen. 2005. Using cultures to investigate the physiological
ecology of microalgae. In *Algal Culture Techniques*, ed. R.A. Anderson, 287–
327. Burlington: Elsevier.

Malham, S.K., P. Rajko-Nenow, E. Howlett, K.E. Tuson, T.L. Perkins, D.W. Pallett, H.
Wang, C.F. Jago, D.L. Jones, and J.E. McDonald. 2014. The interaction of human
microbial pathogens, particulate material and nutrients in estuarine environments
and their impacts on recreational and shellfish waters. *Environmental Science:
Processes and Impacts* 16: 2145–2155. https://doi.org/10.1039/c4em00031e

Malik, A.S., B.A. Larson, and M. Ribaudo. 1994. Economic incentives for agricultural
nonpoint source pollution control. *Journal of the American Water Resources
Association* 30 (3): 471–480. https://doi.org/10.1111/j.1752-1688.1994.tb03306.x

Mallin, M.A., H.W. Paerl, J. Rudek, and P.W. Bates. 1993. Regulation of estuarine
primary production by watershed rainfall and river flow. *Marine Ecology Progress
Series* 93: 199–203.

Manahan, D.T., and D.J. Crisp. 1982. The role of dissolved organic material in the

nutrition of pelagic larvae: amino acid uptake by bivalve veligers. *American Zoologist* 22 (3): 635–646.

May, E.B. 1971. A survey of the oyster and oyster shell resources of Alabama. *Alabama Marine Resources Bulletin* 4: 1–53.

McCarthy, M.J., D.B. Otis, P. Méndez-Lázaro, and F.E. Muller-Karger. 2018. Water quality drivers in 11 Gulf of Mexico estuaries. *Remote Sensing* 10 (2): 255. https://doi.org/10.3390/rs10020255

Mckee, L., and D. Gluchowski. 2011. Improved nutrient load estimates for wastewater, stormwater and atmospheric deposition to South San Francisco Bay (South of the Bay Bridge). Richmond, CA: SFEI Contribution xx, San Francisco Estuary Institute.

Medcof, J.C. 1939. Larval life of the oyster (*Ostrea virginica*) in Bideford River. *Journal of the Fisheries Board of Canada* 4b (4): 287–301. https://doi.org/10.1139/f38-026

Meerhoff, E., L. Castro, and F. Tapia. 2013. Influence of freshwater discharges and tides on the abundance and distribution of larval and juvenile *Munida gregaria* in the Baker River Estuary, Chilean Patagonia. *Continental Shelf Research* 61–62: 1–11. http://dx.doi.org/10.1016/j.csr.2013.04.025

Millar, R.H. 1961. Scottish oyster investigations 1946–1958. *Marine Research Scotland* 3: 1–76.

Miller, S.H., S.G. Morgan, J. Wilson White, and P.G. Green. 2013a. Interannual variability in an atlas of trace element signatures for determining population connectivity. *Marine Ecology Progress Series* 474: 179–190. https://doi.org/-10.3354/meps10119

Miller, S.H., S.G. Morgan, J. Wilson White, and P.G. Green. 2013b. Trace element

    signatures in larval soft tissues reveal transport, but not population connectivity.

    Marine Ecology Progress Series 481: 1–10. https://doi.org/10.3354/meps10340

Milliman, J.D., K.L. Farnsworth, P.D. Jones, K.H. Xu, and L.C. Smith. 2008. Climatic

    and anthropogenic factors affecting river discharge to the global ocean, 1951–

    2000. *Global and Planetary Change* 62 (3–4): 187–194. https://doi.org/10.1016/-

    j.gloplacha.2008.03.001

Montagna, P.A., and R.D. Kalke. 1992. The effect of freshwater inflow on meiofaunal

    and macrofaunal populations in the Guadalupe and Nueces Estuaries, Texas.

    Estuaries 15 (3): 307–326. https://doi.org/10.2307/1352779

Montiel, D., A. Lamore, J. Stewart, and N. Dimova. 2019. Is submarine groundwater dis-

    charge (SGD) important for the historical fish kills and harmful algal bloom events

    of Mobile Bay? *Estuaries and Coasts* 42 (2): 470–493. https://doi.org/10.1007/-

    s12237-018-0485-5

Moore, R.B., C.M. Johnston, R.A. Smith, and B. Milstead. 2011. Source and delivery of

    nutrients to receiving waters in the northeastern and mid-Atlantic regions of the

    United States. *Journal of the American Water Resources Association* 47 (5): 965–

    990.

Moran, A.L. 2000. Calcein as a marker in experimental studies newly-hatched

    gastropods. *Marine Biology* 137 (5–6): 893–898. https://doi.org/10.1007-

    /s002270000390

Moran, A.L., and P.B. Marko. 2005. A simple technique for physical marking of larvae
of marine bivalves. *Journal of Shellfish Research* 24 (2): 567–571.
https://doi.org/10.2983/0730-8000(2005)24[567:ASTFPM]2.0.CO;2

Muggeo, A.M.R. 2019. Package 'segmented': regression models with break-
points/change-points estimation. *R package version* 1.1–0.

Mulholland, P.J., G.R. Best, C.C Coutant, G.M. Hornberger, J.L. Meyer, P.J. Robinson,
J.R. Stenberg, R.E. Turner, F. Vera-Herrera, and R.G. Wetzel. 1997. Effects of
climate change on freshwater ecosystems of the southeastern United States and the
Gulf Coast of Mexico. *Hydrological Processes* 11 (8): 949–970.
https://doi.org/10.1002/(SICI)1099-1085(19970630)11:8<949::AID-
HYP513>3.0.CO;2-G

Murray, C., B. Müller-Karulis, J. Carstensen, D.J. Conley, B.G. Gustafsson, and J.H.
Andersen. 2019. Past, present and future eutrophication status of the Baltic Sea.
Frontiers in Marine Science 6: 2. https://doi.org/10.3389/fmars.2019.00002

Nagieć, M., P. Czerkies, K. Goryczko, A. Witkowski, and E. Murawska. 1995. Mass-
marking of grayling, *Thymallus thymallus* (L.), larvae by fluorochrome tagging of
otoliths. *Fisheries Management and Ecology* 2 (3): 185–195. https://doi.org-
/10.1111/j.1365-2400.1995.tb00111.x

Narragansett Bay Estuary Program. 2017. Nutrient loading. In *State of Narragansett Bay
and it's watershed*, 166–189. Providence, RI.

National Research Council. 2000. Clean coastal waters: understanding and reducing the
effects of nutrient pollution. Washington, DC: National Academies Press.

National Shellfish Sanitation Program. 2015. Guide for the Control of Molluscan

Shellfish 2015 Revision.

Nedwell, D.B., L.F. Dong, A. Sage, and G.J.C. Underwood. 2002. Variations of the
nutrients loads to the mainland U.K. estuaries: correlation with catchment areas,
urbanization and coastal eutrophication. *Estuarine, Coastal and Shelf Science* 54 (6):
951–970. https://doi.org/10.1006/ecss.2001.0867

Nelson, T.C. 1928. Relation of spawning of the oyster to temperature. *Ecology* 9 (2):
145–154. https://doi.org/10.2307/1929351

Nelson, K.A., L.A. Leonard, M.H. Posey, T.D. Alphin, and M.A. Mallin. 2004. Using
transplanted oyster (*Crassostrea virginica*) beds to improve water quality in small
tidal creeks: a pilot study. *Journal of Experimental Marine Biology and Ecology*
298 (2): 347–368. https://doi.org/10.1016/S0022-0981(03)00367-8

Newell, R.I.E., T.R. Fisher, R.R. Holyoke, and J.C. Cornwell. 2005. Influence of eastern
oysters on nitrogen and phosphorus regeneration in Chesapeake Bay, USA. In:
The comparative roles of suspension feeders in ecosystems, ed. R. Dame and S.
Olenin, Vol. 47, 93–120. NATO Science Series: IV - Earth and Environmental
Sciences. Springer, Netherlands.

Newell R.I.E., V.S. Kennedy, J.L. Manuel, and D. Meritt. 2005. Behavioral responses of
Crassostrea ariakensis and *Crassostrea virginica* larvae to environmental change
under spatially realistic conditions. Final Report to Maryland Department of
Natural Resources, Annapolis, MD, 28.

Niemand, C. 2009. The application of elemental fingerprinting techniques to identify
population connectivity using *austrovenus stutchburyi* recruits. The University of
Waikato, Ph.D. Dissertation.

Nixon, S.W., and M.E. Pilson. 1983. Nitrogen in estuarine and coastal marine
ecosystems. In *Nitrogen in the marine environment*, ed. E.J. Carpenter and D.G.
Capone, 565–648. Academic Press.

Nixon, S.W. 1995. Coastal marine eutrophication: a definition, social causes, and future
concerns. *Ophelia* 41 (1): 199–219. https://doi.org/10.1080/00785236.-
1995.10422044

Nixon, S.W. 2003. Replacing the Nile: are anthropogenic nutrients providing the fertility
once brought to the Mediterranean by a great river? *AMBIO: A Journal of the
Human Environment* 32 (1): 30–40.

Nixon, S.W., and B.A. Buckley. 2002. **"A strikingly rich zone"**—nutrient enrichment and
secondary production in coastal marine ecosystems. *Estuaries* 25 (4): 782**–**796.

Norrie, C.R., B.J. Dunphy, J.A. Baker, and C.J. Lundquist. 2016. Local-scale variation in
trace elemental fingerprints of the estuarine bivalve *Austrovenus stutchburyi*
within and between estuaries. *Marine Ecology Progress Series* 559: 89–102.
https://doi.org/10.3354/meps11890

North, E.W., and E.D. Houde. 2003. Linking ETM physics, zooplankton prey, and fish
early-life histories to striped bass *Morone saxatilis* and white perch *M. americana*
recruitment. *Marine Ecology Progress Series* 260: 219–236. https://doi.org/-
10.3354/meps260219

North, E.W., Z. Schlag, R.R. Hood, M. Li, L. Zhong, T. Gross, and V.S. Kennedy. 2008.
Vertical swimming behavior influences the dispersal of simulated oyster larvae in
a coupled particle-tracking and hydrodynamic model of Chesapeake Bay. *Marine
Ecology Progress Series* 359: 99–115. https://doi.org/10.3354/meps07317

Novick, E., and D. Senn. 2014. External nutrient loads to San Francisco Bay.

    Contribution No. 704. Richmond, California: San Francisco Estuary Institute.

O'Bannon, B.K. 2001. Fisheries of the United States 2000. *National Marine Fisheries*

    Service.

O'Connor, M.I., J.F. Bruno, S.D Gaines, B.S. Halpern, S.E. Lester, B.P. Kinlan, and J.M.

    Weiss. 2007. Temperature control of larval dispersal and the implications for

    marine ecology, evolution, and conservation. *Proceedings of the National*

    Academy of Sciences 104 (4): 1266–1271. https://doi.org/10.1073/pnas.-

    0603422104

Ortega, S., and J.P. Sutherland. 1992. Recruitment and growth of the eastern oyster,

    Crassostrea virginica, in North Carolina. *Estuaries* 15 (2): 158–170.

Park, K., C.-K. Kim, and W.W. Schroeder. 2007. Temporal variability in summertime

    bottom hypoxia in shallow areas of Mobile Bay, Alabama. *Estuaries and Coasts*

    30 (1): 54–65.

Park, K., S.P. Powers, G.S. Bosarge, and H.-S. Jung. 2014. Plugging the leak: Barrier

    island restoration following Hurricane Katrina enhances habitat quality for oysters

    in Mobile Bay, Alabama. *Marine Environmental Research* 94: 48–55. https://-

    doi.org/10.1016/j.marenvres.2013.12.003

Paerl, H.W., K.L. Rossignol, S.N. Hall, B.L. Peierls, and M.S. Wetz. 2010.

    Phytoplankton community indicators of short-and long-term ecological change in

    the anthropogenically and climatically impacted Neuse River Estuary, North

    Carolina, USA. *Estuaries and Coasts* 33 (2): 485–497.

Peeler, K.A., S.P. Opsahl, and J.P. Chanton. 2006. Tracking anthropogenic inputs using

    caffeine, indicator bacteria, and nutrients in rural freshwater and urban marine

    systems. *Environmental Science and Technology* 40 (24): 7616–7622. https://-

    doi.org/10.1021/es061213c

Peguero-Icaza, M., L. Sánchez-Velasco, M.F. Lavín, S.G. Marinone, and E. Beier. 2011.

    Seasonal changes in connectivity routes among larval fish assemblages in a semi-

    enclosed sea (Gulf of California). *Journal of Plankton Research* 33 (3): 517–533.

    https://doi.org/10.1093/plankt/fbq107

Pennock, J.R., J.H. Sharp, and W.W. Schroeder. 1994. What controls the expression of

    estuarine eutrophication? Case studies of nutrient enrichment in the Delaware Bay

    and Mobile Bay Estuaries, USA. In *changes in fluxes in estuaries: implications*

    from science to management, ed. K.R. Dyer and R.J. Orth, 139–146. International

    Symposium series.

Pineda, J., J.A. Hare, and S. Sponaugle. 2007. Larval transport and dispersal in the

    coastal ocean and consequences for population connectivity. *Oceanography* 20

    (3): 22–39.

Pollack, J.B., H.-C. Kim, E.K. Morgan, and P.A. Montagna. 2011. Role of flood

    disturbance in natural oyster (*Crassostrea virginica*) population maintenance in

    an estuary in south Texas, USA. *Estuaries and Coasts* 34 (1): 187–197. https://-

    doi.org /10.1007/s12237-010-9338-6

Powell, E.N., J.M. Klinck, E.E. Hofmann, and M.A. McManus. 2003. Influence of water

    allocation and freshwater inflow on oyster production: a hydrodynamic-oyster

    population model for Galveston Bay, Texas, USA. *Environmental Management*

31 (1): 100–121. https://doi.org/10.1007/s00267-002-2695-6

Puckett, B.J., and D.B. Eggleston. 2016. Metapopulation dynamics guide marine reserve design: importance of connectivity, demographics, and stock enhancement. *Ecosphere* 7 (6): e01322. https://doi.org/10.1002/ecs2.1322

Qu, H.J., and C. Kroeze. 2010. Past and future trends in nutrients export by rivers to the coastal waters of China. *Science of the Total Environment* 408 (9): 2075–2086. https://doi.org/10.1016/j.scitotenv.2009.12.015

Quayle, D.B., and G.F. Newkirk. 1989. Farming bivalve molluscs: methods for study and development. In *Advances in World Aquaculture*, Vol. 1.

R Core Team. 2017. R: A language and environment for statistical computing. R Foundation for Statistical Computing, Vienna, Austria. URL https://www.R-project.org/

Rabalais, N.N. 2002. Nitrogen in aquatic ecosystems. *AMBIO: A Journal of the Human Environment* 31 (2): 102-113. https://doi.org/10.1579/0044-7447-31.2.102

Rask, N., S.E. Pedersen, and M.H. Jensen. 1999. Response to lowered nutrient discharges in the coastal waters around the island of Funen, Denmark. *Hydrobiologia* 393: 69–81.

Reeves, R.L., S.B. Grant, R.D. Mrse, C.M. Oancea, B.F. Sanders, and A.B. Boehm. 2004. Scaling and management of fecal indicator bacteria in runoff from a coastal urban watershed in southern California. *Environmental Science and Technology* 38 (9): 2637–2648. https://doi.org/10.1021/es034797g

Reiner, S.L. 2011. Evaluating the use of flow-through larval culture for the eastern oyster, *Crassostrea virginica*. College of William and Mary, MS Thesis.

Reinert, T.R., M.C. Wallin, M.J. Conroy, and M.J. Van Den Avyle. 1998. Long-term

retention and detection of oxytetracycline marks applied to hatchery-reared larval

striped bass, *Morone saxatilis*. *Canadian Journal of Fisheries and Aquatic Sciences*

55 (3): 539–543. https://doi.org/10.1139/f97-280

Rhodes, M.W., and H. Kator. 1988. Survival of *Escherichia coli* and *Salmonella* spp. in

estuarine environments. *Applied and Environmental Microbiology* 54 (12): 2902–

2907.

Richmond, C.E., and S.A. Woodin. 1996. Short-term fluctuations in salinity: effects on

planktonic invertebrate larvae. *Marine Ecology Progress Series* 133: 167–177.

https://doi.org/10.3354/meps133167

Ricker, W.E. 1956. Uses of marking animals in ecological studies: the marking of fish.

Ecology 37 (4): 665–670.

Rikard, F.S., and W.C. Walton. 2010. Use of microalgae concentrations for rearing oyster

larvae, *Crassostrea virginica*. NOAA/MS-AL Sea Grant. MASGP-12-048.

Rippey, S.R. 1994. Infectious diseases associated with moluscan shellfish consumption.

Clinical Microbiology Reviews 7 (4): 419–425. https://doi.org/10.1128/CMR.7-

.4.419

Rippey, S.R., W.N. Adams, and W.D. Watkins. 1987. Enumeration of fecal coliforms

and *E. coli* in marine and estuarine waters: an alternative to the APHA-MPN

approach. *Journal (Water Pollution Control Federation)* 59 (8): 795–798.

Roever, C., N. Raabe, K. Luebke, U. Ligges, G. Szepannek, and M. Zentgraf. 2018. klaR:

classification and visualization. *R package version* 0.6–14.

Roman, M.R., and W.C. Boicourt. 1999. Dispersion and recruitment of crab larvae in the

Chesapeake Bay plume: physical and biological controls. *Estuaries* 22 (3): 563–574.

Rumrill, S.S. 1990. Natural mortality of marine invertebrate larvae. *Ophelia* 32 (1–2): 163–198. https://doi.org/10.1080/00785236.1990.10422030

Saoud, I.G., D.B. Rouse, R.K. Wallace, J. Howe, and B. Page. 2000. Oyster *Crassostrea virginica* spat settlement as it relates to the restoration of Fish River Reef in Mobile Bay, Alabama. *Journal of World Aquatic Society* 31: 640–650. https://-doi.org/10.1111/j.1749-7345.2000.tb00914.x

Scallan, E., R.M. Hoekstra, F.J. Angulo, R.V. Tauxe, M.-A. Widdowson, S.L. Roy, J.L. Jones, and P.M. Griffin. 2011. Foodborne illness acquired in the United States-major pathogens. *Emerging Infectious Diseases* 17 (1): 7–15. https://doi.org/-10.3201/eid1701.P11101

Schindler, D.W. 2006. Recent advances in the understanding and management of eutrophication. *Limnology and Oceanography* 51 (1part2): 356–363. https://-doi.org/10.4319/lo.2006.51.1_part_2.0356

Schöne, B.R. 2008. The curse of physiology—challenges and opportunities in the interpretation of geochemical data from mollusk shells. *Geo-Marine Letters* 28 (5–6): 269–285.

Secor, D.H., and E.D. Houde. 1995. Temperature effects on the timing of striped bass egg production, larval viability, and recruitment potential in the Patuxent River (Chesapeake Bay). *Estuaries* 18 (3): 527–544.

Secor, D.H., E.D. Houde, and D.M. Monteleone. 1995. A mark-release experiment on larval striped bass *Morone saxatilis* in a Chesapeake Bay tributary. *ICES Journal of*

Marine Science 52 (1): 87–101. https://doi.org/10.1016/1054-3139(95)80018-2

Secor, D.H., E.D. Houde, and L.L. Kellogg. 2017. Estuarine retention and production of

    striped bass larvae: a mark-recapture experiment. *ICES Journal of Marine Science*

    74 (6): 1735–1748. https://doi.org/10.1093/icesjms/fsw245

Seitzinger, S.P., R.W. Sanders, and R. Styles. 2002. Bioavailability of DON from natural

    and anthropogenic sources to estuarine plankton. *Limnology and Oceanography* 47

    (2): 353–366. https://doi.org/10.4319/lo.2002.47.2.0353

Seitzinger, S.P., and J.A. Harrison. 2008. Land-based nitrogen sources and their delivery

    to coastal systems. In *Nitrogen in the marine environment*, ed. D.G. Capone, D.A.

    Bronk, M.R. Mulholland, and E.J. Carpenter, 469–510. Academic.

Shoji, J., T. Ohta, and M. Tanaka. 2006. Effects of river flow on larval growth and

    survival of Japanese seaperch *Lateolabrax japonicus* (Pisces) in the Chikugo

    River Estuary, upper Ariake Bay. *Journal of Fish Biology* 69 (6): 1662–1674.

    https://doi.org/10.1111/j.1095-8649.2006.01235.x

Siegel, D.A., S. Mitarai, C.J. Costello, S.D. Gaines, B.E. Kendall, R.R. Warner, and K.B.

    Winters. 2008. The stochastic nature of larval connectivity among nearshore

    marine populations. *Proceedings of the National Academy of Sciences USA* 105

    (26): 8974–8979. https://doi.org/10.1073/pnas.0802544105

Silva, M.A.M., G.F. Eça, D.F. Santos, A.G. Guimarães, M.C. Lima, and M.F.L. de

    Souza. 2013. Dissolved inorganic nutrients and chlorophyll *a* in an estuary

    receiving sewage treatment plant effluents: Cachoeira River Estuary (NE

    Brazil). *Environmental Monitoring and Assessment* 185 (7): 5387–5399.

Sinton, L.W., C.H. Hall, P.A. Lynch, and R.J. Davies-Colley. 2002. Sunlight inactivation

of fecal indicator bacteria and bacteriophages from waste stabilization pond effluent in fresh and saline waters. *Applied and Environmental Microbiology* 68 (3): 1122–1131. https://doi.org/10.1128/AEM.68.3.1122-1131.2002

Skreslet, S. 1986. The role of freshwater outflow in coastal marine ecosystems. NATO Advanced Studies Institute Series G. Ecological Science, Vol 7. Springer-Verlag, Berlin.

Šolić, M., N. Krstulović, S. Jozić, and D. Curać. 1999. The rate of concentration of faecal coliforms in shellfish under different environmental conditions. *Environment International* 25 (8): 991–1000. https://doi.org/10.1016/S0160-4120(99)00067-7

Soniat, T.M., J.M. Klinck, E.N. Powell, and E.E. Hofmann. 2012. Understanding the success and failure of oyster populations: periodicities of *Perkinsus marinus*, and oyster recruitment, mortality, and size. *Journal of Shellfish Research* 31 (3): 635–646. https://doi.org/10.2983/035.031.0307

Soniat, T.M., C.P. Conzelmann, J.D. Byrd, D.P. Roszell, J.L. Bridevaux, K.J. Suir, and S.B. Colley. 2013. Predicting the effects of proposed Mississippi River diversions on oyster habitat quality; application of an oyster habitat suitability index model. *Journal of Shellfish Research* 32 (3): 629–638. https://doi.org/10.2983/035.032.-0302

Snell, J., 2019. The Bonnet Carré Spillway sets a record for the most days operating in a single year. WAFB9 (June 12, 2019). Accessed 17/07/19.

Specker, L., 2019. No oyster season this year, Alabama harvesters told. AL.com (November 8, 2018). Accessed 17/07/19.

Spires, J. 2015. The exchange of eastern oyster (*Crassostrea virginica*) larvae between

subpopulations in the Choptank and Little Choptank Rivers: model simulations, the influence of salinity, and implications for restoration. University of Maryland, College Park, MS Thesis. https://doi.org/10.13016/M2F949

Stańczak, K., S. Krejszeff, M. Dębowska, K. Mierzejewska, M. Woźniak, and P. Hliwa. 2015. Mass marking of *Leuciscus idus* larvae using *Artemia salina* as a vector of fluorescent dyes. *Journal of Fish Biology* 87 (3): 799–804. https://doi.org/10.1111/-jfb.12753

Statham, P.J. 2012. Nutrients in estuaries — An overview and the potential impacts of climate change. *Science of the Total Environment* 434: 213–227. https://doi.org/-10.1016/j.scitotenv.2011.09.088

Steets, B.M., and P.A. Holden. 2003. A mechanistic model of runoff-associated fecal coliform fate and transport through a coastal lagoon. *Water Research* 37 (3): 589–608. https://doi.org/10.1016/S0043-1354(02)00312-3

Stenzel, H.B. 1964. Oysters: composition of the larval shell. *Science* 145: 155−156. https://doi.org/10.1126/science.145.3628.155

Stepanauskas, R., H. Laudon, and N.O. Jørgensen. 2000. High DON bioavailability in boreal streams during a spring flood. *Limnology and Oceanography* 45 (6): 1298–1307. https://doi.org/10.4319/lo.2000.45.6.1298

Stout, J.P. K.L. Heck, J.F. Valentine, S.J. Dunn, and P.M. Spitzer. 1998. Preliminary characterization of habitat loss: Mobile Bay National Estuary Program. *MESC Contribution* 301. Dauphin Island: Alabama.

Strickland, J., and T.R. Parsons. 1972. A practical handbook of seawater analysis, 2nd ed. Ottawa: Bulletin of the Fisheries Research Board of Canada.

Strydom, N.A., A.K. Whitfield, and A.W. Paterson. 2002. Influence of altered freshwater

    flow regimes on abundance of larval and juvenile *Gilchristella aestuaria* (Pisces:

    Clupeidae) in the upper reaches of two South African estuaries. *Marine and*

    Freshwater Research 53 (2): 431–438. https://doi.org/10.1071/MF01077

Supan, J. 2014. High-density rearing of oyster larvae in flow-through systems. *Southern*

    Regional Aquaculture Center Publication Number 4311.

Surge, D.M., K.C. Lohmann, and G.A. Goodfriend. 2003. Reconstructing estuarine

    conditions: oyster shells as recorders of environmental change, Southwest

    Florida. *Estuarine, Coastal and Shelf Science* 57 (5–6): 737–756. https://-

    doi.org/10.1016/S0272-7714(02)00370-0

Swearer, S.E., G.E. Forrester, M.A. Steele, A.J. Brooks, and D.W. Lea. 2003. Spatio-

    temporal and interspecific variation in otolith trace-elemental fingerprints in a

    temperate estuarine fish assemblage. *Estuarine, Coastal and Shelf Science* 56 (5–

    6): 1111–1123. https://doi.org/10.1016/S0272-7714(02)00317-7

Tao, L., W. Shanna, C. Hongying, C. Zhang, L. Haitao, L. Hengpeng, S. Wenchong, and

    C. Zhongyi. 2008. Estimation of ammonia nitrogen load from nonpoint sources in

    the Xitiao River Catchment, China. *Journal of Environmental Sciences* 20 (10):

    1195–1201. https://doi.org/10.1016/S1001-0742(08)62209-3

Tamburri, M.N., M.W. Luckenbach, D.L. Breitburg, and S.M. Bonniwell. 2008.

    Settlement of *Crassostrea ariakensis* larvae: effects of substrate, biofilms,

    sediment and adult chemical cues. *Journal of Shellfish Research* 27 (3): 601−608.

    https://doi.org/10.2983/0730-8000(2008)27[601:SOCALE]2.0.CO;2

Tatum, W.M., M.S. Van Hoose, R.W. Havard, and M.C. Clark. 1995. The 1995 Atlas of major public oyster reefs of Alabama and a review of oyster management efforts 1975–1995. *Alabama Marine Resource Bulletin* 14: 1−15.

Taylor, M.S., and M.E. Hellberg. 2003. Genetic evidence for local retention of pelagic larvae in a Caribbean reef fish. *Science* 299 (3): 107–109. https://doi.org/10.1126/-science.1079365

Thébault, J., L. Chauvaud, J. Clavier, R. Fichez, and E. Morize. 2006. Evidence of a 2-day periodicity of striae formation in the tropical scallop *Comptopallium radula* using calcein marking. *Marine Biology* 149 (2): 257–267. https://doi.org/10.1007-/s00227-005-0198-8

Thébault, J., L. Chauvaud, S. L'Helguen, J. Clavier, A. Barats, S. Jacquet, C. Pécheyran, and D. Amouroux. 2009. Barium and molybdenum records in bivalve shells: geochemical proxies for phytoplankton dynamics in coastal environments? *Limnology and Oceanography* 54 (3): 1002–1014. https://doi.org/10.4319/-lo.2009.54.3.1002

Thorrold, S.R., G.P. Jones, M.E. Hellberg, R.S. Burton, S.E. Swearer, J.E. Neigel, A.G. Morgan, and R.R. Warner. 2002. Quantifying larval retention and connectivity in marine populations with artificial and natural markers. *Bulletin of Marine Science* 70 (1): 291–308.

Thorrold, S.R., D.C. Zacherl, and L.A. Levin. 2007. Population connectivity and larval dispersal using geochemical signatures in calcified structures. *Oceanography* 20 (3): 80–89. https://doi.org/10.5670/oceanog.2007.31

Tiwari, S., and S. Gallager. 2003. Machine learning and multiscale methods in the

    identification of bivalve larvae. *Proceedings Ninth IEEE International*

    Conference on Computer Vision 494–501. https://doi.org/10.1109/I-

    CCV.2003.1238388

Tsukamoto, K., and T. Kajihara. 1987. Age determination of Ayu with otolith. *Nippon*

    Suisan Gakkaishi 53 (11): 1985–1997. https://doi.org/10.2331/suisan.53.1985

Turner, R.E. 2006. Will lowering estuarine salinity increase Gulf of Mexico oyster

    landings? *Estuaries and Coasts* 29 (3): 345–352. https://doi.org/10.1007/-

    BF02784984

United States Environmental Protection Agency. 1986. Ambient water quality criteria for

    bacteria, EPA440/5-84-002. Washington, D.C.

United States Environmental Protection Agency. 2002. Waquoit Bay watershed

    ecological risk assessment: the effect of land-derived nitrogen loads on estuarine

    eutrophication, EPA/600/R-02/079. Washington, D.C.

United States Environmental Protection Agency. 2003. Bacterial water quality standards

    for recreational waters (fresh and marine waters). Washington, DC, USA: Office

    of Water.

United States Environmental Protection Agency. 2006. Volunteer estuary monitoring: a

    methods manual, EPA-842-B-06-003. Washington, DC, USA: Office of Water.

United States Environmental Protection Agency. 2012. Recreational water quality

    criteria, 820-F-12-058. Washington, DC, USA: Office of Water.

United States Geological Survey. 2017. USGS National Hydrography Dataset Best

    Resolution 20170312 for Alabama State or Territory File GDB 10.1 Model

Version 2.2.1. Retrieved from ftp://rockyftp.cr.usgs.gov/vdelivery/datasets/sta-

ged/hydrography/NHD/state/highresolution/shape/NHD_H_Alabama_Shape.zip.

Utting, S.D., and B.E. Spencer. 1991. The hatchery culture of bivalve mollusc larvae and

juveniles. *Ministry of Agriculture, Fisheries, and Food Directorate of Fisheries Research Laboratory leaflet* 68.

Valiela, I., K. Foreman, M. LaMontagne, D. Hersh, J. Costa, P. Peckol, B. DeMeo-

Andreson, C. D'Avanzo, M. Babione, C.-H. Sham, J. Brawley and K. Lajtha.

1992. Couplings of watersheds and coastal waters: sources and consequences of

nutrient enrichment in Waquoit Bay, Massachusetts. *Estuaries* 15 (4): 443–457.

Van Drecht, G., A.F. Bouwman, J.M. Knoop, A.H.W Beusen, and C.R. Meinardi. 2003.

Global modeling of the fate of nitrogen from point and nonpoint sources in soils,

groundwater, and surface water. *Global Biogeochemical Cycles* 17 (4): 1115.

https://doi.org/10.1029/2003GB002060

van der Geest, M., J.A. van Gils, J. van der Meer, H. Olff, and T. Piersma. 2011.

Suitability of calcein as an *in situ* growth marker in burrowing bivalves. *Journal of Experimental Marine Biology and Ecology* 399 (1): 1–7. https://doi.org/-

10.1016/j.jembe.2011.01.003

Vander Putten, E., F. Dehairs, E. Keppens, and W. Baeyens. 2000. High resolution

distribution of trace elements in the calcite shell layer of modern *Mytilus edulis*:

environmental and biological controls. *Geochimica et Cosmochimica Acta* 64 (6):

997–1011. https://doi.org/10.1016/S0016-7037(99)00380-4

Vant, W. 2001. New challenges for the management of plant nutrients and pathogens in the Waikato River, New Zealand. *Water Science and Technology* 43 (5): 137–144. https://doi.org/10.2166/wst.2001.0270

Vargas, C.A., D.A. Narváez, A. Piñones, S.A. Navarrete, and N.A. Lagos. 2006. River plume dynamic influences transport of barnacle larvae in the inner shelf off central Chile. *Journal of the Marine Biological Association of the United Kingdom* 86 (5): 1057–1065. https://doi.org/10.1017/S0025315406014032

Venables, W.N., and B.D. Ripley. 2002. Modern Applied Statistics with S. 4th edition. Springer-Verlag: New York.

Viitasalo, S., J. Sassi, J. Rytkönen, and E. Leppäkoski. 2005. Ozone, ultraviolet light, ultrasound and hydrogen peroxide as ballast water treatments - experiments with mesozooplankton in low-saline brackish water. *Journal of Marine Environmental Engineering* 8 (1): 35–55.

Vollenweider, R.A. 1976. Advances in defining critical loading levels for phosphorus in lake eutrophication. *Memorie dell'Istituto Italiano di Idrobiologia, Dott. Marco de Marchi Verbania Pallanza* 33: 53–83.

Vörösmarty, C.J., P. Green, J. Salisbury, and R.B. Lammers. 2000. Global water resources: vulnerability from climate change and population growth. *Science* 289 (5477): 284–288.

Wallace, R.K., P. Waters, and F.S. Rikard. 2008. Oyster hatchery techniques. *Southern Regional Aquaculture Center*. Publication No. 4302.

Ward Jr., G.H. 1980. Hydrography and circulation processes of Gulf estuaries. In *Estuarine and wetland processes with emphasis on modelling*, ed. P. Hamilton and K.B. MacDonald, 183–215. Plenum: New York.

Webb, B.M., and C. Marr. 2016. Spatial variability of hydrodynamic timescales in a broad and shallow estuary: Mobile Bay, Alabama. *Journal of Coastal Research* 32 (6): 1374–1388. https://doi.org/10.2112/JCOASTRES-D-15-00181.1

Weiskel, P.K., and B.L. Howes. 1992. Differential transport of sewage-derived nitrogen and phosphorus through a coastal watershed. *Environmental Science and Technology* 26: 352–360. https://doi.org/10.1021/es00026a017

Weiskel, P.K., B.L. Howes, and G.R. Heufelder. 1996. Coliform contamination of a coastal embayment: sources and transport pathways. *Environmental Science and Technology* 30 (6): 1872–1881. https://doi.org/10.1021/es950466v

Weiss, I.M., N. Tuross, L. Addadi, and S. Weiner. 2002. Mollusc larval shell formation: amorphous calcium carbonate is a precursor phase for aragonite. *Journal of Experimental Zoology* 293 (5): 478–491. https://doi.org/10.1002/jez.90004

Wetz, J.J., E.K. Lipp, D.W. Griffin, J. Lukasik, D. Wait, M.D. Sobsey, T.M. Scott, and J.B. Rose. 2004. Presence, infectivity, and stability of enteric viruses in seawater: relationship to marine water quality in the Florida Keys. *Marine Pollution Bulletin* 48 (7–8): 698–704. https://doi.org/10.1016/j.marpolbul.2003.09.008

Wetz, M.S., and D.W. Yoskowitz. 2013. An 'extreme' future for estuaries? Effects of extreme climatic events on estuarine water quality and ecology. *Marine Pollution Bulletin* 69 (1–2): 7–18. https://doi.org/10.1016/j.marpolbul.2013.01.020

Whitall, D., S. Bricker, J. Ferreira, A.M. Nobre, T. Simas, and M. Silva. 2007. Assessment of eutrophication in estuaries: pressure–state–response and nitrogen source apportionment. *Environmental Management* 40 (4): 678–690. https://-doi.org/10.1007/s00267-005-0344-6

Whitall, D., and S. Bricker. 2006. Assessment of eutrophication in estuaries: pressure-state-response and source apportionment. USDA Forest Service Proceedings RMRS-P-42CD.

Wilber, D.H. 1992. Associations between freshwater inflows and oyster productivity in Apalachicola Bay, Florida. *Estuarine, Coastal and Shelf Science* 35 (2): 179–190. https://doi.org/10.1016/S0272-7714(05)80112-X

Wilson C.A., D.W. Beckman, and J.M. Dean. 1987. Calcein as a fluorescent marker of otoliths of larval and juvenile fish. *Transactions of the American Fisheries Society* 116 (4): 668–670. https://doi.org/10.1577/15488659(1987)116<668:CAAFMO->2.0.CO;2

Winfield, M.D., and E.A. Groisman. 2003. Role of nonhost environments in the lifestyles of *Salmonella* and *Escherichia coli*. *Applied and Environmental Microbiology* 69 (7): 3687–3694. https://doi.org/10.1128/AEM.69.7.3687-3694.2003

Wood, S. 2012. mgcv: Mixed GAM computation vehicle with GCV/AIC/REML smoothness estimation. *R package version* 1.7–17.

Wood, L.H., and W.J. Hargis. 1971. *Transport of bivalve larvae in a tidal estuary*, 29–44). Cambridge University Press.

Zacherl, D.C., G. Paradis, and D.W. Lea. 2003. Barium and strontium uptake into larval protoconchs and statoliths of the marine neogastropod *Kelletia kelletii*.

Geochimica et Cosmochimica Acta 67 (21): 4091−4099. https://doi.org/-
10.1016/S0016-7037(03)00384-3

Zacherl, D.C. 2005. Spatial and temporal variation in statolith and protoconch trace
elements as natural tags to track larval dispersal. *Marine Ecology Progress Series*
290: 145–163. https://doi.org/10.3354/meps290145

zu Ermgassen, P.S., M.D. Spalding, B. Blake, L.D. Coen, B. Dumbauld, S. Geiger, J.H.
Grabowski, R. Grizzle, M. Luckenbach, K. McGraw, W. Rodney, J.L. Ruesink,
S.P. Powers, and R.D. Brumbaugh. 2012. Historical ecology with real numbers:
past and present extent and biomass of an imperiled estuarine habitat.
Proceedings of the Royal Society B: Biological Sciences 279: 3393–3400.

Zuliani, A., L. Zaggia, F. Collavini, and R. Zonta. 2005. Freshwater discharge from the
drainage basin to the Venice Lagoon (Italy). *Environment International* 31 (7):
929–938. https://doi.org/10.1016/j.envint.2005.05.004

Zuur, A., E.N. Ieno, and G.M. Smith. 2007. Analyzing ecological data. Springer Science
and Business Media.

Zuur, A., E.N. Ieno, N. Walker, A.A. Saveliev, and G.M. Smith. 2009. Mixed effects
models and extensions in ecology with R. Springer Science and Business Media.

APPENDICES

Table A1. Number of stained and unstained oysters found in Niskin samples at 1, 2, 3, and 5 days following the release of stained larvae on May 19 (lower salinity) and July 28 (higher salinity), 2014. Salinity data reflect field measurements on the day of recapture and model outputs from noon each day (closest to field sampling time) for each sampling site from an existing larval transport model.

Release date	Day	Site	Oysters (20 L^{-1})		Salinity	
			Unstained	Stained	YSI	Model
May 19	0	1	-	-	4.7	3.6
		2	-	-	5.2	4.8
	1	1	0	0	-	3.3
		2	2	0	-	4.0
		3	1	0	7.5	5.2
		4	0	0	12.6	11.4
	2	1	0	0	-	3.4
		2	0	0	-	4.0
		3	0	0	-	4.5
		4	0	0	-	9.5
	3	1	0	0	-	3.4
		2	0	0	-	5.8
		3	0	0	-	7.2
		4	0	0	-	12
	5	1	0	0	-	4.5
		2	0	0	-	6.1
		3	0	0	-	7.4
		4	0	0	-	12.1
July 28	0	1	-	-	19.5	12.7
		2	-	-	22.5	21.5
	1	1	0	0	12.0	12.1
		2	0	0	15.0	17.0
		3	0	0	18.6	22.6
		4	4	0	26.3	26.0
	2	1	0	0	11.8	11.9
		2	0	0	13.8	15.8

Table A1 cont.

Release date	Day	Site	Oysters (20 L⁻¹)		Salinity	
			Unstained	Stained	YSI	Model
		3	-	-	16.7	17.7
		4	4	1	26.1	25.0
July 28	3	1	0	0	12.0	12.0
		2	0	0	15.7	15.1
		3	1	0	18.0	16.5
		4	2	0	28.7	24.8
	5	1	0	0	18.2	9.1
		2	0	0	22.5	10.7
		3	0	0	21.9	11.6
		4	2	1	31.0	20.5
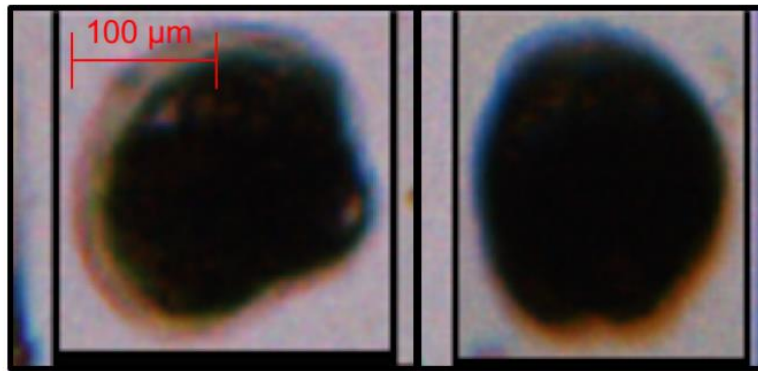
Figure A1. FlowCam images of stained oysters recaptured following the second release (July 28, 2014) at site 4 on day 2 (190 μm, anterior to posterior orientation; left panel) and day 5 (220 μm, posterior orientation; right panel).
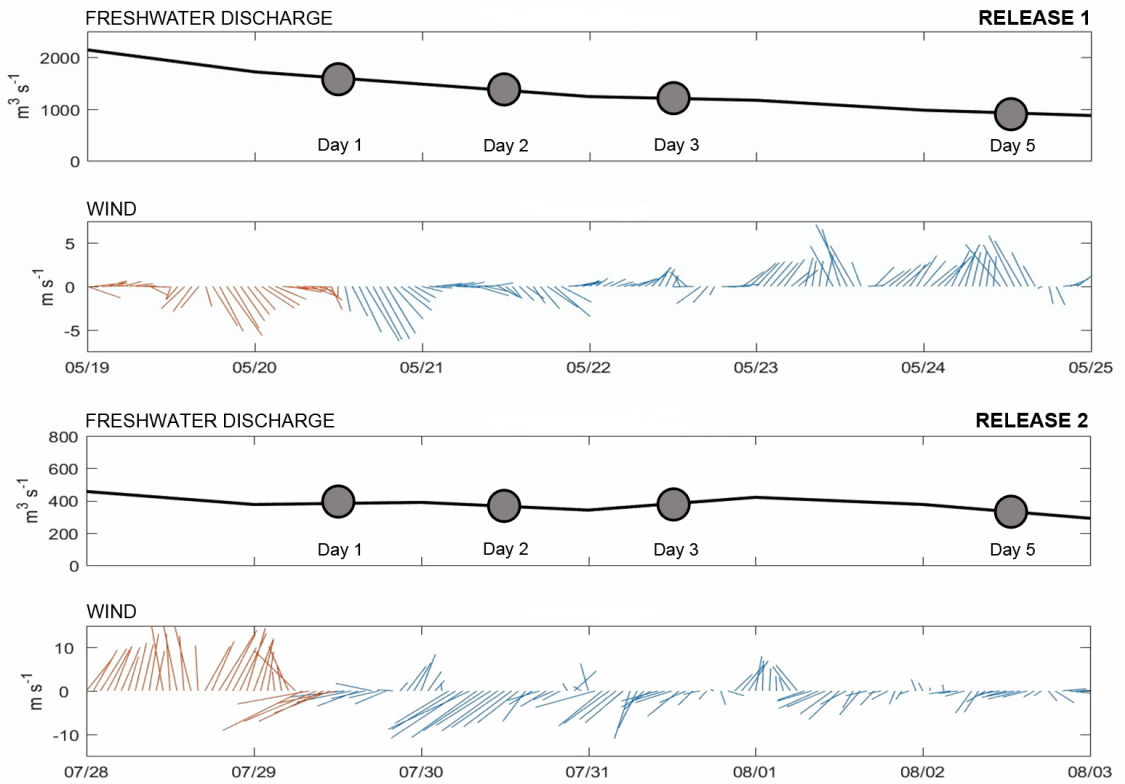
Figure A2. The forcing conditions for freshwater discharge and wind used for the model simulations for the first (May 19, 2014) and the second (July 28, 2014) releases.

Appendix B. Chapter 2 supplemental figures and tables

Table A2. Sites for settlement plate ("S") and native adult oyster ("A").

Site	Latitude (°N)	Longitude (°W)
S1/A1	30.343	-88.349
S2/A2	30.305	-88.273
S3/A3	30.348	-88.232
A3a	30.383	-88.282
A3b	30.339	-88.254
S4/A4	30.299	-88.124
S5	30.336	-88.101
A5	30.349	-88.121
S6	30.332	-87.962
A6	30.319	-87.788
S7	30.412	-88.071
S8	30.547	-88.071
A8	30.651	-88.033

Table A3. Intercept statistics for negative binomial general linear model (2014) and zero-altered negative binomial linear model (2016) lines in Fig. 7. Slopes for 2014 and 2016 sites are 0.38 and 0.34, respectively. 95% confidence intervals, z statistics, and p-values are in relation to site S2. Bold p-values are statistically significant.

Year	Site	Intercept	95% CI	z value	p-value
2014	S1	0.50	2.34	0.82	0.41
	S2	0.32	3.62	-1.44	0.15
	S4	0.06	2.45	-2.71	**0.01**
2016	S1	0.35	2.10	1.14	0.25
	S2	0.19	2.34	-2.79	**0.01**
	S3	0.68	2.17	2.32	**0.02**
	S4	0.29	1.99	0.86	0.39
	S5	0.17	2.19	-0.21	0.83
	S7	0.08	2.77	-1.20	0.23

Table A4. Intercept statistics for regression lines in Fig. 9a, bottom panel showing salinity variation among sites with time in 2016. 95% confidence intervals, t statistics, and p-values are in relation to site S2. Bold p-values are statistically significant.

Site	Intercept	95% CI	t statistic	p-value
S1	20.39	3.82	0.77	0.44
S2	19.66	3.72	21.24	**<0.0001**
S3	16.20	3.82	-3.64	**<0.001**
S4	17.68	3.82	-2.08	**0.04**
S5	16.16	3.82	-3.69	**<0.001**
S7	12.31	3.82	-7.73	**<0.0001**

Table A5. Slope and intercept statistics for regression lines in Fig. A3 showing salinity variation with time in 2014 and 2016. Bold *p*-values are statistically significant.

Year	Slope	Intercept	95% CI	*t* statistic	*p*-value
2014	1.83	2.50	0.80	9.26	**<0.0001**
2016	0.40	18.60	1.14	-5.02	**<0.0001**

Table A6. MANOVA (multivariate) and ANOVA (univariate) results for recent (~single year) and whole (~multiple years) shell used to determine if there were differences in multi-elemental (MANOVA) and individual (ANOVA) trace element ratios among sites. Bold *p*-values are statistically significant.

Shell type	MANOVA	Pillai's Trace	Hypothesis df	Error df	*F*	*p*
Recent	All elements	4.34	72	136	2.24	**<0.0001**
	ANOVA		df	MS	*F*	*p*
	Cr		8	1.32×10^6	4.62	**0.003**
	Mn		8	3.26	1.63	0.19
	Fe		8	1.77	6.35	**<0.001**
	Co		8	6.79×10^6	4.36	**0.005**
	Ni		8	427.25	1.22	0.34
	Cu		8	4.67	5.11	**0.002**
	Zn		8	31.92	0.62	0.75
	Sr		8	0.20	3.19	**0.02**
	Pb		8	4.48×10^3	0.57	0.79
Whole	MANOVA	Pillai's Trace	Hypothesis df	Error df	*F*	*p*
	All elements	4.14	64	144	2.42	**<0.0001**
	ANOVA		df	MS	*F*	*p*
	Mg		8	0.00	0.80	0.61
	Cr		8	3.10×10^5	8.08	**<0.0001**
	Fe		8	1.66	5.11	**0.002**
	Co		8	4.03×10^6	1.94	0.12
	Ni		8	280.02	3.53	**0.01**
	Cu		8	9.89	9.55	**<0.0001**
	Sr		8	0.11	1.16	0.37
	Ba		8	4.44×10^4	1.43	0.25

Table A7. Standardized coefficients explaining the relative contribution of elements to discriminate among sites for recent (~single year) and whole (~multiple years) shell linear discriminant function analyses. Percent variance explained indicates how much variation each linear discriminant explains for site separation.

Shell type	Me:Ca	LD1	LD2	LD3	LD4	LD5	LD6	LD7	LD8
Recent	Cr	0.00	0.00	-0.00	0.00	0.00	0.00	0.00	0.00
	Mn	1.93	0.07	0.02	-0.43	-0.39	-0.37	-0.15	0.22
	Fe	-8.27	1.60	-0.31	-2.17	0.05	-010	-0.94	0.22
	Co	0.00	0.00	0.00	0.00	0.00	0.00	0.00	0.00
	Ni	0.15	-0.06	-0.06	-0.03	0.07	-0.02	-0.03	0.03
	Cu	-0.94	-1.31	0.12	-0.58	-0.07	0.81	0.12	-0.08
	Zn	-0.37	-0.25	0.14	0.15	-0.17	0.14	-0.10	-0.04
	Sr	-7.78	-4.33	-0.64	2.06	0.31	-0.34	2.06	1.33
	Pb	-0.02	0.02	0.01	-0.00	0.01	-0.02	0.01	-0.01
	% variance explained	69.1	21.0	6.6	1.9	0.9	0.3	0.1	0.0
Whole	Mg	-5.80	-8.81	-5.84	16.22	10.83	-6.70	-12.80	12.80
	Cr	-0.00	0.01	-0.00	-0.00	0.00	0.00	0.00	0.00
	Fe	-4.81	-3.79	-0.75	0.85	-0.67	1.34	-0.44	-0.35
	Co	0.00	0.00	0.00	0.00	0.00	-0.00	0.00	0.00
	Ni	0.09	0.01	0.07	0.03	0.04	0.09	-0.06	0.02
	Cu	0.52	-0.77	-0.65	-0.05	0.27	0.03	0.47	0.06
	Sr	-9.35	-1.41	4.07	-3.11	1.56	-0.90	1.88	2.44
	Ba	0.02	0.00	-0.01	0.00	-0.01	0.00	-0.00	-0.00
	% variance explained	78.6	13.8	3.2	1.8	1.5	0.7	0.3	0.1

Table A8. Validation results of recent (~single year) and whole (~multiple years) shell linear discriminant function analyses. Classification matrix indicates the predicted site from the model dataset. Jack-knifed classification matrix indicates the leave-one-out cross-validation used to test the robustness of the adult shell classification. Bold indicates % of total sites correctly classified.

| Shell type | True site | Predicted site | | | | | | | | | % correct |
		A1	A2	A3	A3a	A3b	A4	A5	A6	A8	
Recent	Classification matrix										
	A1	3	0	0	0	0	0	0	0	0	100
	A2	0	3	0	0	0	0	0	0	0	100
	A3	0	0	3	0	0	0	0	0	0	100
	A3a	0	0	0	3	0	0	0	0	0	100
	A3b	0	0	0	0	3	0	0	0	0	100
	A4	0	0	0	0	0	3	0	0	0	100
	A5	0	0	0	0	0	0	3	0	0	100
	A6	0	0	0	0	0	0	0	3	0	100
	A8	0	0	0	0	0	0	0	0	3	100
	Total	3	3	3	3	3	3	3	3	3	**100**
	Jack-knifed classification matrix										
	A1	3	0	0	0	0	0	0	0	0	100
	A2	0	2	0	0	1	0	0	0	0	67
	A3	0	0	0	0	1	0	2	0	0	0
	A3a	0	0	0	3	0	0	0	0	0	100
	A3b	0	1	0	0	2	0	0	0	0	67
	A4	0	0	0	0	0	2	0	0	1	67
	A5	0	0	0	0	1	0	2	0	0	67
	A6	0	0	0	0	0	0	0	3	0	100
	A8	0	0	0	0	0	0	0	0	3	100
	Total	3	3	0	3	5	2	4	3	4	**74**

Table A8 cont.

Shell type	True site	A1	A2	A3	A3a	A3b	A4	A5	A6	A8	% correct
					Predicted site						
Whole	Classification matrix										
	A1	3	0	0	0	0	0	0	0	0	100
	A2	0	2	0	0	0	0	0	0	0	67
	A3	0	0	3	0	0	0	0	0	0	100
	A3a	0	0	0	3	0	0	0	0	0	100
	A3b	0	0	0	0	3	0	0	0	0	100
	A4	0	0	0	0	0	3	0	0	0	100
	A5	0	1	0	0	0	0	3	0	0	100
	A6	0	0	0	0	0	0	0	3	0	100
	A8	0	0	0	0	0	0	0	0	3	100
	Total	3	3	3	3	3	3	3	3	3	**96**
	Jack-knifed classification matrix										
	A1	2	0	0	0	1	0	0	0	0	67
	A2	0	2	0	0	0	0	1	0	0	67
	A3	0	0	1	1	0	0	0	0	1	33
	A3a	0	1	0	2	0	0	0	0	0	67
	A3b	1	0	0	0	2	0	0	0	0	67
	A4	0	0	0	0	0	3	0	0	0	100
	A5	0	2	0	0	0	0	1	0	0	33
	A6	0	0	0	0	0	1	1	1	0	33
	A8	0	0	0	0	0	0	0	0	3	100
	Total	3	5	1	3	3	4	3	1	4	**63**

Table A9. Two-way MANOVA results of spat shells during three time periods to determine if multi-elemental trace element ratios between larval and settled shell of spat were different among sites and between shell types. Bold *p*-values are statistically significant.

MANOVA	Hypothesis df	Error df	Pillai's Trace	*F*	*p*
May-Jun					
Site	48	48	2.96	2.86	**<0.001**
Shell	12	9	0.93	10.77	**<0.001**
Site x shell	48	48	2.46	1.59	0.06
Error					
Jul-Aug					
Site	48	48	2.93	2.74	**<0.001**
Shell	12	9	0.90	6.92	**<0.001**
Site x shell	48	48	2.17	1.19	0.28
Error					
Aug-Sep					
Site	60	85	2.87	1.92	**<0.001**
Shell	12	13	0.80	4.34	**<0.001**
Site x shell	60	85	2.46	1.38	0.09
Error					

Table A10. ANOVA (univariate) results following two-way MANOVAs (Table A8) of spat shells during three time periods to determine which individual trace element ratios differed among sites and between the larval and settled shell of spat. Bold p-values are statistically significant.

		May–Jun				Jul–Aug				Aug–Sep		
	df	MS	F	p	df	MS	F	p	df	MS	F	p
Mg												
Site	4	1.37	3.08	**0.04**	4	14.20	3.41	**0.03**	5	1.39	1.27	0.31
Shell	1	25.00	56.30	**<0.0001**	1	32.30	7.75	**0.01**	1	25.30	23.00	**<0.0001**
Site x shell	4	0.52	1.18	0.35	4	9.75	2.34	0.09	5	2.08	1.90	0.13
Error	20	0.44			20	4.16			24	1.10		
V												
Site	4	1.56	2.49	0.08	4	8.20	7.28	**<0.001**	5	2.13	0.75	0.59
Shell	1	7.10	11.40	**<0.01**	1	1.50	1.33	0.26	1	24.60	8.70	**0.01**
Site x shell	4	0.50	0.79	0.54	4	3.60	3.20	**0.03**	5	2.26	0.80	0.56
Error	20	0.62			20	1.13			24	2.82		
Cr												
Site	4	4.28	2.37	0.09	4	9.05	6.90	**<0.01**	5	1.69	0.63	0.68
Shell	1	16.40	9.08	**0.01**	1	1.34	1.02	0.32	1	24.20	9.06	**0.01**
Site x shell	4	1.48	0.82	0.53	4	4.23	3.22	**0.03**	5	2.04	0.76	0.59
Error	20	1.81			20	1.31			24	2.68		
Mn												
Site	4	2.46	4.40	**0.01**	4	3.00	7.60	**<0.0001**	5	2.12	1.79	0.15
Shell	1	6.25	11.20	**<0.01**	1	0.03	0.07	0.79	1	5.23	4.41	0.05
Site x shell	4	0.35	0.63	0.65	4	1.54	3.89	**0.02**	5	0.96	0.81	0.56
Error	20	0.56			20	0.40			24	1.19		
Fe												
Site	4	4.76	2.50	0.08	4	13.70	7.20	**<0.001**	5	1.40	0.89	0.50
Shell	1	22.90	12.00	**<0.01**	1	3.34	1.76	0.20	1	15.90	10.10	**<0.01**
Site x shell	4	1.24	0.65	0.63	4	5.69	2.99	**0.04**	5	1.29	0.82	0.55

Table A10 cont.

	May–Jun				Jul–Aug				Aug–Sep			
	df	MS	F	p	df	MS	F	p	df	MS	F	p
Error	20	1.91			20	1.90			24	1.58		
Co												
Site	4	2.65	6.64	**<0.01**	4	10.50	7.18	**<0.001**	5	3.98	1.35	0.28
Shell	1	4.23	10.60	**<0.01**	1	1.64	1.12	0.30	1	27.00	9.15	**0.01**
Site x	4	0.16	0.40	0.81	4	5.30	3.61	**0.02**	5	2.79	0.95	0.47
Error	20	0.40			20	1.47			24	2.95		
Ni												
Site	4	1.87	1.11	0.38	4	7.77	5.90	**<0.01**	5	2.90	1.03	0.42
Shell	1	8.51	5.04	**0.04**	1	1.20	0.91	0.35	1	23.40	8.28	**0.01**
Site x	4	0.36	0.22	0.93	4	5.06	3.85	**0.02**	5	1.71	0.61	0.70
Error	20	1.69			20	1.32			24	2.82		
Cu												
Site	4	25.80	2.35	0.09	4	3.29	7.97	**<0.001**	5	5.31	1.60	0.20
Shell	1	0.32	0.03	0.87	1	0.19	0.47	0.50	1	6.66	2.00	0.17
Site x	4	11.30	1.03	0.42	4	2.78	6.72	**<0.01**	5	2.25	0.68	0.64
Error	20	11.00			20	0.41			24	3.32		
Zn												
Site	4	4.11	1.51	0.24	4	10.10	7.60	**<0.001**	5	3.14	1.73	0.17
Shell	1	27.00	9.93	**0.01**	1	1.50	1.13	0.30	1	25.00	13.80	**<0.01**
Site x	4	1.16	0.43	0.79	4	4.47	3.37	**0.03**	5	2.24	1.23	0.32
Error	20	2.71			20	1.33			24	1.81		
Sr												
Site	4	0.50	5.43	**<0.01**	4	0.29	10.20	**<0.001**	5	0.08	3.64	**0.01**
Shell	1	3.23	35.40	**<0.0001**	1	0.29	10.10	**<0.01**	1	0.05	2.59	0.12
Site x	4	0.10	1.10	0.39	4	0.09	3.13	**0.04**	5	0.05	2.15	0.09
Error	20	0.09			20	0.03			24	0.02		

Table A10 cont.

	May–Jun				Jul–Aug				Aug–Sep			
	df	MS	F	p	df	MS	F	p	df	MS	F	p
Ba												
Site	4	3.55	1.95	0.14	4	9.28	5.52	**<0.01**	5	2.93	1.14	0.36
Shell	1	20.00	11.00	**<0.01**	1	4.06	2.41	0.14	1	33.60	13.10	**<0.01**
Site x shell	4	1.93	1.06	0.40	4	3.54	2.10	0.12	5	2.83	1.10	0.39
Error	20	1.83			20	1.68			24	2.57		
Pb												
Site	4	2.85	2.76	0.06	4	10.10	6.68	**<0.01**	5	3.21	0.67	0.65
Shell	1	6.98	6.78	**0.02**	1	0.95	0.63	0.44	1	38.30	7.99	**0.01**
Site x shell	4	1.00	0.97	0.45	4	4.20	2.78	0.05	5	4.14	0.86	0.52
Error	20	1.03			20	1.51			24	4.79		

Table A11. MANOVA (multivariate) and ANOVA (univariate) results for larval and settled shell during three time periods used to determine if there were differences in multi-elemental (MANOVA) and individual (ANOVA) trace element ratios among sites. Bold *p*-values are statistically significant.

Shell type	Time period	MANOVA	Pillai's Trace	Hypothesis df	Error df	*F*	*p*
Larval	May–Jun	All TEs	2.95	24	32	3.75	**<0.001**
		ANOVA		df	MS	*F*	*p*
		Sr		4	0.02	5.28	**0.02**
		Cu		4	56.91	4.77	**0.02**
		Co		4	9.62	4.77	**0.02**
		V		4	10.30	2.08	0.16
		Mn		4	1.57	3.60	0.05
		Ni		4	0.16	2.96	0.07
	Jul–Aug	MANOVA	Pillai's Trace	Hypothesis df	Error df	*F*	*p*
		All TEs	3.13	40	16	1.43	0.22
	Aug–Sep	MANOVA	Pillai's Trace	Hypothesis df	Error df	*F*	*p*
		All TEs	1.09	10	24	2.88	**0.02**
		ANOVA		df	MS	*F*	*p*
		Mn		5	1.17	3.65	**0.03**
		Sr		5	0.02	2.68	0.07
Settled	May–Jun	MANOVA	Pillai's Trace	Hypothesis df	Error df	*F*	*p*
		All TEs	3.37	40	16	2.14	0.05
	Jul–Aug	MANOVA	Pillai's Trace	Hypothesis df	Error df	*F*	*p*
		All TEs	2.23	12	30	7.19	**<0.0001**
		ANOVA		df	MS	*F*	*p*
		Mn		4	4.75	10.42	**<0.001**
		Sr		4	0.31	6.69	**0.01**
		Cu		4	4.26	12.69	**<0.0001**
	Aug–Sep	MANOVA	Pillai's Trace	Hypothesis df	Error df	*F*	*p*
		All TEs	3.01	30	55	2.76	**<0.0001**
		ANOVA		df	MS	*F*	*p*
		Sr		5	0.11	2.93	0.06
		V		5	0.86	0.29	0.91
		Co		5	0.74	0.26	0.93
		Cr		5	0.97	0.32	0.89
		Zn		5	1.39	0.68	0.65
		Ni		5	1.08	0.45	0.81

Table A12. Standardized coefficients explaining the relative contribution of elements to discriminate among sites for larval and settled shell linear discriminant function (LDA) analyses for time periods that had significant MANOVAs. Percent variance explained indicates how much variation each linear discriminant explains for site separation. Larval July–August and settled May–June did not have significant MANOVAs to proceed with LDAs and thus results are not shown.

Shell type	Time period	Me:Ca	LD1	LD2	LD3	LD4	LD5
Larval	May–Jun	Sr	-17.71	-11.98	11.32	-1.21	-
		Cu	-0.59	-0.42	-0.02	0.04	-
		Co	0.35	-2.60	-0.34	0.11	-
		V	2.29	0.60	0.47	-0.40	-
		Mn	-4.31	1.80	-1.65	-0.96	-
		Ni	-6.89	8.97	0.82	3.49	-
		% variance explained	69.6	22.6	5.7	2.1	-
	Aug–Sep	Mn	1.80	1.16	-	-	-
		Sr	-0.46	-15.38	-	-	-
		% variance explained	61.5	38.5	-	-	-
Settled	Jul–Aug	Cu	3.15	-2.02	3.14	-	-
		Sr	-5.11	-3.43	-4.77	-	-
		Mn	-0.34	2.19	-2.49	-	-
		% variance explained	60.0	28.9	11.1	-	-
	Aug–Sep	Sr	-32.73	5.87	-9.52	7.43	4.15
		V	10.63	1.83	-2.78	-8.16	-0.86
		Co	-5.40	7.17	-4.91	6.57	2.06
		Cr	-1.50	-6.90	5.10	5.06	1.85
		Zn	5.10	-1.27	6.47	-2.86	0.19
		Ni	-5.54	-1.52	-2.24	-1.93	-4.02
		% variance explained	75.4	13.1	6.3	4.7	0.6

Table A13. Validation results of larval and settled shell linear discriminant function (LDA) analyses for time periods that had significant MANOVAs. Classification matrix indicates the predicted site from the model dataset. Jack-knifed classification matrix indicates the leave-one-out cross-validation used to test the robustness of the larval and settled shell classification. Bold indicates % of total sites correctly classified. Larval July–August and settled May–June did not have significant MANOVAs to proceed with LDAs and thus results are not shown.

Shell type	Time period	True site	Predicted site							% correct
			S1	S2	S3	S4	S5	S6	S7	
Larval	May–Jun	Classification matrix								
		S1	3	-	0	0	0	0	-	100
		S3	0	-	3	0	0	0	-	100
		S4	0	-	0	3	0	0	-	100
		S5	0	-	0	0	3	0	-	100
		S6	0	-	0	0	0	3	-	100
		Total	3	-	3	3	3	3	-	**100**
		Jack-knifed classification matrix								
		S1	3	-	0	0	0	0	-	100
		S3	0	-	3	0	0	0	-	100
		S4	0	-	1	2	0	0	-	67
		S5	1	-	1	0	1	0	-	33
		S6	1	-	0	0	0	2	-	67
		Total	5	-	5	2	1	2	-	**73**
	Aug–Sep	Classification matrix								
		S1	2	0	0	0	0	-	0	67
		S2	0	2	0	0	0	-	1	67
		S3	0	0	3	0	0	-	0	100
		S4	0	0	0	3	2	-	1	100
		S5	1	0	0	0	1	-	0	33
		S7	0	1	0	0	0	-	1	33
		Total	3	3	3	3	3	-	3	**67**
		Jack-knifed classification matrix								
		S1	0	0	0	0	2	-	1	0
		S2	0	2	0	0	0	-	1	67
		S3	0	0	3	0	0	-	0	100
		S4	0	0	0	3	0	-	0	100
		S5	0	0	0	2	0	-	1	0
		S7	0	1	0	1	0	-	1	33
		Total	0	0	0	0	0	-	0	**50**

205

Table A13 cont.

Shell type	Time period	True site	Predicted site							% correct
			S1	S2	S3	S4	S5	S6	S7	
Settled	Jul–Aug	Classification matrix								
		S1	3	1	0	0	-	0	-	100
		S2	0	2	0	0	-	0	-	67
		S3	0	0	3	0	-	0	-	100
		S4	0	0	0	3	-	0	-	100
		S6	0	0	0	0	-	3	-	100
		Total	3	3	3	3	-	3	-	**93**
		Jack-knifed classification matrix								
		S1	1	1	0	1	-	0	-	33
		S2	1	2	0	0	-	0	-	67
		S3	0	1	2	0	-	0	-	67
		S4	0	0	0	3	-	0	-	100
		S6	2	0	1	0	-	0	-	0
		Total	4	4	3	4	-	0	-	**53**
	Aug–Sep	Classification matrix								
		S1	3	0	0	0	0	-	0	100
		S2	0	3	0	0	0	-	0	100
		S3	0	0	3	1	0	-	0	100
		S4	0	0	0	2	0	-	1	67
		S5	0	0	0	0	3	-	0	100
		S7	0	0	0	0	0	-	2	67
		Total	3	3	3	3	3	-	3	**89**
		Jack-knifed classification matrix								
		S1	1	2	0	0	0	-	0	33
		S2	0	2	0	0	1	-	0	67
		S3	0	0	3	0	0	-	0	100
		S4	0	0	1	2	0	-	0	67
		S5	0	0	1	0	2	-	0	67
		S7	0	0	0	1	0	-	2	67
		Total	1	4	5	3	3	-	2	**67**

Table A14. MANOVA (multivariate) and ANOVA (univariate) results in recent adult shell using trace element (TE) ratios used in the larval origin prediction analyses (i.e., TE ratios present in both larval and recent shell). Differences in multi-elemental (MANOVA) and individual (ANOVA) TE ratios among sites were used to confirm the use of adult shells as a proxy of natal TE ratios. Bold *p*-values are statistically significant.

MANOVA	Pillai's Trace	Hypothesis df	Error df	*F*	*p*
All elements	2.55	35	80	2.37	**<0.001**

ANOVA		df	MS	*F*	*p*
Sr		7	0.21	3.35	**0.02**
Cu		7	12.66	8.08	**0.008**
Co		7	225201.00	3.98	**0.010**
Mn		7	22.37	1.08	0.42
Ni		7	127.81	1.08	0.42

Table A15. Validation results from the larval origin prediction linear discriminant function analysis using trace element ratios in recent adult shell. Classification matrix indicates the predicted site from the model dataset. Jack-knifed classification matrix indicates the leave-one-out cross-validation used to test the robustness of the recent shell classification. Bold indicates % of total sites correctly classified.

True site	Predicted site								% correct
	A1	A2	A3	A3a	A3b	A4	A5	A6	
Classification matrix									
A1	3	0	0	0	0	0	0	0	100
A2	0	3	0	0	0	0	0	0	100
A3	0	0	2	0	0	0	0	0	67
A3a	0	0	0	3	0	0	0	1	100
A3b	0	0	0	0	3	0	0	0	100
A4	0	0	1	0	0	3	0	0	100
A5	0	0	0	0	0	0	3	0	100
A6	0	0	0	0	0	0	0	2	67
Total	3	3	3	3	3	3	3	3	**92**
Jack-knifed classification matrix									
A1	2	0	0	1	0	0	0	0	67
A2	0	2	1	0	0	0	0	0	67
A3	0	0	0	0	1	2	0	0	0
A3a	1	0	0	2	0	0	0	0	67
A3b	0	0	0	0	3	0	0	0	100
A4	0	0	2	0	0	0	1	0	0
A5	0	0	0	0	0	1	2	0	67
A6	0	0	0	1	0	0	0	2	67
Total	3	2	3	4	4	3	3	2	**54**

Table A16. Standardized coefficients explaining the relative contribution of elements to discriminate among sites for the larval origin prediction linear discriminant function analysis using trace element ratios in recent adult shell. Percent variance explained indicates how much variation each linear discriminant explains for site separation.

Shell type	Me:Ca	LD1	LD2	LD3	LD4	LD5
Recent shell	Sr	-4.43	-2.64	-1.39	0.25	-1.75
	Cu	-0.38	-0.07	0.51	0.14	0.02
	Co	0.01	-0.00	-0.00	-0.00	-0.00
	Mn	0.09	0.22	0.06	0.02	-0.16
	Ni	-0.11	0.04	-0.01	-0.09	0.02
	% variance explained	70.9	17.5	9.2	2.2	0.2
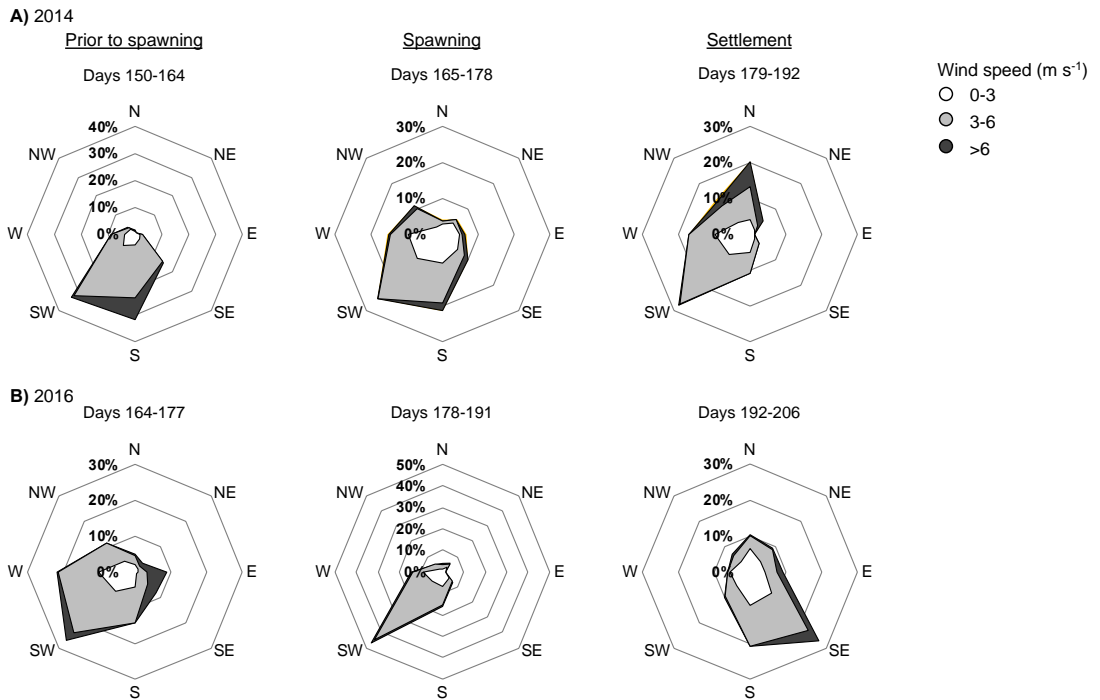
Figure A3. Wind conditions of the Mobile Bay-eastern Mississippi Sound system leading up to the beginning of an exponential increase in spat settlement for 2014 (a) and 2016 (b). The left panels show wind conditions 2-weeks prior to the potential spawning event and 4-weeks prior to the increase in settlement. The middle panels show wind conditions during the potential spawning event. The right panels show the wind conditions during the increase in settlement.
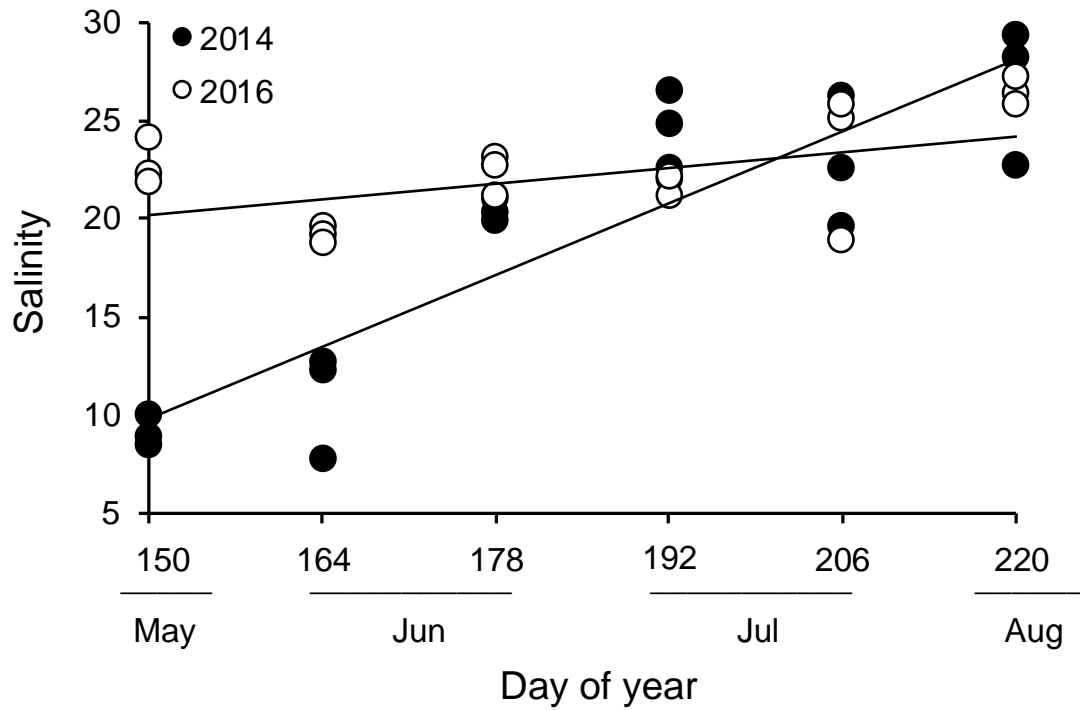
Figure A4. Salinity differences between 2014 and 2016 with time (cf. slope and intercept statistics Table A5). To determine differences between years, sites (S1, S2, S4) and time periods that had appreciable settlement and were measured in both years were used. Sites were not statically different and were used as replicates.
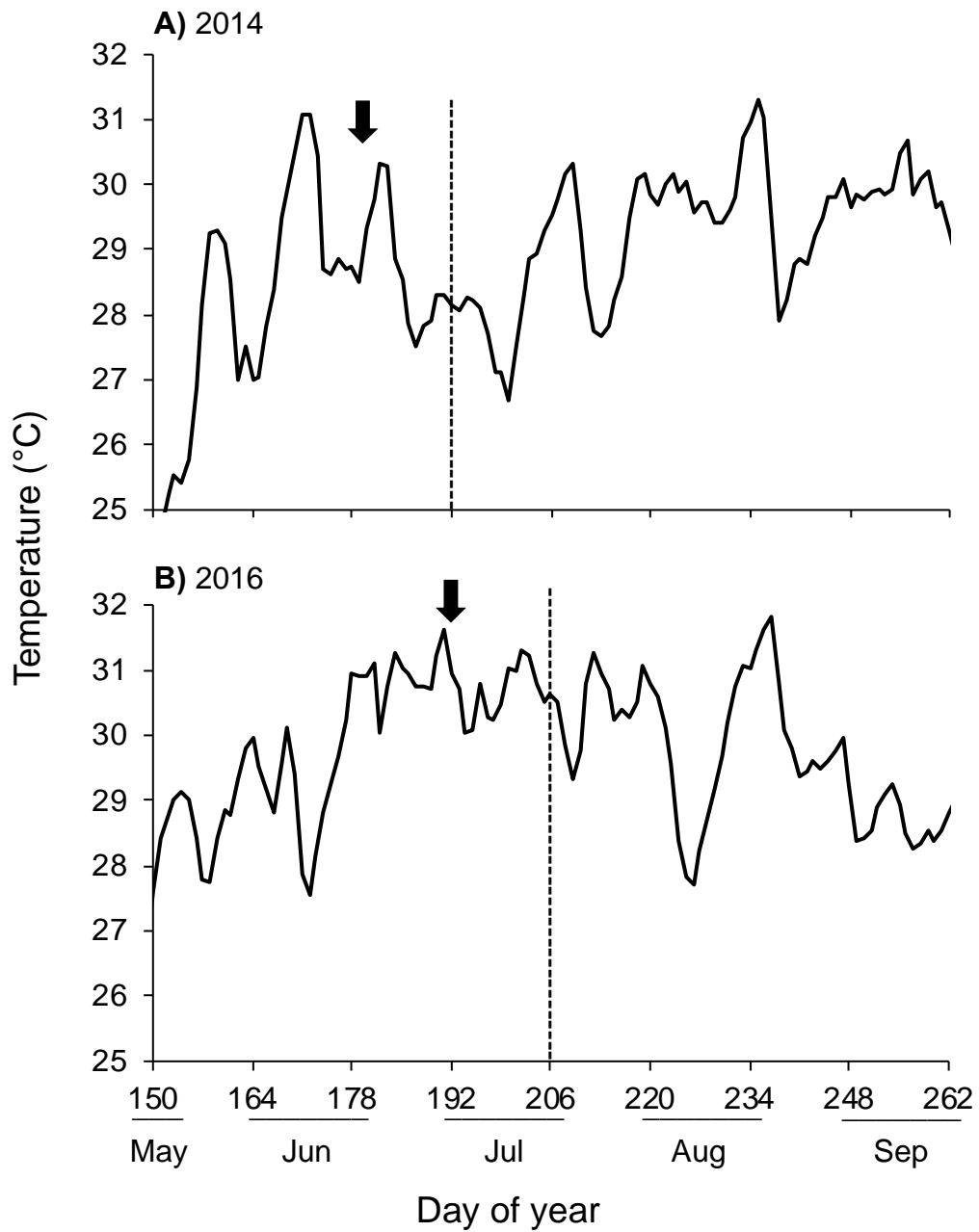
Figure A5. Water temperature (Dauphin Island NOAA tides and currents station) throughout the settlement sampling period during 2014 (a) and 2016 (b), presented as day of year. Dashed lines indicate the beginning of an exponential increase in spat settlement. Arrows indicate possible brood stock spawning events.
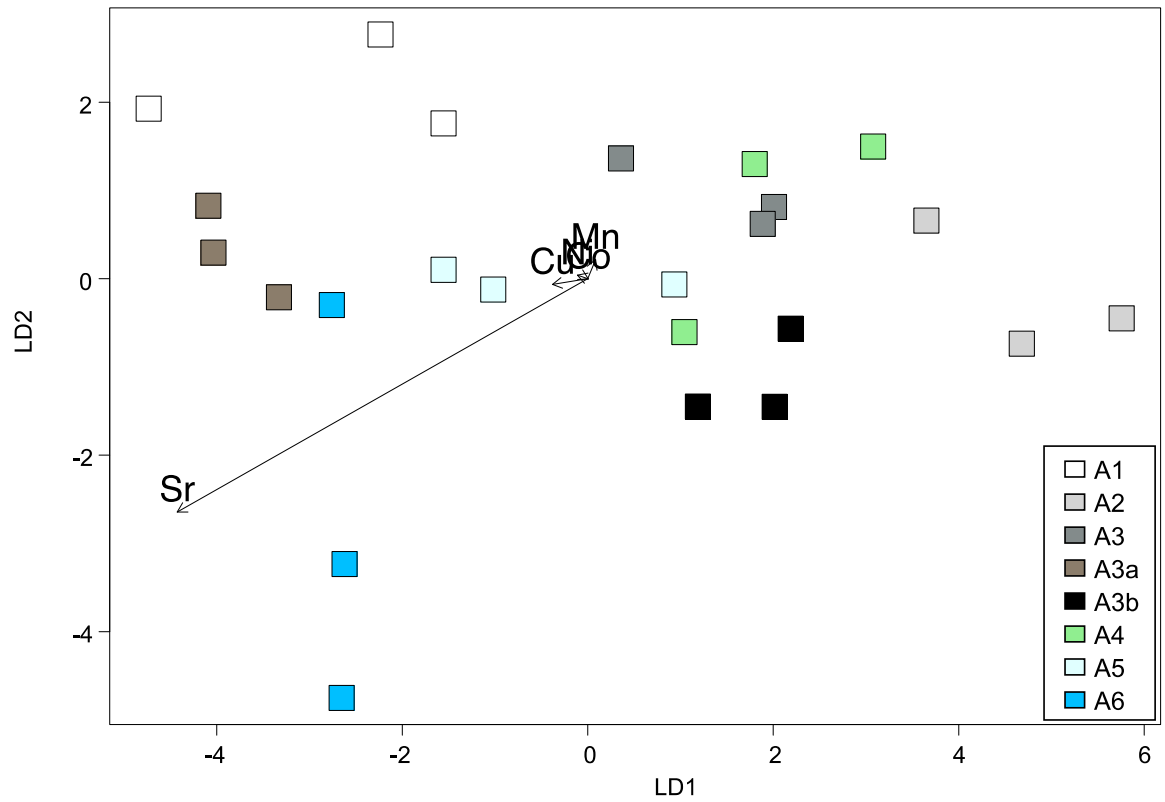
Figure A6. Biplots showing the first two linear discriminates from the larval origin prediction linear discriminant function analysis using trace element (TE) ratios in recent adult shell. Arrows indicate TE ratios causing site differences.

Table A17. GPS coordinates of sources (wastewater treatment plants [WTP] and rivers) and downstream receiving sites sampled in high and low flow subsystems and at additional sites sampled for estuarine-scale analyses.

Site type	Subsystem	Site name	Latitude (°N)	Longitude (°W)
WTP	High	Mobile	30.660	-88.037
	Low	Bayou La Batre	30.385	-88.252
	Additional system site	Fairhope	30.530	-87.904
River	High	Mobile	30.733	-88.042
		Dog	30.565	-88.088
	Low	Bayou La Batre	30.384	-88.271
		West Fowl	30.364	-88.186
	Additional system site	East Fowl	30.447	-88.110
Receiving site	High	MB1	30.651	-88.033
		MB2	30.547	-88.028
	Low	BLB1	30.343	-88.349
		BLB2	30.305	-88.273
		BLB3	30.348	-88.232

Table A18. Explanatory variables considered in each set of wastewater indicator models (dependent variables) for model selection analyses. "X" refers to explanatory variables used; "-" refers to explanatory variables not used. Explanatory variables were measured at source locations to determine the influence of wastewater sources on downstream receiving sites and at receiving sites to determine if variables measured *in situ* explained wastewater concentrations at sites. Dependent variables refer to the wastewater indicators tested (nutrients: $NO_3^- + NO_2^-$, NH_4^+, PO_4^{3-}, TDN, DIN, DON; indicator microbes: fecal coliforms, *E. coli*). Load refers to the nutrient or indicator microbe load that is specific to the nutrient or indicator microbe in question (i.e., the dependent variable). "*" indicates six nutrients measured.

Dependent variables	Explanatory variables											
	Measured at source			Measured at receiving sites								
		Load										
	WTP	River	Chlorophyll *a* river	Nutrients*	Salinity	DO	Chlorophyll *a*	Wind direction	Tidal amplitude	Rainfall	Season	Year
Nutrients	x	x	x	-	-	-	x	x	x	x	x	x
Microbes	x	x	-	x	x	x	-	x	x	x	x	x

Table A19. Nutrient concentrations (µM) measured at wastewater treatment plants (WTP) and rivers in high and low flow subsystems and at nearby receiving sites, separated by season and year sampled. "-" indicates data not available. Error ± SE.

| Flow type | Site type | Site | Season | Year | Nutrient concentration (µM) | | | | | |
					$NO_3^- + NO_2^-$	NH_4^+	PO_4^{3-}	TDN	DIN	DON
High	Source	WTP	Warm	2015	80.62 ± 26.72	409.86 ± 123.75	38.86 ± 5.51	1265.94 ± 113.42	490.48 ± 135.76	775.46 ± 66.07
				2016	181.64 ± 53.84	264.77 ± 60.57	74.69 ± 22.26	921.13 ± 70.52	446.41 ± 89.00	474.72 ± 57.17
			Cold	2015	287.61 ± 94.28	301.38 ± 107.30	71.29 ± 17.58	795.53 ± 31.41	588.99 ± 44.51	262.21 ± 16.74
				2016	123.63 ± 14.51	245.21 ± 85.15	45.80 ± 15.72	942.77 ± 116.10	368.83 ± 71.22	573.93 ± 114.40
		River	Warm	2015	6.75 ± 0.58	3.07 ± 0.99	0.44 ± 0.09	51.03 ± 10.29	9.82 ± 1.02	43.46 ± 9.25
				2016	3.98 ± 1.58	1.69 ± 0.40	0.71 ± 0.08	27.07 ± 2.40	5.67 ± 1.92	21.41 ± 1.66
			Cold	2015	21.29 ± 3.00	2.80 ± 0.61	0.51 ± 0.06	55.88 ± 3.86	24.08 ± 2.45	31.80 ± 2.24
				2016	11.05 ± 0.73	4.30 ± 0.46	0.73 ± 0.15	38.28 ± 2.01	15.35 ± 0.47	22.93 ± 1.86
	Receiving	MB1	Warm	2015	3.54 ± 0.44	17.53 ± 2.14	1.08 ± 0.16	50.06 ± 13.81	21.07 ± 1.92	33.96 ± 14.23
				2016	8.64 ± 2.77	8.15 ± 3.20	1.43 ± 0.15	42.12 ± 5.30	16.79 ± 3.31	25.33 ± 2.33
			Cold	2015	24.88 ± 5.15	6.69 ± 1.70	3.03 ± 1.01	65.03 ± 5.33	31.57 ± 4.31	33.46 ± 2.58
				2016	4.58 ± 1.92	7.03 ± 1.72	1.11 ± 0.19	27.61 ± 5.70	11.60 ± 3.63	16.01 ± 2.07
		MB2	Warm	2015	1.55 ± 0.65	4.37 ± 1.83	1.03 ± 0.11	44.07 ± 16.06	5.93 ± 2.24	38.28 ± 15.12
				2016	1.35 ± 0.60	3.41 ± 1.73	0.79 ± 0.33	27.41 ± 3.24	4.75 ± 2.18	22.66 ± 2.08
			Cold	2015	10.20 ± 2.71	4.04 ± 0.91	1.03 ± 0.68	40.09 ± 7.70	14.24 ± 3.35	25.86 ± 4.57
				2016	4.24 ± 0.84	4.74 ± 0.68	0.77 ± 0.14	26.57 ± 0.64	8.98 ± 1.16	17.59 ± 1.90
Low	Source	WTP	Warm	2015	819.94 ± 276.82	10.25 ± 1.93	151.42 ± 50.04	2316.50 ± 840.67	830.19 ± 274.90	1486.30 ± 678.79
				2016	242.57 ± 114.35	34.99 ± 29.54	185.20 ± 36.95	901.53 ± 109.50	277.56 ± 101.50	623.97 ± 87.22
			Cold	2015	967.72 ± 264.03	24.55 ± 9.66	227.65 ± 17.36	1059.86 ± 340.14	992.27 ± 259.63	370.36 ± 16.74
				2016	131.79 ± 30.79	0.77 ± 0.26	170.73 ± 21.14	672.82 ± 147.32	132.56 ± 30.98	540.26 ± 117.79
		River	Warm	2015	2.24 ± 0.79	4.37 ± 1.38	0.62 ± 0.13	53.04 ± 9.41	6.62 ± 2.13	46.43 ± 9.89
				2016	2.35 ± 1.46	2.17 ± 0.75	0.69 ± 0.11	36.27 ± 6.84	4.44 ± 2.23	31.85 ± 4.68
			Cold	2015	6.46 ± 1.59	6.57 ± 1.29	0.32 ± 0.03	35.85 ± 2.98	13.03 ± 2.69	22.82 ± 0.71
				2016	3.84 ± 1.63	4.84 ± 1.16	0.78 ± 0.19	30.54 ± 3.48	8.68 ± 2.44	21.86 ± 1.76

Table A19 cont.

Flow type	Site type	Site	Season	Year	Nutrient concentration (µM)					
					$NO_3^- + NO_2^-$	NH_4^+	PO_4^{3-}	TDN	DIN	DON
Low	Receiving	BLB1	Warm	2015	0.61 ± 0.17	8.69 ± 4.10	0.73 ± 0.09	36.19 ± 8.92	9.30 ± 4.26	27.34 ± 10.78
				2016	0.23 ± 0.11	0.42 ± 0.18	0.44 ± 0.09	22.72 ± 2.57	0.65 ± 0.11	22.08 ± 2.61
			Cold	2015	2.04 ± 1.40	7.03 ± 2.78	0.71 ± 0.45	21.10 ± 2.26	9.06 ± 3.29	12.04 ± 2.89
				2016	0.26 ± 0.08	2.85 ± 0.08	0.61 ± 0.17	15.23 ± 0.49	3.11 ± 0.15	12.12 ± 0.63
		BLB2	Warm	2015	0.43 ± 0.18	5.87 ± 3.01	0.60 ± 0.07	30.26 ± 5.74	6.30 ± 3.15	24.20 ± 7.69
				2016	0.63 ± 0.41	1.03 ± 0.47	0.60 ± 0.09	23.86 ± 1.86	1.66 ± 0.23	22.19 ± 1.67
			Cold	2015	2.17 ± 1.65	6.29 ± 2.32	0.51 ± 0.25	21.59 ± 3.30	8.46 ± 3.33	13.13 ± 3.30
				2016	0.45 ± 0.05	2.87 ± 0.60	0.62 ± 0.12	20.00 ± 1.92	3.32 ± 0.55	16.69 ± 1.37
		BLB3	Warm	2015	-	-	-	-	-	-
				2016	1.29 ± 0.80	0.70 ± 0.39	0.49 ± 0.16	20.14 ± 0.93	1.99 ± 1.03	18.15 ± 1.72
			Cold	2015	-	-	-	-	-	-
				2016	0.56 ± 0.47	1.02 ± 0.30	0.49 ± 0.13	18.80 ± 2.44	1.59 ± 0.45	17.21 ± 2.01

Table A20. Indicator microbial concentrations (CFU or PFU 100 mL^{-1}) measured at wastewater treatment plants (WTP) and rivers in high and low flow subsystems and at nearby receiving sites, separated by season and year sampled. FC = fecal coliforms, EC = *E. coli*, MSC = male-specific coliphage. "-" indicates data not available. "<" indicates non-detect measurements. Error ± SE.

Flow type	Site type	Site	Season	Year	Indicator concentration		
					FC (CFU 100 mL^{-1})	EC (CFU 100 mL^{-1})	MSC (PFU 100 mL^{-1})
High	Source	WTP	Warm	2015	18 ± 8	15 ± 6	88 ± 22
				2016	20 ± 10	20 ± 10	37 ± 27
			Cold	2015	30 ± 0	27 ± 3	47 ± 27
				2016	277 ± 262	208 ± 196	37 ± 27
		River	Warm	2015	59 ± 22	40 ± 14	20 ± 6
				2016	23 ± 18	15 ± 10	13 ± 3
			Cold	2015	115 ± 41	105 ± 38	<10
				2016	167 ± 142	147 ± 127	37 ± 22
	Receiving	MB1	Warm	2015	149 ± 119	124 ± 109	13 ± 3
				2016	558 ± 546	273 ± 263	<10
			Cold	2015	195 ± 89	127 ± 63	23 ± 7
				2016	85 ± 43	68 ± 43	<10
		MB2	Warm	2015	154 ± 149	141 ± 136	13 ± 3
				2016	<5	<5	<10
			Cold	2015	41 ± 9	37 ± 7	13 ± 3
				2016	17 ± 12	17 ± 12	10 ± 0
Low	Source	WTP	Warm	2015	<5	<5	<10
				2016	<5	<5	<10
			Cold	2015	<5	<5	<10
				2016	20 ± 8	15 ± 5	<10
		River	Warm	2015	89 ± 38	61 ± 32	<10
				2016	142 ± 82	105 ± 73	17 ± 7
			Cold	2015	97 ± 27	87 ± 22	<10
				2016	1222 ± 548	752 ± 320	<10
	Receiving	BLB1	Warm	2015	<5	<5	<10
				2016	<5	<5	<10
			Cold	2015	<5	<5	<10
				2016	987 ± 982	970 ± 965	<10
		BLB2	Warm	2015	<5	<5	<10
				2016	<5	<5	<10
			Cold	2015	<5	<5	<10
				2016	20 ± 15	20 ± 15	<10
		BLB3	Warm	2015	-	-	-
				2016	<5	<5	<10
			Cold	2015	-	-	-
				2016	68 ± 63	68 ± 63	10 ± 0

Table A21. Environmental attributes measured at downstream receiving sites (salinity, temperature, dissolved oxygen [DO], chlorophyll *a*) and from nearby weather stations (wind direction, tidal amplitude, rainfall) in high and low flow subsystems, separated by season and year sampled. Only one rainfall station was used per high and low flow subsystem, thus data are repeated for receiving sites in the respective subsystem. "-" indicates data not available. Error ± SE.

Flow type	Receiving site	Season	Year	Salinity	Temperature (°C)	DO (mg L^{-1})	Chlorophyll *a* (µg L^{-1})	Wind direction (°)	Tidal amplitude (m)	Rainfall (cm)
High	MB1	Warm	2015	19.6 ± 4.6	28.1 ± 1.1	4.1 ± 1.3	4.7 ± 0.9	158	0.05 ± 0.01	12.1 ± 5.1
			2016	15.2 ± 4.1	28.6 ± 0.4	4.2 ± 1.1	6.4 ± 1.7	121	0.06 ± 0.01	10.0 ± 7.6
		Cold	2015	5.4 ± 2.2	15.8 ± 2.1	6.7 ± 0.3	2.4 ± 0.6	320	-0.11 ± 0.03	4.4 ± 3.9
			2016	20.4 ± 3.5	15.6 ± 1.5	7.2 ± 0.6	2.6 ± 0.4	359	-0.11 ± 0.03	17.7 ± 17.7
	MB2	Warm	2015	9.2 ± 4.0	29.4 ± 1.0	6.9 ± 1.0	12.0 ± 2.7	138	0.01 ± 0.02	12.1 ± 5.1
			2016	11.5 ± 2.7	29.4 ± 0.4	6.7 ± 0.7	10.2 ± 1.9	112	0.03 ± 0.03	10.0 ± 7.6
		Cold	2015	5.9 ± 3.1	15.6 ± 2.5	7.4 ± 0.1	7.1 ± 3.5	339	-0.06 ± 0.02	4.4 ± 3.9
			2016	15.6 ± 4.0	13.7 ± 1.6	8.2 ± 1.4	3.9 ± 1.0	12	-0.07 ± 0.03	17.7 ± 17.7
Low	BLB1	Warm	2015	21.1 ± 4.1	29.6 ± 0.5	6.0 ± 1.1	8.7 ± 1.6	147	0.01 ± 0.01	0.8 ± 0.4
			2016	22.7 ± 2.4	29.3 ± 0.6	5.9 ± 1.0	11.3 ± 1.4	128	0.02 ± 0.02	0.9 ± 0.4
		Cold	2015	25.5 ± 2.2	16.1 ± 1.9	7.4 ± 0.4	7.3 ± 1.8	356	-0.05 ± 0.03	0.4 ± 0.3
			2016	28.7 ± 3.3	15.6 ± 1.5	7.9 ± 0.3	5.9 ± 3.1	31	-0.06 ± 0.04	2.2 ± 2.2
	BLB2	Warm	2015	22.3 ± 2.4	29.8 ± 0.6	6.9 ± 0.5	9.0 ± 1.6	150	0.01 ± 0.01	0.8 ± 0.4
			2016	22.8 ± 2.4	29.4 ± 0.5	6.8 ± 0.6	16.7 ± 1.3	134	0.02 ± 0.02	0.9 ± 0.4
		Cold	2015	21.6 ± 2.8	15.2 ± 2.0	7.7 ± 0.4	14.9 ± 3.0	341	-0.16 ± 0.12	0.4 ± 0.3
			2016	28.4 ± 2.2	13.9 ± 1.5	8.5 ± 0.5	5.9 ± 2.6	29	-0.06 ± 0.04	2.2 ± 2.2
	BLB3	Warm	2015	-	-	-	-	-	-	-
			2016	20.7 ± 1.5	30.2 ± 0.2	6.3 ± 0.1	13.4 ± 1.8	134	0.02 ± 0.02	0.9 ± 0.4
		Cold	2015	-	-	-	-	-	-	-
			2016	23.1 ± 4.5	14.7 ± 1.0	9.0 ± 1.0	5.2 ± 2.6	28	-0.06 ± 0.04	2.2 ± 2.2

Table A22. Nutrient loads (mol d^{-1}) calculated from wastewater treatment plants (WTP) and rivers in high and low flow subsystems, separated by season and year sampled. Error ± SE.

Flow type	WTP /River	Season	Year	NO$_3^-$ + NO$_2^-$	NH$_4^+$	PO$_4^{3-}$	TDN	DIN	DON
				Load (mol d^{-1}) × 10^4					
High	WTP	Warm	2015	0.84 ± 0.28	3.32 ± 0.85	0.37 ± 0.05	12.27 ± 1.84	4.16 ± 0.94	8.11 ± 1.81
			2016	1.54 ± 0.39	2.06 ± 0.37	0.56 ± 0.16	7.94 ± 0.52	3.61 ± 0.52	4.33 ± 0.81
		Cold	2015	2.49 ± 0.60	2.97 ± 1.28	0.61 ± 0.09	7.20 ± 0.75	5.46 ± 1.11	2.37 ± 0.27
			2016	0.96 ± 0.10	2.13 ± 0.84	0.32 ± 0.09	7.41 ± 0.96	3.09 ± 0.77	4.32 ± 0.61
	River	Warm	2015	25.40 ± 4.36	9.50 ± 2.93	1.43 ± 0.34	197.13 ± 61.70	34.91 ± 6.10	171.17 ± 54.89
			2016	11.15 ± 3.94	4.51 ± 0.78	1.95 ± 0.18	76.50 ± 8.24	15.66 ± 4.62	60.84 ± 6.64
		Cold	2015	213.09 ± 39.63	28.71 ± 8.33	4.74 ± 0.26	574.68 ± 86.06	241.80 ± 36.87	332.87 ± 54.68
			2016	23.74 ± 4.70	9.37 ± 2.08	1.33 ± 0.20	85.71 ± 18.10	33.12 ± 6.05	52.59 ± 12.17
				Load (mol d^{-1}) × 10^1					
Low	WTP	Warm	2015	27.79 ± 9.18	0.33 ± 0.05	5.27 ± 2.01	75.61 ± 25.87	28.12 ± 9.14	47.49 ± 20.80
			2016	9.16 ± 4.40	1.14 ± 0.93	7.03 ± 1.81	33.75 ± 5.87	10.29 ± 3.94	23.46 ± 4.84
		Cold	2015	35.49 ± 8.15	0.98 ± 0.40	8.61 ± 0.28	39.10 ± 10.23	36.46 ± 7.95	13.82 ± 2.47
			2016	4.98 ± 1.57	0.03 ± 0.01	5.98 ± 0.19	25.19 ± 7.23	5.00 ± 1.57	20.19 ± 5.70
	River	Warm	2015	2.52 ± 0.78	5.05 ± 1.42	0.74 ± 0.15	72.84 ± 20.83	7.58 ± 2.15	65.26 ± 21.24
			2016	4.29 ± 2.65	4.35 ± 1.46	1.28 ± 0.29	70.56 ± 14.47	8.34 ± 4.06	62.22 ± 11.44
		Cold	2015	8.46 ± 2.37	8.41 ± 1.80	0.39 ± 0.02	45.13 ± 5.88	16.87 ± 4.00	28.26 ± 2.11
			2016	5.48 ± 2.68	5.90 ± 1.38	0.92 ± 0.17	41.14 ± 7.77	11.37 ± 3.91	29.76 ± 4.94

Table A23. Indicator microbial loads (CFU or PFU d^{-1}) calculated from wastewater treatment plants (WTP) and rivers in high and low flow subsystems, separated by season and year sampled. FC = fecal coliforms, EC = *E. coli*, MSC = male-specific coliphage. Error ± SE.

Flow type	WTP /River	Season	Year	Indicator microbe load FC (CFU d^{-1})	EC (CFU d^{-1})	MSC (PFU d^{-1})
High	WTP	Warm	2015	$1.70\times10^{11} \pm 7.74\times10^{9}$	$1.55\times10^{10} \pm 6.81\times10^{9}$	$9.47\times10^{10} \pm 3.81\times10^{10}$
			2016	$1.71\times10^{10} \pm 7.62\times10^{9}$	$1.71\times10^{10} \pm 7.62\times10^{9}$	$2.89\times10^{10} \pm 1.93\times10^{10}$
		Cold	2015	$2.74\times10^{10} \pm 3.56\times10^{9}$	$2.49\times10^{10} \pm 5.64\times10^{9}$	$4.00\times10^{10} \pm 2.35\times10^{10}$
			2016	$2.56\times10^{11} \pm 2.46\times10^{11}$	$1.92\times10^{11} \pm 1.84\times10^{11}$	$3.29\times10^{10} \pm 2.56\times10^{10}$
	River	Warm	2015	$1.88\times10^{13} \pm 8.89\times10^{12}$	$1.41\times10^{13} \pm 7.07\times10^{12}$	$7.94\times10^{12} \pm 3.17\times10^{12}$
			2016	$5.51\times10^{12} \pm 3.93\times10^{12}$	$3.66\times10^{12} \pm 2.09\times10^{13}$	$3.60\times10^{12} \pm 5.47\times10^{11}$
		Cold	2015	$1.02\times10^{14} \pm 2.65\times10^{13}$	$9.25\times10^{13} \pm 2.09\times10^{13}$	$1.01\times10^{13} \pm 1.88\times10^{12}$
			2016	$4.56\times10^{13} \pm 4.00\times10^{13}$	$4.00\times10^{13} \pm 3.58\times10^{13}$	$9.92\times10^{12} \pm 6.82\times10^{12}$
Low	WTP	Warm	2015	$1.64\times10^{8} \pm 1.12\times10^{7}$	$1.64\times10^{8} \pm 1.12\times10^{7}$	$3.28\times10^{8} \pm 2.24\times10^{7}$
			2016	$1.85\times10^{8} \pm 1.34\times10^{7}$	$1.85\times10^{8} \pm 1.34\times10^{7}$	$3.69\times10^{8} \pm 2.69\times10^{7}$
		Cold	2015	$1.91\times10^{8} \pm 1.45\times10^{7}$	$1.91\times10^{8} \pm 1.45\times10^{7}$	$3.82\times10^{8} \pm 2.89\times10^{7}$
			2016	$7.09\times10^{8} \pm 2.71\times10^{8}$	$5.40\times10^{8} \pm 1.97\times10^{8}$	$3.60\times10^{8} \pm 3.98\times10^{7}$
	River	Warm	2015	$1.01\times10^{11} \pm 4.44\times10^{10}$	$7.25\times10^{10} \pm 3.65\times10^{10}$	$1.23\times10^{10} \pm 1.89\times10^{9}$
			2016	$3.10\times10^{11} \pm 1.53\times10^{11}$	$2.17\times10^{11} \pm 1.28\times10^{11}$	$3.34\times10^{10} \pm 1.31\times10^{10}$
		Cold	2015	$1.19\times10^{11} \pm 3.37\times10^{10}$	$1.07\times10^{11} \pm 2.83\times10^{10}$	$1.23\times10^{10} \pm 9.94\times10^{8}$
			2016	$1.82\times10^{12} \pm 8.55\times10^{11}$	$1.12\times10^{12} \pm 5.30\times10^{11}$	$1.31\times10^{10} \pm 2.14\times10^{9}$

Table A24. Candidate models for model selection to investigate nutrient concentrations in the high flow subsystem at the receiving site MB1. Each nutrient measured has a set of candidate models. AICc = Akaike information criterion for small sample size. w = Akaike weights. MR = Mobile River nutrient load of the respective nutrient. Dog = Dog River nutrient load of the respective nutrient. WTP = Mobile wastewater treatment plant nutrient load of the respective nutrient. Wind = wind direction.

Nutrient	Model	df	AICc	Δ AICc	w
$NO_3^- + NO_2^-$	y = MR load + error	3	80.46	0.00	0.87
	y = MR load + WTP load + error	4	84.57	4.11	0.11
	y = MR load + WTP load + MR load*WTP load + error	5	89.08	8.62	0.01
	y = Year + MR load + WTP load + MR load*WTP load + error	6	94.03	13.57	0.00
	y = 1 + error	2	100.41	19.95	0.00
	y = Year + MR load + WTP load + Rainfall + MR load*WTP load + error	7	102.19	21.73	0.00
NH_4^+	y = Season + error	3	86.47	0.00	0.47
	y = Season + Dog load + error	4	87.60	1.14	0.27
	y = 1 + error	2	88.03	1.57	0.21
	y = Season + Dog load + WTP load + error	5	91.11	4.64	0.05
	y = Year + Dog load + WTP load + error	5	95.98	9.52	0.00
	y = Year + Season + Dog load + WTP load + error	6	96.60	10.13	0.00
	y = Year + Season + Dog load + WTP load + Wind + error	7	106.46	19.99	0.00
PO_4^{3-}	y = MR load + error	3	36.87	0.00	0.84
	y = MR load + WTP load + error	4	40.63	3.76	0.13
	y = 1 + error	2	43.73	6.86	0.03
	y = Year + MR load + WTP load + error	5	46.19	9.32	0.01
	y = Year + Season + MR load + WTP load + error	6	53.35	16.47	0.00
	y = Year + Season + MR load + WTP load + Wind + error	7	59.47	22.60	0.00

Table A24 cont.

Nutrient	Model	df	AIC$_c$	Δ AIC$_c$	w
TDN	y = MR load + error	3	97.69	0.00	0.88
	y = Year + MR load + error	4	102.14	4.46	0.09
	y = 1 + error	2	105.39	7.70	0.02
	y = Year + Season + MR load + error	5	107.24	9.55	0.01
	y = Year + Season + MR load + Rainfall + error	6	115.32	17.63	0.00
DIN	y = MR load + error	3	92.05	0.00	0.81
	y = MR load + WTP load + error	4	96.10	4.04	0.11
	y = 1 + error	2	97.85	5.79	0.04
	y = Year + MR load + WTP load + error	5	98.06	6.01	0.04
	y = Year + Season + MR load + WTP load + error	6	104.52	12.47	0.00
	y = Year + Season + MR load + WTP load + Rainfall + error	7	114.48	22.43	0.00
DON	y = MR load + error	3	87.29	0.00	0.79
	y = 1 + error	2	91.39	4.09	0.10
	y = MR load + WTP load + error	4	91.50	4.20	0.10
	y = MR load + WTP load + Wind + error	5	95.06	7.76	0.02
	y = MR load + WTP load + Wind + Rainfall + error	6	102.82	15.53	0.00
	y = Year + MR load + WTP load + Wind + Rainfall + error	7	115.94	28.64	0.00
	y = Year + Season + MR load + WTP load + Wind + Rainfall + error	8	137.71	50.41	0.00

Table A25. Model averaging output for candidate models associated with Table A24 for model selection to investigate nutrient concentrations in the high flow subsystem at the receiving site MB1. Each nutrient measured has a model average output. Variables with bold *p*-values are statistically significant. *w* = Akaike weights. MR = Mobile River nutrient load of the respective nutrient. Dog = Dog River nutrient load of the respective nutrient. WTP = Mobile wastewater treatment plant nutrient load of the respective nutrient. Wind = wind direction.

Nutrient	Variable	Intercept	Std. error	*t*	*p*	Sum *w*
$NO_3^- + NO_2^-$	Intercept	3.70	1.52	2.52	0.03	1.00
	Year	3.88×10^{-3}	2.99×10^{-3}	1.31×10^{-3}	1.00	0.00
	MR load	9.33×10^{-6}	1.39×10^{-6}	7.07	**0.0001**	1.00
	WTP load	1.00×10^{-5}	2.28×10^{-5}	5.48×10^{-2}	0.96	0.13
	Rainfall	-1.54×10^{-6}	1.35×10^{-6}	-1.92×10^{-5}	1.00	0.00
	MR load* WTP load	-2.09×10^{-12}	2.31×10^{-12}	-1.16×10^{-2}	0.99	0.01
NH_4^+	Intercept	4.20	1.96	1.82	0.10	1.00
	Year	-0.03	0.02	-0.01	0.99	0.01
	Season	5.27	2.21	1.87	0.09	0.78
	Dog load	2.00×10^{-3}	1.00×10^{-3}	0.48	0.65	0.32
	WTP load	5.60×10^{-6}	4.49×10^{-6}	0.07	0.95	0.05
	Wind	1.84×10^{-7}	3.36×10^{-7}	1.17×10^{-5}	1.00	0.00
PO_4^{3-}	Intercept	0.34	0.41	0.84	0.42	1.00
	Year	-4.00×10^{-4}	4.00×10^{-3}	-7.00×10^{-4}	1.00	0.01
	Season	-1.00×10^{-4}	1.00×10^{-4}	-1.00×10^{-4}	1.00	0.00
	MR load	1.00×10^{-4}	1.48×10^{-5}	3.45	**0.007**	0.97
	WTP load	8.99×10^{-6}	1.34×10^{-5}	0.09	0.93	0.14
	Wind	4.11×10^{-8}	2.49×10^{-8}	1.71×10^{-5}	1.00	0.00

Table A25 cont.

Nutrient	Variable	Intercept	Std. error	t	p	Sum w
TDN	Intercept	31.40	4.42	7.20	**<0.0001**	1.00
	Year	-0.33	0.80	-0.04	0.97	0.10
	Season	0.06	0.06	0.01	0.99	0.01
	MR load	5.12×10^{-6}	1.34×10^{-6}	3.79	**0.005**	0.98
	Rainfall	-2.00×10^{-5}	3.02×10^{-5}	-1.00×10^{-4}	1.00	0.00
DIN	Intercept	14.84	2.51	5.98	**0.0002**	1.00
	Year	-0.28	0.17	-0.07	0.95	0.04
	Season	0.01	0.01	1.30×10^{-3}	1.00	0.00
	MR load	5.77×10^{-6}	1.77×10^{-6}	3.13	**0.01**	0.96
	WTP load	5.38×10^{-6}	1.40×10^{-5}	0.06	0.96	0.15
	Rainfall	-6.96×10^{-7}	1.43×10^{-6}	-5.30×10^{-6}	1.00	0.00
DON	Intercept	15.57	3.13	5.13	**0.0009**	1.00
	Year	5.42×10^{-7}	2.61×10^{-6}	9.87×10^{-8}	1.00	0.00
	Season	1.96×10^{-11}	6.29×10^{-11}	2.76×10^{-12}	1.00	0.00
	MR load	4.13×10^{-6}	1.38×10^{-6}	2.69	**0.02**	0.90
	WTP load	0.00	0.00	0.07	0.95	0.11
	Wind	-4.00×10^{-4}	3.00×10^{-4}	-0.02	0.98	0.02
	Rainfall	0.00	1.00×10^{-4}	-3.00×10^{-4}	1.00	0.00

Table A26. Full candidate models for model selection to investigate nutrient and indicator microbial concentrations in high and low flow subsystems at the receiving sites MB1 and MB2 (high flow) and BLB1 (low flow), with outliers included and excluded from the models. Nutrient = DON with May 2015 outlier. Microbe = Fecal coliforms (FC) with August 2016 outlier. Models in bold indicate a model that had an Akaike weight >0.9, and model averaging was not carried out for that model. w = Akaike weights. AICc = Akaike information criterion for small sample size. Models for indicator microbes in the high flow subsystem with the outlier included are not shown because data were not linear and thus model selection was not performed. In high flow, MR load = Mobile River DON or FC load, WTP load = Mobile wastewater treatment plant (WTP) DON load, Dog load = Dog River DON load. In low flow, BBR load = Bayou La Batre DON load, WTP load = Bayou La Batre WTP DON load. Wind = wind direction. chl$a$ = BLB1 chlorophyll a. Tide = tidal amplitude.

Indicator	Flow	Receiving	Outlier	Model	df	AIC_c	ΔAIC_c	w
Nutrients	High	MB1	Included	**y = MR load + WTP load + error**	**4**	**97.78**	**0.00**	**0.91**
				y = Year + MR load + WTP load + error	5	102.97	5.19	0.07
				y = MR load + error	3	106.56	8.78	0.01
				y = WTP load + error	3	107.78	10.00	0.01
				y = Year + Season + MR load + WTP load + error	6	109.26	11.48	0.00
				y = 1 + error	2	113.71	15.93	0.00
			Excluded	y = MR load + error	3	87.29	0.00	0.79
				y = 1 + error	2	91.39	4.09	0.10
				y = MR load + WTP load + error	4	91.50	4.20	0.10
				y = MR load + WTP load + Wind + error	5	95.06	7.76	0.02
				y = MR load + WTP load + Wind + Rainfall + error	6	102.82	15.53	0.00
				y = Year + MR load + WTP load + Wind + Rainfall + error	7	115.94	28.64	0.00
				y = Year + Season + MR load + WTP load + Wind + Rainfall + error	8	137.71	50.41	0.00

Table A26 cont.

Indicator	Flow	Receiving	Outlier	Model	df	AIC$_c$	Δ AIC$_c$	w
Nutrients	High	MB2	Included	**y = MR load + Dog load + MR load*Dog load + error**	**5**	**94.28**	**0.00**	**0.97**
				y = MR load + Dog load + WTP load + MR load*Dog load + error	6	101.52	7.24	0.03
				y = MR load + Dog load + error	4	104.33	10.05	0.01
				y = MR y = MR load + WTP load + Dog load + WTP load*Dog load + WTP load*Dog load + error	7	111.72	17.45	0.00
				y = 1 + error	2	115.69	21.41	0.00
		MB2	Included	y = Year + MR load + WTP load + Dog load + MR load*Dog load + WTP load*Dog load + error	8	126.71	32.44	0.00
				y = Year + Season + MR load + WTP load + Dog load + MR load*Dog load + WTP load*Dog load + error	9	148.71	54.43	0.00
			Excluded	y = 1 + error	2	81.70	0.00	0.48
				y = MR load + error	3	81.79	0.09	0.46
				y = MR load + Dog load + error	4	85.89	4.20	0.06
				y = Year + MR load + Dog load + error	5	92.08	10.39	0.00
				y = Year + Season + MR load + Dog load + error	6	98.75	17.05	0.00
	Low	BLB1	Included	y = WTP load + error	3	88.03	0.00	0.65
				y = BBR load + WTP load + error	4	89.83	1.79	0.27
				y = BBR load + error	3	93.22	5.19	0.05
				y = BBR load + WTP load + BBR load*WTP load + error	5	94.25	6.22	0.03
				y = Year + BBR load + WTP load + BBR load*WTP load + error	6	101.21	13.17	0.00
				y = Year + Season + BBR load + WTP load + BBR load*WTP load +	7	103.31	15.28	0.00
				y = 1 + error	2	108.07	20.04	0.00

Table A26 cont.

Indicator	Flow	Receiving	Outlier	Model	df	AIC_c	ΔAIC_c	w
Nutrients	Low		Excluded	$y = 1 + error$	2	79.33	0.00	0.66
				$y = BBR\ load + error$	3	81.07	1.75	0.28
				$y = BBRy = BBR\ load + WTP\ load + error$	4	84.78	5.47	0.04
				$y = BBR\ load + WTP\ load + chla + error$	5	86.76	7.44	0.02
				$y = BBR\ load + WTP\ load + chla + Tide + error$	6	93.35	14.02	0.00
				$y = Year + BBR\ load + WTP\ load + chla + Tide + error$	7	104.65	25.32	0.00
Microbes	High	MB1	Excluded	**$y = MR\ load + DON + error$**	**4**	**147.82**	**0.00**	**0.95**
				$y = MR\ load + DON + DIN + error$	5	154.10	6.29	0.04
				$y = 1 + error$	2	159.85	12.03	0.00
				$y = Salinity + DON + DIN + error$	5	160.47	12.65	0.00
				$y = MR\ load + Salinity + DON + DIN + error$	6	161.42	13.60	0.00
				$y = MR\ load + DIN + error$	4	164.47	16.65	0.00
				$y = Season + MR\ load + Salinity + DON + DIN + error$	7	173.83	26.02	0.00

Table A27. Full model averaging output for candidate models associated with Table A26 for model selection of nutrient and indicator microbial concentrations in high and low flow subsystems at the receiving sites MB1 and MB2 (high flow) and BLB1 (low flow), with outliers included and excluded from the models. Nutrient = DON with May 2015 outlier. Microbe = Fecal coliforms (FC) with August 2016 outlier. Variables with bold *p*-values are statistically significant. *w* = Akaike weights. "*" represent model that had a *w* >0.9 and therefore no model average (also shown by "-" in sum *w* column). In high flow, MR load = Mobile River DON or FC load, WTP load = Mobile wastewater treatment plant (WTP) DON load, Dog load = Dog River DON load. In low flow, BBR load = Bayou La Batre DON load, WTP load = Bayou La Batre WTP DON load. Wind = wind direction. chl*a* = BLB1 chlorophyll *a*. Tide = tidal amplitude.

Indicator	Flow	Receiving site	Outlier	Variable	Intercept	Std. error	*t*	*p*	Sum *w*
Nutrients	High	MB1	Included*	Intercept	5.72	3.71	1.54	0.15	-
				MR load	6.29×10^{-6}	1.40×10^{-6}	4.49	**0.001**	-
				WTP load	2.42×10^{-4}	5.80×10^{-5}	4.17	**0.002**	-
			Excluded	Intercept	15.57	3.13	5.13	**0.0009**	1.00
				Year	5.42×10^{-7}	2.61×10^{-6}	9.87×10^{-8}	1.00	0.00
				Season	1.96×10^{-11}	6.29×10^{-11}	2.76×10^{-12}	1.00	0.00
				MR load	4.13×10^{-6}	1.38×10^{-6}	2.69	**0.03**	0.90
				WTP load	1.01×10^{-5}	1.68×10^{-5}	0.07	0.95	0.11
				Wind	-4.00×10^{-4}	3.00×10^{-4}	-0.02	0.98	0.02
				Rainfall	-4.37×10^{-5}	1.00×10^{-4}	-3.00×10^{-4}	1.00	0.00
		MB2	Included*	Intercept	22.24	3.89	5.72	**0.0003**	-
				MR load	-5.26×10^{-6}	1.95×10^{-6}	-2.70	**0.02**	-
				Dog load	-1.00×10^{-4}	5.00×10^{-4}	-0.21	0.84	-
				MR load*Dog load	6.02×10^{-10}	1.32×10^{-10}	4.58	**0.001**	-

Table A27 cont.

Indicator	Flow	Receiving	Outlier	Variable	Intercept	Std. error	t	p	Sum w
Nutrients		MB2	Excluded	Intercept	10.00	1.25	4.26	**0.002**	1.00
				Year	-2.90×10^{-3}	0.01	-7.00×10^{-4}	1.00	0.00
				Season	5.00×10^{-4}	4.00×10^{-4}	1.00×10^{-4}	1.00	0.00
				MR load	1.13×10^{-6}	6.33×10^{-7}	0.93	0.38	0.52
				Dog load	1.73×10^{-5}	2.54×10^{-5}	0.04	0.97	0.06
	Low	BLB1	Included	Intercept	5.16	2.56	2.05	0.07	1.00
				Year	2.70×10^{-3}	4.00×10^{-3}	8.00×10^{-4}	1.00	0.00
				Season	2.40×10^{-3}	1.00×10^{-3}	8.00×10^{-4}	1.00	0.00
				BBR load	4.00×10^{-4}	3.00×10^{-4}	0.69	0.51	0.35
				WTP load	4.00×10^{-3}	8.00×10^{-4}	5.67	**0.0003**	0.95
				BBR load*WTP load	5.31×10^{-9}	5.73×10^{-9}	0.03	0.98	0.03
			Excluded	Intercept	3.69	1.25	1.06	0.32	1.00
				Year	0.00	0.00	0.00	1.00	0.00
				BBR load	3.00×10^{-4}	3.00×10^{-4}	0.40	0.68	0.34
				WTP load	1.00×10^{-4}	1.00×10^{-4}	0.05	0.96	0.06
				Chl$a$	0.01	0.01	0.03	0.97	0.02
				Tide	0.02	0.02	7.00×10^{-4}	1.00	0.00
Microbes	High	MB1	Excluded*	Intercept	-125.00	44.59	-2.80	**0.02**	-
				MR load	1.18×10^{-12}	4.28×10^{-13}	2.77	**0.02**	-
				DON	7.02	1.33	5.28	**0.0005**	-

Table A28. Candidate models for model selection to investigate nutrient concentrations in the high flow subsystem at the receiving site MB2. Each nutrient measured has a set of candidate models. Models in bold indicate a model that had an Akaike weight >0.9, and model averaging was not carried out for that nutrient. AICc = Akaike information criterion for small sample size. w = Akaike weights. MR = Mobile River nutrient load of the respective nutrient. Dog = Dog River nutrient load of the respective nutrient. WTP = Mobile wastewater treatment plant nutrient load of the respective nutrient. Wind = wind direction. Tide = tidal amplitude. chl$a$ = MB2 chlorophyll a. MR chl$a$ load = Mobile River chlorophyll a load.

Nutrients	Model	df	AIC$_c$	Δ AIC$_c$	w
NO$_3^-$ + NO$_2^-$	y = MR load + Dog load + error	4	50.02	0.00	0.76
	y = Dog load + error	3	52.75	2.73	0.19
	y = MR load + WTP load + Dog load + error	5	55.58	5.56	0.05
	y = MR load + WTP load + Dog load + MR load*WTP load + error	6	62.46	12.43	0.00
	y = MR load + WTP load + Dog load + MR load*WTP load + MR load*Dog load + error	7	66.00	15.97	0.00
	y = MR load + WTP load + error	4	71.83	21.81	0.00
	y = Year + MR load + WTP load + Dog load + MR load*WTP load + MR load*Dog load + error	8	75.73	25.70	0.00
	y = 1 + error	2	78.61	28.59	0.00
	y = Year + MR load + WTP load + Dog load + chl$a$ + MR load*WTP load + MR load*Dog load + error	9	99.29	49.26	0.00
NH$_4^+$	**y = Dog load + MR chl$a$ load + error**	**4**	**53.04**	**0.00**	**0.92**
	y = WTP load + Dog load + MR chl$a$ load + error	5	58.59	5.54	0.06
	y = Season + WTP load + Dog load + MR chl$a$ load + error	6	62.15	9.11	0.01
	y = WTP load + MR chl$a$ load + error	4	62.16	9.11	0.01
	y = 1 + error	2	63.74	10.70	0.00
	y = Season + WTP load + Dog load + error	5	67.73	14.69	0.00

231

Table A28 cont.

Nutrients	Model	df	AIC_c	ΔAIC_c	w
NH_4^+	y = Season + WTP load + Dog load + MR chl$a$ load + Wind + error	7	71.44	18.40	0.00
PO_4^{3-}	y = 1 + error	2	26.37	0.00	0.38
	y = Tide + error	3	27.13	0.76	0.26
	y = Wind + Tide + error	4	27.89	1.51	0.18
	y = Wind + error	3	28.18	1.81	0.15
	y = Year + Wind + Tide + error	5	31.79	5.42	0.03
	y = Year + Season + Wind + Tide + error	6	37.55	11.17	0.00
TDN	y = MR load + Dog load + MR load*Dog load + error	5	82.92	0.00	0.75
	y = MR load + Dog load + error	4	85.29	2.37	0.23
	y = 1 + error	2	91.05	8.13	0.01
	y = MR load + Dog load + Tide + MR load*Dog load + error	6	91.70	8.78	0.01
	y = Year + MR load + Dog load + Tide + MR load*Dog load + error	7	104.72	21.80	0.00
	y = Year + Season + MR load + Dog load + Tide + MR load*Dog load + error	8	126.70	43.78	0.00
DIN	y = Dog load + error	3	68.00	0.00	0.89
	y = MR load + Dog load + error	4	72.32	4.33	0.10
	y = MR load + Dog load + MR load*Dog load + error	5	77.00	9.01	0.01
	y = MR load + error	3	79.95	11.95	0.00
	y = MR load + WTP load + Dog load + MR load*Dog load + error	6	83.60	15.61	0.00
	y = 1 + error	2	84.20	16.20	0.00
	y = MR load + WTP load + Dog load + chl$a$ + MR load*Dog load + error	7	89.88	21.89	0.00
	y = MR load + WTP load + Dog load + chl$a$ + Tide + MR load*Dog load + error	8	98.66	30.67	0.00

Table A28 cont.

Nutrients	Model	df	AIC$_c$	Δ AIC$_c$	w
DON	y = 1 + error	2	81.70	0.00	0.48
	y = MR load + error	3	81.79	0.09	0.46
	y = MR load + Dog load + error	4	85.89	4.20	0.06
	y = Year + MR load + Dog load + error	5	92.08	10.39	0.00
	y = Year + Season + MR load + Dog load + error	6	98.75	17.05	0.00

Table A29. Model averaging output for candidate models associated with Table A28 for model selection to investigate nutrient concentrations in the high flow subsystem at the receiving site MB2. Each nutrient measured has a model average output. Variables with bold *p*-values are statistically significant. *w* = Akaike weights. "*" represent model that had a *w* >0.9 and therefore no model average (also shown by "-" in sum *w* column). MR = Mobile River nutrient load of the respective nutrient. Dog = Dog River nutrient load of the respective nutrient. WTP = Mobile wastewater treatment plant nutrient load of the respective nutrient. Wind = wind direction. Tide = tidal amplitude. chl*a* = MB2 chlorophyll *a*. MR chl*a* load = Mobile River chlorophyll *a* load.

Nutrient	Variable	Intercept	Std. error	*t*	*p*	Sum *w*
$NO_3^- + NO_2^-$	Intercept	1.56	0.42	3.78	**0.005**	1.00
	Year	2.34×10^{-6}	1.27×10^{-6}	3.68×10^{-6}	1.00	0.00
	MR load	1.06×10^{-6}	4.02×10^{-7}	2.13	0.07	0.81
	WTP load	2.70×10^{-7}	2.50×10^{-6}	0.01	1.00	0.05
	Dog load	1.70×10^{-3}	2.00×10^{-4}	7.24	**0.0001**	1.00
	chl*a*	-1.25×10^{-12}	1.23×10^{-12}	-1.55×10^{-11}	1.00	0.00
	MR load*WTP load	-1.89×10^{-14}	1.00×10^{-13}	-5.00×10^{-4}	1.00	0.00
	MR load*Dog load	-4.01×10^{-13}	1.82×10^{-13}	-6.00×10^{-4}	1.00	0.00
NH_4^+ *	Intercept	3.81	0.98	3.90	**0.003**	-
	Dog load	3.30×10^{-3}	8.00×10^{-4}	3.91	**0.003**	-
	MR chl*a* load	-5.47×10^{-12}	1.71×10^{-12}	-3.21	**0.009**	-
PO_4^{3-}	Intercept	0.49	0.14	2.90	0.03	1.00
	Year	-0.01	0.01	-0.03	0.98	0.03
	Season	-7.00×10^{-4}	6.00×10^{-4}	-1.50×10^{-3}	1.00	0.00
	Wind	7.00×10^{-4}	4.00×10^{-4}	0.56	0.59	0.36
	Tide	2.18	1.21	0.84	0.42	0.47

Table A29 cont.

Nutrient	Variable	Intercept	Std. error	t	p	Sum w
TDN	Intercept	24.90	3.20	7.66	**<0.0001**	1.00
	Year	-1.53×10^{-5}	5.06×10^{-5}	-4.18×10^{-6}	1.00	0.00
	Season	1.02×10^{-10}	1.19×10^{-9}	2.01×10^{-11}	1.00	0.00
	MR load	-2.76×10^{-6}	1.70×10^{-6}	-1.19	0.27	0.98
	Dog load	4.00×10^{-4}	3.00×10^{-4}	1.13	0.30	0.99
	Tide	-0.03	0.22	-1.10×10^{-3}	1.00	0.01
	MR load*Dog load	2.60×10^{-10}	8.94×10^{-11}	2.20	0.07	0.76
DIN	Intercept	4.82	0.92	5.27	**0.0005**	1.00
	MR load	1.16×10^{-08}	1.42×10^{-7}	0.01	1.00	0.11
	Dog load	2.10×10^{-3}	4.00×10^{-4}	5.95	**0.0003**	1.00
	WTP load	-1.27×10^{-8}	1.88×10^{-8}	-3.00×10^{-4}	1.00	0.00
	chl$a$	-5.37×10^{-6}	3.30×10^{-6}	-2.58×10^{-5}	1.00	0.00
	Tide	5.66×10^{-6}	2.78×10^{-6}	3.94×10^{-7}	1.00	0.00
	MR load*Dog load	-4.96×10^{-12}	6.17×10^{-12}	-0.01	0.99	0.01
DON	Intercept	10.00	1.25	4.26	**0.002**	1.00
	Year	-2.90×10^{-3}	0.01	-7.00×10^{-4}	1.00	0.00
	Season	5.00×10^{-4}	4.00×10^{-4}	1.00×10^{-4}	1.00	0.00
	MR load	1.13×10^{-6}	6.33×10^{-7}	0.93	0.38	0.52
	Dog load	1.73×10^{-5}	2.54×10^{-5}	0.04	0.97	0.06

Table A30. Candidate models for model selection to investigate nutrient concentrations in the low flow subsystem at the receiving site BLB1. Each nutrient measured has a set of candidate models. AICc = Akaike information criterion for small sample size. w = Akaike weights. BBR = Bayou La Batre River nutrient load of the respective nutrient. WTP = Bayou La Batre wastewater treatment plant nutrient load of the respective nutrient. Wind = wind direction. Tide = tidal amplitude. chl$a$ = BLB1 chlorophyll a. BBR chl$a$ load = Bayou La Batre River chlorophyll a load.

Nutrients	Model	df	AICc	Δ AICc	w
$NO_3^- + NO_2^-$	y = WTP load + error	3	3.39	0.00	0.77
	y = Year + WTP load + error	4	6.51	3.12	0.16
	y = 1 + error	2	8.45	5.06	0.06
	y = Year + Season + WTP load + error	5	12.66	9.27	0.01
NH_4^+	y = BBR load + error	3	84.26	0.00	0.34
	y = Year + error	3	84.59	0.33	0.29
	y = Year + BBR load + error	4	84.92	0.66	0.24
	y = 1 + error	2	86.36	2.10	0.12
	y = Year + Season + BBR load + error	5	90.27	6.01	0.02
	y = Year + Season + BBR load + Wind + error	6	95.94	11.68	0.00
PO_4^{3-}	y = BBR chl$a$ load + Tide + error	4	22.22	0.00	0.54
	y = Tide + error	3	23.17	0.95	0.33
	y = 1 + error	2	26.30	4.08	0.07
	y = Year + BBR chl$a$ load + Tide + error	5	27.79	5.57	0.03
	y = BBR chl$a$ load + error	3	28.54	6.32	0.02

Table A30 cont.

Nutrients	Model	df	AIC$_c$	Δ AIC$_c$	w
TDN	y = WTP load + chl$a$ + error	4	74.41	0.00	0.87
	y = BBR chl$a$ load + WTP load + chl$a$ + error	5	80.34	5.93	0.05
	y = 1 + error	2	80.59	6.18	0.04
	y = BBR chl$a$ load + chl$a$ + error	4	81.49	7.07	0.03
	y = BBR chl$a$ load + WTP load + error	4	82.62	8.21	0.01
	y = BBR chl$a$ load + WTP load + chl$a$ + Wind + error	6	88.99	14.58	0.00
	y = Season + BBR chl$a$ load + WTP load + chl$a$ + Wind + error	7	100.62	26.21	0.00
	y = Year + Season + BBR chl$a$ load + WTP load + chl$a$ + Wind + error	8	118.44	44.03	0.00
DIN	y = WTP load + error	3	87.06	0.00	0.41
	y = 1 + error	2	88.61	1.55	0.19
	y = BBR load + error	3	88.70	1.63	0.18
	y = BBR load + WTP load + error	4	88.74	1.68	0.18
	y = Year + BBR load + WTP load + error	5	91.45	4.39	0.05
	y = Year + Season + BBR load + WTP load + error	6	98.72	11.66	0.00
	y = Year + Season + BBR load + WTP load + Wind + error	7	107.24	20.18	0.00
DON	y = 1 + error	2	79.33	0.00	0.66
	y = BBR load + error	3	81.07	1.75	0.28
	y = BBR load + WTP load + error	4	84.78	5.46	0.04
	y = BBR load + WTP load + chl$a$ + error	5	86.76	7.44	0.02
	y = BBR load + WTP load + chl$a$ + Tide + error	6	93.35	14.02	0.00
	y = Year + BBR load + WTP load + chl$a$ + Tide + error	7	104.65	25.32	0.00

Table A31. Model averaging output for candidate models associated with Table A30 for model selection to investigate nutrient concentrations in the low flow subsystem at the receiving site BLB1. Each nutrient measured has a model average output. Variables with bold *p*-values are statistically significant. *w* = Akaike weights. BBR = Bayou La Batre River nutrient load of the respective nutrient. WTP = Bayou La Batre wastewater treatment plant nutrient load of the respective nutrient. Wind = wind direction. Tide = tidal amplitude. chl*a* = BLB1 chlorophyll *a*. BBR chl*a* load = Bayou La Batre River chlorophyll *a* load.

Nutrients	Variable	Intercept	Std. error	*t*	*p*	Sum *w*
$NO_3^- + NO_2^-$	Intercept	0.22	0.10	2.03	0.07	1.00
	Year	-0.03	0.03	-0.19	0.85	0.17
	Season	-3.00×10^{-4}	1.00×10^{-3}	-2.30×10^{-3}	1.00	0.01
	WTP load	1.00×10^{-4}	3.94×10^{-5}	2.78	**0.02**	0.94
NH_4^+	Intercept	2.57	2.36	1.31	0.22	1.00
	Year	-3.03	1.45	-1.14	**<0.0001**	0.55
	Season	0.02	0.05	0.01	1.00	0.02
	BBR load	0.01	2.30×10^{-3}	1.31	0.22	0.60
	Wind	1.81×10^{-5}	1.68×10^{-5}	1.10×10^{-3}	1.00	0.00
PO_4^{3-}	Intercept	-0.34	0.14	-2.33	**0.04**	1.00
	Year	-2.00×10^{-4}	0.01	-8.00×10^{-4}	1.00	0.03
	BBR chl*a* load	-4.07×10^{-11}	1.88×10^{-11}	-1.30	0.22	0.60
	Tide	6.56	2.04	2.93	**0.02**	0.91

Table A31 cont.

Nutrients	Variable	Intercept	Std. error	t	p	Sum w
TDN	Intercept	7.14	3.18	2.15	0.06	1.00
	Year	-1.02×10^{-9}	7.07×10^{-10}	-3.47×10^{-10}	1.00	0.00
	Season	5.39×10^{-6}	5.88×10^{-6}	1.63×10^{-6}	1.00	0.00
	BBR chl$a$ load	-5.84×10^{-12}	3.28×10^{-11}	-0.02	0.99	0.09
	WTP load	1.50×10^{-3}	6.00×10^{-4}	2.54	**0.04**	0.93
	Chl$a$	0.92	0.28	3.11	**0.02**	0.95
	Wind	2.34×10^{-6}	8.11×10^{-6}	2.00×10^{-4}	1.00	0.00
DIN	Intercept	1.19	2.09	0.45	0.66	1.00
	Year	-0.27	0.18	-0.07	0.95	0.05
	Season	1.10×10^{-3}	3.70×10^{-3}	4.00×10^{-4}	1.00	0.00
	BBR load	1.20×10^{-3}	7.00×10^{-4}	0.67	0.52	0.40
	WTP load	1.10×10^{-3}	5.00×10^{-4}	1.28	0.23	0.63
	Wind	3.31×10^{-7}	3.18×10^{-7}	1.76×10^{-5}	1.00	0.00
DON	Intercept	3.69	1.25	1.06	0.32	1.00
	Year	6.39×10^{-6}	6.29×10^{-6}	2.14×10^{-6}	1.00	0.00
	BBR load	3.00×10^{-4}	3.00×10^{-4}	0.42	0.68	0.34
	WTP load	1.00×10^{-4}	1.00×10^{-4}	0.05	0.96	0.06
	Chl$a$	0.01	0.01	0.03	0.98	0.02
	Tide	0.02	0.02	7.00×10^{-4}	1.00	0.00

Table A32. Candidate models for model selection to investigate nutrient concentrations in the low flow subsystem at the receiving site BLB2. Each nutrient measured has a set of candidate models. $NO_3^- + NO_2^-$ did not have relationships to explanatory variables measured at BLB2 and model selection was not performed. AICc = Akaike information criterion for small sample size. w = Akaike weights. BBR = Bayou La Batre River nutrient load of the respective nutrient. WTP = Bayou La Batre wastewater treatment plant nutrient load of the respective nutrient. Wind = wind direction. Tide = tidal amplitude. chl$a$ = BLB2 chlorophyll a. BBR chl$a$ load = Bayou La Batre River chlorophyll a load.

Nutrients	Model	df	AIC$_c$	Δ AIC$_c$	w
NH$_4^+$	y = BBR load + error	3	40.06	0.00	0.86
	y = BBR load + Tide + error	4	44.36	4.30	0.10
	y = 1 + error	2	47.25	7.19	0.02
	y = Year + BBR load + Tide + error	5	48.24	8.18	0.01
	y = Year + Season + BBR load + Tide + error	6	53.75	13.70	0.00
PO$_4^{3-}$	y = 1 + error	2	2.04	0.00	0.60
	y = BBR load + error	3	3.68	1.64	0.26
	y = BBR load + Tide + error	4	5.03	3.00	0.13
	y = Year + BBR load + Tide + error	5	10.43	8.40	0.01
	y = Year + Season + BBR load + Tide + error	6	15.31	13.27	0.00
TDN	y = 1 + error	2	69.87	0.00	0.67
	y = WTP load + error	3	71.96	2.08	0.24
	y = WTP load + chl$a$ + error	4	73.94	4.06	0.09
	y = WTP load + chl$a$ + Tide + error	5	77.88	8.01	0.01
	y = Year + WTP load + chl$a$ + Tide + error	6	86.39	16.52	0.00
	y = Year + Season + WTP load + chl$a$ + Tide + error	7	99.32	29.44	0.00

Table A32 cont.

Nutrients	Model	df	AIC$_c$	Δ AIC$_c$	w
DIN	y = BBR load + error	3	79.22	0.00	0.41
	y = BBR load + WTP load + error	4	80.07	0.86	0.27
	y = WTP load + error	3	81.02	1.80	0.17
	y = 1 + error	2	81.62	2.41	0.12
	y = BBR load + WTP load + Tide + error	5	84.71	5.49	0.03
	y = Year + BBR load + WTP load + Tide + error	6	90.82	11.61	0.00
	y = Year + Season + BBR load + WTP load + Tide + error	7	101.12	21.90	0.00
DON	y = BBR chl$a$ load + error	3	78.44	0.00	0.56
	y = 1 + error	2	80.21	1.77	0.23
	y = WTP load + error	3	81.79	3.35	0.11
	y = WTP load + BBR chl$a$ load + error	4	82.38	3.93	0.08
	y = WTP load + BBR chl$a$ load + Tide + error	5	84.98	6.54	0.02
	y = Year + WTP load + BBR chl$a$ load + Tide + error	6	93.29	14.85	0.00
	y = Year + Season + WTP load + BBR chl$a$ load + Tide + error	7	106.23	27.79	0.00

Table A33. Model averaging output for candidate models associated with Table A32 for model selection to investigate nutrient concentrations in the low flow subsystem at the receiving site BLB2. Each nutrient measured has a model average output. $NO_3^- + NO_2^-$ did not have relationships to explanatory variables measured at BLB2 and model selection was not performed. Variables with bold p-values are statistically significant. w = Akaike weights. BBR = Bayou La Batre River nutrient load of the respective nutrient. WTP = Bayou La Batre wastewater treatment plant nutrient load of the respective nutrient. Wind = wind direction. Tide = tidal amplitude. chl$a$ = BLB2 chlorophyll a. BBR chl$a$ load = Bayou La Batre River chlorophyll a load.

Nutrients	Variable	Intercept	Std. error	t	p	Sum w
NH_4^+	Intercept	-0.82	0.52	-1.55	0.15	1.00
	Year	-0.01	0.01	-0.02	0.99	0.02
	Season	-6.00×10^{-4}	6.00×10^{-4}	-1.00×10^{-3}	1.00	0.00
	BBR load	2.60×10^{-3}	7.00×10^{-4}	3.58	**0.005**	0.98
	Tide	-0.04	0.28	-0.02	0.99	0.12
PO_4^{3-}	Intercept	0.19	0.05	1.52	0.16	1.00
	Year	-5.00×10^{-4}	1.40×10^{-3}	-3.80×10^{-3}	1.00	0.01
	Season	-2.00×10^{-4}	1.00×10^{-4}	-1.00×10^{-3}	1.00	0.00
	BBR load	6.00×10^{-4}	5.00×10^{-4}	0.43	0.68	0.40
	Tide	0.12	0.08	0.23	0.82	0.14
TDN	Intercept	6.31	0.91	2.36	**0.04**	1.00
	Year	-2.00×10^{-4}	4.00×10^{-4}	-1.00×10^{-4}	1.00	0.00
	Season	2.75×10^{-7}	7.38×10^{-7}	10.00×10^{-8}	1.00	0.00
	WTP load	2.00×10^{-4}	2.00×10^{-4}	0.39	0.71	0.33
	Chl$a$	0.03	0.02	0.15	0.88	1.00
	Tide	0.14	0.10	0.02	0.99	0.01

Table A33 cont.

Nutrients	Variable	Intercept	Std. error	t	p	Sum w
DIN	Intercept	0.99	1.60	0.55	0.59	1.00
	Year	-3.80×10^{-3}	4.10×10^{-3}	-1.20×10^{-3}	1.00	0.00
	Season	5.00×10^{-6}	2.08×10^{-5}	1.75×10^{-6}	1.00	0.00
	BBR load	2.10×10^{-3}	9.00×10^{-4}	1.68	0.13	0.71
	WTP load	6.00×10^{-4}	3.00×10^{-4}	0.86	0.41	0.46
	Tide	-0.21	0.27	-0.02	0.98	0.03
DON	Intercept	10.55	2.00	5.03	**0.0008**	1.00
	Year	6.00×10^{-4}	1.00×10^{-3}	2.00×10^{-4}	1.00	0.00
	Season	-8.71×10^{-7}	2.40×10^{-6}	-1.89×10^{-7}	1.00	0.00
	WTP load	4.00×10^{-4}	4.00×10^{-4}	0.21	0.84	0.21
	BBR chl$a$ load	5.71×10^{-10}	2.46×10^{-10}	1.54	0.16	0.66
	Tide	0.46	0.27	0.04	0.97	0.02

Table A34. Candidate models for model selection to investigate nutrient concentrations in the low flow subsystem at the receiving site BLB3. BLB3 was only sampled one year, and data were supplemented with data from another study, which did not measure nutrients in wastewater treatment plant effluent, thus only river load could be tested. In addition, chlorophyll a was not tested in the other study and could not be included in model selection. Only NH_4^+ and PO_4^{3-} had relationships to nutrient concentrations at BLB3. Each nutrient measured has a set of candidate models. Models in bold indicate a model that had an Akaike weight >0.9, and model averaging was not carried out for that nutrient. AICc = Akaike information criterion for small sample size. w = Akaike weights. WFR = West Fowl River nutrient load of the respective nutrient. Wind = wind direction. Tide = tidal amplitude.

Nutrients	Model	df	AICc	Δ AICc	w
NH_4^+	**y = WFR load + error**	**3**	**24.40**	**0.00**	**0.91**
	y = WFR load + Rainfall + error	4	29.35	4.95	0.08
	y = WFR load + Rainfall + WFR load*Rainfall + error	5	33.62	9.22	0.01
	y = 1 + error	2	34.89	10.50	0.00
	y = Season + WFR load + Rainfall + WFR load*Rainfall + error	6	43.46	19.07	0.00
PO_4^{3-}	y = Tide + error	3	1.50	0.00	0.41
	y = 1 + error	2	1.76	0.26	0.36
	y = WFR load + Tide + error	4	3.32	1.82	0.17
	y = WFR load + Wind + Tide + error	5	6.18	4.68	0.04
	y = WFR load + Wind + error	4	8.30	6.80	0.01
	y = Season + WFR load + Wind + Tide + error	6	15.18	13.68	0.00

Table A35. Model averaging output for candidate models associated with Table A34 for model selection to investigate nutrient concentrations in the low flow subsystem at the receiving site BLB3. Only NH_4^+ and PO_4^{3-} had relationships with explanatory variables to be tested via model selection and have model average outputs. BLB3 was only sampled for half of the sampling periods and data were supplemented from another project, and wastewater treatment plant loads could not be included. Variables with bold *p*-values are statistically significant. *w* = Akaike weights. "*" represent model that had a *w* >0.9 and therefore no model average (also shown by "-" in sum *w* column). WFR = West Fowl River nutrient load of the respective nutrient. Wind = wind direction. Tide = tidal amplitude.

Nutrients	Variable	Intercept	Std. error	*t*	*p*	Sum *w*
NH_4^+ *	Intercept	0.42	0.17	2.42	**0.04**	-
	WFR load	1.30×10^{-3}	3.00×10^{-4}	4.94	**0.0008**	-
PO_4^{3-}	Intercept	0.32	0.05	4.68	**0.002**	1.00
	Season	1.00×10^{-4}	4.97×10^{-5}	5.00×10^{-4}	1.00	0.00
	WFR load	-5.00×10^{-4}	3.00×10^{-4}	-0.36	0.73	0.22
	Wind	-1.00×10^{-4}	1.00×10^{-4}	-0.09	0.93	0.05
	Tide	1.06	0.48	1.37	0.21	0.62

Table A36. Candidate models for model selection to investigate indicator bacterial concentrations in the high flow subsystem at the receiving site MB1. Each indicator bacteria measured has a set of candidate models. Models in bold indicate a model that had an Akaike weight >0.9, and model averaging was not carried out for that indicator microbe. AICc = Akaike information criterion for small sample size. w = Akaike weights. FC = fecal coliforms. EC = *E. coli*. MR load = Mobile River FC load.

Indicator	Model	df	AIC$_c$	Δ AIC$_c$	w
FC	**y = MR load + DON + error**	**4**	**147.82**	**0.00**	**0.95**
	y = MR load + DON + DIN + error	5	154.10	6.29	0.04
	y = 1 + error	2	159.85	12.03	0.00
	y = Salinity + DON + DIN + error	5	160.47	12.65	0.00
	y = MR load + Salinity + DON + DIN + error	6	161.42	13.60	0.00
	y = MR load + DIN + error	4	164.47	16.65	0.00
	y = Season + MR load + Salinity + DON + DIN + error	7	173.83	26.02	0.00
EC	y = DON + error	3	144.97	0.00	0.88
	y = Salinity + DON + error	4	149.61	4.63	0.09
	y = Season + Salinity + DON + error	5	152.16	7.19	0.02
	y = 1 + error	2	156.07	11.09	0.00
	y = Year + Season + Salinity + DON + error	6	160.96	15.99	0.00

Table A37. Model averaging output for candidate models associated with Table A36 for model selection to investigate indicator bacterial concentrations in the high flow subsystem at the receiving site MB1. Each indicator bacteria measured has a model average output. Variables with bold *p*-values are statistically significant. w = Akaike weights. FC = fecal coliforms. EC = *E. coli*. "*" represent model that had a $w > 0.9$ and therefore no model average (also shown by "-" in sum w column). MR load = Mobile River FC load.

Indicator	Variable	Intercept	Std. error	*t*	*p*	Sum *w*
FC*	Intercept	-125.00	44.59	-2.80	**0.02**	-
	MR load	1.18×10^{-12}	4.28×10^{-13}	2.77	**0.02**	-
	DON	7.02	1.33	5.28	**0.0005**	-
EC	Intercept	-96.22	48.46	-2.05	0.07	1.00
	Year	-4.00×10^{-4}	0.02	-7.46×10^{-6}	1.00	0.00
	Season	-2.17	1.27	-0.04	0.97	0.02
	Salinity	0.17	0.37	0.05	0.96	0.11
	DON	6.69	1.38	4.83	**0.001**	1.00

Table A38. Candidate models for model selection to investigate indicator bacterial concentrations in the high flow subsystem at the receiving site MB2. Each indicator bacteria measured has a set of candidate models. AICc = Akaike information criterion for small sample size. w = Akaike weights. FC = fecal coliforms. EC = *E. coli*. MR load = Mobile River FC or EC load. Tide = tidal amplitude.

Indicator	Model	df	AICc	Δ AICc	w
FC	$y = (NO_3^- + NO_2^-)$ + error	3	94.94	0.00	0.56
	$y = $ MR load + $(NO_3^- + NO_2^-)$ + error	4	95.61	0.67	0.40
	$y = $ MR load + $(NO_3^- + NO_2^-)$ + Tide + error	5	100.63	5.69	0.03
	$y = $ MR load + error	3	103.45	8.52	0.01
	$y = 1$ + error	2	109.17	14.23	0.00
EC	$y = $ MR load + $(NO_3^- + NO_2^-)$ + error	4	89.99	0.00	0.76
	$y = (NO_3^- + NO_2^-)$ + error	3	93.07	3.07	0.16
	$y = $ MR load + $(NO_3^- + NO_2^-)$ + Tide + error	5	95.42	5.43	0.05
	$y = $ MR load + error	3	97.28	7.28	0.02
	$y = 1$ + error	2	106.20	16.21	0.00

Table A39. Model averaging output for candidate models associated with Table A38 for model selection to investigate indicator bacterial concentrations in the high flow subsystem at the receiving site MB2. Each indicator bacteria measured has a model average output. Variables with bold *p*-values are statistically significant. w = Akaike weights. FC = fecal coliforms. EC = *E. coli*. MR load = Mobile River FC or EC load. Tide = tidal amplitude.

Indicator	Variable	Intercept	Std. error	*t*	*p*	Sum w
FC	Intercept	0.68	3.72	0.17	0.87	1.00
	MR load	5.09×10^{-14}	2.65×10^{-14}	0.84	0.42	0.44
	$NO_3^- + NO_2^-$	3.40	0.68	5.02	**0.0007**	0.99
	Tide	-1.58	1.67	-0.03	0.98	0.03
EC	Intercept	1.06	2.92	0.34	0.74	1.00
	MR load	1.30×10^{-13}	4.50×10^{-14}	2.41	**0.04**	0.84
	$NO_3^- + NO_2^-$	2.40	0.58	4.08	**0.003**	0.98
	Tide	-1.64	2.13	-0.04	0.97	0.05

Table A40. Wastewater treatment plant (WTP) and river nutrient loads (mol d^{-1}) to the whole system and to the whole system with the exclusion of the high flow WTP and river. Error ± SE. Error was propagated as the square root of the sum of squares.

Nutrient	WTP/ River	∑ system loads (mol d^{-1})	∑ load excluding high flow WTP and river (mol d^{-1})
$NO_3^- + NO_2^-$	WTP	$1.72\times10^4 \pm 2.85\times10^3$	$3.07\times10^3 \pm 5.85\times10^2$
	River	$6.52\times10^5 \pm 2.66\times10^5$	$1.84\times10^3 \pm 5.58\times10^2$
NH_4^+	WTP	$2.70\times10^4 \pm 5.46\times10^3$	$2.57\times10^2 \pm 1.14\times10^2$
	River	$1.29\times10^5 \pm 3.87\times10^4$	$1.70\times10^3 \pm 1.83\times10^2$
PO_4^{3-}	WTP	$5.82\times10^3 \pm 7.41\times10^2$	$1.24\times10^3 \pm 1.56\times10^2$
	River	$2.32\times10^4 \pm 4.20\times10^3$	$2.81\times10^2 \pm 2.95\times10^1$
TDN	WTP	$9.90\times10^4 \pm 1.07\times10^4$	$9.19\times10^3 \pm 1.23\times10^3$
	River	$2.33\times10^6 \pm 6.78\times10^5$	$2.29\times10^4 \pm 2.90\times10^3$
DIN	WTP	$4.41\times10^4 \pm 5.94\times10^3$	$3.25\times10^3 \pm 6.30\times10^2$
	River	$7.81\times10^5 \pm 2.86\times10^5$	$3.33\times10^3 \pm 6.87\times10^2$
DON	WTP	$5.67\times10^4 \pm 1.04\times10^3$	$6.32\times10^3 \pm 9.98\times10^2$
	River	$1.58\times10^6 \pm 4.28\times10^5$	$1.96\times10^4 \pm 2.70\times10^3$

Table A41. Wastewater treatment plant (WTP) and river indicator microbial loads (CFU or PFU d^{-1}) to the whole system and to the whole system with the exclusion of the high flow WTP and river. FC = fecal coliforms, EC = *E. coli*, MSC = male-specific coliphage. Error ± SE. Error was propagated as the square root of the sum of squares.

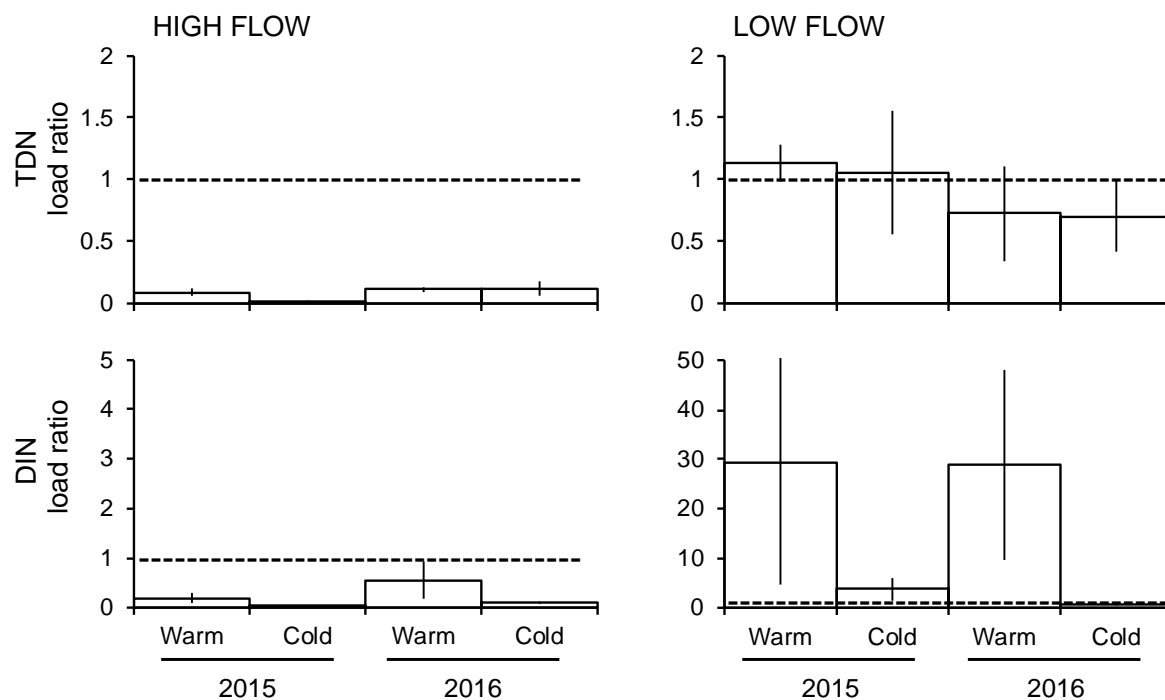| Microbe	WTP/ River	$\sum$ system loads (CFU or PFU d^{-1})	$\sum$ load excluding high flow WTP and river (CFU or PFU d^{-1})
FC	WTP	$7.67 \times 10^{10} \pm 5.61 \times 10^{10}$	$2.11 \times 10^{9} \pm 7.36 \times 10^{8}$
	River	$4.23 \times 10^{13} \pm 1.43 \times 10^{13}$	$1.15 \times 10^{12} \pm 3.67 \times 10^{11}$
EC	WTP	$6.09 \times 10^{10} \pm 4.19 \times 10^{10}$	$1.99 \times 10^{9} \pm 6.49 \times 10^{8}$
	River	$3.66 \times 10^{13} \pm 1.28 \times 10^{13}$	$8.62 \times 10^{11} \pm 2.76 \times 10^{11}$
MSC	WTP	$5.38 \times 10^{10} \pm 1.55 \times 10^{10}$	$1.15 \times 10^{9} \pm 2.19 \times 10^{7}$
	River	$8.00 \times 10^{12} \pm 1.80 \times 10^{12}$	$1.12 \times 10^{11} \pm 4.00 \times 10^{10}$

Figure A7. Ratio of wastewater treatment plant (WTP) to river nutrient loads (TDN and DIN) for high flow and low flow subsystems (note the difference in scale), separated by seasons and years. Dashed line indicates where WTP:river load = 1; >1 indicates the WTP is a larger source and <1 indicates the river is a larger source. Error ± SE. TDN and DIN load ratios were lower from the high flow subsystem than the low flow subsystem (p < 0.0001 for all significant ANOVAs). DIN load ratios within both subsystems were higher in the warm season compared to the cold season (p = 0.04) and not different between years. TDN load ratios were not different between seasons or years.
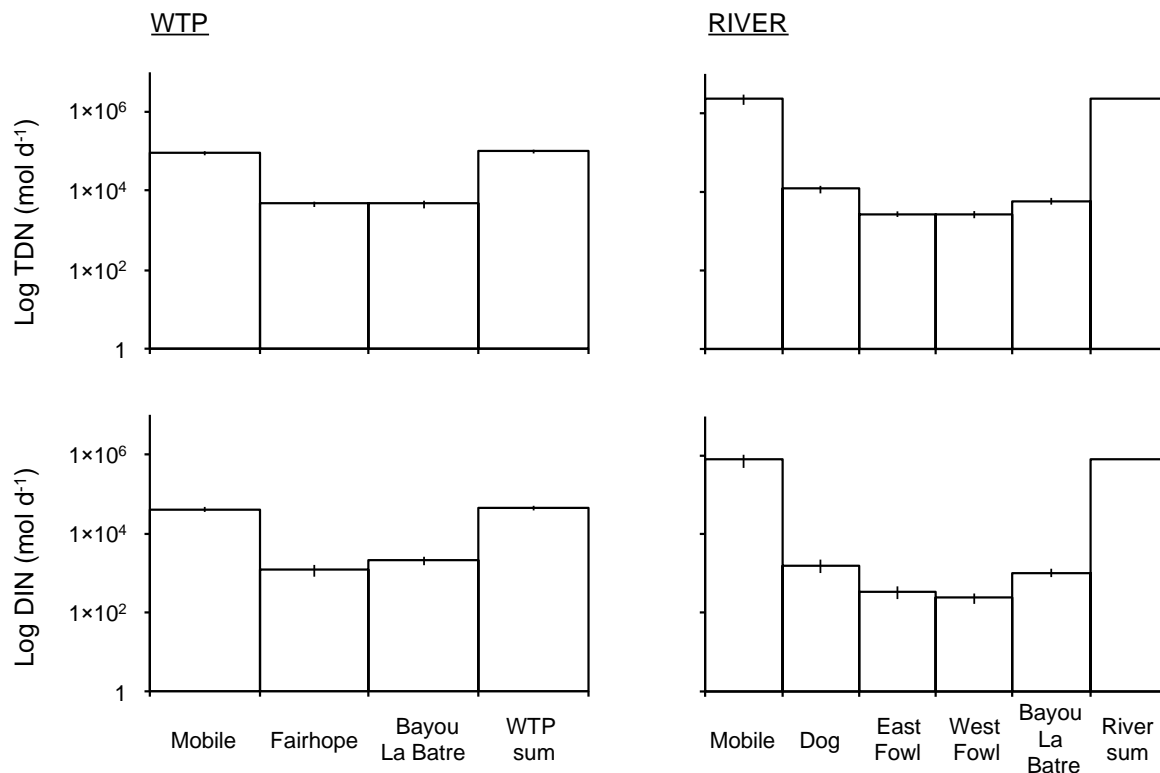
Figure A8. Sum of sampled average ($n = 13$; $n_{Fairhope} = 6$) wastewater treatment plant (WTP) and river TDN and DIN loads to the system. Error $\pm$ SE. Error was propagated as the square root of the sum of squares.

BIOGRAPHICAL SKETCH

BIOGRAPHICAL SKETCH

Name of Author: Haley Nicholson Gancel

Place of Birth: San Diego, California

Date of Birth: March 5, 1991

Graduate and Undergraduate Schools Attended:

University of South Alabama, Mobile, Alabama
University of Miami, Coral Gables, Florida

Degrees Awarded:

Doctor of Marine Science, 2020, Mobile, Alabama
Bachelor of Science, 2013, Coral Gables, Florida

Awards and Honors:

Gulf Estuarine Research Society Biennial Meeting student oral presentation 1st place, 2018, Galveston, Texas
32st Alabama Water Resource Conference student oral presentation 1st place, 2018, Orange Beach, Alabama
Graduate Research Symposium honorable mention oral presentation, 2018, Dauphin Island, Alabama
31st Alabama Water Resource Conference student oral presentation 2nd place, 2017, Orange Beach, Alabama
DISL-FDA Graduate Fellowship, 2014-2019

Publications:

Cartolano, M. C., **Gancel, H. N.,** Lonthair, J., Wood, C. M., and McDonald, D. Pulsatile urea excretion in Gulf toadfish: the role of circulating serotonin and additional 5-HT receptor subtypes. *Journal of Comparative Physiology B*. Accepted.

Gancel, H. N., Carmichael, R. H., Park, K., Krause, J. W., and Rikard, S. 2019. Field mark-recapture of calcein-stained larval oysters (*Crassostrea virginica*) in a freshwater-dominated estuary. *Estuaries and Coasts*. https://doi.org/10.1007/s12237-019-00582-6

Darnell, M. Z., **Nicholson, H. S.,** and Munguia, P. 2015. Thermal ecology of the fiddler crab *Uca panacea*: thermal constraints and organismal responses. *Journal of Thermal Biology* 52: 157-165. https://doi.org/10.1016/j.jtherbio.2015.06.004